Department of Engineering Science

Energy and Power Group



Thesis - MScR

The Development of a Methodology to Approach Carbon Neutrality Using Temperate and Tropical Climates as Case Studies

Andreas Alkiviades

St Catherine's College

Supervisor: Dr Malcolm McCulloch

August 2014

This thesis is dedicated in loving memory of my grandfather, a man who actions were inspiring and kindness touched many lives.

Andreas Alkiviades

(1933-2011)

Acknowledgements

First and foremost, I would like to express my sincere gratitude to my supervisor, Dr Malcolm McCulloch, for the opportunity he gave me to be a part of the Energy and Power Group. The knowledge he has passed on to me as well as his continuous support, guidance and patience throughout the preparation of this thesis have been a source of inspiration and learning.

I am very grateful to Dr Justin Bishop for his advice and support throughout the many hours spent together discussing my work and especially his help and assistance in troubleshooting the Matlab codes developed for the purposes of this study. His help has been integral in writing this thesis.

I would like to thank Dr Barbara Hammond and the team at the Low Carbon Hub for providing me with the opportunity to collaborate with them as well as the funding provided as part of the Leaf Project.

I thank all my fellow group members at the Energy and Power Group for their continuous support and stimulating discussion we have had that have in many ways helped my development and learning. They are great people and I have been lucky to have met and worked beside them.

I am very grateful to Michael Athanson of the Bodleian Library for his training on GIS software. His assistance helped me realize the power of GIS and the applications it has with regards to my research.

A sincere thank you also goes to my housemate, Abdur, for all his support throughout the many hours and late nights spent working together while this thesis was written.

A special thank you to my family who have given me unequivocal support at all stages of my life.

Last, but definitely not least, I would like to express my gratitude to Evyenia for her understanding and endless support throughout my studies; she has been a source of inspiration to me.

Abstract

The threat of climate change has become one of the major issues facing mankind over recent decades and its severity is escalating significantly with increased atmospheric greenhouse gas levels, due to the combustion of fossil fuels, exacerbating the situation. This study develops a methodology to design a renewable energy supply mix to meet demand.

Economic and environmental factors are included in the decision-making process in order to be consistent with the definition of sustainability set out by the United Nations. The economic criterion is represented by the total annual cost and the environmental criterion is represented by the emissions reduction. Analytical techniques are applied to assess the temporal, climatic and growth factors of demand. The supply mix is examined as the potential resource and available conversion technology components. Resources are statistically categorized by availability as determinative, dispatchable and stochastic. This study considers biomass as a dispatchable resource; solar as a determinative resource and wind as a stochastic resource. A constrained exhaustive search algorithm is adapted for supply mix design, including a search space minimization method for greater computational efficiency. The Lagrangian multipliers of cost and emissions reduction are calculated to determine the optimum supply mix.

In order to assess this methodology at different locations with temperate and tropical climates as well as dissimilar demand characters, it is implemented in two case studies attempting to achieve carbon neutrality. The first location is the island of Hanimaadhoo in the Republic of the Maldives. The island is classed as a poor wind regime, but high wind availability is apparent with low solar availability and so both resources have been examined as potentially complementing one another. The annual demand is 1.5 GWh_e and can achieve carbon neutrality at a cost of $ 582,000 per year with a supply mix comprised of 1710 kW_e PV and 6500 kWh_e lead-acid battery storage. The second case study is the county of Oxfordshire in the UK and the Christ Church site, located within the county, as a model smaller-scale site. Oxfordshire has been examined under a land usage scenario that maximizes biomass establishment and 52 % emissions reduction can be achieved at a total annual cost of £ 182 million. A second scenario is examined that aims to create a net food import/export position in the county and allocates remaining land for biomass. This scenario can achieve a 76 % emissions reduction at a total annual cost of £ 169 million. The 60 % emissions reduction target set by Christ Church can be achieved with a 250 kW_e energy crop Anaerobic digester and a 93 kW_e PV array.

Table of Contents

Chapter 1 - Introduction 1

1.1 Metrics Used in the Decision-Making Process of the Supply Mix Design 2

1.2 Statistical Characterization of Renewable Energy Resources 4

1.3 Introduction to Case Studies 5

1.4 Thesis Roadmap 8

Chapter 2 - Literature Review 12

2.1 The Role of the 1973 Oil Crisis on the Energy Supply Mix Design Literature 12

2.2 Available Renewable Energy Supply Mix Design Methodologies 15

Chapter 3 - Methodology 24

3.1 Energy Demand Analysis 27

3.2 Potential Renewable Energy Source Assessment 31

3.3 Available Renewable Energy Conversion Technologies 69

3.4 Renewable Energy Supply Mix Design Methodology 84

3.5 Chapter Summary 93

Chapter 4 - Republic of the Maldives Case Study 95

4.1 Energy Demand Analysis – Hanimaadhoo Case Study 99

4.2 Renewable Energy Resource Assessment – Hanimaadhoo Case Study 102

4.3 Available Conversion Technology Assessment 109

4.4 Renewable Energy Supply Mix Design – Hanimaadhoo Case Study 111

4.5 Chapter Summary 114

Chapter 5 – Oxfordshire Case Study 116

5.1 County of Oxfordshire 117

5.2 Renewable Energy Supply Mix Design – Oxfordshire 151

5.3 Case Study Summary 153

5.4 Christ Church Site 155

5.5 Case Study Summary 171

Chapter 6 - Conclusion 173

Appendix A 180

Works Cited 186

Nomenclature

Symbol	Definition
4PSD	4-Parameter Single Diode
5PSD	5-Parameter Single Diode
A	Vertical Cross-sectional Area of Wind Extraction
A	Diode Quality Factor (Photovoltaic Module)
AD	Anaerobic Digestion
AI	Artificial Intelligence
ANN	Artificial Neural Networks
BMP	Bio-Methane Potential
C&I	Commercial and Industrial
CDD	Cooling Degree Days
CHP	Combined Heat and Power
C_p	Power Coefficient
COE	Cost of Energy
CRF	Capital Recovery Factor
D	Shade Length
D'	Photovoltaic Array Spacing
DC	Direct Current
$D_{deficit}$	Maximum Daily Energy Demand Deficit
$D_{surplus}$	Maximum Daily Energy Surplus
E_B	Energy Stored in a Lead-acid Battery
E_{ch}	Energy Flowing to Charge a Lead-acid Battery
E_{disch}	Energy Discharging from a Lead-acid Battery
E_G	Energy Generated from a Renewable Technology
E_L	Energy Demand used for Battery Strategy
E_{Bmax}	Maximum Energy that can be Stored in a Battery Bank
E_{Bmin}	Minimum Energy that can be Stored in a Battery Bank
$E_{batt,max}$	Maximum Energy Storage Capacity for Battery (Exhaustive Search)
$E_{charging,discharging}$	Energy used to Charge or supplied by Discharge of Battery
E_{PV}	Energy Generated by 1 PV panel
E_{Pot}	Biogas Energy Potential per mass of Biomass Feedstock
E_{site}	Energy Demand of Case Study

E_w	Potential Energy in Wind Resource
E_{wind}	Energy Generated by 1 Wind Turbine
FL	Fuzzy Logic
GA	Genetic Algorithm
G_{diesel}	Energy Generation from Diesel Generator
GDP	Gross Domestic Product
GHG	Greenhouse Gas
GIS	Geographic Information System
HDD	Heating Degree Days
HHV	Higher Heating Value
I_{mpp}	Maximum Power Point Current
I_o	Dark Saturation Current
I_{ph}	Photo-generated Current
K	Potassium
LHV	Lower Heating Value
LPSP	Loss of Power Supply Probability
MADM	Multi-Attribute Decision Making
MCA	Multi-Criteria Assessment
MCDM	Multi-Criteria Decision Making
MODM	Multi-Objective Decision Making
MPPT	Maximum Power Point Tracking
MSW	Municipal Solid Waste
M_T	Mass of Total Solids
M_{VS}	Mass of Volatile Solids
N_{batt}	Number of Battery units (Exhaustive Search)
N_{PV}	Number of PV units (Exhaustive Search)
N_{Wind}	Number of Wind Turbine units (Exhaustive Search)
N	Nitrogen
NOCT	Nominal Operating Cell Temperature
O&M	Operation and Maintenance
P_{Bio}	Potential energy content per cubic metre of biogas
P_{BMP}	Bio-methane potential per mass of Feedstock
P_t	Average Power Demand

$P_{max}^{t_i}$	Maximum value of the average power in time interval t_i maximized over the days of the year
$P_{min}^{t_i}$	Minimum value of the average power in time interval t_i maximized over the days of the year
P_{Max}	Maximum Extractable Wind Power
P_{mpp}	Maximum Power Point
P_w	Power of the Wind Resource
$P_w(V)$	Electrical Power Output of a Wind Turbine at Speed (V)
P_r	Rated Power Output of Wind Turbine
P	Phosphorous
PPA	Power Purchase Agreement
PV	Photovoltaic
R	Gas Constant
$R_{Diffuse}$	Diffuse Solar Radiation
$R_{Diffuse}$	Diffuse Radiation on a Horizontal Surface
R_{Direct}	Direct Radiation on a Horizontal Surface
R_{Global}	Global Radiation on a Horizontal Surface
$R_{Reflected}$	Reflected Radiation on a Horizontal Surface
R_s	Series Resistance of Photovoltaic Module
R_{sh}	Shunt Resistance of Photovoltaic Module
R_{Total}	Total Solar Radiation
SOC	State of Charge of Lead-acid Battery
SRC	Short Rotation Coppice
STC	Standard Testing Conditions
T_{stc}	Air Temperature at Standard Testing Conditions
T	Air Temperature
TAC	Total Annual Cost
V_{ci}	Cut-in Wind Speed of Wind Turbine
V_r	Rated Wind Speed of Wind Turbine
V_{co}	Cut-out Wind Speed of Wind Turbine
V	Wind Velocity
V_{mpp}	Maximum Power Point Voltage
V_o	Friction Velocity
V_1, V_2	Wind Speed at Height (1) and (2)
VS	Volatile Solid Content

WAB	Weighted Average Boiler Efficiency
Y	Methane Yield per unit Mass of Biomass Feedstock
a-e	Multi-Criteria Assessment Scores
c	Volumetric Ratio of Methane to Biogas
c	Building Base Load (for Climate Energy Factors of Demand)
c	Weibull Scale Parameter (for Wind Distribution Calculations)
f	Weibull Wind Speed Frequency Distribution
k	Boltzmann's Constant
h	Vertical Height of Photovoltaic Panel from Ground Level
ha	Hectare
h_1, h_2	Vertical height (1) and (2) for Wind Speed Calculation
n	Julian Day
p	Air Pressure
i	Discount Factor (for Capital Recovery Factor Calculation)
i	Number of Hours in a Day (For Average Power Analysis Calculation)
k	Weibull Shape Parameter
m	Factor of Energy Loss in a Building
m_i	Size of each Dimension of the Exhaustive Search Matrices
$m_{i,u}$	Upper Bound Number of Units
$m_{i,l}$	Lower Bound Number of Units
$m_{i,s}$	Step Change Number of Units
n	Number of Days in a year [1:365]
odt	Oven Dry Ton
q	Charge of one electron
t_i	Hours in 1 day
u	Wind Speed in Weibull Calculation
v	Terminal Voltage of Photovoltaic Module
w1-w5	Multi-Criteria Assessment Weightings
w	Weighting of Multi-Criteria Assessment Score
z_o	Surface Roughness
Greeks	
a	Altitude Angle of the Sun (for Solar Positioning Calculations)
β	Inclination Angle of a Solar Collector

δ	Solar Declination
δ	Solar Declination
η_{gas}	Biomass to Syngas Conversion Efficiency
η_{inv}	Inverter Efficiency
$\eta_{batt,in}$	Charging Efficiency of Lead-Acid Battery
$\eta_{batt,out}$	Discharging Efficiency of Lead-Acid Battery
η_{wab}	Weighted Average Boiler Efficiency
ρ	Ground Reflectivity
ρ	Air Density (For Wind Resource Potential Calculation)
φ	Geographical Latitude
ψ	Sun Azimuth Angle
ω	Hour Angle
ω_o	Minimum of ω_s and ω_s'
ω_s	Sunrise Hour Angle
ω_s'	Sunrise Hour Angle Above an nclined Plane

Chapter 1 - Introduction

This thesis explores the development of a methodology that can be implemented by decision makers investigating the approach to carbon neutrality using renewable energy resources to meet demand and create a sustainable supply mix.

Climate change is strengthened and enhanced by the excessive presence of Green House Gases (GHG) in the atmosphere to which conventional fossil fuel power generation is a major contributor (Hester & Harrison, 1999). Climate change is broadly defined as "a change of climate which is attributed directly or indirectly to human activity that alters the composition of the global atmosphere and which is in addition to natural climate variability observed over comparable time periods" (UNFCCC, 1992). The main characteristics are: the increase in average global temperatures; the melting of glaciers and ice caps causing a rise in sea levels; a change in cloud cover; precipitation; the presence of extreme weather conditions; and the increase in ocean temperatures and acidity (UNFCCC, 2007). The global climate is normally determined by the thermal equilibrium between the solar radiation inflow, the trapping of a part of this heat by the "natural greenhouse gas effect" and the re-radiation of heat into space. Since the industrial revolution, the increasing energy demand and fossil fuel combustion have caused a subsequent increase in atmospheric GHG volumes above accepted levels. The industrialization of agriculture has caused larger volumes of methane emissions from livestock as well as large-scale deforestation and land usage change that also contribute significantly to climate change (Josephson, 2002). The diagram, in Figure below, shows a complete breakdown of the global GHG emissions sources (Herzog, 2005).

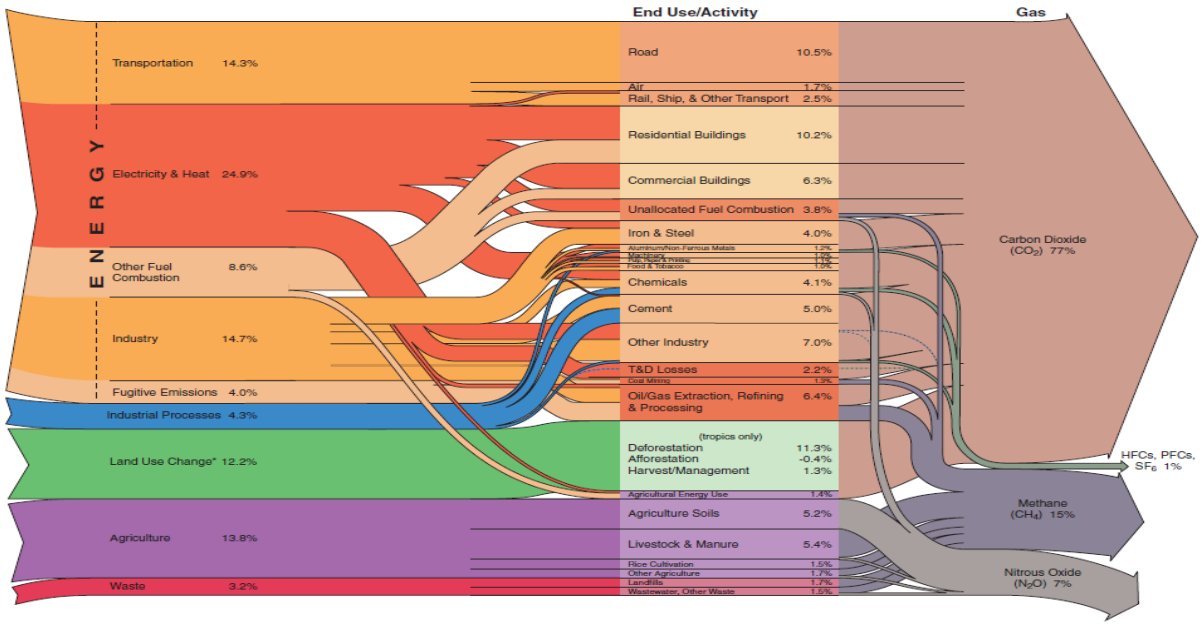


Figure 1-1 Sankey Diagram of the Global GHG Emissions Sources (Source: (Herzog, 2005))

The sources listed above are anthropogenic effects that cause higher levels of solar radiation to become trapped in the atmosphere, thus increasing the global warming risk (Jepma & Munasinghe, 1998). Annual GHG emissions from the energy sector continue to increase on a global scale since the combustion of fossil fuels is the dominant process for power generation (BP, 2012a). Since the mid-19th century, this global dependence on fossil fuels has led to an estimated emission of more than 1100 $GtCO_2$ into the atmosphere (Metz et al., 2007).

This association can be seen both on a national level, where large-scale systems export energy on the national grid, and on smaller local scale systems where generators are used to power local communities and industrial requirements.

1.1 Metrics Used in the Decision-Making Process of the Supply Mix Design

The United Nations World Commission on Environment and Development was mandated in 1987 to re-examine environmental issues and propose an innovative and realistic framework to deal with them. Due to the strong interlinking of these development aspects, the main focus of attention was on food security, area of population, human settlement, energy and industry. One of the most significant findings of this study was that sustainability could be defined as the economic, environmental and social metrics of a proposed development solution. This report is also referred to as the Brundtland Report (UNWCED, 1987).

The main drive behind this study is to propose a renewable energy supply mix that can substitute conventional systems at a reduced or zero operational carbon dioxide emissions level, both for newly built and retrofit installations on a local and national level. The assessment of the proposed solution is based on the aforementioned economic and environmental metrics of the Brundtland Report. The social aspects have not been included as they are considered out of the scope of this study.

The economic metric is critical because every user will be financially impacted by an increasing cost of energy. As energy markets start to deregulate, there is greater competition between suppliers that leads to reduced profit margins. Therefore, stakeholders pay a great deal of attention to the economic aspect which is one of the main drivers of decision-making in the energy industry today.

Conventional energy generation plants have a high capital cost and high operational cost mainly dictated by fuel prices. Renewable energy generation plants also demonstrate a high capital cost but typically have a low operational cost due to freely available resources such as solar and wind energy. Dedicated biofuels typically have a related fuel cost that, as shown in Chapter 3, is minimal in comparison to conventional oil and natural gas prices. To compare the two types of generation, an economic indicator is needed that adequately captures the capital and operational costs applicable to both existing and new systems in an unbiased way. It will be shown, in Chapter 3, that the total annual cost is the best indicator to use as part of the economic metric assessment. This cost is a summation of the annualized capital cost and annual operation and maintenance cost incurred by a supply mix. The annualized capital cost is the equivalent capital cost calculated by discounting the one-off capital cost at the defined discount rate and lifetime for the site under investigation. The main benefit of using this cost is twofold. Firstly it considers the intensive initial capital cost over the project lifetime, thereby examining the effect of this cost over the time period within which it is utilized, and, secondly, it can compare the effective weighting of the same capital cost between two or more sites that may have different discount rate or lifetime requirements. This can make an identical supply mix more or less competitive between sites. The annual operation and maintenance cost is considered as the annual cost required to operate the supply mix and maintain it at the standard required to achieve the estimated lifetime and energy generation performance. The cost of conventional energy, if any, to meet demand deficit is also included in this variable. This has the benefit of including the renewable energy supplied directly to demand at the time of requirement in the overall

assessment. The higher the renewable energy to demand, the lower the conventional energy generation cost required.

To assess the environmental metric, a range of indicators, such as the equivalent carbon dioxide emissions reduction, land usage, water usage, waste generation, resource consumption and visual impacts, can be used. The reduction in carbon dioxide emissions is used as the indicator of the environmental metric because it can compare the proportion of all avoided types of green house gas emissions due to the introduction of a renewable energy supply mix. Furthermore, this indicator can account for the specific fuel type(s) powering a site and investigate the magnitude of effect the renewable energy element will have to match equivalent carbon dioxide emissions. The biomass assessment addresses the land usage factor even though it is not used explicitly in the final metric.

Green house gases that contribute to climate change include carbon dioxide, methane and nitrous oxide. These emissions are typically expressed as equivalent carbon dioxide emissions by accounting for the global warming potential, thus, allowing the real contribution of each gas to be compared (WorldBank, 2010). This study only considers the operational carbon dioxide emissions, and not the emissions in the material extraction, sourcing and technology manufacturing process. The emissions reduction is calculated by first finding the renewable energy generated to meet demand. Energy that is oversupplied to demand, due to a mismatch between time of generation and time of usage, is not considered in the emissions reduction calculation. This is because the scope of this study constrains the boundaries of the case study to its internal demand profile only. The operational emissions of the proposed supply mix, which are dependent on the fuel type used to power demand, are then compared against the carbon dioxide currently emitted by the site.

The economic and environmental indicators are then examined simultaneously to identify the renewable energy supply mix to meet demand.

1.2 Statistical Characterization of Renewable Energy Resources

Renewable energy resources can be statistically categorized by either a determinative, dispatchable or stochastic nature. This statistical characterization is required because the time of availability of each resource is a main factor in matching the time of demand usage on a temporal scale such as that of the diurnal and seasonal.

The appropriate selection of a resource, and the balancing of resources from each category, is required to maximize the direct conversion of the potential resource to useful energy and meet demand on a time scale ranging from diurnal to seasonal. One type of renewable energy resource is considered as an example of each statistical category. Each category represents how easy it is for the operator to predict, ahead of time, if the resource will be available or not.

A determinative resource is defined as a resource that has a predictable magnitude and diurnal and seasonal profile over the annual time scale. The randomness involved in resource availability is assumed as minimal and reliable forecasting can be made at least on the day-ahead time scale. This study assumes that solar energy is a determinative resource. Although, the short term intraday forecasting of solar energy can be impaired by cloud coverage, the variability is negligible on a seasonal and annual scale. Furthermore, the knowledge that solar energy is unavailable during night hours and peaks at midday enhances the element of statistical predictability. A dispatchable resource is defined as a resource that can provide spatial and temporal energy storage. This provides the operator with guaranteed control over the supply availability and magnitude on all time scales. This study assumes that biomass energy is a dispatchable resource.

A stochastic resource is defined as a resource that has an intermittent nature and can be assessed using probability distribution functions. There is minimal reliance on accurate diurnal availability patterns and it is, therefore, a resource type that is typically used to complement other renewable resources in a supply mix. This study assumes that wind energy is a stochastic resource.

Moving from dispatchable resource reliance to a determinative and stochastic resource creates an increased energy storage requirement. This will be shown by the lead-acid battery at Hanimaadhoo, in Chapter 4, and in the form of energy crops as an inter-seasonal storage at Christ Church in Chapter 5.

1.3 Introduction to Case Studies

The use of case studies is required to test the implementation and output of the renewable energy supply mix methodology developed in this study. The selection of the case studies used has been conducted using the four main requirements listed below.

- The case study must be a system that can be easily defined in terms of its geographical and administrative boundaries
- There must be a reasonably well known energy demand available
- The case studies must be found in different geographic locations so that different types of resources and existing supply mix characteristics can be considered
- A need to introduce renewable energy sources to meet demand and reduce carbon dioxide emissions must be defined by stakeholders

In 2008, the Maldivian government announced a countrywide carbon neutrality target to be achieved by 2020 (PresidentOffice, 2009). To accomplish this, a range of measures, including the installation of renewable energy technologies and energy efficiency techniques, must be implemented. This study examines the renewable energy technology aspect of achieving these goals on the island of Hanimaadhoo, as an example of an "outer island" site. This island has a population of 1184 and is populated only by locals and is not used as a tourist destination (MPND, 2007). The average of the daily peak demand is 220 kW_e and the annual consumption is 1.5 GWh_e that is currently met by 2 x 160 kW_e and 1 x 200 kW_e diesel generators (STELCO, 2009).

The main issue faced by this case study is the fact that, as it is a relatively small island, it is heavily constrained in terms of available space for renewable energy installations. This constraint also means that a renewable energy resource may exist in abundance around the island but there is no available land to utilize it physically.

The second case study investigates the potential of renewable energy installations in the county of Oxfordshire, as a representative section of the UK. Christ Church is a college of the University of Oxford and is located within the county of Oxfordshire. This site is examined in further detail as a model site with a commercial and residential demand mix. Christ Church has committed to reducing its carbon emissions by 60 % by 2050 (Harris, 2008).

The county of Oxfordshire is located in the southeast region of England and has a population of 650,000 occupying 260,000 households. It is an important academic center and tourist attraction in the region. The average daily electrical peak demand is 645 MW_e and the annual consumption is 3500 GWh_e which is currently met by connection to the national grid. Its economic contribution in 2009 was £14.2 billion representing approximately 8 % of the south-east region's gross value added together (OCC, 2012). There

are five administrative districts in the county namely, Cherwell, Oxford, South Oxfordshire, Vale of White Horse and West Oxfordshire (OCC, 2012). The main stakeholder in this case study is the Low Carbon Hub (LCH), a non-governmental organization that is committed to working towards lower carbon emissions across Oxfordshire by developing energy efficiency and renewable energy projects for the benefit of local communities (LCH, 2013). The LCH has been involved in examining the decommissioning of the Didcot A power station in 2013 and what the potential renewable energy alternatives to a complete fossil fuel replacement are.

The Christ Church site is located in Oxford City Centre. The population is comprised of academic and administrative staff working throughout normal office hours and a student population working and living on-site. The number of academic staff is 130 (ChristChurch, 2013). The total student population is 600 (ChristChurch, 2013a). The average daily electrical peak demand is 310 kW_e and the annual consumption is 3.3 GWh_e which is currently met by importing electricity from the national grid via two substations that distribute energy to the north and south parts of the site. The grid also powers a large element of night storage heating at the north substation. The site imports gas from the national gas grid that provides the remaining space heating, water heating and kitchen cooking requirements. There are two main constraints faced in the attempt to install renewable energy technologies at the site. Firstly, as the site is located in Oxford City Centre, there is a tight geographical boundary in terms of infrastructure development due to the minimal space available. Secondly, as Christ Church is comprised of a number of listed buildings, such as the Tom Quadrangle (Grade I) and the Blue Boar Quadrangle (Grade II) (Goodge, 2006), the site is further constrained as to the real options available for physical resource utilization.

The selection of the aforementioned case studies allows the examination of the methodology on large and localized scale systems operating in tropical and temperate climates. They allow a detailed investigation of the implementation of renewable energy technologies in economically developed and developing parts of the world, which experience dissimilar resource patterns and energy demand characteristics in terms of intensity and time of usage.

1.4 Thesis Roadmap

A review is conducted, in Chapter 2, to examine the renewable energy supply mix design methodologies currently available in the literature. This review focuses on the three main sections of the overall methodology developed in this study. The first section examines the available assessment methodologies relating to biomass, solar and wind energy resources in terms of the magnitude and availability of each. The second section examines the conversion technologies of each resource relating to the technical modelling, in order to estimate useful energy generated from an input resource. Combined Heat and Power (CHP) is considered for the biomass energy conversion technology, Photovoltaic (PV) technology is considered for the solar converter and wind turbines are considered for wind. The final section examines the literature relating to the methodologies developed to design renewable energy supply mixes. The literature is investigated in terms of the core functionalities currently available, identified as the mathematical optimization, multi-criteria decision making and dedicated software.

Since the main aim is to design a supply mix to meet demand, a series of analyses techniques is presented to assess these factors and characteristics of demand. These analyses aim to consider the temporal, climatic and growth factors of demand.

The potential renewable energy resource assessment for the different types of biomass, solar and wind energy is conducted in terms of the resource availability and magnitude and the economic and environmental indicators.

The methodology developed in this study, using a Geographic Information Systems (GIS) approach, to assess the potential solar energy on rooftop planes in an urban area, is presented and tested. The main input requirement of this methodology is a GIS map of the urban area. The main outputs are the total horizontal surface area suitable for solar installations and the estimated utilizable area for PV systems after accounting for optimum tilt and orientation angles of the array. Finally, the maximum total installed capacity of PV installations is calculated with a GIS output map of the specific houses suitable to assess the geographic distribution of the rooftop systems.

The animal waste, energy crop and refuse biomass types are examined in terms of their potential energy assessment content normalized per unit mass of each. An economic and environmental analysis of the preparation of each type to a usable form is then conducted.

The energy crop type of biomass is grown specifically for its utilization in a renewable energy supply mix, unlike animal waste or refuse that is a biomass originating as a by-product of other activities. Due to the wide range of available species, as well as the advantages and disadvantages of each, a Multi-Criteria Assessment (MCA) methodology is developed to identify the optimum species with respect to the economic and environmental decision-making indicators. The MCA is developed for biomass to be converted into solid biomass systems or anaerobic digestion systems for biogas generation.

Wind energy is assessed by the Weibull distribution method, a statistical technique used to estimate the probability of a wind speed occurring, thereby, identifying the potential wind energy content at a site. This method is widely used both in academia and industry.

The modelling techniques of the conversion technologies used in the final supply mix design for each resource are presented in detail. The economic analysis is conducted in terms of the capital and annual Operation and Maintenance (O&M) costs to determine the total annual cost incurred per unit of each technology. The environmental analysis is conducted in terms of the avoided annual carbon dioxide emissions per unit of each technology.

The construction and development of the final renewable energy supply mix methodology, based on the constrained exhaustive search algorithm, is then presented. Since this algorithm is associated with a large search space that is computationally expensive, this study proposes a search space minimization technique tailored to the design of a renewable energy supply mix to meet demand. This is required for the technologies operating with the determinative and stochastic resources that cannot be energized at the operators' request. Each technology is considered independently with a conventional power supply to identify the number of units that cannot further reduce the conventional power requirement. At that specific unit number, the search space is considered as a minimum and the constrained exhaustive search algorithm can be implemented at a higher computational efficiency. The total annual cost and emissions reduction indicators of a renewable energy supply mix, commencing at zero units and saturating at the search space maxima, is then conducted. To determine the optimum capacity per technology, the Lagrangian Multipliers of the cost and emissions reduction indicators are calculated for each step change interval unit. A test case scenario is presented, using constructed resource and demand data to illustrate the functionality of the methodology developed.

Once the methodology developed has been presented in detail, it is implemented, in Chapter 4, on the island of Hanimaadhoo in the Republic of the Maldives. The renewable energy resource assessment is conducted for the solar and wind resources. An initial overview of the biomass availability on the island shows an insignificant energy potential that is not further considered. Although the wind energy shows a poor potential, its maximum availability is present when the solar energy is at a minimum on a seasonal scale and, therefore, further investigation is conducted for the possibility of using the wind to complement solar. The final renewable energy supply mix design is then presented for a PV, wind turbine, lead-acid battery storage and a PV, lead-acid battery supply mix. This chapter presents the island's approach to carbon neutrality using the economic and environmental indicators in the decision-making process.

Chapter 5 examines the implementation of a renewable energy supply mix in the county of Oxfordshire and Christ Church as a model site within the county. The potential energy assessment is conducted for biomass and rooftop solar energy. The results of the wind energy assessment, conducted by BVG Associates, as part of the "Oxfordshire Capacity Study", are presented in this chapter.

To examine the biomass assessment, a reallocation of land area in the county is first presented using the results of the collaboration with LandShare, a social enterprise established to investigate alternative options to the way land and resources are managed. This collaboration has identified two land usage strategies, the "Energy Focus" that maximizes land usage for energy purposes and the "Food Focus" that maximizes land usage for feeding purposes. The energy crop MCA is then conducted for the "Food Focus" scenario to identify the optimum species. To assess the rooftop solar potential in the county, the towns of Abingdon, Banbury, Bicester and Oxford are examined using the GIS methodology developed in Chapter 3. The results are then extrapolated to find the entire rooftop potential in Oxfordshire. The conversion technologies, utilizing the determined potential energy content of the aforementioned resources in the county, are then examined under both land usage scenarios.

The renewable energy supply mix methodology is then implemented at Christ Church, as a model site within Oxfordshire. The Christ Church site is examined first in terms of the energy demand analysis, potential resource and available conversion technology assessment process developed in this study. As there is also a thermal energy demand, this, too, is examined using the same factors. The resources considered are solar energy and energy crop biomass. The optimum biomass species for solid and biogas

applications is determined using the MCA analysis. Wind energy is not examined due to the very low resource potential on site. The constrained exhaustive search algorithm is implemented on the site's resource and demand profiles to develop the final renewable energy supply mix based on the total annual cost and emissions reduction indicators.

Chapter 2 - Literature Review

The main aim of this study is to design a renewable energy supply mix to meet the energy demand at a site under investigation. The supply mix is separated into two components; the potential renewable energy resource and the available conversion technology. The diagram, in Figure 2-1 below, illustrates the main supply mixes that could be constructed from the biomass, solar and wind resources investigated in this study.

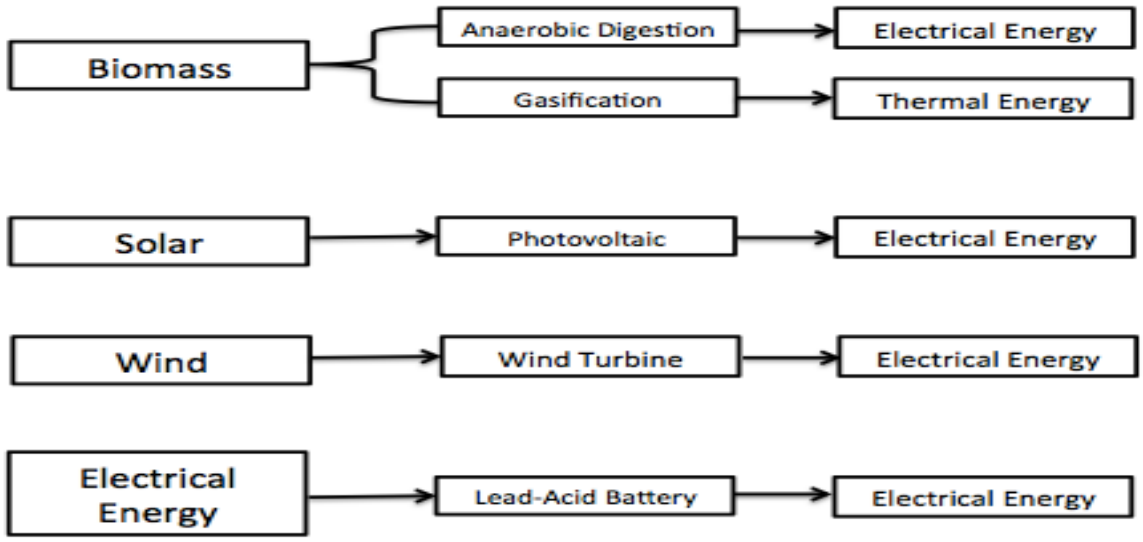


Figure 2-1 Renewable Energy Supply Mix Pathways Examined

A review of the energy supply mix literature identifies the current gaps in knowledge and the suitability of current methods for this study.

This chapter aims to address the following topics of the available literature:

1) *What role did the 1973 oil crisis have on the energy supply mix design?*
2) *What are the key techniques and methodologies used by authors in this field?*
3) *What are the suitable parameters for the assessment of a supply mix?*

2.1 The Role of the 1973 Oil Crisis on the Energy Supply Mix Design Literature

In October 1973, members of the Organization of Arab Petroleum Exporting Countries known as the OAPEC declared an embargo on oil that led to a shortage of availability in energy supply and the quadrupling of world oil prices. This in turn caused an unprecedented escalation of energy prices accompanied by a major economic shock (Yergin, 1991). The development of renewable energy has been

motivated by diverse drivers, which have evolved over time. The early demonstration programmes of the 1970s were mainly motivated by the 1973 crisis. At the time, governments and stakeholders realized that their economies were excessively dependent on imported fuels with unpredictable costs. This section examines the literature in the energy supply mix design field in the pre and post oil crisis years to understand the effect this event had on objectives, assessment indicators and techniques used.

2.1.1 Pre 1973 Investigation of Renewable Energy Resources

Golding (1958), examined the supply of energy to improve living conditions and assist in the development of developing regions. The author considered the wind, solar, water and vegetable waste resources in comparison to conventional diesel energy as well as animal power as a main element of energy provision in remote developing areas. The aim of this study was to attempt to answer two questions. The first question was to identify the means of energy provision in terms of conventional and renewable energy sources. The second question was in relation to planning the supply mix and what sort of behavioural aspects may be required by users to maximize the energy service provided. The author examined specific time of day energy usage requirements against time of day energy supply per technology in his attempt to develop a supply mix design methodology. Emphasis was given on the cost of energy (£/kWh) per technology and for a combination of technologies. A summary of the author's conclusions is shown in Table 2-1 below (Golding, 1958).

Table 2-1 Supply Technologies and Demand Characteristics (Golding, 1958)

Types of Equipment	Probable Cost of Energy (pence/kWh)	Load to be Supplied	Timing Requirements	Annual Electric Consumption (kWh)	Annual Cost of Energy (£ Sterling)
Wind Generator	2.2	Irrigation, Pumping, Agriculture	Random Daytime Precise time (night)	65,000	600
Water Pumping Windmills	8	Domestic Water Pumping	Random	3,000	100
Solar Collectors (Flat-Plate)	0.85	Water & space heating, refrigeration distillation	Random	56,400	200

Concentrating Solar Collectors	0.4	Cooking	Precise times in the day Random	15,000	25
Solar Pumping Engine	8.6	Water pumping	Random	2,500	90
Steam Engine	6	Agriculture, stand-by power	Stand-by	10,000	250
Electric Battery	-	Lighting and small loads	Precise times	-	200

The Modele des Trois Plans uses linear programming to determine the optimal technology mix based on a minimum cost function and is constrained to supply meeting demand at all times. The cost function is calculated as the sum of the annualized capital cost, operation and maintenance and fuel cost requirements (Boiteux & Bessiere, 1961). The methodology was mainly used by electric utilities for strategy development.

2.1.2 Post 1973 Investigation of Renewable Energy Resources

On the national level, Denmark, which currently has the largest amount of installed wind capacity globally, started the commercialization of wind technology after the 1973 crisis. Up until then, the Danish electricity industry was highly dependent on oil, with over 90 % of supply based on imported oil. This crisis stimulated the country to move from oil to coal for electricity generation. Furthermore, the national energy policy imposed taxes on electricity prices that were then used to support research and development for renewable energy (IRENA, 2012).

The Brookhaven model uses linear programming to optimize the energy supply mix created for the American energy system. The independent objectives are cost, fuel consumption and environmental considerations. Since the development of this model started before the 1973 oil crisis, its main drawback is that it assumes that an energy shortage can be met using low cost fuel imports, which, in hindsight, has proven to not be the case (Hoffman, 1973). Schweizer (1974), developed an energy supply mix methodology to determine the optimum fuel mix based on environmental performance to be used by electricity utilities and industrial complexes with relatively high energy demands. This study was driven by the oil crisis and the introduction of the Air Quality Act of 1967 and the Clean Air Act of 1970 (Schweizer, 1974). Quareshi (1984), initiated his work on the techno-economic analysis of energy modelling before the oil crisis and was initially only concerned with investigating oil and gas. As it is an

open-ended model, the renewable energy element was added in light of the crisis. This model is mainly concerned with investigating the Cost of Energy (COE) of solar PV and wind technologies, defined as the sum of the annualized capital cost and operation and maintenance cost per unit of energy generated. Since PV and wind were relatively young technologies at the time, the author's main aim was to establish at which price per barrel of oil the renewables would be competitive on a COE based approach (Quareshi, 1984). The results showed that a site with a mean wind speed of 8 m/s could compete with oil generating technologies at a price of $ 18 per barrel1.

A review of the literature pre and post oil crisis shows an introduction of energy security in stakeholders' objectives by shifting from oil to coal and natural gas as primary fuels and the increasing attention and research conducted on renewable energy sources. Furthermore, the crisis established that future electricity supply mix planning, that aimed to minimize a cost function, accounted for the competiveness of renewable energy sources due to the zero fuel cost involved in these technologies.

2.2 Available Renewable Energy Supply Mix Design Methodologies

This section presents a review of the available literature related to renewable energy supply mix design. The methodologies identified are separated into three types based on their functional characteristics listed below:

1) Mathematical Optimization
2) Multi-Criteria Assessment (MCA) Analysis
3) Artificial Intelligence (AI)

The following sub-sections are dedicated to reviewing the literature available on each type of methodology identified above.

2.2.1 Mathematical Optimization

This sub-section examines the mathematical optimizations available in the supply mix design literature. An optimization is a mathematical tool used to maximize or minimize an objective function, such as cost, in terms of the process variables under a set of constraints (King & Mody, 2010). The objective functions found in supply mix design are single and multi-objectives.

1 The price of oil in 1984 was $ 26 per barrel (EIA, 2013). This is equivalent to $ 56 in 2013

A summary of the literature on mathematical optimizations for renewable energy supply mix design is shown, in Table 2-2 below, per author and technologies included in the processes.

Table 2-2 Technologies Examined in the Renewable Energy Supply Mix Optimization Literature

Author(s)	PV/Diesel/ Battery	PV/Wind/ Battery	PV/Wind/Diesel/Battery	PV/Wind/Diesel/Battery/Biomass
(Borowy, 1996)		✓		
(Chedid & Saliba, 1996)			✓	
(El-Hefnawi, 1998)	✓			
(Protogeropoulos et al., 1997)		✓		
(Ashok, 2007)			+ Micro-Hydro	
(Koroneos et al., 2004)				+ Geothermal
(Chedid et al., 2005)			✓	
(Yang et al., 2007)			✓	
(Diaf et al., 2007)		✓		
HOMER ENERGY			+ Hydro	

Borowy (1996), used linear programming to develop a minimum capital cost function for a wind, solar PV and battery storage system under a Loss of Power Supply Probability (LPSP) constraint. This constraint is defined as the long-term average load proportion not powered by the stand-alone hybrid system. Therefore, a LPSP of 0 ensures continuous supply of all the demand and a LPSP of 1 means that the demand is never met. The LPSP is a user-defined constraint and a specific probability is selected based on operational strategy (Borowy, 1996). The main limitation identified in this methodology is the use of the capital cost function. The optimization converges at the lowest capital cost not accounting for the longer-term operational costs that are also incurred, and, therefore, a non-biased comparison between a conventional and renewable power supply cannot be made. Furthermore, since there is no backup supply in the model, a maximum LPSP may exist due to the availability of the resource to meet demand. If this maximum is exceeded, a LPSP input by the user can then result in the optimization diverging.

Therefore, a trial and error approach is initially required by the user to identify this LPSP that is expected to require computational and time resource.

Chedid & Saliba (1996), developed a linear program to minimize the Cost of Energy (COE) of a PV/Wind/Battery/Diesel supply mix at an hourly resolution using recorded resource and demand data for one year. This method functions with one constraint, namely, that at all time intervals, the supply must equal the demand (Chedid & Saliba, 1996). By only minimizing the COE and not constraining the optimization to a renewables contribution or emissions reduction, the optimization is expected to converge to the lowest cost solution, which is typically diesel generation. This is true apart from geographically remote case studies with a high resource potential that are expected to incur a high diesel and relatively low renewables COE. Therefore, the main limitation of this method is its applicability and function in different case studies with low and high resource potentials.

El-Hefnawi (1998), used linear programming to develop a system sizing program to minimize the cost of a PV/Diesel/Battery hybrid supply mix. This method is divided into 3 steps. The first step is the selection of a battery capacity that is capable of meeting demand over the largest period of time without any sunshine or during the night. The second step is the addition of the maximum discharge depth of the battery under expected seasonal solar fluctuations. The third step is the selection of the array required, proposed as sizing for the average daily demand (El-Hefnawi, 1998). The main limitation identified for this method is that, even though there is sufficient battery capacity to meet demand during the minimum solar time, it is unclear as to how the battery is capable of discharging. This is because the authors have not allowed for a renewables surplus to charge the battery during the maximum solar period. Therefore, it is expected that this method may oversize the battery system as there is a pre-set upper bound constraint set on the PV array.

Protogeropoulos et al (1997), developed a techno-economic analysis to optimally size a Wind/PV/Battery hybrid system. The authors defined the autonomy level as the main driver behind decision-making and implemented this method in a case study in Cardiff, Wales, first using the “worst-case” renewables resource and then the “average” resource. The limitation of this method is that it uses an autonomy level as a matrix to the system’s performance and only considers the resource magnitude as a “worst-case’ and “average”. The respective demand data is not presented or included in the algorithm. There may be cases

where the minimum resource coincides with a minimum demand and, thus, the resource-demand difference could have been considered as a "worst-case" and "average" scenario to overcome this issue (Protogeropoulos et al., 1997).

Ashok (2007), proposed a non-linear constrained optimization technique for a PV/Wind/Micro-Hydro/Diesel/Battery supply mix for a rural community based hybrid system. The main objective used by the author was a minimization of the COE, constrained to meet the hourly demand for an annual period (Ashok, 2007). The main advantage of this method is that the author only accounted for the energy generated that meets the demand in the COE calculations and not the surplus energy that is dumped. Therefore, a COE representing the demand is expressed so that fair comparisons can be made between the proposed supply mix and other solutions.

Koroneos et al (2004), developed a multi-objective function for a wind, solar PV, biomass, geothermal and conventional energy supply mix. A linear program was developed to minimize the cost per unit energy of the total mix whilst simultaneously minimizing the environmental impact factor derived from the system's gross emissions (Koroneos et al., 2004). A review of this method concludes that it is a useful high-level approach to the supply mix design. However, since this method functions with the annual time resolution, caution must be shown to ensure that there is a good match between resource availability and demand. If this is not the case, this optimization may converge to a supply mix not truly representative of the optimum.

Chedid et al (2005), developed a wind, solar PV, battery storage and diesel supply mix methodology using a multi-objective linear program. The functions used are the maximization of emissions reduction and minimization of cost. To model the demand profile, this model assigns a light load period to the first half of the day and a peak load period to the second part of the day. The battery is assumed to charge in the light load and discharge in the dark load (Chedid et al., 2005). Due to the assignment of two demand magnitudes per day, this model is unable to recognize demand spikes and troughs that occur and so it is vulnerable to demand dynamics. Therefore, this model is most suited to case studies with predictable demand profiles due to constant loads such as airports and hospitals.

Yang et al (2007), developed a Wind/PV/Battery/Diesel hybrid model to optimize the capacity sizes of each technological component of the supply mix. This model is comprised of three parts: 1) The hybrid

systems components model; 2) The LPSP model; and 3) The COE model. The system sizes that meet the LPSP criteria, determined by the user, progress to a COE calculation to identify the hybrid capacity that meets the LPSP and minimizes the COE of the system (Yang et al., 2007). The main limitation identified in this method is that the optimization considers every technology per kW of installed capacity as opposed to the number of units. Therefore, the results obtained represent a total installed capacity per technology that may not be physically available on the market.

Diaf et al (2007), developed a minimum (COE) function for a wind, solar PV and battery storage supply mix. The COE is expressed as the annualized cost of generating the entire system output (Diaf et al., 2007). The main constraint used is a user defined LPSP to establish that demand can be met for a certain proportion of the year. Even though the COE is considered as a useful energy and cost indicator, calculating it using the entire energy generated, and not the energy generated that meets demand, does not allow for the amount of energy oversupplying demand which is "wasted". HOMER, available for free, is the second most downloaded energy related software (Connollya et al., 2010). It functions with a bottom-up approach simulating the mainstream renewable energy sources and individual unit capacities selected down to the 1-minute time resolution. HOMER performs an Exhaustive Search on all the possible capacity options and progresses to the second stage of the process with only the feasible capacity options that can meet demand. After running the simulations, the software ranks the feasible cases in order of net present cost. This cost is defined as the present value of the capital, operation and maintenance and fuel costs (NREL, 2011). The user benefits from this software as it is freely available and has a user friendly interface that requires minimal training to handle. The selection of the net present cost as the optimization objective is the main advantage of this software, as this cost will fairly account for the different capital and operation and maintenance cost between technologies, as well as the conventional fuel requirement to meet demand. The main disadvantage is that the only constraint in the system is that supply must meet demand. This means that the optimization process does not have any specific requirement in a minimum renewables installation or emission reduction. Where conventional fuel is available at relatively low cost, the optimization will select conventional power and not include a renewable element to the supply mix.

2.2.2 Multi-Criteria Assessment Analysis

This sub-section examines the supply mix design literature that uses Multi-Criteria Decision Making

(MCDM) as the main functionality of the methodology developed. MCDM is a branch of operational research and a field of decision-making. MCDM can work with both qualitative and quantitative criteria and analyze possible conflict in decision making (Pohekar & Ramachandran, 2004). In general, MCDM can be categorized as Multi-Objective Decision Making (MODM) and Multi-Attribute Decision Making (MADM) (Climaco, 1997). MODM characterizes the problem by the existence of numerous and competitive objects that must be scored against a set of constraints (Diakaki et al., 2004). MADM evaluates a set of alternative solutions against the criteria and is one of the most popular MCDM categories (Wang, 2010). The literature on MCDM in the renewable energy field is separated into four categories namely: 1) Renewable Energy Planning and Policy; 2) Renewable Energy Evaluation; 3) Project Selection; and 4) Environmental main overall objectives. The Project Selection category is the most relevant to this study and this review is consequently constrained to this area only.

Begic and Afgan (2007), evaluated the options of power systems for Bosnia-Herzegovina using a multi-criteria sustainability assessment framework in order to investigate the possible solutions for selecting the new technological options for building supply capacity with conventional and renewable energy sources (Begic & Afgan, 2007). This methodology uses indicators criteria that are evaluated quantitatively. These are the resource, economic, environmental and social indicators. The resource indicator is assessed using a mass per unit of potential energy sub-indicator. The economic indicator is assessed using the total investment and cost of energy sub-indicator. The environmental indicator is assessed using a GHG emissions sub-indicator and the social indicator is assessed using a job and workforce-generated sub-indicator. A weighting coefficient is then introduced to prioritize the output solution based on a selection of the aforementioned indicators. The main advantage of this methodology is that it can include multiple indicators in the assessment from any type of source, such as environmental or economic. Also, although this particular publication does not demonstrate this, the methodology can be easily adapted to include qualitative indicators such as, for example, the social acceptance of each technology providing a more complete assessment of the examined options. The main disadvantage is that the examined options are proposed based on meeting an annual energy demand only. Therefore, the temporal factor of demand that may provide supply deficits due to supply / demand mismatches on the intraday or seasonal scale is not examined. Also, this methodology is unable to cope with the examination of numerous technologies operating in the supply mix. Cherni et al (2007), investigated the application of a multi-criteria decision

support system methodology to identify the optimal technologies to be used in rural Columbia (Cherni et al., 2007).

Kaya & Kahramanb (2010), used multi-criteria decision making to establish the most favourable renewable energy technologies in Istanbul and the most suitable areas that can accommodate each of these technologies (Kaya & Kahramanb, 2010).

Evans et al (2009), developed an MCA analysis for the selection of technologies for a renewable energy supply mix. This analysis identified seven sustainability indicators to categorize the wind, solar PV, hydro and geothermal technologies for global conditions. These indicators are, namely, the cost of energy, operational emissions, availability of technology, conversion efficiency, land demand, water consumption and social acceptance (Evans et al., 2009). This methodology can be adapted to particular case studies attempting to identify which technologies should be considered in the supply mix design and does not specifically dictate the optimum supply mix in terms of installed capacity and operational strategy.

A similar approach was taken by Tzeng et al (1992), who attempted to construct an MCA that functions with a range of technological, economic, societal and environmental criteria. This study aims to identify the optimum technologies to be used in a new energy supply mix for Taiwan and scored the above criteria using qualitative data (Tzeng et al., 1992). Similarly to Evans et al (2009), referred to above and common across MCA for supply mix design, this approach can be adopted to identify the favourable technologies to be used in specific resource and demand cases. The output technologies must be further examined to establish the capacities and specific criteria performance.

Afgan & Carvalho (2002), developed an MCA using a set of predetermined sustainability indicators, namely the conversion efficiency, installation cost, cost of electricity, emissions factor and land area requirement. The aim of this MCA is to assess a set of conventional and renewable technologies to be used in the development of a new power plant. The weightings of the MCA were then alternated per indicator to examine the change in technological preference with respect to specific user and site requirements (Afgan & Carvalho, 2002).

Due to the numerous criteria, environmental conditions and constraints that need to be considered simultaneously, project selection is a complex decision-making procedure that must account for all of the

aforementioned conditions and constraints whilst obeying the user's requirements. Therefore, MCDM is a powerful tool that can be used in this field to identify sites and technologies for renewable installations. The main limitation in the nature of the aim of this thesis is that the supply mix capacity can only be considered as an input in this methodology and not an output. The appropriate supply mix is, therefore, selected from a range of possible options that must be initially determined for the methodology to function.

2.2.3 Artificial Intelligence

This sub-section examines the Artificial Intelligence methodologies available in the supply mix design literature. AI can be applied to computer systems in order to perform more complicated tasks than straight programming. AI is comprised of branches including, but not restricted to, Genetic Algorithms (GA), Artificial Neural Networks (ANN) and Fuzzy Logic (FL) as well as hybrid approaches that are combinations of the aforementioned branches (Mellita et al., 2009). AI has been increasingly noted in the renewable energy literature as a functional methodology in this field.

Koutroulis et al (2006), develop a GA methodology for designing a solar PV, wind and battery supply mix by selection of available commercial equipment and optimum unit number. This methodology minimizes the total annual cost of the system defined as the capital and operation and maintenance cost over a 20-year lifetime. The main constraint is that supply must meet demand throughout each time interval and that the number of units per technology must be greater than or equal to zero (Koutroulis et al., 2006). The total annual cost objective function is advantageous to the function of this methodology, used by several authors reviewed above. However, there is no consideration of conventional fuels used in the supply mix, such as backup diesel or grid generation system. Therefore, the main disadvantage is that this methodology cannot cope with case studies that have concurrent periods of low wind and solar resource. The optimization is, therefore, forced to oversize the supply mix to meet demand throughout a low resource potential period. This oversizing may be redundant for the majority of the year, but should still be considered the optimum solution due to the lack of backup supply. The battery bank can, to a certain extent, reduce this effect, but no guarantee can be made as the battery is only charged using surplus energy from the renewable sources.

Yang et al (2008), developed a GA to optimize the unit size of a wind, PV and battery supply using a minimum total annual cost function and loss of power supply probability constraint at the hourly time scale. The main differentiation between this methodology and other similar approaches in the literature, such as the publication by Koutroulis et al (2006), discussed previously, is that the PV tilt angle and wind turbine hub height is optimized for maximum generation with respect to the time of day demand usage (Yang et al., 2008). If the site demonstrates a conventional intra-day demand profile, the maximum solar resource will be during the same hours as the peak demand, and therefore, searching for the optimum tilt in an optimization format is computationally unnecessary. Otherwise, including the PV tilt angle in the optimization will assist in matching direct electricity generated from the PV panel to demand, thereby, minimizing the PV capacity in the supply mix.

Chapter 3 - Methodology

The measurement of sustainability can be defined by the environmental, social and economic metrics of the proposed solution (Brundtland, 1987). Only the economic and environmental metrics are used as indicators in the decision-making process of the supply mix design as the social metrics are out of the research scope of this work.

This chapter presents the methodology developed to create a tool that can be used to identify the renewable energy supply mix of a country/region seeking to achieve a carbon neutral status and meet demand. The renewable energy supply mix is considered as two components: the renewable energy resource; and the conversion technology selected for the utilization of the resource.

Economic Decision Making Metric

Multiple supply mix configurations may exist in terms of the resources, technologies and installed capacities utilized. This study aims to design a supply mix that is able to maximize the tangible benefits against the economic cost involved. Due to its ability to measure the cost-effectiveness of various assets with differing lifespans, the Total Annual Cost is selected as the indicator of the economic metric (NAPEE, 2008). The total annual cost is calculated using Equation (3-1) below.

$$TAC(£/yr) = Annualized\ Capital\ Cost(£/yr) + O\&M\ Cost(£/yr) + Fuel\ Cost(£/yr) \quad \textbf{(3-1)}$$

Where the O&M cost is the annual Operation and Maintenance cost and the annualized capital cost is a technique used to compare the magnitude of a capital cost at current value by converting it to a future annual capital charge, as calculated using Equation (3-2) below (Towler & Sinnott, 2012).

$$Annualized\ Capital\ Cost\ = Capital\ Recovery\ Factor\ x\ Capital\ Cost \quad \textbf{(3-2)}$$

Where the Capital Recovery Factor (CRF) converts the present capital cost value into a stream of equivalent annual payments at a specific interest rate over a specified time period, as expressed by Equation (3-3) below (Sepulveda et al., 1984).

$$CRF = \frac{i(1+i)^n}{(1+i)^n - 1} \quad \textbf{(3-3)}$$

Where *i* is the interest rate and *n* is the number of annual payments over the project's lifetime.

Environmental Decision Making Metric

Environmental indicators examine the effect of human activities on the environment and their implications on ecosystems, health and quality of life. A number of environmental indicators could be used to assess the environmental performance of a proposed solution. These include, but are not limited to, land and water usage, waste generation and soil erosion. Since this study aims to design a renewable energy supply mix to approach carbon neutrality, the environmental performance is assessed by the achieved reduction in emissions. Therefore, the emissions reduction is used as the indicator of the environmental decision-making metric. This indicator is calculated by finding the percentage difference between the carbon dioxide emissions of the proposed solution and the emissions of the existing energy supply mix as shown in Equation (3-4) below.

$$Emissions\ Reduction\ (\%) = \left[1 - \frac{Proposed\ \ Emissions\ (kgCO_2)}{Current\ \ Emissions\ (kgCO_2)}\right] \times 100\% \quad \textbf{(3-4)}$$

The proposed emissions component depends on the proportion of energy generated from each technology in relation to demand and is calculated at the available time interval. In case the renewable technologies oversupply demand, the emissions reduction for the time interval reach a maximum limit of 100 %. This study only considers the operational emissions and so the emissions generated from any embodied energy are out of the scope of this work.

Classifications of Renewable Energy Resources

This study has identified and analyzed the three distinct classifications of the mainstream renewable energy resources which are:

1) Deterministic resource; a resource with an occurrence and magnitude pattern that has a future state of development with little randomness involved;

2) Dispatchable resource; a resource able to provide an energy content that can be used at a specific time and place, allowing an adjustable supply at the operator's request; and

3) Stochastic resource; a resource that has a non-deterministic, intermittent manner described using probability distributions.

Figure 3-1 below illustrates the combinations of renewable energy resources, conversion technologies,

energy storage and backup pathways considered in this study to create a supply mix.

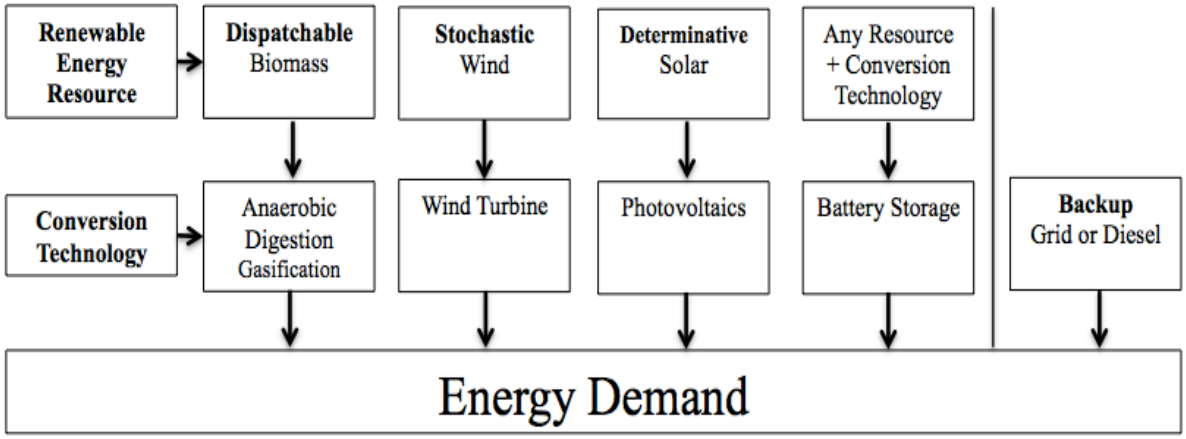


Figure 3-1 Energy Supply Mix Chain Based on the Statistical Characteristics of the Resources

It is noted that solar energy can also be considered as a stochastic resource due to variable cloud coverage. However, this cloud coverage is expected to have a negligible annual effect on the resource forecasting and, in addition, the number of night time hours confirm that this resource will not be available. Furthermore, the solar radiation data recorded incorporates the effect of cloud coverage due to a reduction of radiation intensity that would otherwise not be expected under a clear sky. Therefore, this study assumes that solar is a determinative classification.

Having identified the total annual cost and emissions reduction indicators, this study has established a methodology to assess the above resource classifications operating within the same system. Although the same indicators are used, the evaluation process of each resource is conducted differently to ensure that demand is met.

A review of the literature, in Chapter 2, has shown that the available renewable energy supply mix design software or existing methodologies do not base their processes on the decision-making indicators identified in this study. In order to complete this gap in knowledge, this chapter presents a renewable energy supply mix methodology, using these indicators in the decision-making process.

Since the main aim of the proposed system is to meet demand, this chapter is structured to initially present a series of techniques for energy demand analysis and characterization. A resource and conversion technology assessment of the components, illustrated in Figure 3-1 above, is then conducted using the elements of the decision-making indicators. A final renewable energy supply mix methodology, which requires all of the aforementioned supply-demand constituents, is then presented, based on the

economic and environmental decision-making indicators of this study. The main aim of this methodology is to identify the number of units and, thus, the installed capacity of the technologies considered in the optimum range, under the decision-making indicators used.

3.1 Energy Demand Analysis

The main aim of this study is to design a renewable energy supply mix to meet demand. Therefore, an assessment is required to analyze and understand the factors and characteristics of this demand. Energy demand is variable with time and typically has diurnal, weekly, seasonal and monthly profiles. Three key aspects of energy demand have been identified as the temporal, climatic and growth effects that are further examined in this section.

3.1.1 Temporal Analysis

The Average Power Analysis is used to examine the diurnal timing and magnitude of the peak and minimum demand.

The possible seasonal nature of energy demand can be identified by the monthly temporal analysis. The effect of influences on demand, such as uneven population patterns that can affect changes on this scale, can then be assessed.

To allow for long-term energy demand forecasting, a potential shift in demand on a larger scale, for example annually, must be considered to calculate the expected requirement of additional supply capacity to meet the rate of demand increase.

Average Power Analysis

The Average Power is used to represent the maximum and minimum extremities in demand behaviour for a certain time interval. This study focuses on the maximum average power and the time this occurs in Equation (3-5) and the minimum average power and the time this occurs in Equation (3-6).

$$P_{max}^{t_i} = Max|_n(Pt_i^n) \quad \textbf{(3-5)} \qquad P_{min}^{t_i} = Min|_n(Pt_i^n) \quad \textbf{(3-6)}$$

Where t_i represents the hours in a day; t_i = [0:24] and n represents the number of days in a year n = [1:365]. $P_{max}^{t_i}$ represents the maximum value of the average power in time interval t_i maximized over the days of the year. Similarly, $P_{min}^{t_i}$ represents the minimum value of the average power in time interval t_i minimized over the days of the year.

3.1.2 Climatic Effects

A significant proportion of demand is due to weather related effects. When energy is used for space heating or cooling purposes, the demand should be dependent on the difference between ambient temperature and the required internal building temperature. This is because the energy demand for heating and cooling purposes is used to maintain a constant internal temperature at a selected level. By only accounting for ambient temperature, the magnitude of energy demand cannot be assessed in terms of the time and intensity of the heating or cooling requirements. However, the degree-day unit is able to quantify the magnitude and time of heating or cooling requirements that a building may have (Vesma, 2011). Therefore, using a degree-day and demand analysis, climate is considered as a factor of the energy demand.

This sub-section examines the climatic factor of demand using the degree-day unit to assess the space heating/cooling load of a building with the respective energy demand. This analysis is used to prove and quantify a potential correlation between external temperature and demand. The results from this analysis also identify the weather and non-weather related demand components.

The Heating Degree Day (HDD) and Cooling Degree Day (CDD) are representations of the degree Celcius-Hour units. They are constructed using the same methodology except that the HDD accounts for an ambient temperature lower than the internal and the CDD accounts for an ambient temperature higher than the internal. For reasons of simplicity, the explanation of the degree-day representation and the process of this construction use the HDD.

Figure 3-2 below shows an internal and ambient air temperature 24-hour profile for a chosen internal temperature of 18°C. The shaded area separating the two temperature profiles is effectively the demand for space heating.

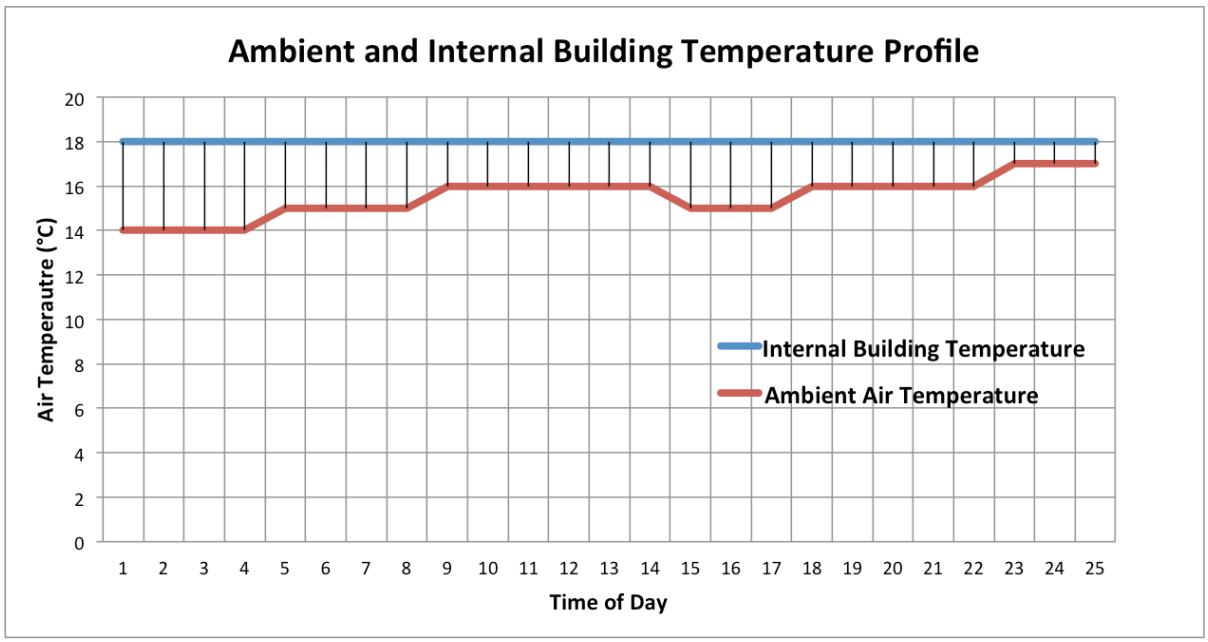


Figure 3-2 Building Heating Demand - 24 hour Period

In order to quantify the intensity and duration of this heating demand and calculate the total daily HDD, the area between the internal and ambient temperature is calculated using Equation (3-7) below (Cesaraccio et al., 2001).

$$HDD = \frac{1}{24} * \int_0^{24} (Internal\ Temperature - Ambient\ Air\ Temperature)dt \quad \textbf{(3-7)}$$

The methodology used to determine the relationship between the heating or cooling degree day data and the electricity or gas demand is identical. For simplicity, the process explained below is presented in terms of electrical energy demand and HDD.

The statistical tool used in this analysis is a simple linear regression analysis that correlates the HDD with the respective demand. The results are in a form similar to Equation (3-8) below.

$$E = mHDD + c \quad \textbf{(3-8)}$$

Where E is the total electrical energy demand; m is the factor of building energy loss expressed as kWh $(^{\circ}Chr)^{-1}$; HDD is the number of heating degree days ($^{\circ}Chr$); and c is the buildings' base load, which is the non-weather related demand (e.g. IT equipment) expressed as kWh (Layberry, 2008).

The relationship between the degree-days and energy demand depends on the correlation coefficient R^2. It is generally accepted that the correlation coefficient value of a linear regression analysis must be greater than or equal to 0.75, equating to a 75 % confidence of a strong linear relationship between the two data

sets (Bernstein & Bernstein, 1999). A correlation coefficient value less than 0.75 is deemed to have a weak relationship between the energy demand and degree-day value and so the *m* and *c* components of Equation (3-8) above cannot be determined confidently.

3.1.3 Growth

Infrastructure and population are the two major elements of energy requirement and so a change in either element results in an expected change in demand. In addition, a change in economic wealth is expected to shift the energy demand in the direction in which wealth is moving. Therefore, the elements of growth identified in this study that must be further considered are the projected changes in infrastructure, population and wealth of the current scenario.

The infrastructure growth element is examined by considering expected developments to the site that will change the number and type of energy conversion technologies within the demand mix. A substantial introduction of more efficient appliances and technologies operating within the demand mix may reduce the rate of increasing demand. However, this does not necessarily mean that there will be a decrease in demand over a large scale caused by this increase in conversion efficiency. Apart from the expected change in demand, the usage of infrastructure must be examined more closely to assess an expected temporal profile. A comparison between the current and new profile must be conducted to estimate the effect of integrating the new with the current infrastructure.

The population growth element is examined in a similar way to the infrastructural growth element, due to the direct relation between infrastructure and occupiers. The population element is examined by considering expected change in the number of people using the conversion technologies in the demand mix. The population growth must be considered to account for potential changes to the demand profiles and magnitude.

The wealth element of growth can be examined in two different perspectives that yield a similar result. The first perspective is the assessment of whether the availability of energy is a driver of economic growth and, therefore, generation of wealth. The second perspective is the assessment of whether energy demand is a side product of wealth and economic growth. In any case, a relationship between energy consumption and economic activity is expected. Figure 3-3 below shows the recorded global Gross Domestic Product (GDP), Energy Consumption and CO_2 emissions between 1970 and 2010 and the

projections of each up to 2030 (BP, 2012). A decoupling of energy and GDP can be seen starting from the 1980s. There is a significantly higher recorded GDP per unit energy in 2010 compared to 1970. The similarities in the energy trends and CO_2 emissions up to 2010 is evident, and, more importantly, the reducing nature, due to the effects of the global financial crisis between 2008 - 2010.

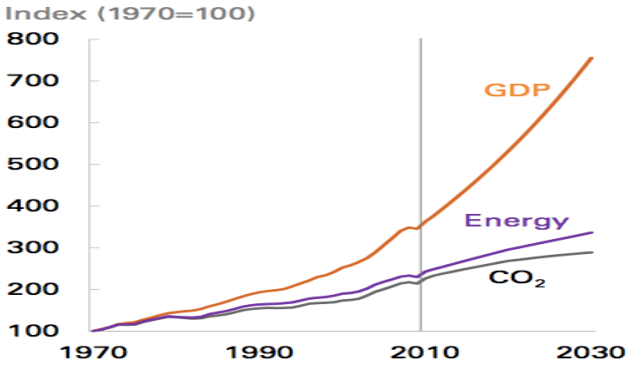


Figure 3-3 Global GDP, Energy and Carbon Dioxide Growth Trend 1970 – 2030 (Source: BP Energy Outlook 2039 (BP, 2012))

It is important to note the high uncertainty involved with the growth factor of demand in terms of the difference between the behaviour of the growth elements and the overall expected and real trend that demand will follow.

To summarize, this study considers three factors affecting energy demand shown in Figure 3-4 below.

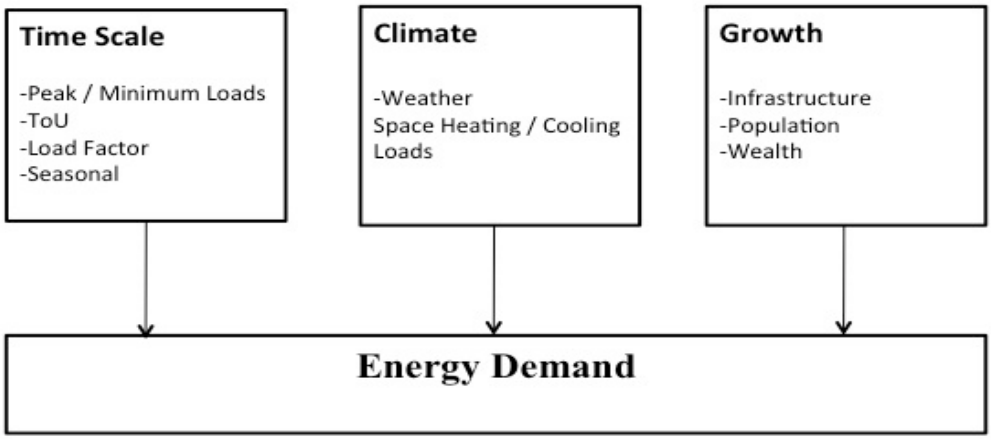


Figure 3-4 Factors Affecting Energy Demand

3.2 Potential Renewable Energy Source Assessment

The following section describes the development of the methodologies used to assess the renewable energy resource component of a supply mix. Solar energy is used as an example of a determinative resource, biomass energy is used as an example of a dispatchable resource and wind energy is used as an

example of a stochastic resource. Solar and wind energy are continuously renewable resources that have no GHG emissions involved with their provision and, therefore, an environmental analysis of these resources is not considered in this section (Hester & Harrison, 2003).

3.2.1 Determinative Resource Assessment

This section presents the potential energy assessment and economic analysis of the determinative resource classification using solar energy as an example. The solar resource can be utilized via centralized or decentralized systems. Centralized systems are large-scale installations developed to supply the national grid. Decentralized systems are usually domestic or commercial rooftop installations that supply an internal demand and export any excess energy to the national grid.

To determine the energy available for both utilization systems, the total incident radiation on a suitable collector must be calculated. This is a function of the relative path that the sun takes[2]. This path is used to calculate the shading effect between solar collectors and identify the minimum installation distance necessary to avoid shading and, thus, find the credible surface area for solar installations.

The viable size of the collector surface for a decentralized system is determined by examining the available rooftop area. A statistical methodology, using Geographic Information Systems (GIS) and Google Earth™, is developed.

Annual Sun Path

This sub-section presents the construction of the hourly annual sun path at a site envisaged for solar applications. The sun path is illustrated by graphically presenting the hourly altitude angle (a) against the hourly azimuth angle. The altitude angle is the angle between a line pointing from the observation point towards the centre of the sun and the horizon. The azimuth angle (ψ) is the angle on a horizontal plane that, for northern hemisphere latitudes, is measured from the south to the horizontal projection of the sun's rays (Garag & Prakash, 2000). An illustration of the solar azimuth and altitude angles is shown in Figure 3-5 below (La Roche, 2011).

[2] The effects of cloud cover are not considered as an individual component in this study as they are a factor of the recorded solar radiation at the site under investigation

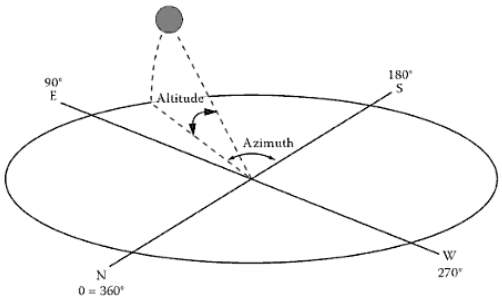


Figure 3-5 Diagram of Solar Azimuth and Altitude Angles

Altitude Angle of the Sun

The altitude angle (a) is calculated using Equation (3-9) below (Markvart, 2000).

$$\sin a = sin\delta sin\phi + cos\delta cos\phi cos\omega \quad \textbf{(3-9)}$$

Where φ is the geographical latitude of the site under investigation and ω is the hour angle that can be measured in degrees or time[3].

The solar declination (δ) is defined as the degrees north or south of the equator. The solar declination varies from +23.5º (North) to -23.5º (south) in December and is calculated on a daily scale using Equation (3-10) below. The variable n is the day in the year, where January 1st is n=1.

$$\delta = \pi \frac{23.45}{180} sin\left(2\pi \frac{284 + n}{365}\right) \quad \textbf{(3-10)}$$

Azimuth Angle of the Sun

The azimuth angle (ψ) is calculated using Equation (3-11) below (Markvart, 2000).

$$cos\psi = \left(\frac{sina\ sin\phi - sin\delta}{cosa\ cos\phi}\right) \quad \textbf{(3-11)}$$

Where each of the variables has been previously defined above.

Example Sun Path Diagram for Hanimaadhoo and Oxford

This sub-section presents an example of an annual sun path diagram, using the latitude for the island of Hanimaadhoo in the Maldives and the city of Oxfordshire in the United Kingdom. To outline the position

[3] 24 hours = 2π radians

that the sun follows throughout the year, four days that define the path boundaries are used. These are the summer and winter 'solstices' and the March and September 'solar equinoxes'.

The solstices are used because they represent the longest and shortest days of the year, which are 21st of June and 21st of December respectively. The equinoxes are used because they represent the only two days of the year where the day is precisely 12 hours long and the sun rises due east and sets due west of the equator. The equinoxes are on the 20th of March and 22nd of September (Boxwell, 2010). For illustrative purposes, a sun diagram is presented, in Figure 3-6 below, for the city of Oxford and, in Figure 3-7 below, for the island of Hanimaadhoo on the days of the solstices and equinoxes.

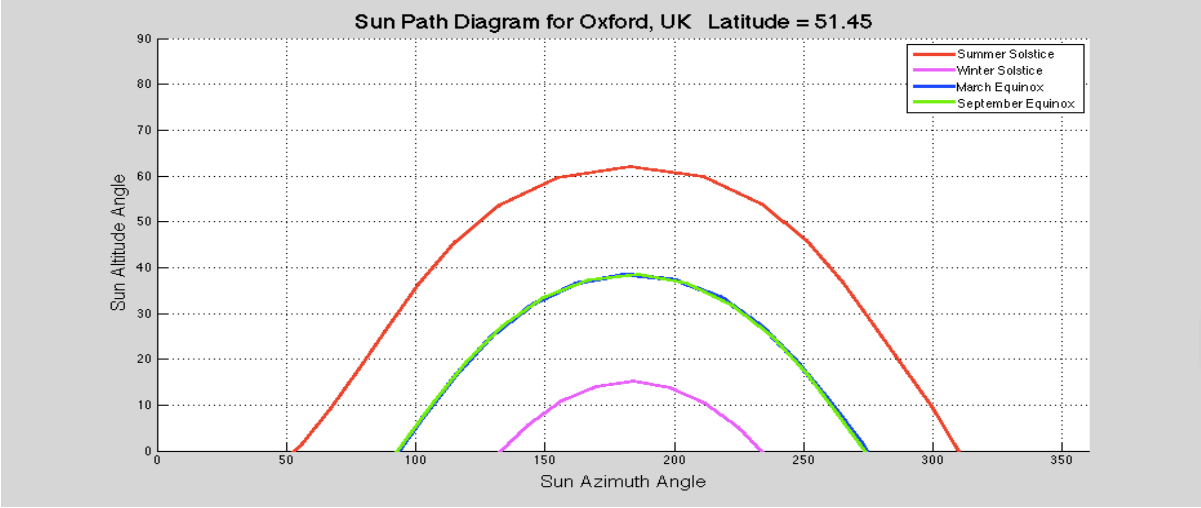


Figure 3-6 Sun Path Diagram - Oxford

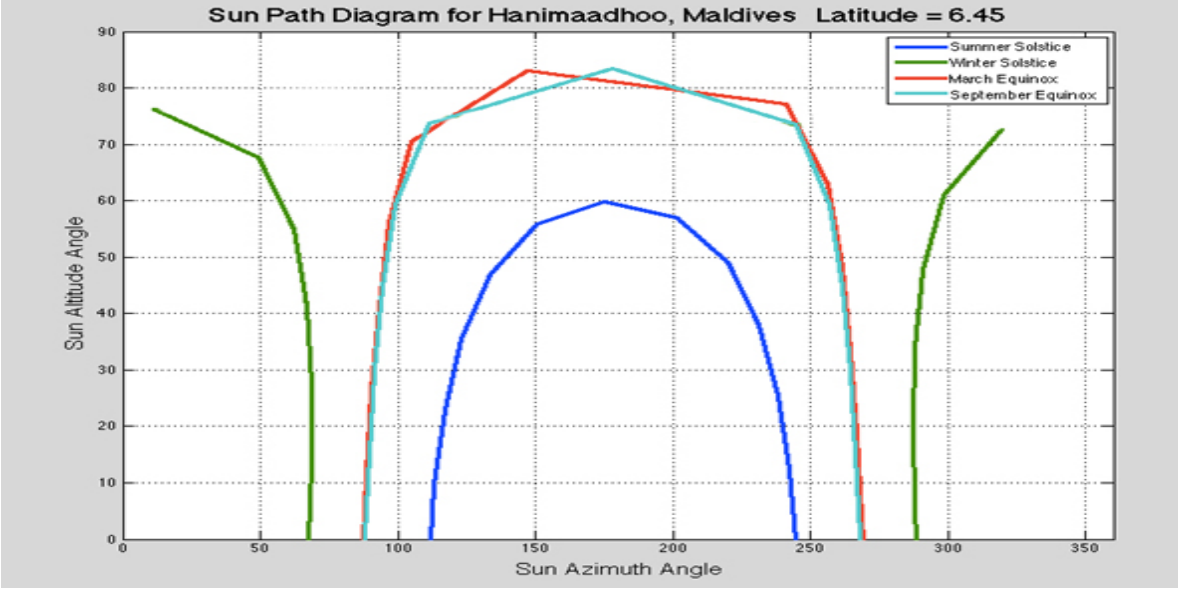


Figure 3-7 Sun Path Diagram - Hanimaadhoo

From the Oxford sun path diagram, in Figure 3-6 above, the solar elevation reaches its lowest point of approximately 15º at the winter solstice, and its highest point of approximately 62º at the summer

solstice. The Hanimaadhoo diagram, in Figure 3-7 above, shows that the solar elevation reaches its lowest point at approximately 60° at the winter solstice, and its highest point of approximately 80° at the summer solstice. The graphs above confirm the fact that, at both equinoxes, the sun rises exactly from the east and sets exactly in the west and so the equinox lines follow the same path.

Magnitude of Total Solar Radiation

The total solar radiation is defined as the sum of the direct, diffuse and reflected radiation components (Markvart, 2000). The magnitude of each of these components depends on the orientation and inclination angle of the collector illustrated in Figure 3-8 below (Surles et al., 2011).

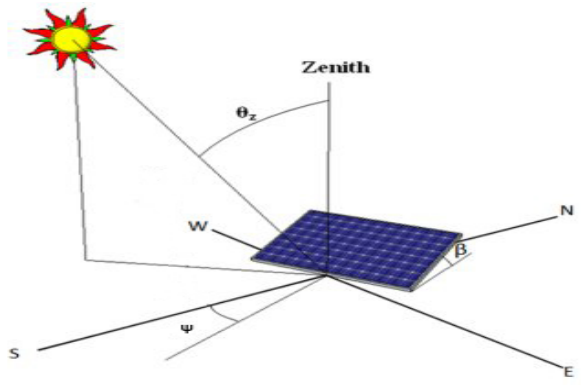


Figure 3-8 Solar Collector Installation Angles

In the northern hemisphere an orientation angle of true south yields the maximum annual energy absorbed by collectors. Similarly, for collectors in the southern hemisphere, orientation of due north is optimal (Goetzberger & Hoffmann, 2005). Provey & Barber (2000), show that for a 20°-orientation range to the east or west there is a 2 % decrease in the total energy yield (Provey & Barber, 2010). Due to the minimal reduction in energy yield and additional availability of utilizable surface area, this study assumes that the solar collector is positioned true south within a 20° -orientation range. Once the latitude and solar radiation is known, the optimum inclination angle in terms of maximum total annual radiation absorbed can be found.

This section examines the process of calculating the total solar radiation at an inclined plane using the direct, diffuse and reflected radiation components. A summary of the required symbols and definitions is shown in Table 3-1 below.

Table 3-1 List of symbols and definitions required for total solar radiation process

Symbol	Definition	Unit
R_{Direct}	Direct Radiation on a Horizontal Surface	J / m^2
$R_{Diffuse}$	Diffuse Radiation on a Horizontal Surface	J / m^2
$R_{Reflected}$	Reflected Radiation on a Horizontal Surface	J / m^2
R_{Global}	Global Radiation on a Horizontal Surface	J / m^2
δ	Solar Declination	Radians
β	Inclination Angle	Radians
ρ	Ground Reflectivity	-
ω	Hour Angle	Radians
ω_s	Sunrise Hour Angle	Radians
ω_s'	Sunrise Hour Angle Above an Inclined Plane	Radians
ω_o	Minimum of ω_s and ω_s'	Radians
φ	Geographical Latitude	Radians

Direct Radiation at an Inclined Plane

Assuming a south facing collector and there is an isotropic radiation distribution, the direct radiation at an inclination angle (β) to the horizontal is given in Equation (3-12) (Liu & Jordan, 1960).

$$R_{direct}(\beta) = R_{direct}\left(\frac{\cos(\phi-\beta)\,cos\delta sin\omega_o + \omega_o sin(\phi-\beta)sin\delta}{cos\varphi cos\delta sin\omega_o + \omega_o sin\varphi sin\delta}\right) \quad \textbf{(3-12)}$$

Where ω_o is defined as the minimum value between the sunrise hour angle (ω_s) and the sunrise hour angle above an inclined plane (ω_s') as shown in Equation (3-13) below (Jordan & Liu, 1962).

$$\omega_o = min\{\omega_s, \omega_s'\} \quad \textbf{(3-13)}$$

Where ω_s' and ω_s' are found using Equations (3-14) and (3-15) respectively below.

$$\omega_s' = cos^{-1}(-\tan(\varphi-\beta)\,tan\delta) \quad \textbf{(3-14)}$$

$$\omega_s = cos^{-1}(-tan\varphi.tan\delta) \quad \textbf{(3-15)}$$

Diffuse Radiation at an Inclined Plane

For an isotropic distribution of diffuse radiation over the sky, the diffuse radiation on an inclined plane, $R_{Diffuse}$ (β), is found using Equation (3-16) below (Jordan & Liu, 1962).

$$R_{Diffuse}(\beta) = \frac{1}{2}(1 + cos\beta).R_{Diffuse} \quad \textbf{(3-16)}$$

Reflected Radiation at an Inclined Plane

The ground reflectivity (ρ) is defined as the ratio of radiation reflected from the ground surface to the incident global radiation striking it. This radiation component is calculated using Equation (3-17) (Markvart, 2000).

$$R_{Reflected}(\beta) = \frac{1}{2}[R_{Global}.\rho(1 - cos\beta)] \quad \textbf{(3-17)}$$

Where $R_{Reflected}(\beta)$ is the reflected solar radiation at inclination angle β; R_{Global} is the global solar radiation and (ρ) is the ground reflectivity ratio representing a range of ground types in Table 3-2 below (Markvart, 2000).

Table 3-2 Ground reflectivity values

Ground Type	Reflectivity
Bare Dry Ground	0.2
Dry Grassland	0.3
Desert Sand	0.5
Snow	0.5-0.8

The reflectivity ratios, in Table 3-2 above, indicate that snow is the most preferable surface for solar installations, due to the high reflectivity, while dry ground is the least preferable surface.

Total Solar Radiation at an Inclined Plane

The results from Equations (3-12), (3-16) and (3-17) above can now be used to populate Equation (3-18) below and calculate the total radiation striking an inclined plane, $R_{Total}(\beta)$.

$$R_{Total}(\beta) = R_{Direct}(\beta) + R_{Diffuse}(\beta) + R_{Reflected}(\beta) \quad \textbf{(3-18)}$$

Solar Rooftop Assessment Methodology for Urban Areas

The existence of unused space on building rooftops means that a considerable surface area can be allocated to solar energy applications on an urban-wide scale. From a total area perspective, the large

number of buildings and different types of rooftops make the task of calculating the individual available rooftop space for solar installations extremely resource expensive and practically unfeasible.

This section presents the methodology developed to assess a statistical overview of the maximum surface area that can be used to utilize solar energy on rooftops in an urban location. This methodology can be conducted in a reasonably short computational time period without incurring financial cost. To conduct this methodology, the individual building and urban area characteristics are required, as listed below.

1. Orientation of Each Building
2. Credible Surface Area per Rooftop
3. Rooftop Mix of an Urban Area

Each of the above characteristics is considered as a step in the urban area assessment methodology described in further detail in each of the following three sub-sections below.

Step 1 - Orientation of Each Building

A building may be considered suitable for solar installations if it is south facing with a flexibility of 20º due south-east or south-west (Thomas, 2003). To identify the orientation of a building and its relation to the 20º ranges, a GIS spatial analysis algorithm, examined in further detail in the next sub-section, is created to identify the number of suitable buildings.

Geographic Information Science Spatial Analysis Algorithm for Orientation

This sub-section presents the GIS algorithm and main assumptions developed in this study to identify the number of buildings in an urban area that are within the required orientation constraints.

The Ordinance Survey MasterMap facility records all of the existing buildings and structures in Great Britain, in a digital mapping format, and is used to extract a map of the area examined (OS, 2012). The required area for implementation of the GIS algorithm is extracted from the MasterMap.

The aerial image, in Figure 3-9 below, is used to show a set of houses with various orientations extracted from a Google Earth™ image of Abingdon, Oxfordshire (GoogleEarth, 2010). By observation, it can be noted that the orientation is equivalent to the bearing of the longest side relative to the north.



Figure 3-9 Google Earth™ Image Extract of Abingdon, Oxfordshire (Source: Google Earth™)

Based on the assumption that the longest side of the building is also its orientation, the algorithm developed to identify the orientation of all the houses in a particular area first identifies which side of each house has the longest length. Since the MasterMap GIS format is geographically referenced, the orientation of this length can be calculated.

The angular limits assigned to the algorithm are the houses that are south facing within a +/- 20º range. Furthermore, a second angular constraint is required since houses that are north facing will also provide a south facing rooftop. Therefore, this angular constraint is for houses that are north facing within a +/- 20º range. The orientations that do not fall within the aforementioned angular constraints are then excluded from the process.

To summarize, the GIS algorithm, shown in the Visual Basic code in Table 0-1 of Appendix A, works in the process shown in the flowchart, in Figure 3-10 below, for any number of buildings.

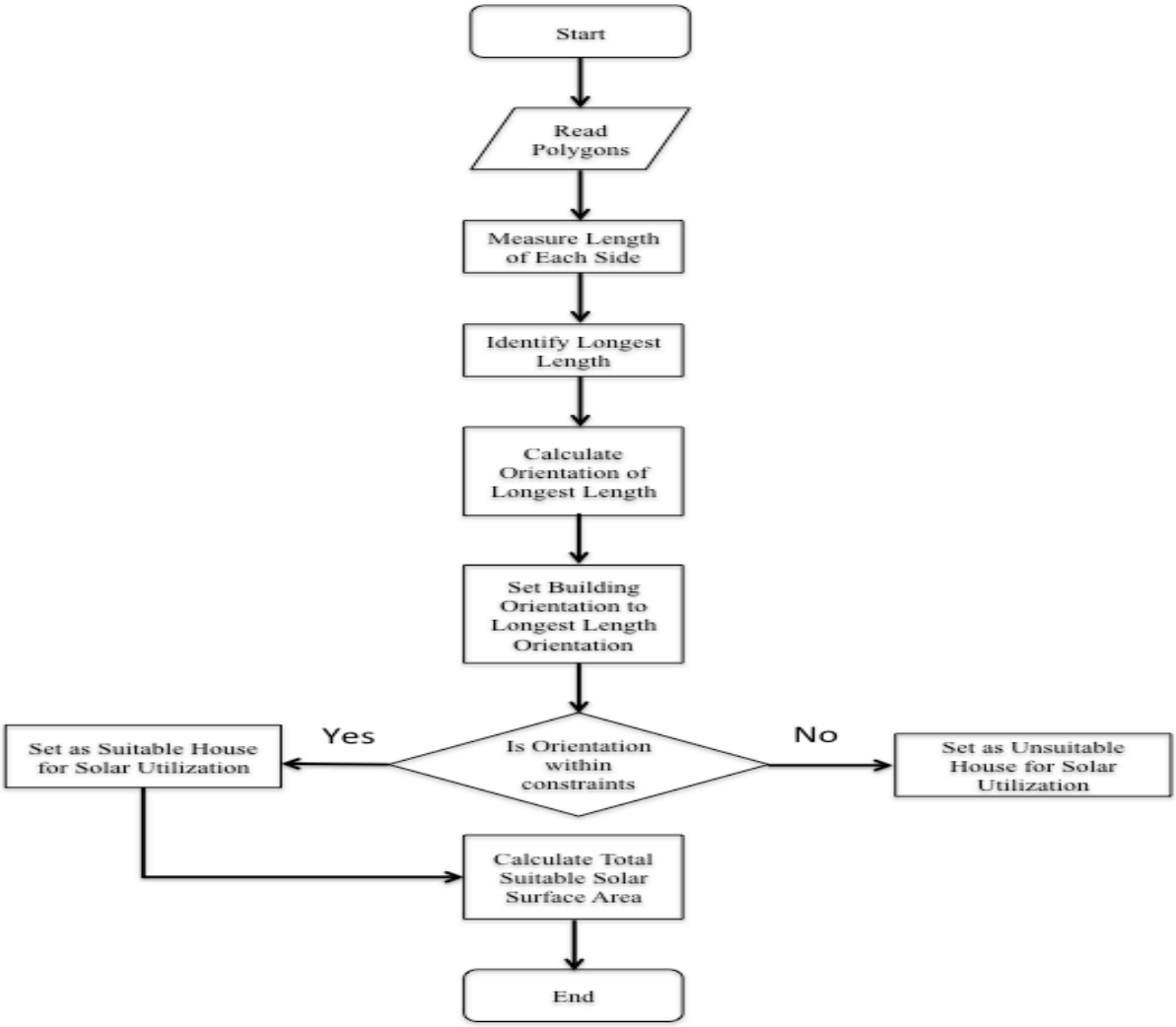


Figure 3-10 Flowchart for the Suitable Solar Rooftop Algorithm

Example of the GIS Spatial Analysis Rooftop Algorithm

This sub-section presents a test case of the GIS algorithm implementation on the residential area shown in Figure 3-9 above. The GIS format is overlaid on a Google Earth™ image and the houses within the orientation constraints are highlighted in purple and the houses outside the constraints are highlighted in red, as shown in Figure 3-11 below. A slight offset between each house and the selection polygon has been made for a clearer representation of the test case.



Figure 3-11 GIS Algorithm of Buildings within Orientation Constraint (Source: Base Map, Google Earth ™, MapInfo™)

The diagram, in Figure 3-11 above, shows that the GIS algorithm is able to correctly identify the houses within the orientation constraint limits and, thus, highlights them as potential buildings for solar applications. However, this GIS algorithm is unable to identify the available solar area per rooftop as the digital map only represents the floor area of each building. In order to overcome this weakness, the Google Earth™ approach described in the next step, is required.

Step 2 – Credible Surface Area per Rooftop

This sub-section presents the second step of the overall solar resource assessment methodology to identify the available area per type of rooftop and the estimated distribution of each type of rooftop in the area under examination. The main assumption used is that the solar area is equivalent to the maximum surface area that can be physically used for a solar installation.

The available area for solar utilization per rooftop type is dependent on the type of each rooftop. In order to create a cross-sectional view of the architectural building style that accounts for both residential and commercial developments, four rooftop types typical to UK architecture have been identified. Photographs of each type are shown in Figure to Figure of Appendix A and are, namely, the gable, double gable, hipped and flat rooftops. An additional rooftop category, of no solar area potential, is

included in the mix that represents the buildings that do not have any available rooftop space, regardless of their orientation. Within this category, there are flat rooftops that are covered with other equipment and machinery and cannot accommodate solar installations due to space constraints and large shading effects.

The following sub-sections are dedicated to presenting the trigonometric relationship between the rooftop type and respective solar area.

Gable Rooftop

This sub-section presents the trigonometric relationship between a gable rooftop and the available area that can be utilized for solar energy applications. Figure 3-12 below shows the geometric parameters required to calculate the solar area shaded in yellow and calculated in Equation (3-19).

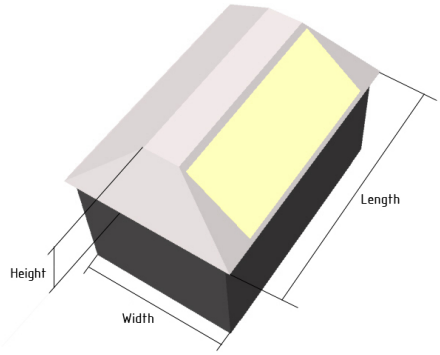


Figure 3-12 Gable Rooftop

$$Solar\ area\ (m^2) = slant\ width * length \quad \textbf{(3-19)}$$

Where:

$$slant\ width = .\left(\frac{0.5 * width}{\cos\ (tilt\ angle)}\right)$$

Double Gable Rooftop

This sub-section presents the trigonometric relationship between a double gable rooftop and the available area that can be utilized for solar energy applications. The geometric relationship, shown in Equation (3-20) below, is similar to the gable rooftop above. However, the total solar area per rooftop is not the same due to different magnitudes of each dimension. Figure 3-13 below shows the parameters required to calculate this area.

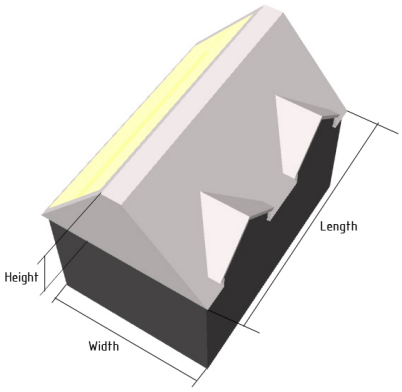


Figure 3-13 Double Gable Rooftop

$$\boldsymbol{Solar\ area\ (m^2) = slant\ width * length} \quad \textbf{(3-20)}$$

Where:

$$slant\ width = .\left(\frac{0.5 * width}{\cos\ (tilt\ angle)}\right)$$

Flat Rooftop

This sub-section presents the trigonometric relationship between a flat rooftop and the available area that can be utilized for solar energy applications by accounting for the effect of array shading. The solar area is shown, in Equation (3-21) below, using the parameters in Figure 3-14.

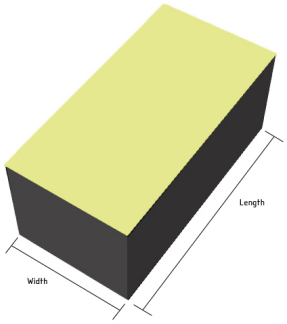
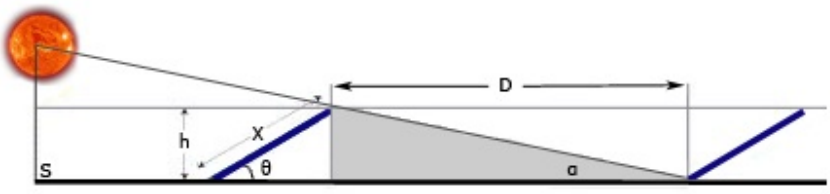


Figure 3-14 Flat Rooftop

$$Solar\ area\ (m^2) = width * length \quad \textbf{(3-21)}$$

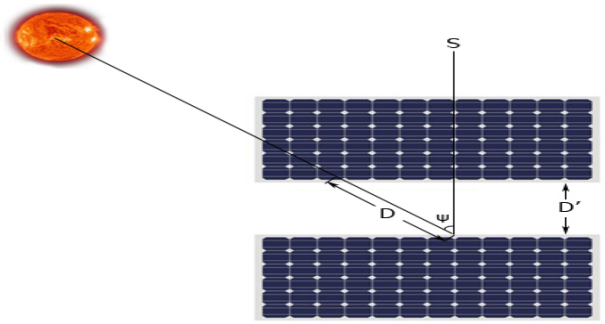
Inter-collector shading, that does not allow shade caused by the first collector to cover and reduce the performance of the second collector, is avoided by finding the smallest distance between two arrays. The sun path diagram is required to find the sun altitude on the winter solstice when it is at its lowest point of the year. This altitude determines the shade length (*D*) behind the solar collector. Figure 3-15 below shows the parameters required to calculate the shade length in Equation (3-22) below.



$$D = \frac{h}{\tan(a)} \qquad \textbf{(3-22)}$$

Figure 3-15 Length of Solar Collector Shading (Meck, 2012)

Once the shade length is established, the minimum inter-collector spacing is found by correcting the solar azimuth, extracted at the same time and date as the altitude. Figure 3-16 shows the parameters required to calculate the azimuth correction in Equation (3-23) below.



$$D' = D.cos(180 - \psi) \qquad \textbf{(3-23)}$$

Figure 3-16 Top View of an Inclined Solar Collector with the Azimuth Correction ((Meck, 2012))

Hipped Rooftop

This sub-section presents the trigonometric relationship between a hipped rooftop and the available area that can be utilized for solar energy applications. Figure 3-17 shows the parameters required to calculate the solar area in Equation (3-24) below.

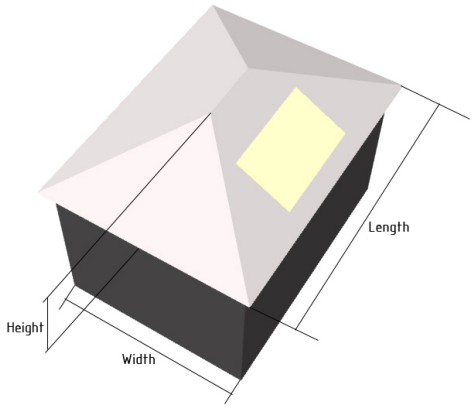


Figure 3-17 Hipped Rooftop

$$\boldsymbol{Solar\ area\ (m^2)} = \mathbf{x} * (\boldsymbol{length - 2b}) \quad \textbf{(3-24)}$$

Where b is the length of each right angle triangle on the rooftops' solar plane

Where

$$x = \frac{height}{\sin(tilt\ angle)}$$

Step 3 - Rooftop Mix of an Urban Area

The rooftop mix of an urban area is defined as the proportion of each rooftop type in relation to the total number of buildings in the area under investigation. The rooftop mix is characterized by first counting the number of rooftops in the area that are relevant to each type presented in the previous sub-section. This survey can be conducted by a site visit or a Google Earth™ approach. The proportion of each type, from an investigation of 1000 buildings, is considered as a sample number representative of an average city in the UK.

Summary of Solar Rooftop Assessment Methodology for Urban Areas

The main advantage of this methodology is that it can be used to identify the magnitude of accessible solar resource striking an urban area at a minimum computational and at no financial cost. Due to the extremely high number of buildings examined, the alternative of an individual assessment of each building has proven to be an unfeasible task.

The main disadvantage of this methodology is that it does not account for the shading effect of surrounding buildings, trees or other causes of shading. In order to account for the aforementioned shading, the use of aerial imagery from Lidar sources is required. This data set is considered extremely costly and has not, therefore, been examined further.

Economic Analysis of the Solar Resource

The solar resource is freely available in nature and so no fuel cost is involved in its use. An envisaged project operating with this resource typically requires a desk study of which the cost can be assumed as negligible and is, thus, assumed at no financial cost. There is, however, a financial cost related to the conversion technology that is later examined in the respective conversion technology subsection.

3.2.2 Dispatchable Resource Assessment

This section presents the potential energy assessment and economic analysis of the dispatchable resource classification using biomass as an example. To determine the potential energy, the end form must first be established. This depends on the biomass category and conversion pathway followed. The scope of this study is the anaerobic digestion for biogas and pelletizing/chipping for solid biomass as shown in Table 3-3 below.

Table 3-3 Examined Biomass Pathways to a Fuel Form in this Study

Biomass Category	Description	Preparation to End Fuel Form	End Fuel Form
Animal Waste	Livestock Manure/slurry	Anaerobic Digestion	Biogas
Energy Crops	Crops grown specifically for the energy industry	Anaerobic Digestion	Biogas
		Pelleting/Chipping	Solid
Forestry Waste	Woody biomass from forest harvesting	Pelleting/Chipping	Solid
Refuse (Organic Content)	- Municipal Solid Waste (MSW) – Domestic food and garden waste	Anaerobic Digestion	Biogas
	- Commercial & Industrial (C&I) – C&I food and green waste	Anaerobic Digestion	Biogas

The resource assessment is divided into each of the end fuel forms in order to consider the potential energy and economic indicator of each category. The energy assessment is conducted in terms of the energy content per unit mass (kWh/t) and energy content per unit volume (kWh/m^3) for the solid and

biogas fuel forms respectively. The economic assessment is conducted in terms of the cost of raw feedstock (£/t), cost of utilizable mass (£/t) and cost of biogas (£/kWh)[4].

For energy crops in particular, one of the main decisions in the project development is the selection of the appropriate species, which depends on the indicator performance of each. Due to the multiple components driving the selection, a multi-criteria assessment analysis based on the indicators, is developed for each fuel form. Since the implementation process for both is the same, it is presented in the relevant part of the following biogas fuel form section.

3.2.2.1 Assessment of Biomass Feedstock for the Biogas Utilizable Fuel Form

This section presents the potential energy and economic indicator assessment methodology for the biomass categories utilized as biogas. The potential energy assessment of a biomass feedstock, using a generic biogas yield equation, and the construction of an MCA analysis and implementation process for the selection of the optimum species for solid and biogas end fuel forms, are presented.

The potential energy from the anaerobic digestion of a biomass feedstock is a function of the biogas yield and the potential energy of the biogas generated. The biogas yield is derived using a methane yield equation and the known volumetric proportions of methane and carbon dioxide in biogas.

The potential energy of biogas is expressed using Equation (3-25) below.

$$E_{pot} = Y * \frac{P_{Bio}}{c} \quad \textbf{(3-25)}$$

Where E_{pot} is the biogas potential energy per mass of a feedstock; Y is the methane yield per mass of a feedstock; P_{Bio} is the potential energy content per cubic metre of biogas and c is the volumetric ratio of methane to biogas[5]. This ratio is required as the biogas potential is expressed in terms of biogas volume and so the methane volume must be converted to the biogas volume to account consistently for the potential energy.

The main parameters for feedstock characterization are the Volatile Solids (VS) content and Bio-Methane Potential (BMP) (Cho & Park, 1995). The VS content is the organic fraction of the feedstock that can be

[4] The cost of biogas is only considered for the biogas end fuel form
[5] This study assumes that the volumetric composition of biogas is 60% methane and 40% carbon dioxide

converted into biogas (Wilkie, 2005)[6]. The methane generation is expressed as the Bio-Methane Potential (BMP) per VS content of a particular feedstock.

The general equation for the methane yield calculation of a biomass feedstock is shown in Equation (**3-26**) below (Chynoweth et al., 1993).

$$Y = VS * P_{BMP} \quad (3\text{-}26)$$

Where *VS* is the Volatile Solids content per mass of the feedstock and P_{BMP} is the bio-methane potential per mass of volatile solids in the feedstock.

As the efficiency of the conversion technologies is based on the LHV, the energy density of the resource must be considered in consistent terms (Petchers, 2003). The LHV of biogas depends on the methane content in the gas. As this study assumes a ratio of 60 % methane and 40 % carbon dioxide, the LHV is equivalent to 6 kWh/m^3 (Khoiyangbam et al., 2011). A comprehensive data bank that includes the required parameters, constructed from the literature and the author's own investigations, has been developed by the EU funded "CROPGEN" project and is used in this study (Braun et al., 2011).

3.2.2.1.1 Animal Waste

This section presents the potential energy and economic assessment of the animal waste category normalized per head of livestock type. The economic analysis is presented by comparing the Nitrogen content of raw waste typically used for fertilizing to that of the digestate. This analysis shows that the diversion of animal waste from a fertilizer to an anaerobic digestion feedstock provides the land with a similar nitrogen content that is also an energy generating solution.

Potential Energy Content of Biogas from Animal Waste

The raw waste quantity and characteristics identified in the previous section are required to determine the biogas yield per head of livestock. Cattle (including dairy cattle) and pigs are typically used to fuel AD systems. The waste quantity considered is the accessible waste generated while the livestock is in the housing period (Nix, 2012).Table 3-4 below shows the annual potential energy yield performance of the animal waste generated per livestock type using Equations (3-24) and (**3-26**).

[6] The VS per total mass is converted from the VS per total solids content available in the literature

Table 3-4 Biogas Yield Performance of Animal Waste per Head of Livestock

Livestock	Average Annual Waste Generation (M_T/year) (Nix, 2012)	VS Content $\left(M_{VS}/M_T\right)$ (Banks, 2007)	Bio-methane volume per VS amount $\left(m^3CH_4/M_{VS}\right)$ (Banks, 2007)	Biogas Yield $\left(m^3Biogas/M_T\right)$	Annual Potential Energy Content (kWh / head livestock)
Dairy Cattle	11.6	0.086	144	21	1460
Cattle	8.2	0.069	200	23	1130
Pigs	1.6	0.033	272	31	298

The results, in Table 3-4 above, indicate that the dairy cattle livestock generates the highest potential energy content per head to the order of five times higher than the pig livestock which performs at the lowest comparative potential.

Economic Analysis of Animal Waste

During the AD process, a bio-chemical change occurs that modifies the organic compounds where the nutrients are stored and improves their accessibility to crops. A proportion of the organic nitrogen in the manure is converted to ammonium, but the nitrogen content in the digestate is similar to that of the raw feedstock content (Lukehurst et al., 2010). Table 3-5 below compares the difference in nitrogen content in dairy cattle manure and its digestate from a field trial example conducted in Northern Ireland (Frost & Gilkinson, 2010).

Table 3-5 Average Nutrient Composition of Dairy Cattle and Digestate

Product	Dry Matter (g/kg)	Total N (g/kg)
Dairy Cattle Manure	72.2	3.5
Digestate	59.3	3.6

The displacement of digestate over manure as a fertilizer is a practical benefit, from the farmer's perspective, in terms of the similar nitrogen content, storing, handling and spreading of the product (Lukehurst et al., 2010). The digestate formed from the AD process can, therefore, be supplied to the farms for agricultural use with a zero net change in fertilizer value. In this case only a transportation cost is incurred. The total cost per unit of energy is calculated as the transportation cost of waste from the farm to the AD plant and the cost of the digestate transportation from the AD plant to the farm. The

transportation data and assumptions required in order to calculate the transport cost of a road and farm tanker are presented in Table 3-6 below (FEC, 2003).

Table 3-6 Road and Farm Tanker Waste Transport Performance

Vehicle	Average Speed (km/hour)	Other Time Demand - Slurry pumping, hooking up (hours)	Hourly Cost (£/hour)	Volume Transported (m^3)
Road Tanker	25	0.73	40	20
Farm Tanker	20	0.73	32	8

The manure density is assumed at 1 t/m^3 (Nix, 2012). The biogas cost of each transportation mode is calculated as a round-trip distance for a range of travel radii shown in Figure 3-18 below.

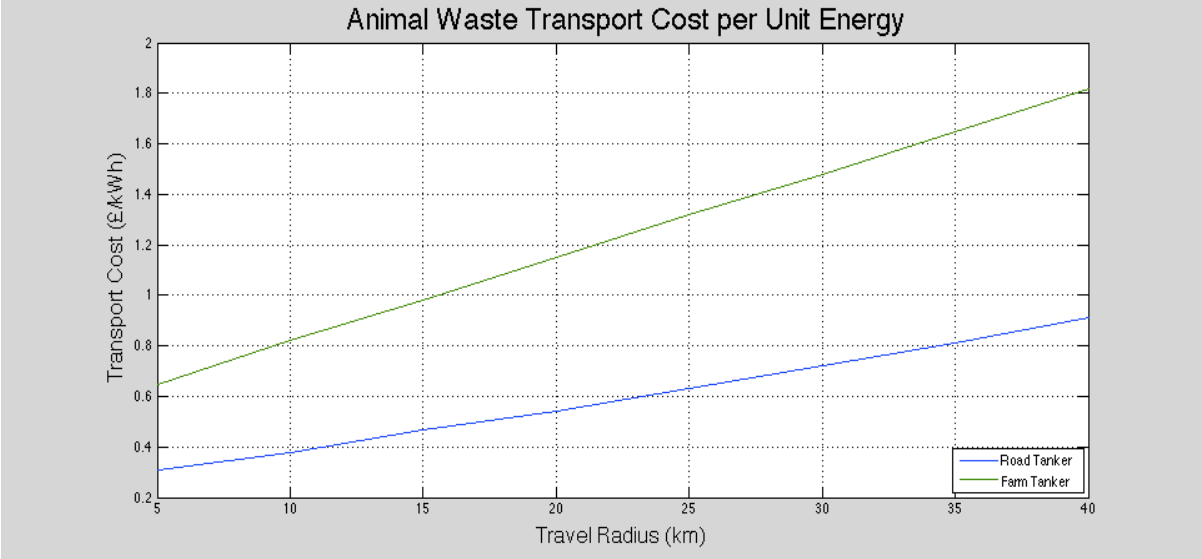


Figure 3-18 Transportation Cost of Animal Waste

3.2.2.1.2 Energy Crops

This section presents the potential energy and economic assessment of energy crops envisaged for biogas generation. The energy crop species selection tool, developed for the biogas fuel form, is also presented. Due to the number of indicators and subsequent elements that must be examined simultaneously over a number of species, an MCA analysis is used.

Potential Energy Content of Biogas from Energy Crops

The biogas energy potential of energy crops is a function of the annual yield tonnage per land area used for crop growth and the achievable biogas generation. Table 3-7 below reports the required species characteristics and annual potential energy yield performance of a range of energy crops, using Equation (**3-26**) above (Banks, 2007).

Table 3-7 Yield and Potential Energy Performance of Energy Crop Species

Crop Species	VS Content $\left({M_{VS}}/{M_T}\right)$ (Banks, 2007)	Bio-Methane Potential $\left({m^3 CH_4}/{M_{VS}}\right)$ (Banks, 2007)	Methane Content of Biogas (%) (Banks, 2007)	Biogas Yield $\left({m^3}/{M_T}\right)$	Crop Yield (t/ha) (Nix, 2012)	Biogas Yield (m^3/ha)	Biogas Potential Energy Content (MWh/ha)
Barley	0.24-0.34	353-658	61-70	157-294	5	785-1470	5.1-9.5
Maize	0.31-0.39	205-450	54	133-292	40	5320-11680	28.7-63.1
Oilseed Rape	0.24	240-340	69	84-118	3	252-354	1.7-2.5
Sugar Beet	0.19	236-381	50	90-145	67	6030-9715	30.2-48.6

Co-digestion of Biomass Feedstock

It is widely accepted that the co-digestion process of animal waste substrates with energy crops increases the biogas yield (Soetaert & Vandamme, 2005). Currently, the most popular combination for co-digestion in Europe is maize and cattle manure (IEA, 2010). This sub-section presents a potential energy assessment of co-digestion and a comparison between the single feedstock digestion of either cattle manure or maize.

Cattle manure is, in practice, considered at a fixed annual tonnage based on the livestock population as opposed to an energy crop that can be planted on requirement. Therefore, the annual maize tonnage and land area requirement for the optimum mixture for co-digestion with cattle manure is examined.

The organic loading rate of the two substrates is assumed at a 1:1 ratio and, thus, an equal VS content of each feedstock in the digester must be established (de Vries et al., 2010). As shown in Table 3-4 above, the VS content of cattle manure is 8.6 %. Therefore, 1 t of cattle manure entering the digester is equivalent to an organic loading rate of 0.086 t. The average VS content of maize is 35 % and so 1 t of maize entering the digester is equivalent to an organic loading rate of 0.35 t. To achieve the required loading ratio, 1 t of maize must be available for every 4 t of manure. In land and livestock terms, 1 ha of maize is required to co-digest 14 t of dairy cattle manure.

The fresh weight ratio of manure to maize is, therefore, 4:1 which provides a total methane and subsequent biogas yield per tonne of mixture shown in Table 3-8 below.

Table 3-8 Methane Yield of Maize and Manure Co-Digestion

Substrate	VS (kg)	Volume CH_4 (m^3/t VS)	Volume CH_4 (m^3/t mixture)
Manure	350	144	51
Maize	350	328	115

The total methane yield from the mixture is the sum of the manure and maize substrates equal to 166 m^3 of methane. Assuming a 60:40 ratio of methane to carbon dioxide in the biogas, the co-digestion yields 277 m^3 of biogas per tonne of mixture. This volume is substantially higher than the biogas yield when the same quantity of either feedstock is digested independently.

Economic Analysis of Energy Crops for Biogas

This sub-section examines the economic analysis of energy crops. The main assumption used is that the crop species already exists on the land area grown and the end usage shifts from the food to the energy markets. Therefore, this analysis accounts only for the variable and not for the establishment costs of the crop[7]. The variable cost components considered include the seed, fertilizer, spray (fungicides, herbicides, insecticides) and harvest costs reported in Table 3-9 below (Nix, 2012).

Table 3-9 Energy Crop Costs

	Cost Component (£/ha)					Min Energy Cost (£/MWh)	Max Energy Cost (£/MWh)
Energy Crop	Seed	Fertilizer	Spray	Harvest	Total	Biogas	Biogas
Barley	63	222	115	85	485	51	95
Maize	170	189	42	96	497	8	17
Oilseed Rape	52	254	136	86	528	211	311
Sugar Beet	171	257	180	355	963	20	32

A comparative review of the cost per biogas potential energy of the species, in Table 3-9 above, indicates a relatively large cost range. This range is mainly due to the growth and biogas yield performance of each

[7] The storage cost of energy crops is accounted for in the capital cost of the conversion technology

species individually. The lowest cost per energy unit is achieved by the Maize species and the highest cost by the oilseed rape species.

Environmental Analysis of Energy Crops

The primary ingredients of fertilizers are Nitrogen (N), Phosphorous (P) and Potassium (K) (Herren, 2011). Table 3-10 below presents the fertilizer demand and embodied energy of each species considered in the UK farming system (FAO, 2007). The embodied energy is defined as the energy input required to manufacture the fertilizer used for cultivation of the examined crops. This input is determined by the fertilizer needs of each crop expressed as the mass per unit area of land (kg/ha) and the specific energy needed to produce 1 kg of each type of fertilizer (MJ/kg). The values of the embodied energy are taken from Dalgaard et al (2001), and are quoted as 50 MJ/kg for Nitrogen, 12 MJ/kg for Potassium and 7 MJ/kg for Phosphorous.

Table 3-10 NPK Requirements of Energy Crops

Energy Crop	Nitrogen		Phosphorous (kg/ha)		Potassium (kg/ha)		Total
	Demand (kg/ha)	Embodied Energy (MJ/ha)	Demand (kg/ha)	Embodied Energy (MJ/ha)	Demand (kg/ha)	Embodied Energy (MJ/ha)	Embodied Energy (MJ/ha)
Barley	188	9400	44	2200	55	2750	14350
Maize	100	5000	47	2350	55	2750	10100
Oilseed Rape	185	9250	45	2250	48	2400	13900
Sugar Beet	100	5000	50	2500	120	6000	13500

Based on this comparison, barley is the most energy intensive by fertilizer requirement species and maize is the least energy intensive with a difference of 4250 MJ/ha between each species.

Biogas Fuel Form Energy Crop Species Assessment Tool

This sub-section presents the biogas energy crop species selection tool using the MCA analysis technique. The criteria, and subsequent elements driving these criteria, are initially identified and explained. The species performance scoring mechanism and final MCA tool are then presented. The implementation of this tool on two or more species can then be used to identify the species that will satisfy the decision-

making indicators.

MCA Analysis Criteria

Since this study bases the decision-making process on the economic and environmental indicators, the MCA allocates a criterion to represent each metric. Furthermore, as the potential energy content is identified above as the main factor affecting the performance of each indicator, an energy yield criterion is also introduced. The elements driving each of these criteria are defined and explained in the respective sub-sections below.

It must be noted that this is an indicative and not exhaustive MCA analysis since there may be other factors, such as the cost of crop storage, which could potentially drive the selection to another species not consistent with the output of this tool.

Energy Yield Criterion

The Energy Yield criterion is comprised of 3 elements that are the VS content, the Bio-Methane Potential and the crop yield discussed previously. Each element is considered to have the same relative importance with respect to the overall energy yield.

Economic Criterion

This study assumes that the crops are already established on arable land and that their use as a fuel is the shift from the food to the energy supply. Therefore, the economic criterion is comprised of the annual O&M cost that includes the cost of maintaining, fertilizing and harvesting the crop for preparation into the required form.

Environmental Criterion

The environmental analysis discussed above has identified the fertilizer requirement as the main embodied energy of a crop species. The embodied energy determines the gross emissions and, thus, the emissions reduction indicator of the proposed supply, expressed as the energy requirement per unit of potential energy unit (MJ/MJ).

Implementation of the Energy Crops Species Selection Tool

The application of the MCA analysis, used to identify the most favourable species under the indicators, is

a five-step process. These steps are listed and explained in further detail below.

1. Collection of site-specific information for each element per species
2. Scoring of elements per species
3. Selection of category weighting value
4. Final result per species
5. Sensitivity analysis

Step 1 - Collection of Necessary Site-Specific Element Data per Species

The quantitative and qualitative data per species, required to complete the first step of the MCA, is available in the respective energy crop resource assessment section above.

Step 2 – Scoring of Elements per Species

This step is conducted to populate the MCA table with the comparative scores for each element. The energy yield element is scored numerically ranging from 1-10 where the most favourable species is also the one with the largest value, i.e. the species with the highest energy yield per unit area is scored with a 10. The economic and environmental elements are populated with qualitative information ranging between very low, low, medium, high and very high, which are then converted to numerical data ranging equally between 0 and 10.

The most favourable species of the two latter criteria are those with the smallest numerical score. Therefore, the elements of these criteria are scored by inversing the 0-10 values to allow an even comparison of these elements and species.

Step 3 – Selection of Category Weighting Value

The element's weighting value depends on its relative importance amongst other elements, governed by the user's strategy (DCLG, 2009). For example, if the O&M cost is considered twice as important as the other elements, due to its continuous cost requirement, it is weighted with a value of 2 and the other elements with a value of 1.

Step 4 – Final Result per Species

This step is required to calculate the final score of each crop species and is conducted by substituting the element score and weight value from steps 2 and 3 above in Equation (3-27) below.

$$Species\ Score = (a * w1) + (b * w2) + (c * w3) \quad \textbf{(3-27)}$$

The energy crop species with the highest scoring value is identified as the most preferable species to be used in the resource component of the energy supply mix.

Step 5 – Sensitivity Analysis

On completion of the MCA, a sensitivity analysis must be conducted to identify the robustness of this methodology and the results obtained. This is conducted by repopulating the MCA, both with the minimum and the maximum values of the reported species range performances. The results of each part of each range extremity can then be compared and further examined to understand the sensitivity level of the selection process. If there is a high sensitivity, the elements causing this can be identified and further risk mitigation techniques can be developed to minimize this effect.

MCA Analysis Structure – Biogas Fuel Form

The functional structure of the MCA analysis is shown, in Table 3-11 below, where *w1–w3* are the weighting values and *a-c* are the element scores.

Table 3-11 Biogas MCA Functional Structure

Criteria	Energy Yield	Economic	Environmental
Elements	Energy Yield (MWh/ha) Function of [VS, BMP, Growth]	O&M (£/t)	Fertilizer Demand (MJ/MJ)
Weighting	*w1*	*w2*	*w3*
Performance	*a*	*b*	*c*

3.2.2.1.3 Refuse

This sub-section presents the methodology developed for the potential energy assessment and economic analysis of the MSW and C&I refuse categories. Due to the multiple waste constituents and management techniques, Article 4 of the revised EU Waste Framework Directive known as the 'waste hierarchy' is used to identify the suitable waste for biogas generation.

Potential Energy Content of Biogas from Refuse

A summary of the waste hierarchy strategy is shown in Figure 3-19 below. The hierarchy strategy advises that where possible prevention and re-use is prioritize for all waste products (EC, 2008).

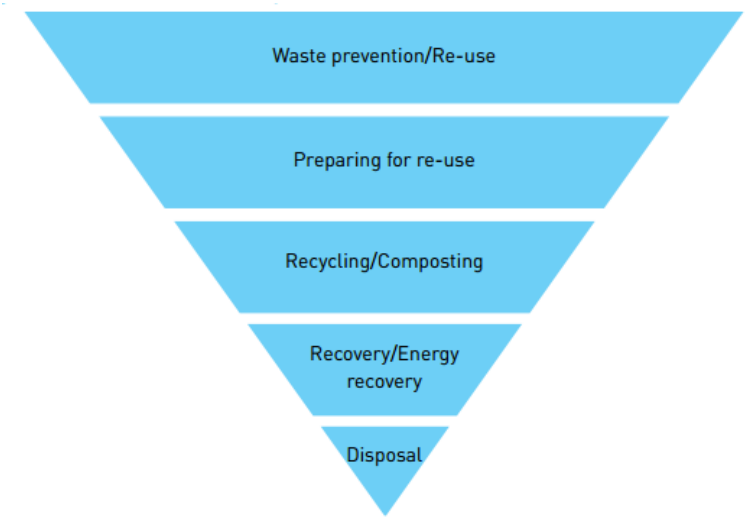


Figure 3-19 Waste Management Hierarchy (EC, 2008)

Current research shows that the anaerobic digestion of food is an environmentally superior recovery technique to composting and other options. This is also true for garden and green waste that require a dry anaerobic digestion recovery. Based on the UK government's approach to waste management and the waste hierarchy, this study assumes that any type of refuse waste that cannot be recycled or reused should be moved to the energy supply mix for anaerobic digestion (DEFRA, 2007). Therefore, this study assumes that food and green waste are used as feedstock for biogas generation.

To assess the biogas energy content of raw MSW and C&I waste, the quantity of each category's food and green waste constituents is required. Typically, the refuse waste quantity is recorded on a total annual basis per unit mass, which is converted to its individual constituents using the England average MSW shown in Figure 7.5 and C&I waste compositions shown in Figure 7.6 of Appendix A.

Table 3-12 below shows the performance of the food and green waste materials in terms of their potential energy yield performance. The feedstock characteristics of food and green waste from MSW and C&I are assumed as the same and, thus, no differentiation in energy content is made.

Table 3-12 Biogas Yield Performance of Waste Material

Waste Material	VS Content (M_{VS}/M_T) (Banks, 2007)	Biogas Yield (m^3/M_{VS})	Biogas Yield (m^3/M_T)	Potential Energy Content (kWh/ M_T)
Food Waste	0.08	500-600	40-48	240-288
Green Waste	0.63	200-500	108-315	648-1890

Economic Analysis of Refuse

This sub-section presents the economic analysis of biogas from refuse in terms of the raw feedstock and biogas yield costs of MSW and C&I waste. A refuse AD plant charges the authority or private firm a gate fee for waste collection and so the feedstock cost for the plant operators is a financial income and not an expense. The Waste Resources and Actions Programme (WRAP) reports a median fee of £41 per tonne which is equivalent to £ 0.15 per kWh of biogas potential energy (WRAP, 2012).

In order to achieve an effective digestion due to the presence of wood, a "dry" AD system operating at a longer degradation time is needed to handle green waste. The number of this type of AD plant is currently limited in the UK (DEFRA, 2011a). Furthermore, the WRAP report does not include a gate fee cost of garden waste since it is typically composted and not digested.

Assessment of Biomass Feedstock for the Solid Biomass Utilizable Fuel Form

This section presents the methodology for assessing the economic and environmental indicators of the biomass categories utilized as a solid fuel form. The potential energy content is a function of the energy density and annual yield tonnage per land area used for crop growth. A normalized format of potential energy content, per unit area of land, is used to compare the different species. The methodology is implemented in the energy crop and forestry waste biomass. The construction of the MCA analysis for energy crops is then presented for optimum species identification.

3.2.2.2 Potential Energy Content of Solid Biomass Feedstock

The efficiency of the solid biomass conversion technologies is based on the LHV and, therefore, the energy density, considered as an element affecting the energy yield of the crop, is also considered in terms of the LHV (Petchers, 2003). The amount of useful heat, per mass of the crop, is affected by the crop's moisture content as it reduces the available energy from combustion. This moisture content is expressed as a percentage of the crop weight and is reported as the relative content in relation to the LHV (McKendry, 2001). The LHV and moisture content relationship is shown, in Figure 3-20 below, for the miscanthus energy crop and wood forestry waste categories (BEC, 2011). The LHV of both species exhibit a linear relationship with moisture content and a similar gradient between each other.

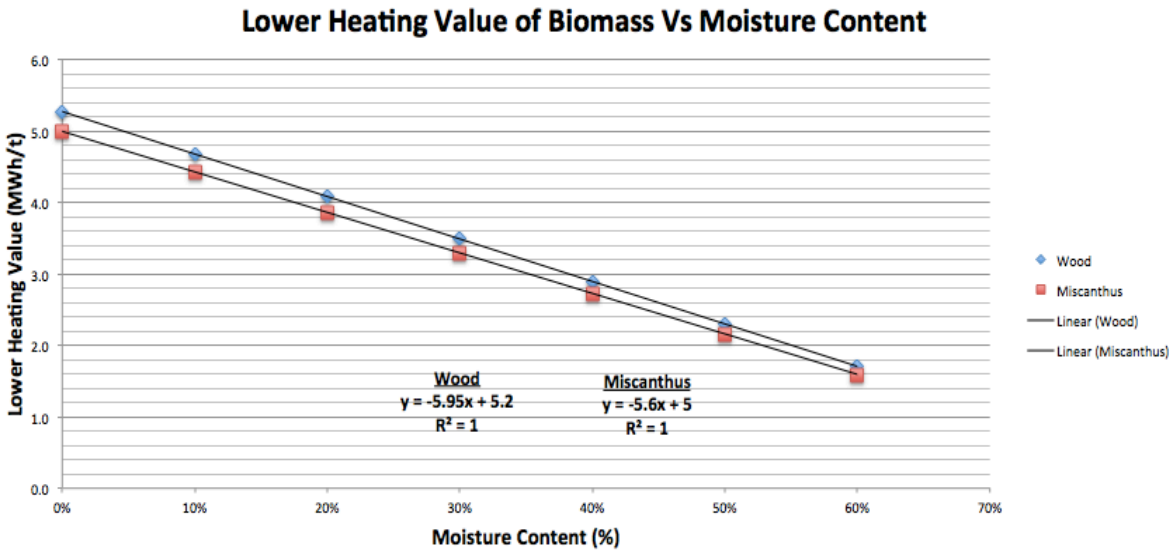


Figure 3-20 Lower Heating Value for a Range of Biomass Moisture Contents

The production of a crop species is based on the ability of the geographic region investigated to grow the species. The expected crop mass per area of land is described as the crop growth. It is considered as a factor of the potential energy content in terms of the raw mass per unit area (t/m^2).

3.2.2.2.1 Energy Crops

This sub-section presents the potential energy and economic analysis of the energy crops that can be used for solid form utilization. The environmental analysis is conducted using the fertilizer demand of each species. The energy crop species selection tool, developed to identify the most favourable species for solid form utilization based on the decision-making indicators, is also presented.

Potential Energy Content of Energy Crops for Solid Utilization

Perennial biomass crops can offer sustainable bioenergy production when established on sub-prime arable land and, thus, avoid the food-energy land usage competition. This is because perennial crops recycle the majority of their nutrients and so require less fertilizer input (Karp & Shield, 2008).

In the UK, two species of perennial energy crops, grasses and coppiced tress, are envisaged for large-scale deployment in the energy industry. Of these, miscanthus and Short-Rotation Coppice (SRC) willow are the most agronomically advanced and common in terms of existing plantings and are, therefore, further considered in this study (Winter & Lobley, 2009).

Table 3-13 below presents the production yield potential, based on average UK values, of both species (Nix, 2012). The energy content reduces as moisture content increases and, thus, Table 3-13 below

divides the LHV ranging from the oven dry tonne (odt) to 20 % moisture content considered a maximum for practical conversion of biomass to useful energy (Breeze, 2005).

Table 3-13 Annual Potential Energy Content of Perennial Crop Species

Species	Yield (odt/ha)	LHV (MWh/t)	LHV (MWh/t)	LHV (MWh/t)	LHV (MWh/ha)	LHV (MWh/ha)	LHV (MWh/ha)
		Oven Dry Tonne	10% Moisture Content	20% Moisture Content	Oven Dry Tonne	10% Moisture Content	20% Moisture Content
Miscanthus	14	5	4.4	3.9	70	61.6	54.6
SRC Willow	25	5.1	4.5	3.9	127.5	112.5	97.5

Economic Analysis of Energy Crops for Solid Utilization

Miscanthus and willow are envisaged for establishment on rough grazing land, specifically for end usage in the energy chain. Therefore, the reallocation of land usage must be accounted for which is achieved by including an establishment cost in the economic analysis. The cost components required are listed and analyzed in further detail below.

1) Annualized Establishment and Maintenance
2) End Form Preparation - Chipping or Pelletizing
3) Transportation

Annualized Establishment and Maintenance Costs

The annualized establishment and maintenance costs for each species are shown in Table 3-14 below (Nix, 2012). The establishment costs are annualized, using a 5 % discount rate over a 20-year period[8]. Even though willow is harvested every 3 years, this cost component is presented as the equivalent cost per annum which is the normalized time period used in this assessment.

[8] 20 years is the minimum standing lifetime of both crops before replanting is required

Table 3-14 Annualized Establishment and Maintenance Costs

Process	Miscanthus			Willow		
	(£/t)	(£/ha)	(£/MWh)	(£/t)	(£/ha)	(£/MWh)
Annualized Establishment	22	310	4.4	10	250	3
Fertilizer	1	14	0.2	2	48	0.4
Harvest	5	70	1	14	350	2.8
Drying (Caslin et al., 2010)	10	140	2	10	250	2

End Form Preparation - Chipping and Pelletizing Costs

As the envisaged service of these crops is to fuel biomass boilers, the cost of chipping and pelletizing are considered and shown in Table 3-15 below (E4tech, 2010).

Table 3-15 Biomass End Form Preparation Costs

Form	Cost (£/t)	Cost (£/MWh)
Chips	10	2
Pellets	34	6.8

Transportation Cost

The main factors affecting the transportation costs are the energy density of the product and distance transported. The cost ranges for the bulk road transportation of oven dry chips and pellets are shown in Table 3-16 below (E4tech, 2010).

Table 3-16 Biomass Chips and Pellets Transport Costs

Biomass Type	Transport Cost (£/odt km)	Transport Cost (£/MWh km)
Chips	0.35 – 0.69	0.07 – 0.14
Pellets	0.27 – 0.51	0.05 – 0.10

The transport costs in Table 3-16 above indicate a large range for both chips and pellets. This range is also sensitive to diesel prices and so average prices of £ 0.52 / odt for chips and £ 0.39 / odt for pellets are considered in this study. It must be noted that the transport costs relate to oven dry tonnes and so an increase in moisture content will decrease the density of biomass transported, thus increasing the overall cost. As expected, chips incur a larger transport cost than pellets due to their lower density.

Total Cost of Energy Crops

The final cost per unit of potential energy for both species is shown, in Table 3-17 below, at 10 % moisture content considered realistic for utilization. For indicative purposes, a transport distance of 30 km is assumed, using the average transport costs previously reported.

Table 3-17 Costs per Unit Energy of Miscanthus and SRC Willow

Species	Miscanthus		SRC Willow	
Form	Chips	Pellets	Chips	Pellets
Cost per Unit Energy (£/MWh)	13	20	20	30

Environmental Analysis of Energy Crops for Solid Utilization

As with the energy crops for biogas utilization section above, the environmental analysis of the energy crops for solid utilization is based on the NPK requirement of each species[9]. The annual mass requirement, per hectare of land, and the total embodied energy of each species is shown in Table 3-18 below (Uellendahl et al., 2008).

Table 3-18 Annual NPK Requirements and Embodied Energy of Miscanthus and SRC Willow

		Miscanthus	SRC Willow
Fertilizer Demand	N (kg/ha/year)	90	100
	P (kg/ha/year)	6	6
	K (kg/ha/year)	45	45
Embodied Energy	Total NPK (MJ/MJ)	0.02	0.02

Solid Fuel Form Energy Crop Species Assessment Tool

The MCA for biogas and solid biomass is identical in the scoring and weighting techniques. There are two differences in terms of the elements used in the functional structure. The first difference is that, since the main factors of the potential energy content of a solid biomass fuel are identified above as the LHV, moisture content and crop growth performance, these are the factors used in the MCA tool as the elements of the energy yield criterion. These factors are considered to have an equal importance to the overall energy yield element. The second difference is that since solid biomass plantations are expected to

[9] The embodied energy for the production of N = 50MJ/kg, P = 12 MJ/kg and K = 7MJ/kg (Dalgaard et al., 2001).

be new establishments and not entering the energy chain from the food chain, a capital cost is involved and considered as of equal importance to the O&M cost in the economic element.

3.2.2.2.2 Forestry Waste

Forestry waste is considered as a renewable, sustainable and low carbon alternative to fossil fuels (Mokyr, 1985). This section presents the methodology developed in this study to assess the potential energy content and economic indicator of forestry waste.

The classification of wood types is divided into two main species known as broadleaf and coniferous wood (Hart, 1991). The main difference between the two is that the wood from broadleaf is denser than conifer. Therefore, the broadleaf species will burn for a longer period of time in comparison to the same volume of the coniferous species and will also require less space for storing the same potential energy content (FC, 2009).

Potential Energy Assessment of Forestry Waste

To calculate the potential energy of wood fuel per forestry area, the wood species volume (m^3/ha) and energy content (MWh/m^3) are required. This depends on the species of wood, classified above as coniferous or broadleaf. The wood fuel proportion, per forestry area, is reported in the latest wood fuel progress report published by the Forestry Commision, shown in Table 3-19 below, with the LHV and annual yield performance of each wood species (Woodcock, 2012). The breakdown of each species is not available in forestry surveys in the UK and so this study considers that a mixed wood category, characterized by the average performance of broadleaf and conifer, is present.

Table 3-19 Yields and Energy Content of Broadleaf Species

Species	Wood Fuel Proportion (%)	Total Annual Yield (m^3/ha/year)	LHV (MWh/m^3)	LHV (MWh/ha/year)
Broadleaf	50	8	2.5	10
Conifer	50	4	1.8	3.6
Mixed	50	6	2.2	6.6

Economic Analysis of Forestry Waste

A breakdown of the estimated production costs and average wood fuel type is presented in Table 3-20 below (FC, 2009a). As shown, the expected costs are subject to a wide variation. For example, harvesting

shows a cost per tonne (£/t) ranging from 8-20. The exact cost depends on weather conditions at the time of harvesting, which is difficult to forecast and quantify.

Table 3-20 Wood fuel cost requirements and market value (FC, 2009a)

Activity	Cost Range (£/t)
Harvesting	8 - 20
Extraction	3 – 8
Processing	8 - 44
Transportation	2 - 11

By choosing the average costs, shown in Table 3-20, the potential energy cost is 2.3 p/kWh.

3.2.3 Stochastic Resource Assessment

This section presents the potential energy assessment and economic analysis of the stochastic resource type using wind energy as an example. The energy content is proportional to the cube of the wind speed, which is determined by the Weibull frequency distribution. The estimation technique of the speed at different heights to those recorded is also presented.

Potential Energy Assessment of the Wind Resource

This sub-section presents the methodology used to calculate the potential energy content at a wind site. A classification system using a numerical range of 1 – 7 and a qualitative description of each class in terms of the potential energy at the site is used (Elliott et al., 1986).

Since the meteorological data sets required may not be recorded or provide for the required vertical height above ground level, a vertical wind shear assessment is presented to calculate the expected wind speeds at a range of heights.

Input Data Requirements of Wind Assessment Methodology

The data required includes the wind speed recorded at a time resolution of at least one-hour intervals, wind direction and air density, recorded at a 50 m vertical height for a period of at least 12 months, which is standard procedure for reporting a wind class (Manwel et al., 2002). In case this particular data set is unavailable, the vertical wind shear technique, explained below, is used to adapt the available data set to 50 m. The 12-month period is required to cover the four seasons and, thus, gain a complete understanding

of the wind characteristics over the course of a year. Furthermore, a description of the topography is required in order to calculate the rate of change of wind speed with increase in vertical height.

Potential Energy Content of the Wind Resource

The energy yield is the factor that considers the level of intensity and duration and, thus, the suitability of the wind resource over a 12-month period. The energy yield is expressed as the integral of the wind power (P_w) over the time period investigated, as shown in Equation (3-28) below (Gipe, 2004).

$$E_w = \int P_w dt \tag{3-28}$$

Where P_w is expressed in Equation (3-29) below

$$P_w = \frac{1}{2} A\, p\, V^3 \tag{3-29}$$

Where A = cross sectional area of wind flow; ρ = density of air (kg/m^3) and V = wind speed (m/s). Due to the fact that the power in the wind varies with the cube of the wind speed, a small change in wind speed leads to a large change in the available power. To assess the maximum extractable power from the wind, an account of the wind conversion technology must be included. This is achieved by introducing the Betz limit, a power coefficient expression that considers the maximum fraction of power garnered from the wind. This limit, C_p, is 0.593, thereby, modifies Equation (3-29) above to derive the maximum extractable wind power, P_{MAX}, in Equation (3-30) below (Betz, 1920).

$$P_{MAX} = C_p \frac{1}{2} A\, p\, V^3 \tag{3-30}$$

Due to the stochastic nature of this resource and the critical effect that wind speed has on power generation, the level and duration of the wind speed is required to determine the extractable energy content. A detailed assessment of the energy yield factor requires the identification of the wind speed range and the presence of this speed on an annual scale. The methodology followed to calculate the energy yield is a three-step process. The first step is the calculation of the vertical wind shear at a range of heights above ground level. The second step is the calculation of the maximum probability of a wind speed and the third step is the calculation of the wind power density of the vertical cross-sectional area parallel to the wind flow.

Step 1 - Vertical wind shear

The vertical wind shear analysis is conducted by using the logarithmic law, the origins of which come from boundary layer fluid mechanics (Kubik et al., 2011). On flat terrain and in neutral conditions, Equation (3-31) expresses the change of wind speed as a function of surface roughness (Prandtl, 1935).

$$V(h) = \frac{V_o}{k} \ln\left(\frac{h}{z_o}\right) \quad \textbf{(3-31)}$$

Where $V(h)$ is the horizontal velocity at height h; V_o is the friction velocity; z_o is a measure of the surface roughness and k is the von Karman constant equal to 0.41 (von Karman, 1931). When the wind velocity V_1 is known at a height h_1 and required at a height h_2 then Equation (3-32) below can be derived from Equation (3-31) above.

$$V_2(h_2) = V_1(h_1) \frac{\ln\left({}^{h_2}/_{z_o}\right)}{\ln\left({}^{h_1}/_{z_o}\right)} \quad \textbf{(3-32)}$$

Where V_1 is the known wind speed at height h_1 and V_2 is the target wind speed at height h_2. The surface roughness constant is chosen, from Table 3-21 below, and represents the effect that different topographies have on vertical wind shear.

Table 3-21 Surface roughness constant per land topography (Tong, 2010)

Surface Roughness (m)	Land Topography Description
0.0002	Water surface
0.03	Agricultural area, few scatter buildings
0.1	Agricultural area, tall plantations
0.4	Small town, rough uneven terrain
0.8	Large city
1	Large city, skyscrapers

The logarithmic law can be demonstrated in Figure 3-21 below using a sample wind speed of 5 m/s at a recorded vertical height of 10m for a range of sites defined by varying the surface roughness values in Table 3-21 above.

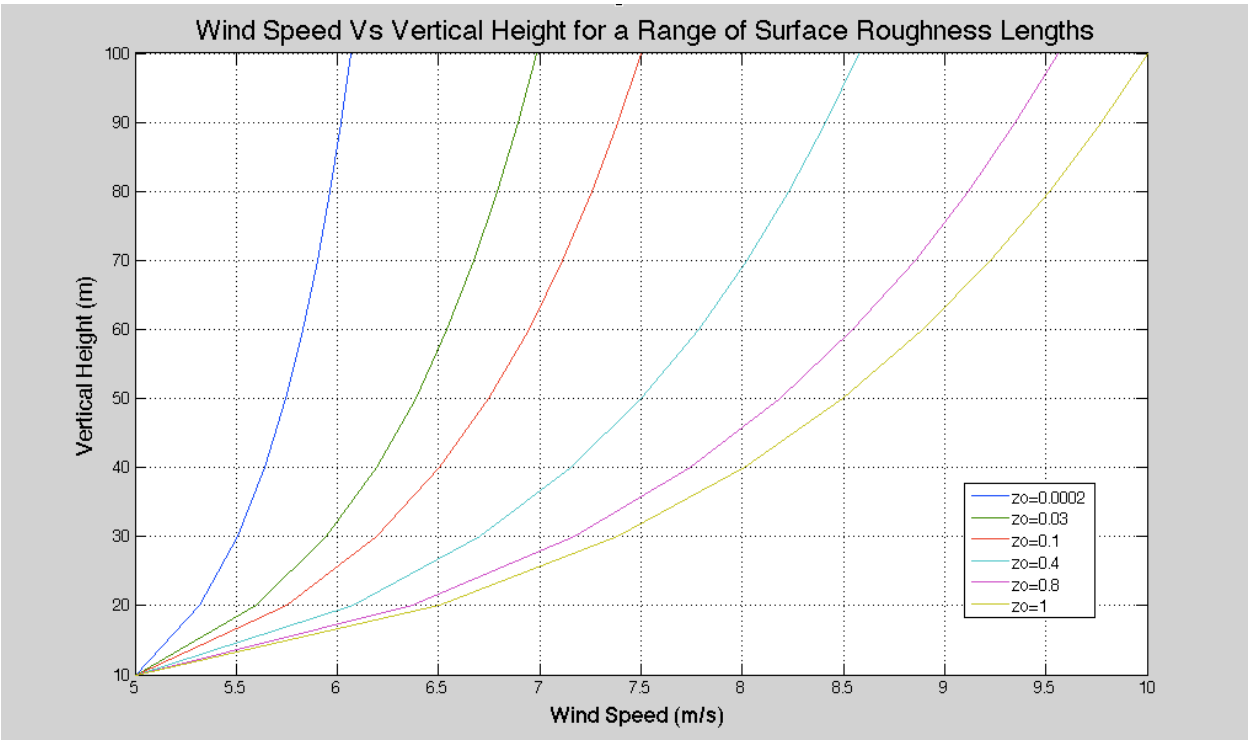


Figure 3-21 Wind Speed Vs Height for a Range of Surface Roughness Lengths using the Logarithmic Law

The graph, in Figure 3-21 above, illustrates that there is a higher rate in wind speed increase for sites with a higher surface roughness length.

The analysis provides the increased rate of wind speeds with height and, thus, the economic feasibility of installing taller wind turbines in terms of the increased energy output. The results are then used to find the maximum probability of a wind speed occurring at the respective extrapolated vertical heights.

Step 2 - Wind Speed Occurrence Probability

As the power in the wind varies largely with the cube of the wind speed and because the wind resource is stochastic in nature, knowledge and use of the mean annual wind speed is insufficient and misleading for the calculation of the wind energy content. Therefore, the frequency distribution of the wind speed at a particular site must be calculated. By creating a histogram of wind speeds with bin sizes of 1m/s intervals from 0m/s to the maximum wind speed present, the percentage frequency is plotted on the *y*-axis and the respective wind speed interval on the *x*-axis. Based on empirical results, the shape of the frequency distribution of a wind site has shown to fit well with the Weibull distribution, which is currently the most commonly used probability distribution for the description of wind speeds (Wizelius, 2007). The Weibull distribution is, therefore, used to calculate the probability of all wind speed ranges occurring and, thus, the maximum wind speed probability as shown in Equation (3-33) below (Stevens & Smulders, 1979).

$$f(u) = \frac{k}{c}\left(\frac{u}{c}\right)^{(k-1)} exp\left[\left(\frac{u}{c}\right)^{k}\right] \quad \textbf{(3-33)}$$

The Weibull distribution is governed by the unit less shape parameter *k* and the scale parameter *c* that will affect the shape and size of the curve respectively whilst maintaining the area under the graph constant. Finally, the observed maximum occurrence probability wind speed value on the Weibull curve is used as the speed for further calculations of the wind energy content.

Step 3 – Wind power density

The wind power density (W/m^2) is calculated, using Equation 9 above, where the air density value is used from the average air density obtained from the recorded data and the wind speed is the Weibull curve peak found in Step 2. The power density is then allocated to the subsequent wind class range found using Table 3-22 below (NREL, 2011a).

Table 3-22 Wind resource potential per class

Wind Class	Average Wind Speed (m/s)	Cross-sectional surface area requirement per unit of wind power (W/m^2)	Resource Potential
1	0 - 5.6	0 - 200	Poor
2	5.6 – 6.4	200 - 300	Poor
3	6.4 – 7.0	300 - 400	Fair
4	7.0 – 7.5	400 - 500	Good
5	7.5 – 8.0	500 - 600	Excellent
6	8.0 – 8.8	600 - 800	Outstanding
7	8.8 – 11.9	800 - 2000	Superb

The main drawback of solely relying on the wind class for decision-making is that the temporal variation of wind speed cannot be deduced. Further analysis must be made at the seasonal and diurnal temporal scales, particularly if there is an envisaged co-operation between wind and other resources.

Economic Analysis of the Wind Resource

The stochastic nature of this resource requires good knowledge of the wind potential. A feasibility study comprised of the wind speed, direction and density readings must be conducted at a 15 – 30 minute resolution range for a minimum period of 12 months. This service is expressed as a budgetary cost of £

19/kW_e of the envisaged installed wind capacity and is used in the total annual cost calculation as an inclusion in the capital cost of the wind technology (Ozerdem et al., 2006).

3.3 Available Renewable Energy Conversion Technologies

This section presents the methodologies developed to assess the available conversion technologies under the decision-making indicators used in this study. The Anaerobic Digestion, Gasification, Photovoltaic and Wind Turbine technologies, which utilize the resources examined above, are considered in this section. The Battery Storage technology, which can store energy from any of the aforementioned technologies, is also examined in this section.

To calculate the decision-making indicators per unit of each technology, the hourly power and annual energy generation is required. The results are then used to consider the technology individually and as a component of the overall renewable energy supply mix.

3.3.1 Anaerobic Digestion Technology

This section examines the assessment of the Anaerobic Digestion technology using the indicators of this study. A summary of the AD supply mix is shown in Figure 3-22 below.

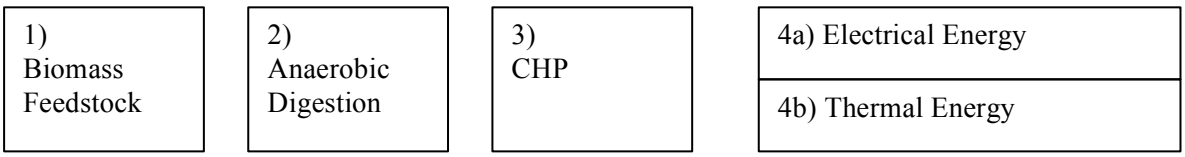


Figure 3-22 Anaerobic Digestion Supply Mix

Since the AD process fuels the CHP unit, the optimal operating strategy of this generator is initially established under the decision-making indicators of this study. An economic and environmental analysis of this supply mix is then examined in further detail.

Combined Heat and Power Operational Strategy

A CHP unit provides a simultaneous supply of electrical and thermal energy and, thus, operates at a higher total efficiency than an individual electrical or thermal generator. The most cost-effective operational strategy requires the maximum possible useful energy generation. Therefore, the AD CHP plant must be considered as a continuous load system with an annual capacity factor of 90 % to allow for maintenance and fault time (IPCC, 2012).

Economic Analysis of the Anaerobic Digestion Technology

This sub-section presents the economic factor of the AD technology by using the relevant cost data from the Arup (2011), review on generation costs in the UK (ARUP, 2011). The two costs examined are the capital cost and the operation and maintenance per installed capacity.

The capital cost of an Anaerobic Digestion plant is driven by the digestion and feedstock processing, storing and handling equipment and the power generation equipment (ARUP, 2011). Food waste plants are considered to be more capital intensive than manure or crop systems, due to the requirement of additional pre-processing equipment. Plants with a larger installed capacity experience economies of scale since the required equipment does not increase linearly with size (ARUP, 2011). A capital cost comparison of the farm and food waste AD systems is shown in Table 3-23 below.

Table 3-23 Capital Costs of Farm and Food Waste Anaerobic Digesters

Feedstock Type	High (£ million /MW_e)	Median (£ million /MW_e)	Low (£ million /MW_e)
Farm Waste	6.7	3.9	1.7
Food Waste	6.9	5.2	3.7

The operating costs of an Anaerobic Digestion plant are principally driven by the labour required to operate and maintain feedstock processing, digestion and generation equipment. Larger plants experience noticeable economies of scale since cost items, such as labour, do not increase linearly with capacity (ARUP, 2011). Cost variations between projects are mainly due to economies of scale and feedstock types examined in further detail in Table 3-24 below.

Table 3-24 Operation and Maintenance Costs of Farm and Food Waste Anaerobic Digesters

Feedstock Type	High (£ million /MW_e)	Median (£ million /MW_e)	Low (£ million /MW_e)
Farm Waste	1.0	0.8	0.4
Food Waste	0.7	0.5	0.2

Environmental Analysis of the Anaerobic Digestion Technology

This sub-section examines the GHG emissions savings of displacing conventional energy generation with the Anaerobic Digestion of biomass. Zwart & Kuikman, (2011) presented a detailed methodology for calculating these GHG using Equation (3-34) below (Zwart & Kuikman, 2011).

$$GHG\ Reduction = Energy\ Related\ GHG\ Savings + Other\ Related\ GHG\ Savings \quad \textbf{(3-34)}$$

The "Energy Related GHG Savings" component is consistent for each of the biomass types previously examined. The "Other Related GHG Savings" are feedstock specific.

The "Energy Related GHG Savings" are calculated in Equation (3-35) below.

$$Energy\ Related\ GHG\ Savings = GHG(A + B) - (C + D) \quad \textbf{(3-35)}$$

GHG A is expressed in Equation (3-36) and *GHG B* is expressed in Equation (3-37) below.

$$GHG\ A = A * GHG_{electricity} \quad \textbf{(3-36)} \qquad GHG\ B = B * GHG_{gas} \quad \textbf{(3-37)}$$

Where A is the net electricity generated (kWh_e) from the AD system and, thus, avoided from the grid calculated in Equation (3-38) below; $GHG_{electricity}$ is the GHG emissions of the electricity grid ($kgCO_2/kWh_e$) ; B is the net thermal energy generated from the AD system (kWh_{th}) and, thus, avoided from the grid calculated in Equation (3-39) below and GHG_{gas} is the GHG emissions of grid natural gas ($kgCO_2/kWh_{th}$)[10]. Since the CHP unit output is thermal energy, the gas emissions factor must be converted from the combustion emissions to thermal energy generated. The efficiency is assumed at 86 % as this is the minimum efficiency requirement under UK building regulations for new and existing dwellings (EnergySavingTrust, 2008).

$$A = gross\ electricity\ production - digester\ parasitic\ electrical\ consumption \quad \textbf{(3-38)}$$

$$B = gross\ thermal\ production - digester\ parasitic\ thermal\ consumption \quad \textbf{(3-39)}$$

The parasitic electricity consumption is 9.2 kWh_e / t feedstock and parasitic thermal consumption is 43.6 kWh_{th} / t feedstock (Zwart & Kuikman, 2011). This mass requirement per feedstock differs and so the total parasitic digester consumption is a factor of the feedstock type. (DEFRA, 2009)

GHG C is the GHG emissions from transporting biomass expressed in Equation (3-40) below.

[10] The equivalent carbon dioxide emissions factor for electricity generated by the UK national grid is 0.457 $kgCO_2$ / kWh_e. The equivalent carbon dioxide emissions factor for thermal energy generated by natural gas combustion from the UK national gas grid is 0.184 $kgCO_2/kWh_{th}$ (DEFRA, 2009)

$$GHG\ C = C * GHG_{\ biomass\ transport} \quad \textbf{(3-40)}$$

Where *C* is the embodied energy of the diesel fuel required for transporting the biomass (kWh) and $GHG_{biomass\ transport}$ is the carbon dioxide emissions factor per unit energy in the diesel fuel ($kgCO_2$/kWh). A typical 30 t payload truck consumes 33.6 litres of diesel / km and, therefore, emits 0.88 $kgCO_2$ / km (DAF, 2007).

Variable *D* is only applicable to energy crop AD systems and represents the GHG emissions from crop production and fertilizer usage combined in Equation (3-41).

$$GHG\ D = Maize\ Area * 1350 \quad \textbf{(3-41)}$$

Where the *Maize Area* is the land area used for crop growth (ha) and 1350 is the emissions factor ($kgCO_2$ / ha) of maize cropping, seed, pesticide and fertilizer production (Zwart & Kuikman, 2011).

The *"Other Related GHG Savings"* account for the avoided carbon dioxide emissions due to the utilization of a biomass in the AD system.

The *"Other Related GHG Savings"* of animal waste digestion are the avoided emissions from methane production and emissions during storage. This analysis assumes that storage emissions are reduced by 95 %. The avoided methane emissions from the digestion of animal waste are 4.65 kg CH_4/t, equivalent to 4.88 kgCO2 / t of waste (Zwart & Kuikman, 2011)[11].

Energy crops are not included in this part of Equation (3-34) because they are grown and harvested specifically for this process and not diverted from another system or supply chain.

The avoided equivalent carbon dioxide emissions, due to the anaerobic digestion of refuse, is the reduction of food waste in landfill sites that undergo an uncontrolled decomposition to generate and emit methane (Metz, 2001). The avoided emissions from digesting and not landfilling refuse is 500 kg CO_2/t of refuse (DEFRA, 2011).

The construction of Equation (3-35) is shown, in Table 3-25 below, for a 1 MW_e CHP (1.12 MW_{th}). The non-energy related emissions (*GHG C* and *GHG D)* are weighted per useful energy output using the proportion of each type of conversion efficiency to the total system efficiency.

[11] The equivalent carbon dioxide conversion assumes a methane global warming potential of 25 over a 100 year time period (Boucher et al., 2009).

Table 3-25 GHG Emissions Reduction due to the Operation of a 1 MW_e Anaerobic Digester

GHG Reduction Component	Animal Waste ($kgCO_2$ reduction)	Energy Crops ($kgCO_2$ reduction)	Animal Waste + Energy Crops Co-Digestion ($kgCO_2$ reduction)	Refuse ($kgCO_2$ reduction)
GHG A	389	448	451	418
GHG B	67	210	215	137
GHG C	14.3	1.8	1.3	8.1
GHG D	300	68.5	254	0.5
Electric Savings ($kgCO_2/MWh_e$)	529	482	573	422
Thermal Savings ($kgCO_2/MWh_{th}$)	231	247	349	142

The emissions reduction factors show that the co-digestion of animal waste has the highest emissions savings per unit energy generated. This is due to the highest energy potential this combination can offer compared to other biomass sources.

3.3.2 Gasification Technology

This section examines the assessment of the gasification technology using the indicators of this study. The solid biomass energy crops and forestry waste are considered as suitable feedstock for this technology. A summary of the gasification supply mix is shown in Figure 3-23 below.

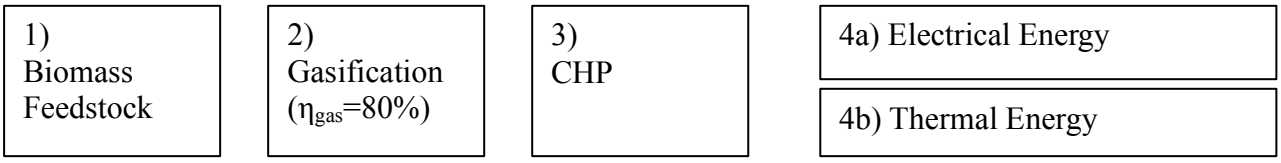


Figure 3-23 Gasification Supply Mix

It is noted that the Gasification and AD supply mix have a similar order apart from part 2, the main feedstock processor which, in this case, is the gasification of biomass. The biomass to syngas conversion (η_{gas}) is assumed as 80 % efficient (Peacocke, 2008). Since the gasification fuels the CHP unit, the optimal operating strategy of this generator is similar to that described previously in the Anaerobic Digestion sub-section. The gasification CHP plant is considered as a continuous load plant and so the annual capacity factor is 90 % to allow for maintenance and fault time (IPCC, 2012).

Economic Analysis of the Gasification Technology

This sub-section presents the economic factor of the gasification technology. The costs examined are the capital and the operation and maintenance costs, shown in Table 3-26 below (ARUP, 2011).

Table 3-26 Economic Analysis of Gasification (Solid Biomass Conversion)

Installed Capacity	< 50 MW_e		> 50 MW_e	
£ million /MW_e	Capital Cost	O&M Cost	Capital Cost	O&M Cost
High	3.9	0.25	2.8	0.22
Median	3.3	0.17	2.4	0.14
Low	2.6	0.12	2.3	0.11

The operating costs are principally driven by the labour required to operate and maintain feedstock processing, digestion and generation equipment. The reduction in cost for the higher capacity band (>50 MW_e) is due to the fact that larger plants experience noticeable economies of scale since cost items, such as labour, do not increase linearly with capacity (ARUP, 2011).

Environmental Analysis of the Gasification Technology

This sub-section presents the environmental analysis factor of the gasification technology. The Environment Agency has extensively published emissions savings from biomass feedstock classified as "Good Practice" and "Bad Practice". A summary of the results for the "Good Practice" classification is shown in Table 3-27 below (Bates et al., 2009). The emissions reduction is calculated as the difference between the national grid electricity and gas emissions and the respective biomass emissions. The grid emissions have been discussed in the environmental analysis of Anaerobic Digestion above.

Table 3-27 Environmental Analysis of Energy Crop and Forestry Waste Gasification under Good Practice

Feedstock Format	Feedstock Type	Carbon Dioxide Emissions Reduction	
		Electrical ($kgCO_2/MWh_e$)	Thermal ($kgCO_2/MWh_{th}$)
Chips	Forestry Waste (UK)	432	158
	SRC Willow	414	142
	Miscanthus	412	140
Pellets	Forestry Waste (UK)	362	96
	SRC Willow	207	-42
	Miscanthus	294	36

Table 3-27 above shows that all types of biomass, except for SRC willow pellets, perform at higher environmental standards than the national electricity and gas grids. An audit of the "Good Practice" and "Bad Practice" practice standards is divided into the biomass preparation and conversion sections of the supply chain. The preparation depends mainly on the transportation distance and the nitrogen fertilizer usage that, in turn, affect the biomass lifecycle emissions. For example, UK forestry waste will have a higher environmental performance than the same type of waste imported from the Baltic regions or Canada (Bates et al., 2009). The biomass conversion depends on the electrical and thermal efficiencies of the CHP generator, which in turn depends on the system size. This study assumes an electrical efficiency of 40 % and a thermal efficiency of 45 %.

3.3.3 Energy Storage

This section presents the energy storage element of an energy supply mix. A selection of storage technologies is presented to identify the most suitable technology for the application requirements and decision-making indicators. The mathematical models of the chosen technology, describing the conversion between electrical to stored energy and vice versa, are then presented.

Selection of an Energy Storage Technology

A comparative review of the technical suitability of the different storage technologies is shown in Table 3-28 below (Connolly, 2010). This study aims to create a storage - technology integration to meet demand for a time period of at least 1 day.

Table 3-28 Technical Suitability of Energy Storage Technologies

Technology	Power Rating (MW_e)	Discharge Duration	Renewables Integration	Maturity
Pumped Hydro	100 - 4000	4 - 12h	Suitable	Commercial
Compressed Air	50 - 100	1 - 4h	Suitable	Concept
Lead-Acid Batteries	< 50	1min - 8h	Suitable	Commercial
Nickel Cadmium Batteries	< 50	1min - 8h	Suitable	Commercial
Flywheels	> 1.7	3 - 120 s	Suitable	Commercial
Hydrogen Fuel Cell	< 0.25	As needed	Suitable	Testing

Table 3-28 above shows that the pumped hydro storage and compressed air storage technologies are suitable for power ratings over 50 MW_e. Although the demand levels in the Oxfordshire case study are at this level, the examination of energy storage on the MW_e or GW_e scale is out of the scope of this thesis.

The Flywheel technology has a suitable power rating and commercial maturity but has a discharge duration of 3 – 120 seconds that is too short for the applications required in this study. Since the Hydrogen storage is not currently at the commercial maturity stage, it cannot be considered for immediate installation and so is also further excluded. The commercial maturity and highest discharge duration of up to 8 hours means that the suitable selections remaining, for the purposes of this study, are the Lead-acid and Nickel-cadmium batteries. However, the higher efficiency of the Lead-Acid battery and its power rating cost that ranges from £ 125/kW_e - £ 375/kW_e provides a more cost-effective option than the Nickel-cadmium power rating cost of £ 390/kW_e - £ 970/kW_e (Connolly, 2010). Therefore the Lead-Acid battery is the only storage option considered further in this study.

Lead Acid Battery Capacity Model

This sub-section presents the hourly energy storage model of a Lead-acid battery. Since the battery is used to complement the renewable energy sources of a supply mix, the battery's charging or discharging mode depends on whether there is an energy deficit or surplus.

Battery Charging Mode

In the case of a surplus, the battery is charging and is modelled using Equation (3-42) (Borowy, 1996)

$$E_B(t) = E(t-1) + \left(E_{G(t)} - \frac{E_{L(t)}}{\eta_{inv}}\right).\eta_{batt,in} \quad \textbf{(3-42)}$$

Where $E_B\ (t)$ and $E_B\ (t\text{-}1)$ is the energy stored in the battery at hours t and $t\text{-}1$ respectively; $E_G\ (t)$ is the energy generated from the renewable technology; $E_L\ (t)$ is the energy demand at time t; η_{inv} is the inverter efficiency and $\eta_{batt,in}$ is the charging efficiency of the battery assumed at 80 %. In case there is a surplus in supply and the battery bank reaches E_{Bmax}, the excess energy cannot be stored or consumed and is, therefore, dumped.

Battery Discharging Mode

In the case of a deficit, the batteries discharge to the amount needed to meet demand and can be modelled using Equation (3-43) below. If there is insufficient energy stored to meet demand, the batteries discharge to their minimum capacity where the battery discharging efficiency, $\eta_{batt,out}$, is assumed to be 100 % (Borowy, 1996).

$$E_B(t) = E_{B(t-1)} - \left(\frac{E_{L(t)}}{\eta_{inv}} - E_{G(t)}\right).\eta_{batt,out} \quad \textbf{(3-43)}$$

In order to preserve batteries from damage, the stored energy is constrained to avoid excessive charging or discharging as shown in Equation (3-44) below.

$$E_{Bmin} \leq E_{B(t)} \leq E_{Bmax} \quad \textbf{(3-44)}$$

Economic Analysis of the Lead Acid Battery Technology

The main costs incurred by a Lead-Acid Battery are shown in Table 3-29 below (IRENA, 2012b).

Table 3-29 Lead Acid Battery Cost Analysis

System Size (MW_e)	Lifetime (cycles)	Lifetime (years)	Capital Cost per Capacity (£/kW_e)	Annual Operating Cost (£/kW-year)
≤ 10	500-800	3-10	125-375	20

A breakdown of the capital cost components is shown in Table 3-30 below (NREL, 2012).

Table 3-30 Capital Cost Breakdown of the Lead-Acid Battery Technology

Cost Component	Breakdown (%)
Battery	48
Power Conversion	33
Pre-Development Cost	15
Engineering and Procurement Services	4

Environmental Analysis of the Lead Acid Battery Technology

This study assumes that the storage system is charged by a renewable energy technology. Therefore, the energy discharged to meet demand originates from renewable energy sources and so there are zero operational carbon dioxide emissions.

3.3.4 Photovoltaic Technology

This section examines the assessment of the Photovoltaic (PV) technology using the decision-making indicators of this study. To do this, the electrical energy generation at the site under investigation must first be determined. Widely used PV models include the linear, 4 Parameter Single Diode (4PSD) and 5

Parameter Single Diode (5PSD) models. Due to the trade-off between accuracy and computational simplicity, especially with the inclusion of shunt resistance in the process, the 5 Parameter Single Diode Model is preferred over the other options and used in this study. The electrical power output modelling and its main characteristics are explained in the following subsection.

Electrical Power Output Modelling of Photovoltaics - 5 Parameter Single Diode Model

The input requirements of the model are the solar radiation, ambient temperature and data sheet parameters of the panel under investigation. The solar resource required is the total solar radiation examined in section 3.2.1 above. Using this model, the terminal current and voltage characteristics, and assuming Maximum Power Point Tracking (MPPT), the Direct Current (DC) power output at different radiation and temperature conditions can be estimated. The DC power is calculated as the product of the terminal current and voltage both found from the 5PSD model (Prasad, 2005). The AC power output is calculated as the product of the DC power and a known DC/AC inverter efficiency.

The 5PSD equivalent circuit of a PV panel under Standard Testing Conditions (STC) is shown in Figure 3-24 below (Sera et al., 2007). STC is used to measure a photovoltaic cell's nominal output power where the total radiation is 1000 W/m^2, the module junction temperature is 25 ºC and the reference air mass is 1.5 (Balfour et al., 2011).

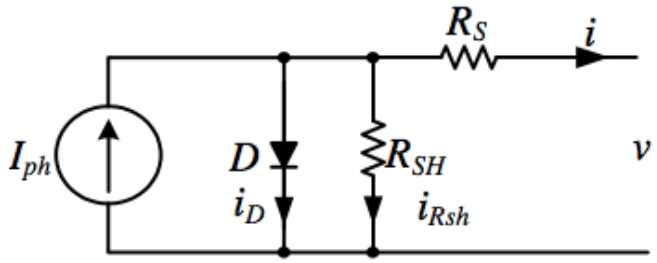


Figure 3-24 PV Panel Equivalent Circuit (Source: Extracted from (Sera et al., 2007))

The current-voltage relationship of this model is shown in Equation (3-45) below (Sera et al., 2007).

$$i = I_{ph} - I_o\left(e^{\frac{v+iR_s}{n_s V_t}} - 1\right) - \frac{v + iR_s}{R_{sh}} \quad \textbf{(3-45)}$$

Where i is the terminal current; v is the terminal voltage; I_{ph} is the photo-generated current at STC; I_o is the dark saturation current in STC; R_s is the panel series resistance; n_s is the number of cells in series; R_{sh} is the panel shunt resistance and V_t is the junction thermal voltage[12].

The junction thermal voltage is expressed in Equation (3-46) below (Sera et al., 2007).

$$V_t = \frac{AkT_{stc}}{q} \quad \textbf{(3-46)}$$

Where *A is* the diode quality factor; *k* is the Boltzmann's constant; q is the charge of the electron and T_{stc} *(K)* is the STC temperature (Sera et al., 2007). The *I-V* relation of a photovoltaic panel is shown graphically in Figure 3-25 below (Balfour et al., 2011).

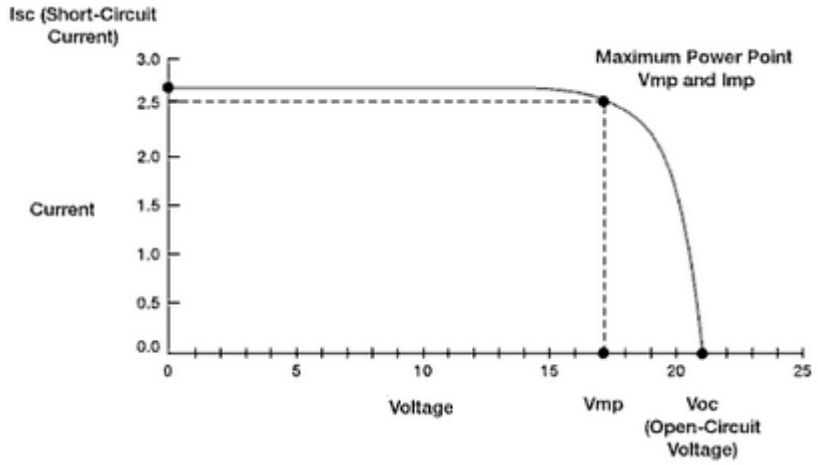


Figure 3-25 Current - Voltage Relationship of a Photovoltaic Panel (Source: Graph Extracted from (Balfour et al., 2011))

Further background information on this model can be found from Sera et al. (2007), who have presented a construction of this model, which is replicated and validated using the parameters of a selected PV panel in this study (Sera et al., 2007).

Testing the 5 Parameter Single Diode Model

To demonstrate the accuracy of this model, a specific PV panel is simulated using the Matlab code developed in this study. The results are compared and reviewed against the datasheet values reported by the respective manufacturer's datasheet values. The specific panel used in this demonstration is the

[12] The dark saturation current in silicon devices is very small compared to the exponential term so the "-1" is neglected

Suntech Power STP190S-24/Ad and its datasheet is shown in Figure 7.7 of Appendix A. The maximum power point current, voltage and DC power of the constructed model and datasheet values are shown in Table 3-31 below. The meteorological conditions examined range from 400 to 1000 W/m^2 of solar radiation assuming a constant ambient temperature of 25 ºC.

Table 3-31 Suntech 190W Module Datasheet and Model Output

Radiation (W/m^2)	Data Sheet Values (Suntech, 2010)			5 Parameter Model			Percentage Difference (%)		
	I_{mpp} (A)	V_{mpp} (V)	P_{mpp} (W)	I_{mpp} (A)	V_{mpp} (V)	P_{mpp} (W)	I_{mpp} (A)	V_{mpp} (V)	P_{mpp} (W)
1000	5.4	38	190	4.8	40	192	11	5	1
800	4.3	37	145	3.9	38.4	148	9	4	2
600	3.2	37.5	110	2.9	35	101	9	6	8
400	2.1	38	73	1.9	37.1	72	9	2	1

The percentage difference between the maximum power point predicted by the 5PSD and the manufacturer's data sheet shows a constant percentage difference of less than 10 % at all radiation levels. Therefore, this model can be used with considerable confidence in the further assessment of the PV technology in this study.

Economic Analysis of the Photovoltaic Technology

This sub-section presents an economic analysis of the PV technology. The main costs examined are the budgetary capital cost for a turnkey operation and the annual operational and maintenance costs required to calculate the total annual cost. The data presented below must be used as an indicative measure of PV economics. It must be noted that these costs are continuously shifting downwards due to a highly competitive solar PV market, especially between Chinese, German and North American manufacturers. The costs are shown in Table 3-32 below (ParsensBrinckerhoff, 2012).

Table 3-32 Economic Analysis of the Photovoltaic Technology

Cost Scenario	Capital Cost (£ million /MW$_e$)	O&M Cost (£ million /MW$_e$)
High	1.5	0.028
Median	1.3	0.023
Low	1.2	0.016

The capital cost item breakdown is shown in Figure 3-26 below (ParsensBrinckerhoff, 2012)

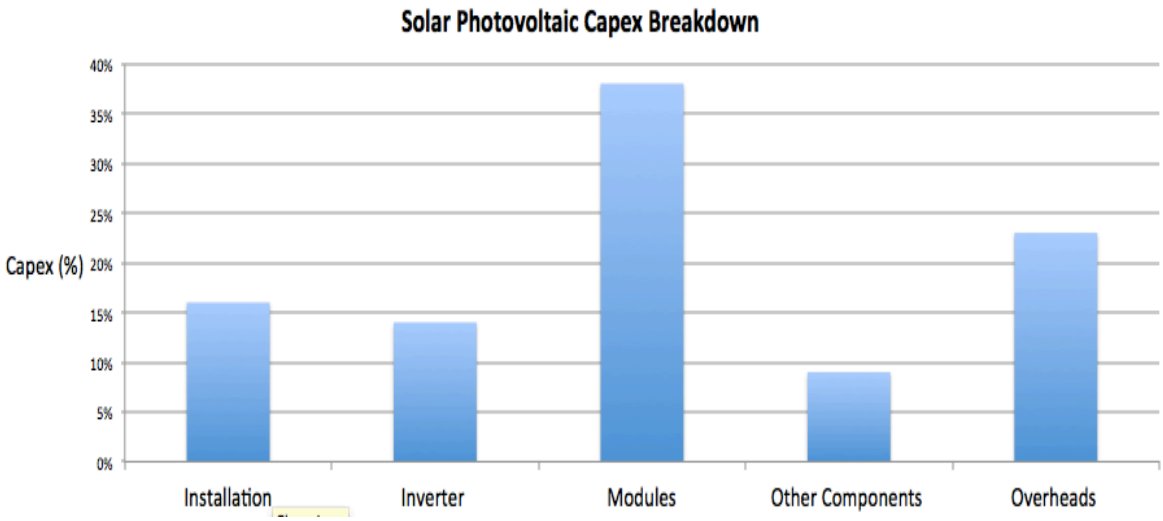


Figure 3-26 Solar Photovoltaic Capex Breakdown

Figure 3-26 above shows that the two main equipment requirements are the PV modules and the inverters that make up 52 % of the total capex.

Environmental Analysis of the Photovoltaic Technology

The PV panel operates without any carbon dioxide related emissions. Therefore, this study assumes that the emissions reduction indicator is equivalent to the amount of carbon the PV array avoids emission into the atmosphere by a conventional fuel.

3.3.5 Wind Turbine Technology

This section examines the assessment of the wind turbine technology using the decision-making indicators of this study. To do this, the electrical energy generation at the site investigated must first be determined. The energy generation is estimated using a mathematical model that incorporates the site's wind speed and air density with a turbine's operational characteristics.

Wind Turbine Power Output Modelling

This sub-section presents the methodology for modelling the electrical power output of a wind turbine. The generation performance of a wind turbine is characterized by a power curve that reports the wind speed and subsequent electrical power output curve for 1 m/s intervals ranging from 0 m/s to the cut-out speed, at a standard air density of 1.225 kg/m^3. Air density is the air mass per unit volume which is concentrated near the ground resulting in density being highest near the ground. Air density decreases

exponentially with altitude (Jacobson, 1999). Air density is found using the gas law that substitutes the recorded pressure and temperature readings in the gas law shown in Equation (3-47) (Gipe, 2004).

$$\rho = \frac{p}{RT} \tag{3-47}$$

Where ρ is the air density; p is the air pressure; R is the gas constant (287.04 J/kgK for air); and T is the air temperature. By substituting a standard air temperature of 288 K and a sea level pressure of 101.3 kPa, in Equation (3-47) above, the air density is equal to 1.225 kg/m3.

A generic power curve is shown in Figure 3-27 below (Rivkin et al., 2012).

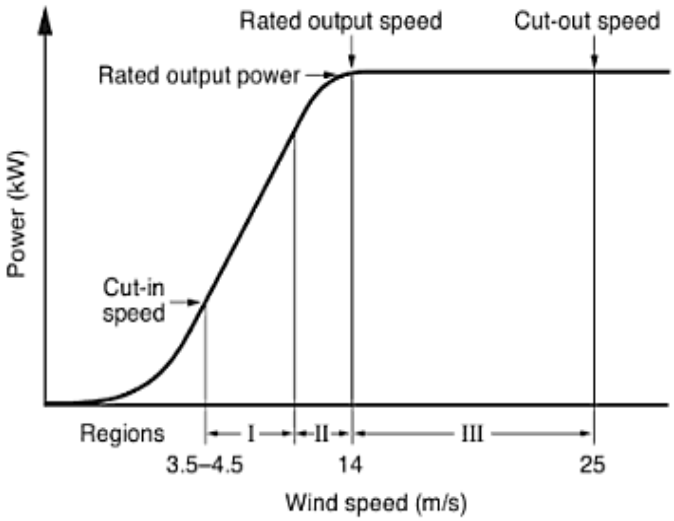


Figure 3-27 Wind Turbine Power Curve (Source: Extracted from (Rivkin et al., 2012))

The power output can then be found by a cubic spline interpolation of the wind speed-power values reported in the power curve. The fitting equation of power output with respect to wind speed is expressed by Equation (3-48) below (Akai, 1994).

$$P_w(V) = \begin{cases} 0 & V \le V_{ci} \text{ or } V \ge V_{co} \\ a_1V^3 + b_1V^2 + c_1V + d_1 & V_{ci} < V < V_1 \\ P_r & V_r \le V < V_{co} \end{cases} \tag{3-48}$$

Where $P_W(V)$ is the electrical power output of the wind turbine at wind speed V; P_r is the turbine rated power; V_{ci} is the cut-in wind speed; V_r is the rated wind speed; and V_{co} is the cut-out speed. Finally, *a,b,c,d* are the polynomial coefficients of the cubic spline interpolation extracted from the specific wind turbine speed-power curve.

Economic Analysis of Wind Turbine Technology

This sub-section presents an economic analysis of the wind turbine technology. The main costs examined are the budgetary capital cost for a turnkey operation and the O&M cost required to calculate the total annual cost economic indicator of this study. The wind turbine capacities are separated into three groups for the micro (<50 kW), small-scale (50 kW – 5 MW) and large-scale sizes (>5MW). These costs are shown in Table 3-33 below (ARUP, 2011).

Table 3-33 Economic Cost Analysis of the Wind Turbine Technology

Installed Capacity	< 50 kW		50 kW – 5 MW		> 5 MW	
£ million /MW_e	Capital Cost	O&M Cost	Capital Cost	O&M Cost	Capital Cost	O&M Cost
High	4.3	0.061	1.9	0.070	1.8	0.073
Median	3.7	0.041	1.0	0.048	1.5	0.057
Low	2.8	0.034	1.0	0.039	1.2	0.030

A breakdown of the capital cost components is shown in Table 3-34 (NREL, 2012).

Table 3-34 Capital Cost Breakdown of the Wind Turbine Technology

Capital Cost Component	Cost Breakdown (%)
Wind Turbine	68
Balance of Plant / Construction	13
Distribution	10
Pre-Development	5
Engineering and Procurement Services	4

The capital cost breakdown shows that the wind turbine unit is the main cost element, followed by the construction costs totalling a combined requirement of 81 %.

Environmental Analysis of the Wind Turbine Technology

The wind turbine operates without any carbon dioxide related emissions. Therefore, this study assumes that the emissions reduction indicator is equivalent to the amount of carbon the wind turbine avoids emission into the atmosphere by a conventional fuel.

3.4 Renewable Energy Supply Mix Design Methodology

This chapter has so far examined independent assessment methodologies for the energy demand, renewable energy resource and conversion technologies. To link these components, this section presents the methodology developed to design a renewable energy supply mix that meets demand and operates using one or more of the resources studied in this chapter.

The literature review on energy supply mix design, in Chapter 2, has not identified an available software or methodology that uses the economic and environmental indicators in the decision-making process. This section targets the gap in knowledge by developing a methodology using the total annual cost and emissions reduction performance of the supply. This methodology must be able to size the technologies to meet demand over a specific time period as illustrated in Figure 3-28 below.

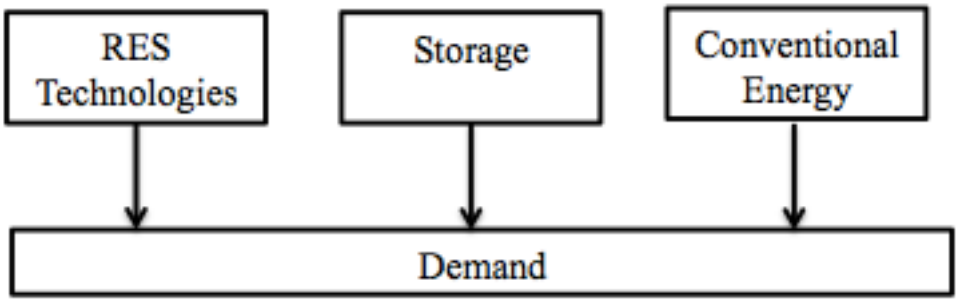


Figure 3-28 Supply Mix Design Algorithm Components

The technology component is characterized by its installed capacity given by the number of units and capacity per unit. The first output must constitute both of these characteristics. Since the technologies are available in discrete sizes, the algorithm to be developed must account for this. The supply is expected to require back-up generation fuelled by conventional sources to meet demand when the renewable element is insufficient. Therefore, the second output must be the capacity and operational strategy of the back-up generator. Finally, the performance of the total annual cost and emissions reduction indicators of the supply mix must be the third output. It is noted that this methodology must function with a known renewable energy power output and an unknown power output within the same time interval which represents the conventional generator that increases to meet a supply deficit or decreases if there is a surplus. A summary of the input/output parameters and functional characteristics of the supply mix design methodology is shown in Table 3-35 below.

Table 3-35 Required Parameters and Functional Characteristics of Supply Mix Methodology

Input Parameters	Functional Requirements	Output Parameters
• Meteorological Conditions • Energy Demand	• Function with any of the Determinative, Dispatchable and Stochastic Resources • Function with expected Renewables Energy Source (RES) power profile and unknown conventional power generation • Storage of RES Power in Energy Surplus Scenarios • Discharge of Storage Power in Energy Deficit Scenarios	• Discretized number of Technology Units • Operational Strategy of Conventional Fuel Generator • Total Annual Cost / Emissions Reduction Performance of each Supply Mix

3.4.1 Selection of Algorithm for Supply Mix Design

To satisfy the requirements in Table 3-35 above, the constrained exhaustive search algorithm is considered as the most favourable selection for the renewable energy supply mix design methodology. The constrained exhaustive search algorithm is a problem solving technique that functions by systematically enumerating all the potential candidates for the solution and confirming if each of these candidates satisfies the main problem statement (Fereidouni, 2012).

The main disadvantage of this algorithm is that it is a resource expensive technique that is dependent on the number of candidate solutions. To overcome this issue, this study presents a heuristic approach to minimizing the search space and resource cost of this algorithm for renewable energy supply mix design. The remainder of this section presents a detailed explanation of the search space minimization technique and implementation of the modified constrained exhaustive search on an example test case.

Modified Constrained Exhaustive search Algorithm for Renewable Energy Supply Mix Design

This section presents the construction of the constrained exhaustive search algorithm for the renewable energy supply mix design methodology. An identification of the search space comprised of the lower bound, step change and upper bound is conducted. The minimization technique of the search space, using a heuristic approach is presented, thereby, creating a constrained exhaustive search space algorithm. Operation of the energy storage technology is determined from the renewable supply surplus/deficit and

is, therefore, examined individually. The methodology is then implemented on a test case scenario to illustrate its functionality.

Search Space Minimization for Power Generation Technologies

This sub-section defines the minimum search space identification of the wind turbine and PV generation technologies in the constrained exhaustive search algorithm. The search space is defined by the lower bound, upper bound and step change interval size. The main factor causing the initial large search space is the unidentified upper bound.

Lower Bound Limits

In order to examine the physically realistic candidate number and type of technology, the lower bound must be set to 0 for each technology. This will also allow the comparison of the decision-making indicator performance between including and not including a technology in the mix.

Upper Bound Limits

To identify an upper bound that does not interfere with an optimal solution, the number of units per technology that will not provide further energy to demand, if increased by an additional unit, is identified as the "saturation point". A range of units per individual technology is then assessed against the conventional generation required to meet demand whilst maintaining the other technologies at 0. Since the first sweep is a linear multiplication of the units of one technology only, implementing an initially large upper bound will not compound the number of solutions and so this analysis can be conducted in a resource efficient manner.

Step Change Interval

To provide a physically sensible change in unit number, there must be an integer change in the number of units per technology. To provide an accurate view of the effects any increase in number of units has on the decision-making indicators a high resolution of intervals must be created. This will also assist in the final supply mix optimization discussed in the next sub-section.

Modified Search Space Minimization for Energy Storage Technologies

This sub-section defines the minimum search space identification for the storage technologies in the constrained exhaustive search algorithm. The lower and upper bounds and the step change representing the number of units examined define the search space of this technology.

Lower Bound Limits

In order to examine all physically realistic candidate number of units, the lower bound must be set to 0 for this technology. This will also allow the determination of the difference between the effect of including or removing storage from the supply mix.

Battery Storage Upper Bound Limits

The methodology followed to find the battery storage upper bound limits is dependent on the number of days the storage system is required to operate for before recharging is necessary. This study considers the battery cycle charge/discharge time of a 24-hour period. To find the absolute upper bound limit of the number of batteries, the maximum energy demand deficit over 24 hours ($D_{deficit}$) and the maximum energy supply surplus ($D_{surplus}$) from renewable energy sources over 24 hours must be calculated. The battery upper bound ($E_{batt,max}$)is the smallest of the energy demand deficit and energy supply surplus as shown in Equation (3-49) below. The smaller of the 2 parameters is required so as not to oversize the storage in the case where surplus renewable energy is available but there is no energy demand to absorb it. Also, using the smaller of the 2 parameters avoids oversizing the storage in cases where there is a high deficit in demand but insufficient renewable energy supplied.

$$E_{batt,max} = min\left(D_{deficit}, D_{surplus}\right) \quad \textbf{(3-49)}$$

The $D_{deficit}$ and $D_{surplus}$ are calculated from the scenario where the upper bound limits of all the generations are operating and, therefore, an absolute search space is defined.

Step Change Interval

Similarly to the step change of the power generation units, the storage step change is proposed at an even number of integer units between the lower and upper bound limits identified above.

3.4.1 (b) Exhaustive Search Modelling Approach

The previous section has defined the search space and interval step change that are examined in the Exhaustive Search methodology. This section examines the modelling approach that is required to construct the final graphical decision making tool in this study. The output is an *m*-dimensional matrix of total annual cost and emissions reduction outputs where *m* is the number of technologies examined. The size of each dimension is given by Equation (**3-50**) below.

$$m_i = \frac{m_{i,u} - m_{i,l}}{m_{i,s}} \tag{3-50}$$

Where m_i is the size of each dimension; $m_{i,u}$ is the upper bound number of units; $m_{i,l}$ is the lower bound number of units and $m_{i,s}$ is the step change of each technology examined. The data required to run this model is the hourly supply profile over a 1-year period for each technology examined and the site's demand profile for the respective time period.

General Equation used in the Model

The general equation that describes this model is a function of the number of units examined at each iteration as the supply per technology and demand are fixed inputs, as shown in Equation (**3-51**) below. The total annual cost indicator per supply mix combination is calculated by the total annual cost to operate the renewable energy supply mix that is determined by the number of units of the Exhaustive Search including the cost of diesel required to meet demand. The emissions reduction indicator is calculated by the emissions reduction achieved by the supply mix determined by the number of units of the Exhaustive Search while also accounting for the emissions released from the diesel generation required to meet demand.

$$G_{diesel}(t) = E_{site}(t) - [N_{PV} * E_{PV}(t) + N_{wind} * E_{wind}(t) + N_{batt} * E_{ch}(t) + N_{batt} * E_{disch}(t)] \tag{3-51}$$

Where t is 1:8760 representing each hour of a year; G_{diesel} is the diesel generation required to meet demand; N_{PV} is the number of units of the PV technology; E_{PV} is the energy generated by 1 unit of the PV technology; N_{wind} is the number of units of the wind turbine technology; E_{wind} is the energy generated by 1 unit of the wind turbine technology; N_{batt} is the number of units of the battery storage technology; E_{ch} is the energy flow involved with charging the battery and E_{disch} is the energy flow involved with discharging the battery. Note that the battery can either be charging or discharging and so E_{ch} and E_{disch} cannot both be greater than 0 within the same time interval and G_{diesel} cannot be less than 0 under any circumstances.

The battery charge and discharge protocol is defined by the following regime:

1) It is assumed that the batteries are not power constrained but are energy constrained. This implies that they can accept the full power up to their energy limits
2) The efficiency for charging is assumed to be 80% and for discharging is assumed to be 100%
3) If there is a surplus of renewable energy and the battery is not fully charged then the battery is charged by the surplus energy
4) If there is a deficit of energy from the renewables and there is available energy in the battery bank then the battery is discharged to meet this requirement
5) If the renewables and the battery cannot deliver sufficient energy then the diesel generator is used to makeup this deficit but the diesel generator is not used to charge the battery

Following the process presented allows the construction of a contour plot that is comprised of a set of contour lines for the total annual cost and emissions reduction indicators for the range of renewable energy technology capacities examined.

The following section will examine the determination of the optimum supply mix based on a required predetermined total annual cost or emissions reduction level.

3.4.2 Determination of the Optimum Renewable Energy Supply Mix

The results from the exhaustive search algorithm present a large number of supply mix combinations that will achieve a certain economic and environmental indicator performance. The final step in the methodology is required to identify the supply mix that simultaneously minimizes the cost and maximizes the emissions reduction indicators. A 2D contour plot can be generated to present the economic and environmental indicators of the search space examined. To identify the optimum supply mix, the Lagrangian multipliers are used and expressed in Equation (3-52) below.

$$\left(\frac{df}{dx}, \frac{df}{dy}\right) = -\lambda\left(\frac{dg}{dx}, \frac{dg}{dy}\right) \quad \textbf{(3-52)}$$

Where f is the total annual cost; x is the number of PV units; y is the number of batteries; and g is the emissions reduction performance of each supply mix combination from the exhaustive search.

The final cost matrix in Equation (3-53) and emissions matrix in Equation (3-54) can then be derived, where the number of rows and number of columns correspond to each technology size extracted directly from the exhaustive search output.

Total Annual Cost Matrix

$$\begin{bmatrix} \frac{df_1}{dx_1} \Big/ \frac{df_1}{dy_1} & \cdots \\ \cdots & \frac{df_n}{dx_n} \Big/ \frac{df_n}{dy_n} \end{bmatrix}$$

Equation (3-53)

Emissions Reduction Matrix

$$\begin{bmatrix} \boldsymbol{\frac{dg_1}{dx_1} \Big/ \frac{dg_1}{dy_1}} & \cdots \\ \cdots & \boldsymbol{\frac{dg_m}{dx_m} \Big/ \frac{dg_m}{dy_m}} \end{bmatrix}$$

Equation (3-54)

Where *n* is the upper bound limit units of the first technology and *m* is the upper bound limits of the second technology considered. The optimum combination per technology is the point where the gradient of the cost curve is the same as the gradient of the emissions reduction curve and, therefore, the matrices above have the same value, i.e. they are tangent to each other. This is the point where for a given value on curve 1, curve 2 is optimal (either maximum or minimum). This process is conducted for each step change in technology units to find the optimum capacity for each cost and emissions reduction.

Generation of the Final Renewable Energy Supply Mix Design Tool

The final part of this methodology is the main output tool that will be used to design the renewable energy supply mix. As a reminder, the general aim of this methodology is to create a tool that can be used to determine the optimum renewable energy capacity based on either a required total annual cost or emissions reduction performance.

This chapter has so far shown 2 main parts of the design methodology. These are:

1) The creation of a contour plot of total annual cost and emissions reduction over a range of renewable energy capacities
2) The identification of optimum size of each technology using the Lagrangian Multipliers using the points determined in Equation (3-53) and Equation (3-54).

The final step is to combine parts 1 and 2 listed above. This is done by plotting the total annual cost and the emission reduction indicator on the same graph whose axis is the number of units of each technology. The Lagrangian Multiplier process is then applied to identify the optimum trajectory through the design

space, i.e. this trajectory connect the points where the two contours are tangential to each other and are therefore optimal. A specific example is discussed in the next section, around Figure 3-31.

Test Case Study

This sub-section presents a test case for the constrained exhaustive search algorithm to demonstrate the methodology developed using a constructed simplified hourly power demand profile and the PV and lead-acid battery technologies. The supply deficit is assumed to be met using a diesel generator that incurs a cost of £ 0.25 / kWh_e. An indicative diurnal profile is shown, in Figure 3-29, for a 190 kW_e PV array and 400 kWh_e of lead acid battery storage created using the Matlab programming language.

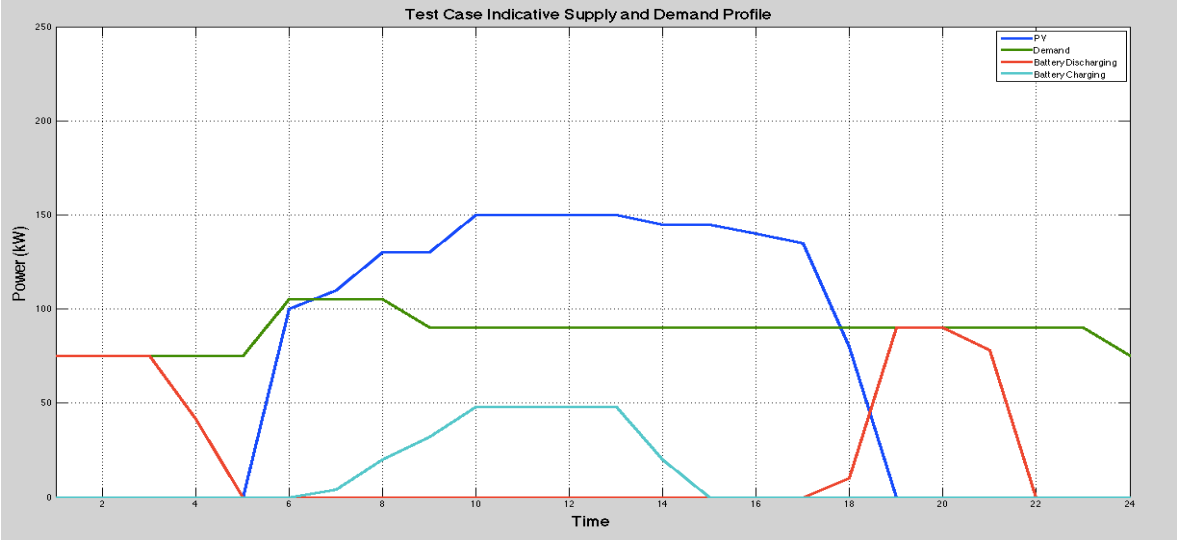


Figure 3-29 Test Case Supply and Demand Profile

Photovoltaic and Wind Turbine Upper Bound Limits

Figure 3-30 below shows that the PV technology saturates at 1500 units, equivalent to 285 kW_e capacity.

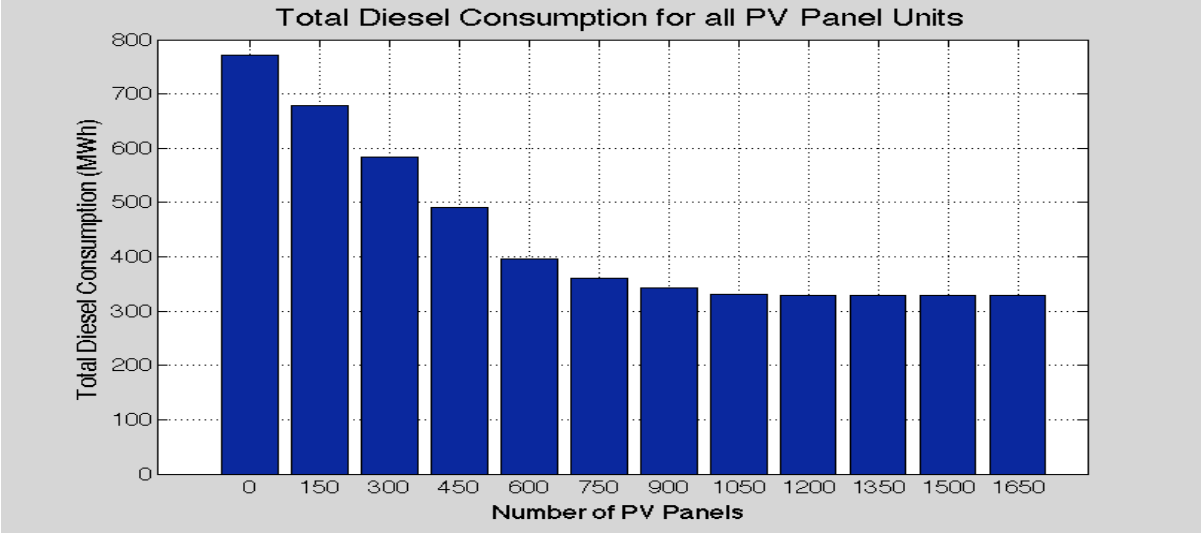


Figure 3-30 PV Saturation of Diesel Generation

Battery Storage Upper Bound Limits

The maximum demand peak and surplus is shown, in Table 3-36 below, with the absolute upper bound limit for the battery technology.

Table 3-36 Upper Bound Battery Storage

PV Capacity (kW_e)	Maximum Daily Demand Deficit (MWh_e)	Maximum Daily Demand Surplus (MWh_e)
285	0.9	1.6

The maximum daily demand deficit is smaller than the maximum daily surplus and, therefore, the 0.9 MWh_e is the energy that is targeted for storage. Assuming the minimum battery SOC is 33 %, the accessible storage availability is translated to 1.3 MWh_e, equivalent to 680 units of the 2 kWh_e batteries. The search space has now been defined and the optimum supply max can now be examined.

Renewable Energy Supply Mix Design

The final output is a 2D contour plot with a blue line overlay of the Lagrangian multipliers, which allows the user to select the supply mix composition based on a required total annual cost or emissions performance. This is shown for the test case in Figure 3-31 below.

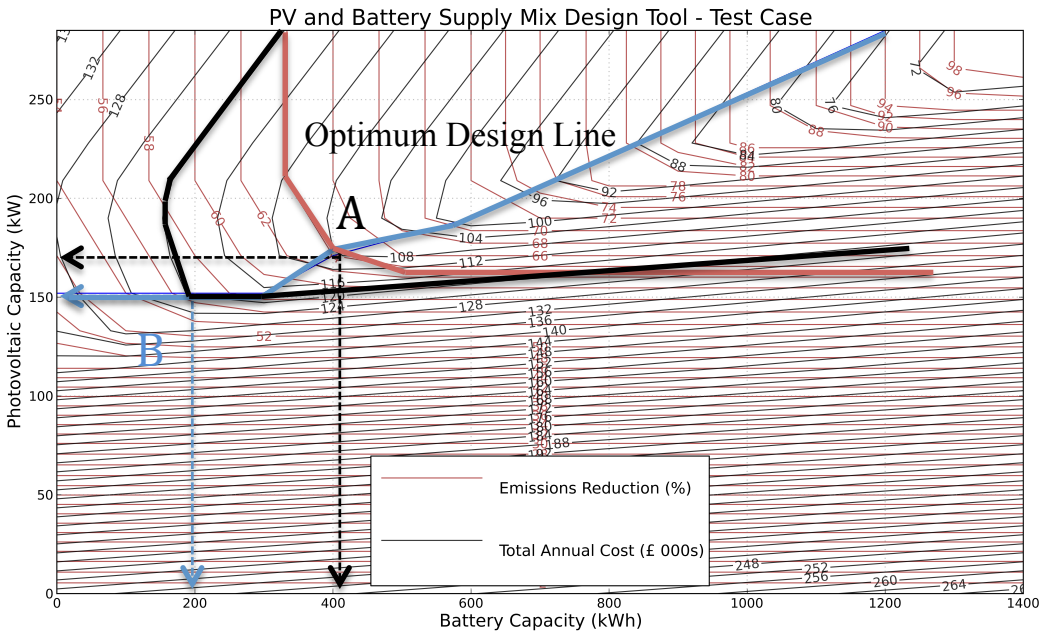


Figure 3-31 Final Supply Mix Design Tool including Optimum Design Line and Contour Plots

To demonstrate the usage of this tool, consider the case where one wants to achieve an emissions reduction of 64 %. This condition is fulfilled along the contour line of emissions reduction target of 64 %. For each point along this contour, there is an associated Total Annual Cost. At point 'A', the Total Annual Cost is minimal. It is also the point where the two contours are tangential to each other, as determined by the Lagrangian multiplier method and is hence on the Optimised Design Line. The supply mix selected at this point 'A' is 160 kW of PV and 400 kWh of battery storage.

As a second example, if the total annual cost that can be allocated is £120 k, then following the black contour line, at point "B", the maximum emissions reduction of 56% is achieved. This results in a design of 150 kW of PV and 200 kWh of battery storage.

3.5 Chapter Summary

This chapter has presented the methodology developed in this study to design a renewable energy supply mix to meet demand whilst optimizing the economic and environmental decision-making indicators. The economic indicator selected is the total annual cost and the environmental indicator selected is the reduction in carbon dioxide emissions.

A series of demand analysis techniques have been presented to assess the demand of a case study in terms of the temporal, climatic and growth factors that are expected to be the main drivers of demand. The renewable energy supply mix has been initially separated into the potential energy and conversion technology components of the mix. The renewable energy resources have then been defined to operate under determinative, dispatchable and stochastic statistical categories and an example of each has been analyzed in further detail. The conversion of potential to electrical energy has then been examined in respect of the total annual cost and emissions reduction indicators. The final renewable energy supply mix design methodology has been based on a constrained exhaustive search algorithm. Due to the fact that this algorithm can be considered as a resource expensive method, a heuristic approach has been implemented to minimize the search space for the power generation and storage technologies whilst making sure that the optimum range is not removed from further investigation.

To identify the optimum supply mix design that will simultaneously minimize the total annual cost and maximize the emissions reduction, the Lagrangian multipliers of these indicators have been calculated. This technique allows the methodology to progress from a large number of possible solutions to a single

capacity per technology for each total annual cost and emissions reduction output. The general supply mix design methodology can be implemented in any case study, regardless of size, usage or geographical location. This is shown in further detail in the following chapters that investigate the renewable energy supply mix design on the island of Hanimaadhoo in the Maldives, the county of Oxfordshire and the Christ Church site in the UK.

Chapter 4 - Republic of the Maldives Case Study

The previous chapter has presented the methodology developed in this study to meet demand. This chapter presents the implementation of this methodology on the island of Hanimaadhoo in the Republic of the Maldives, which is located in the Indian Ocean and spread over 26 atolls comprised of approximately 1200 islands (Masters, 2009). An analysis of the energy demand factors is presented and discussed in detail. A renewable energy resource assessment is conducted to propose the types of renewable energy that must be considered further under the decision-making indicators used. An individual performance assessment of the technologies that operate with the proposed resources is then conducted and a final supply mix is designed that satisfies this study's indicators.

In 2008, the Maldivian Government announced a countrywide carbon neutrality target to be achieved by 2020 (PresidentOffice, 2009). To achieve this target, a range of measures must be enforced including an increase in energy efficiency and renewable energy technology implementation. The main interest of this study lies within the renewable energy technology element of the attempt to achieve carbon neutrality.

Review of the Hanimaadhoo Case Study

The island of Hanimaadhoo is located in the northern part of the country in the Haa Dhaalu Atoll on coordinates 06.45.57 N and 73.10.33 E (GCMAP, 2009). Figure 4-1 below shows a map of the Republic of the Maldives in terms of the 26 atolls and the relative position of the island of Hanimaadhoo examined in detail in this thesis (GunaTravel, 2013). The island's size has been estimated using Google Earth™ and shows a length of 7 km and a width of 0.8 km.

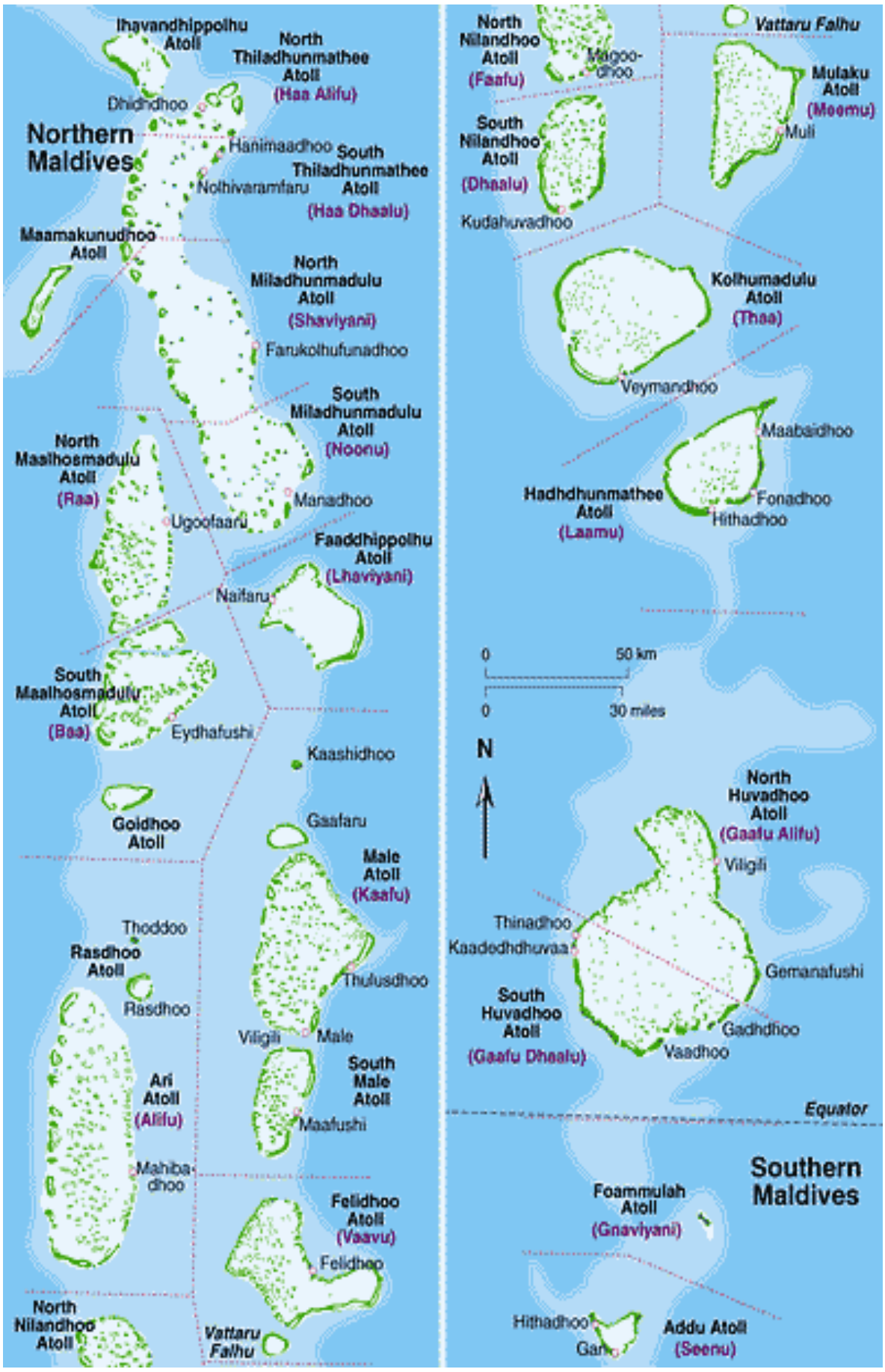


Figure 4-1 Map of the Republic of the Maldives (Source: (GunaTravel, 2013))

The island is not a tourist destination and is only populated by local islanders that are mainly involved with farming and fishing activities. The latest official census, conducted in 2006 by the Ministry of Planning and National Development, recorded a total population of 1184 (MPND, 2006). Between December and April, the northern part of the Maldives is affected by the hot and dry Iruvai monsoon which causes a humid climate and low wind speeds (USAID, 2012). The meteorological data used has been directly obtained from a meteorological station operated by the United Nations Development Program (UNDP) on the island[13].

Review of the Hanimaadhoo Energy Supply Mix

The State Electricity Company, STELCO, is the sole electricity provider on the island and operates in the local powerhouse, which contains 2 x 160 kW_e and 1 x 200 kW_e diesel generators. This study uses the data obtained by the Hanimaadhoo powerhouse for the 2007 – 2009 period (STELCO, 2009). Nasheed Ahmed, the Deputy Under Secretary of the Policy Office in the Maldives, was the main contact in receiving this data. STELCO records the daily peak and minimum demand magnitude and respective Average Power Analysis as well as the total daily energy consumption. However, this resolution is insufficient for demand analysis and renewable energy supply mix design. To overcome this issue, the island's typical load profile found in the literature is used with the 3 aforementioned available demand data points to construct an annual hourly profile.

Construction of Hanimaadhoo Energy Demand Profile

This sub-section presents the construction of the Hanimaadhoo annual hourly electricity demand profile. Van Alphen et al. (2007) was able to obtain the Hanimaadhoo hourly demand profile over a 1-day period[14] from STELCO that is typical of the 2000-2004 period (van Alphen et al., 2007). The average hourly constructed profile is compared with the Van Alphen (2007), profile in Figure 4-2.

[13] This station records air temperature, pressure, wind speed, direct and diffuse solar radiation

[14] No clarification has been made of the seasonal character of the reported typical daily profile

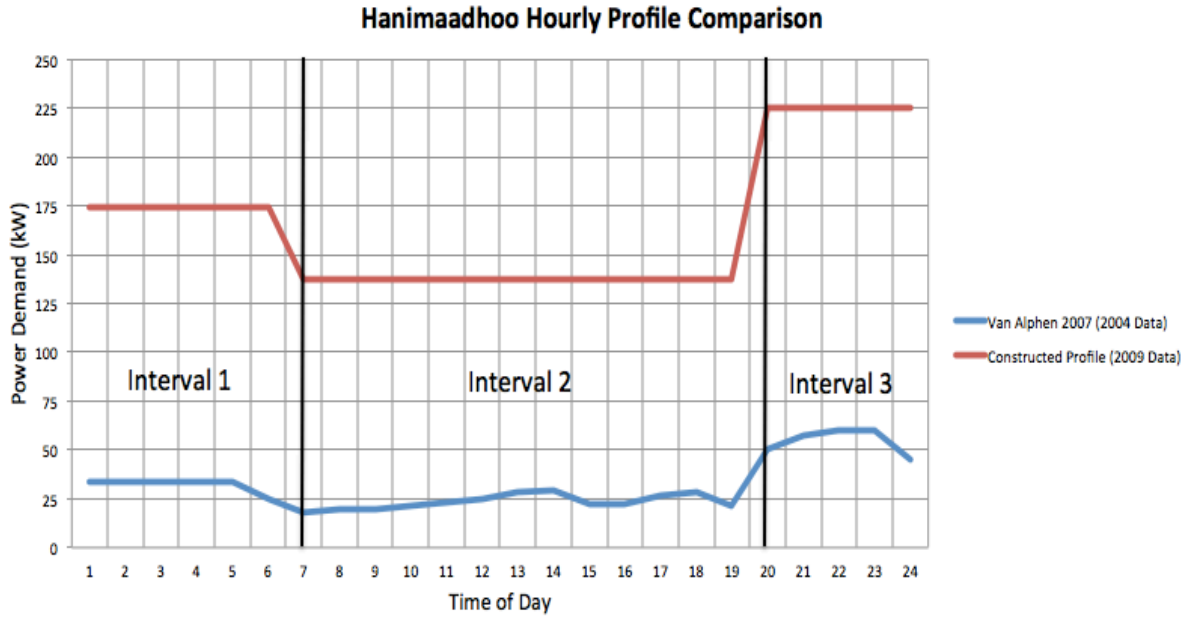


Figure 4-2 Comparison of Constructed Profile and van Alphen profile (van Alphen et al., 2007)

The construction technique developed is comprised of a 5-step process that is repeated per day for 1 year. The steps are reported and explained below:

1) **Review of Van Alpen et al. (2007) profile –** A review of the given profile shows that it is comprised of 3 distinct shapes within the intraday demand. These are marked and labelled in Figure 4-2 above.
2) **Determination of ratio of energy demand between shapes** – The ratio of the energy demand between each interval of the given profile is calculated. Since the minimum demand is at 0700 and the shape of interval 2 is relatively flat, it is assumed as continuously flat at the daily minimum demand. The ratio between intervals 1-2 is 0.72 and is required because the STELCO data gives no indication of the demand magnitude over interval 1. It is assumed that this ratio is the same in the constructed profile.
3) **Determination of constructed profile interval demand magnitudes** – The peak and minimum demand obtained from the STELCO data are overlaid on the graph at the respective Average Power Analysis. The demand of interval 1 is found using the known daily minimum demand and the interval 1-2 ratio mentioned in Step 2.
4) **Peak load interval** – It is assumed that interval 3 is has a flat profile at the peak demand from the time of peak to 0000. The ratio of interval 3 with any of the others is, therefore, not required.

5) **Comparison of constructed profile and STELCO demand** – The annual energy demand of the constructed profile and the STELCO profile is then compared and a percentage difference of 3.3 % is calculated. This difference is considered a minimal amount that can allow a relatively confident use of the constructed profile in further analysis.

Several issues have been faced with the availability of hourly demand data at Hanimadhoo. Firstly, the van Alphen (2007), profile shows a peak demand of 60 kW_e and the data obtained from STELCO reports a peak demand of 295 kW_e which is approximately a 5 fold difference. Furthermore, it is unclear if the authors were referring to the entire island demand or just for one of the 3 generators operating in the powerhouse. However, the following section shows that between 2006 - 2009, the island has experienced a 15 % annual increase in demand. If it were assumed that this growth is traced back to the year 2000, the peak demand would be 210 kW_e which is in a closer range. It can be concluded that this study has had to deal with incomplete and difficult demand data that has presented various challenged. A set of assumptions explained above has been made to refine the demand data in a form that can be used both practically (hourly annual demand format) and confidently (3.3 % difference in annual demand with STELCO data).

4.1 Energy Demand Analysis – Hanimaadhoo Case Study

This section examines the implementation of the energy demand analysis, developed in section 3.1, in relation to the energy demand at Hanimaadhoo. The results allow the assessment and understanding of the temporal, climatic and growth factors on the energy demand.

4.1.1 Temporal Analysis

The Average Power Analysis and seasonal indicators of the temporal demand factors are considered in this section for the Hanimaadhoo demand.

Average Power Analysis

The Average Power Analysis is shown in Figure 4-3 below as the minimum, average and maximum demand at each time interval throughout 2009.

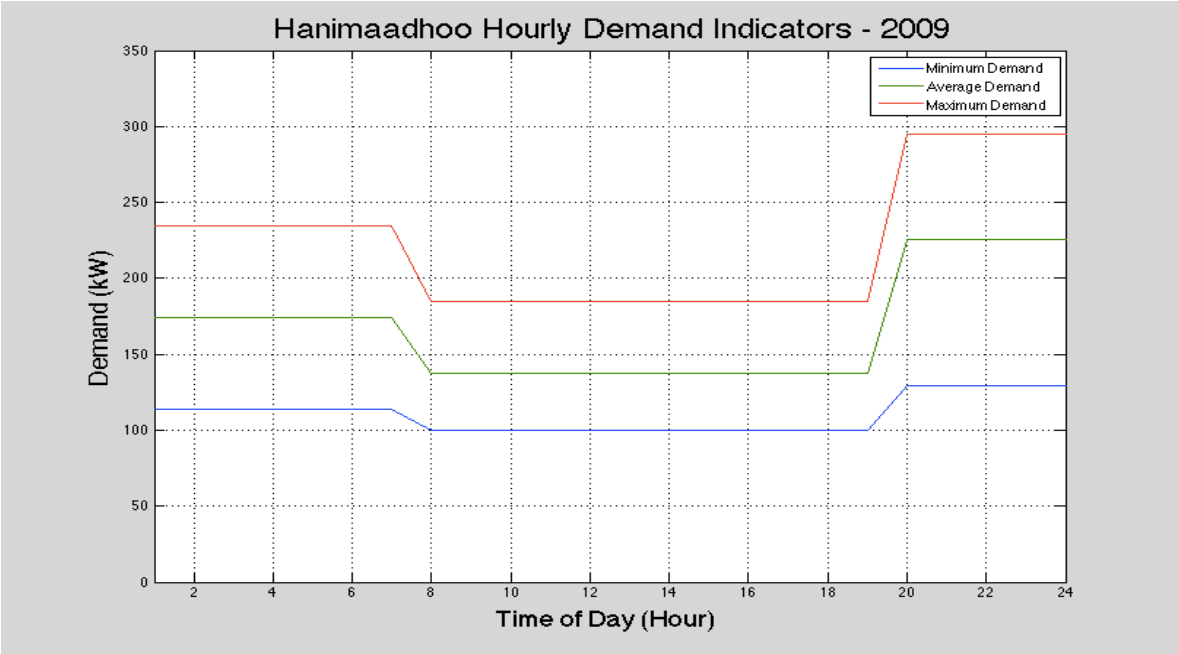


Figure 4-3 Intraday Demand 2009 (Source: Adjusted Data from Utility (STELCO, 2009))

The Average Power Analysis, in Figure 4-3 above, shows a minimum demand at 0700 and a peak demand at 2000. The flat profile throughout between 0700 and 2000 is expected to be due to outdoor activities carried out by the islanders that require a minimal electricity demand, such as farming and fishing. The relatively late peak demand is expected to be due to the evening lighting requirements.

Seasonal Change

The seasonal demand for 2009[15] is shown in Figure 4-4 below. The minimum annual demand is recorded in February at 111 MWh_e and the maximum demand in October at 141 MWh_e.

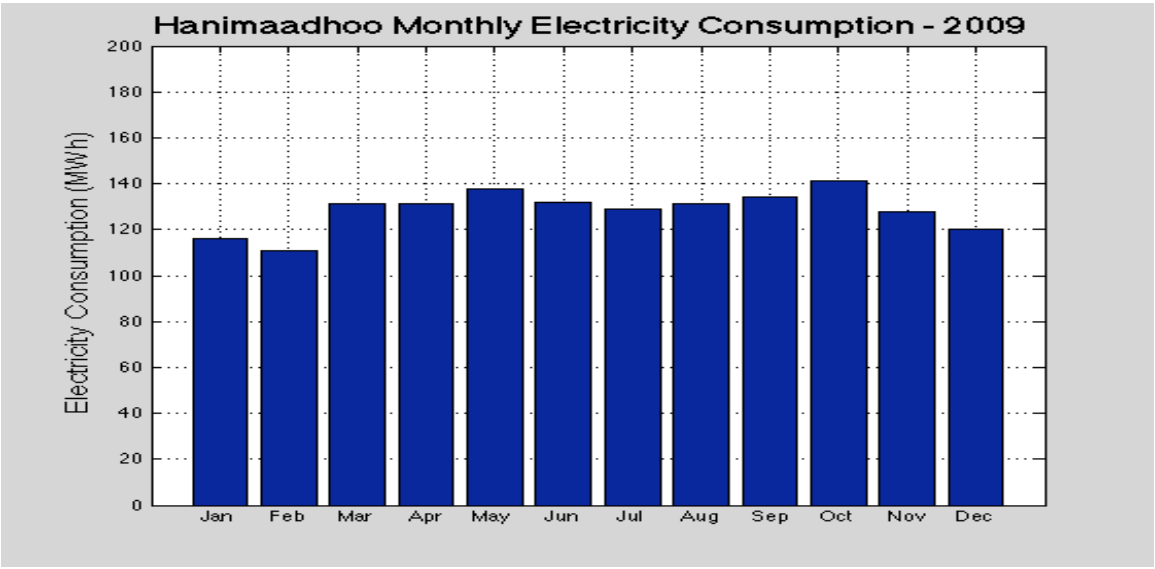


Figure 4-4 Hanimaadhoo Monthly Energy Consumption-2009

[15] At the time of this study 2009 was the most recent period of demand data available from STELCO

As previously mentioned, Hanimaadhoo is not a tourist resort island and so no relation is expected between the tourist period and demand. Moreover, demand extremities cannot be related to the monsoon season, which might affect demand, since it occurs during other periods of the year. It is unclear why the demand behaves in this way and so further analysis is required at a local level to understand this pattern.

Annual Change

The annual change in energy consumption between 2007 and 2009 is shown in Figure 4-5 below. Although this is a limited data set, the years available show a consistent 15 % increase between the years 2007 – 2008 and 2008 – 2009.

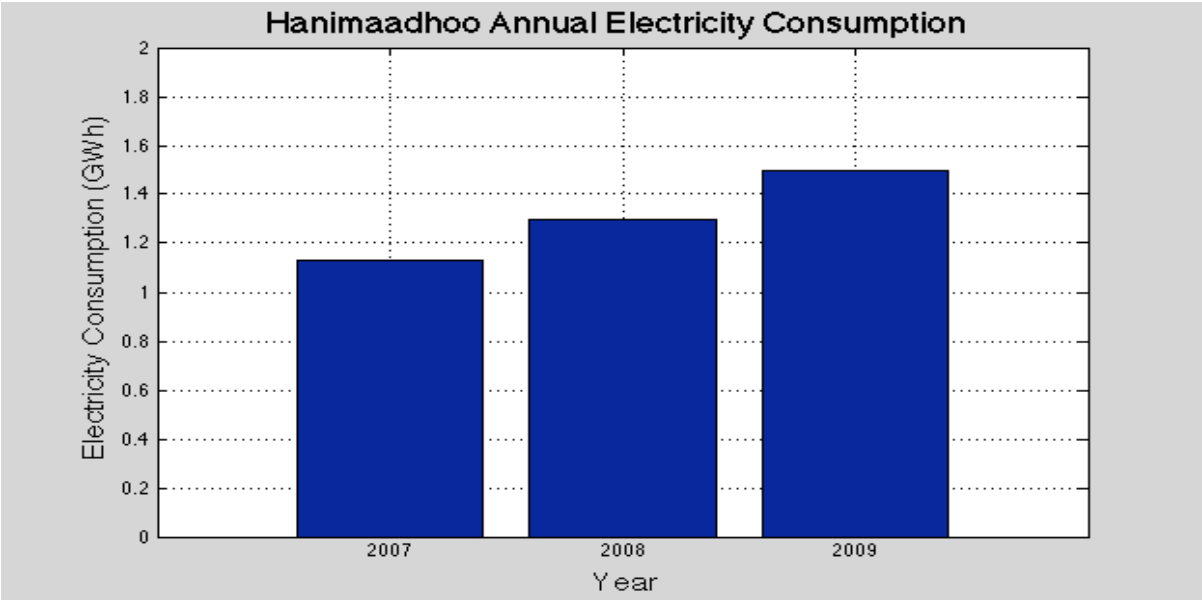


Figure 4-5 Hanimaadhoo Annual Electricity Consumption

4.1.2 Climatic Effects

The climatic effects of demand on Hanimaadhoo are examined in this sub-section. The average hourly ambient air temperature between 2004-2007 was recorded as 28 ºC and indicates that space cooling is the required heating/cooling service. The demand and Cooling Degree Day (CDD) correlation is conducted against an internal building temperature range of 21°C – 26°C with 1°C intervals (DegreeDays.net, 2011). The correlation coefficients for the aforementioned temperature range are shown in Table 4-1 below.

Table 4-1 Internal Building Temperature Range for CDD Data

Internal Temperature (°C)	21	22	23	24	25	26
Correlation Coefficient (R^2)	0.49	0.49	0.47	0.45	0.42	0.41

Table 4-1 above shows that there is a low correlation coefficient throughout the range of examined internal building temperatures. Although this coefficient increases with a decrease in internal temperature, it is still not at a level that can prove a strong linear relationship between the two variables. Therefore, it can be concluded that the energy demand of this island does not show a strong correlation with climatic factors.

4.1.3 Growth

The main factors of growth on Hanimaadhoo can be credited to a change in population or the infrastructure operating on the island. The total population on Hanimaadhoo rose from 1009 to 1184 in the years between 2000 and 2006, equivalent to a 15 % increase over this 6-year period (MPND, 2007). In terms of infrastructure, the island accommodates the Hanimaadhoo Airport, which was upgraded by the addition of more flights from a domestic to international airport in February 2012. The main reason for this upgrade was to foster development and growth in the region (MTCA, 2005). In terms of energy demand, the infrastructure and growth rates are expected to be evident from the increase in future demand and the subsequent need for a larger supply capacity.

Hanimaadhoo Energy Demand Summary

This section has provided an energy demand analysis for the island of Hanimaadhoo in the Maldives using the temporal, growth and climatic demand factors. On an annual basis, a consistent 15 % increase in demand is identified. Finally, demand does not show a strong correlation with climate.

4.2 Renewable Energy Resource Assessment – Hanimaadhoo Case Study

This section examines the implementation of the renewable energy resource assessment methodologies presented in 3.2. The usefulness of this assessment's result is two-fold: firstly, it identifies the resources that should be further considered in the supply mix; and, secondly, it presents the magnitude and occurrence of each resource that is later used to estimate the power and energy generation of each technology.

1.1.1 Determinative Resource Assessment

This section examines the determinative resource assessment on Hanimaadhoo using solar energy as an example. The methodology followed to conduct this assessment is presented in section 3.2.1. The results from this assessment allow an understanding of the magnitude and occurrence of this resource on the

island and a decision is made for its further consideration in the renewable energy supply mix design process.

4.2.1.1 Solar Energy

The solar energy assessment is conducted by the optimum solar collector tilt and annual energy absorbed on the island. The collector spacing, to determine the land area requirement, is found using the sun path over the island. The data used in this analysis has been obtained from the local meteorological station.

Optimum Solar Collector Tilt Angle - Hanimaadhoo

The Maldives is located in the northern hemisphere and so the collector must be south facing. To determine the optimum collector position for maximum annual solar energy, the total radiation is calculated for a range of tilts with 5º intervals. To model the island's sea coverage, an albedo constant of 0.05 is used and the results are shown in Figure 4-6 below.

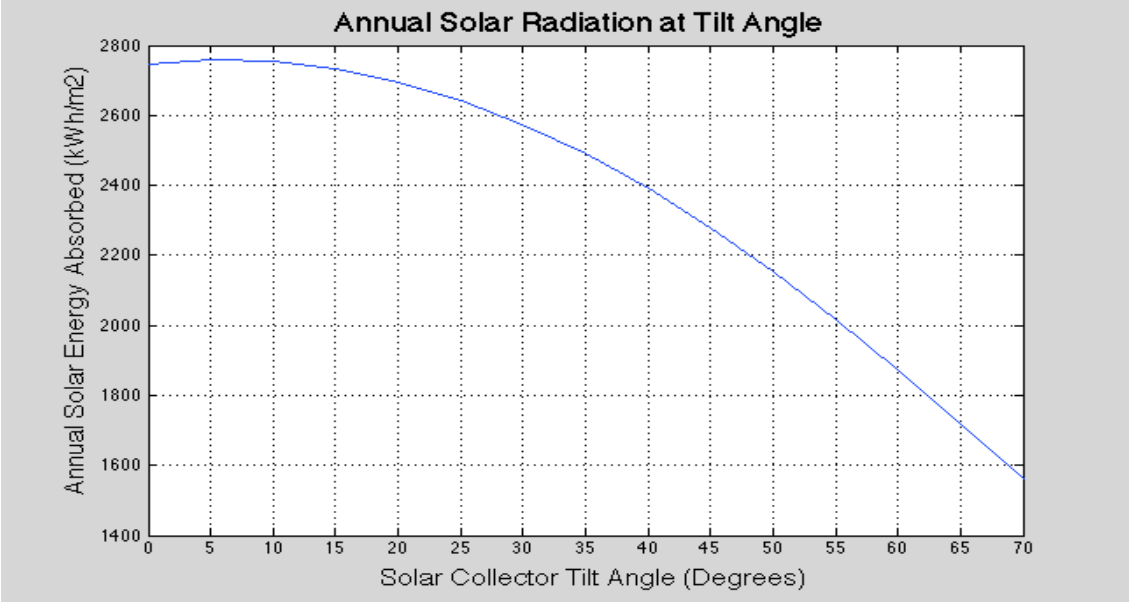


Figure 4-6 Total Solar Radiation Absorbed per Tilt Angle

From the graph in Figure 4-6 above, a tilt angle of 6º is selected as it provides the maximum solar energy absorbed on the island.

Minimum Collector Spacing

Table 4-2 below presents the azimuth and altitude of the sun at the winter solstice. These angles are inserted in Equations (3-9) to (3-11) in section 3.2.1 above to identify the minimum spacing below.

Table 4-2 Minimum Collector Spacing at Hanimaadhoo

Altitude (º)	Azimuth (º)	D (m)	D' (m)
55	150	1.98	1.72

Solar Energy Absorbed at the Optimum Tilt Angle

The average hourly radiation per annum at a 6º tilt angle is shown in Figure 4-7 below. This graph is constructed by an average of the total solar radiation at each time point throughout the year. The annual total solar energy that can be absorbed on Hanimaadhoo is equivalent to 2700 kWh / m^2.

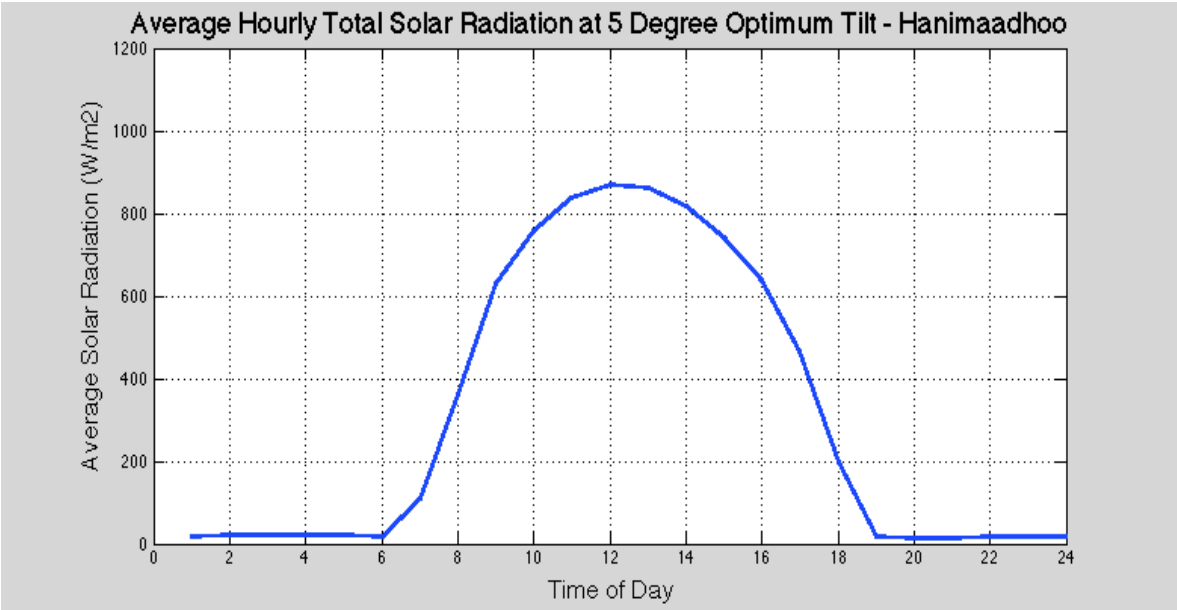


Figure 4-7 Hourly Average Total Solar Radiation

The minimum daily solar energy absorbed occurs on the 3rd of May which is within the monsoon period boundaries.

4.2.2 Dispatchable Resource Assessment

This section examines the dispatchable resource assessment on Hanimaadhoo using biomass energy as an example. The results from this assessment allow an understanding of the magnitude and occurrence of this resource on the island. A decision is then made for its further consideration in the renewable energy supply mix design process.

4.2.2.1 Biomass Energy

This sub-section examines an assessment of the biomass resource on the island of Hanimaadhoo. The island of Hanimaadhoo does not practise any agricultural or commercial activities at a significant scale and, thus, the agricultural waste, energy crop and C&I biomass categories are further excluded.

MSW generation data shows that, for outer islands, the per capita waste is 0.55 kg per day of which the organic composition is 53 % (Mohamed, 2011). Using the 1184 person population and an average biogas yield of 44 m^3 per tonne of organic waste, the potential energy content from MSW is 62 MWh. In terms of installed capacity, and assuming an expected annual performance of 8000 hours per year with an electrical conversion efficiency of 40%, this potential energy content can satisfy the consumption of a 3.1 kW_e plant (Baldwin & Katers, 2009). This energy content is considered to be too low for a cost-effective utilization and does not, therefore, satisfy the indicators of this study. However, it is suggested that an organic waste management scheme should be further examined for groups of islands or atolls fuelling a centralized anaerobic digestion. This investigation is considered out of the scope of this thesis.

4.2.3 Stochastic Resource Assessment

This section examines the stochastic resource assessment on Hanimaadhoo using wind energy as an example. The methodology followed to conduct this assessment is presented in section 3.2.3. The results allow an understanding of the magnitude and occurrence of this resource on the island. A decision is then made for its further consideration in the renewable energy supply mix design process.

4.2.3.1 Wind Energy

The power in the wind is proportional to the cube of the wind speed. To illustrate how this resource behaves on an hourly time scale, throughout all seasons of the year, the cube of the hourly wind speed, recorded at a vertical height of 15 m height is shown in Figure 4-8 below.

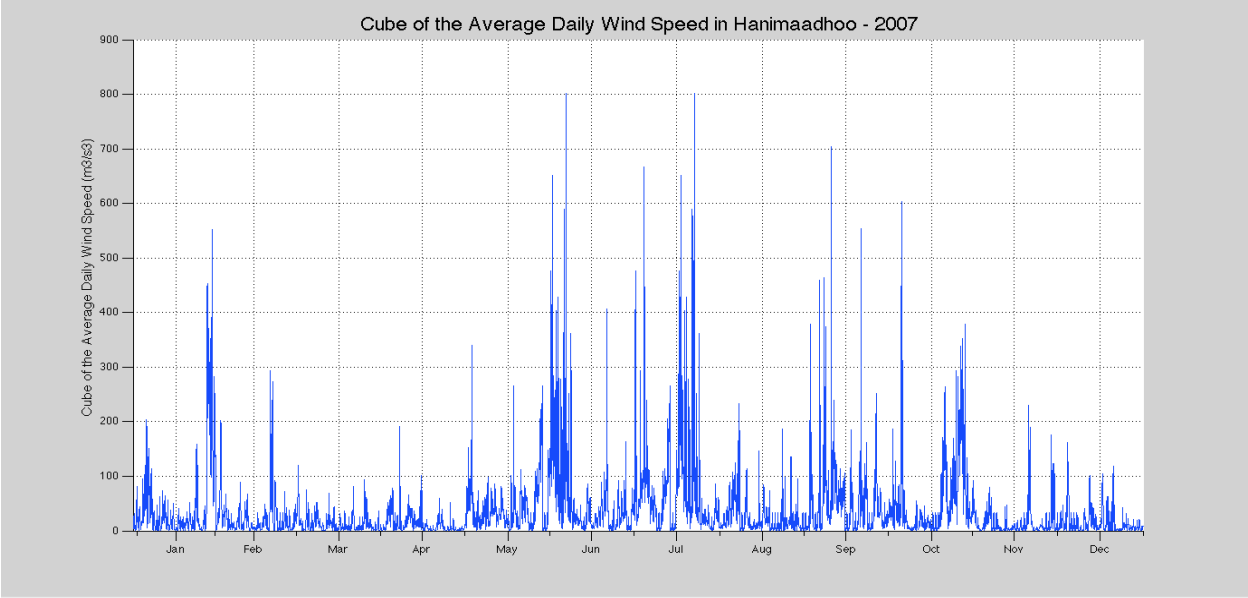


Figure 4-8 Cube of the Average Hourly Wind Speed over 1-year

The seasonal distribution shows consistent peaks that occur between May and July which will allow further analysis of a potential wind – solar resource complement as it may be possible to generate a continuous seasonal renewable energy supply by utilizing this seasonal wind peak.

Vertical Wind Shear

This sub-section uses the vertical wind shear methodology to extrapolate the wind speed data to 30 m, 50 m, 60 m and 80 m vertical heights, as shown in Table 4-3 below. The surface roughness constant used is 0.003 based on the topographical mixture of open sea and agriculture observed on the island.

Table 4-3 Hanimaadhoo Vertical Wind Shear

Height (m)	15	30	50	80
Average wind speed (m/s)	2.8	3	3.2	3.3

Table 4-3 above shows that there is a minimal difference between the wind speeds at a 15 m and 80 m vertical height. The flat topography and minimal height above sea level are the main factors behind this effect since there are a lack of physical obstructions, such as mountains and hills, which could cause a larger surface friction value and, thus, higher rate of increase in wind speed with height.

Wind Speed Occurrence Probability

The Weibull shape and scale parameters have been determined using the maximum likelihood method approach. The Weibull plot of probability density against corresponding wind speed for a 15 m vertical height is shown in Figure 4-9 and for a 50 m vertical height in Figure 4-10 below.

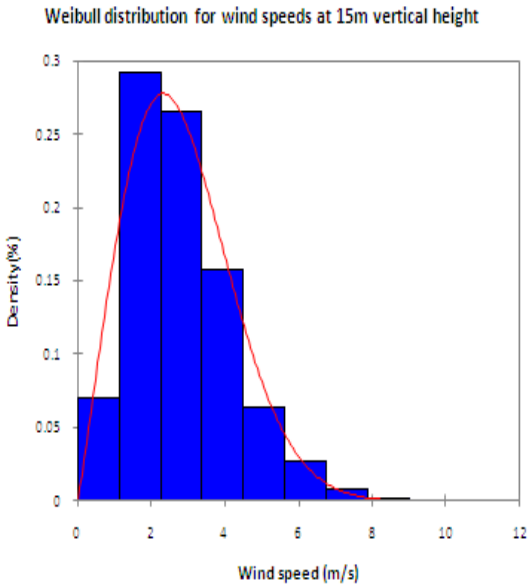


Figure 4-9 Weibull Plot at 15 m

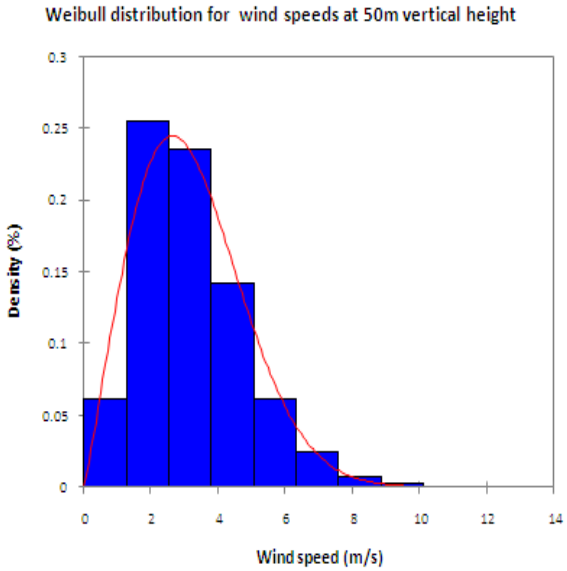


Figure 4-10 Weibull Plot at 50m

Wind Power Density

The wind power density at Hanimaadhoo at various vertical heights is shown in Table 4-4 below.

Table 4-4 Wind Power Density at the Range of Heights Examined

Height (m)	Wind Power (W/m^2)	Wind Class
15	16	1 (Poor)
30	20	1 (Poor)
50	20	1 (Poor)
80	25	1 (Poor)

The results in Table 4-4 above show that for all the vertical heights examined, Hanimaadhoo shows a consistently "poor" wind resource. The utilization of wind as a prime driver in the renewable energy supply mix to meet demand is not suggested. However, the seasonal availability has identified the possibility to use wind to complement other resources, and is examined in the next sub-section.

4.2.3.1.1 Potential for Wind – Solar Resource Combination

The wind resource analysis in this section shows a class 1 wind site, described as "poor" for the utilization of this resource. However, the Weibull distribution and site classification methods do not allow for the possibility of using this resource to complement another type, in this case solar. To identify the prospective combination of resources, the graph in Figure 4-11 below shows the average monthly wind power and solar energy on Hanimaadhoo.

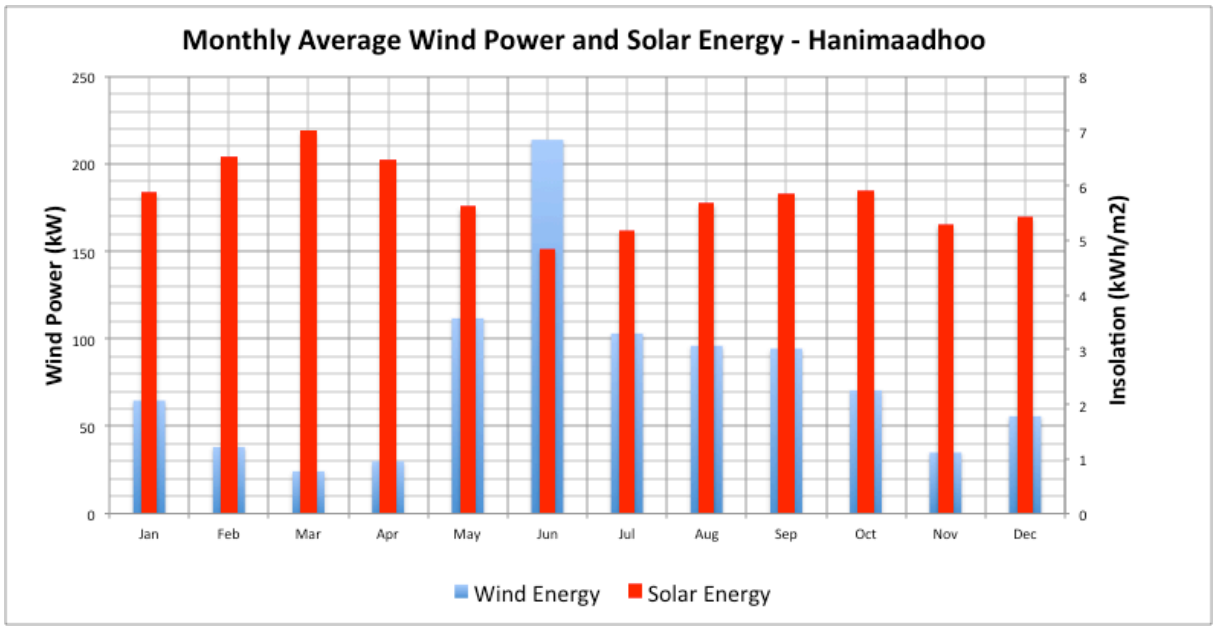


Figure 4-11 Average Monthly Wind Power and Solar Energy - Hanimaadhoo

The graph, in Figure 4-11 above, shows that especially during the May to July period, the solar resource is at an annual minimum. During the same time period, the wind resource is at an annual maximum and may be used to complement the reduced solar availability. Therefore, even though Hanimaadhoo is classed as a "poor" wind site, this resource will be considered further in the design process as a solar complement to provide a constant supply of renewable energy throughout the year.

4.2.4 Hanimaadhoo - Potential Renewable Resource Assessment Summary

To summarize, due to its low potential, the biomass resource is not a cost-effective solution and is not further considered in the supply mix design process. As can be expected of the geographic location of the island, the solar resource is calculated at a relatively high potential and so is further considered in the design process. The wind resource on the island is calculated as a class 1 wind site indicating that this resource should not be further considered in the design process. However, due to the relatively high wind speeds, especially between May and July, when solar is at a minimum, the wind resource is further considered in the supply mix design process. This is due to the possibility of a wind – solar complement to provide a constant energy supply from renewable sources throughout the year.

4.3 Available Conversion Technology Assessment

The previous section identified the solar and wind resources as the renewable energy resource elements of the proposed Hanimaadhoo supply mix. This section examines the implementation of the available conversion technology methodologies, examined in Chapter 3, in the solar PV and wind turbine technologies on Hanimaadhoo. The indicator assessment methodologies are conducted, assuming the installation and operation of one unit of each technology on the island.

4.3.1 Solar Photovoltaic Assessment

This sub-section examines the energy generation and indicator performance of one PV unit on the island of Hanimaadhoo. The 5-parameter single diode model, presented in detail in section 3.3.4, is used to represent the Suntech STP 190 W device assuming a 6º and 0º tilt and orientation installation respectively. The results are shown in Table 4-5 below. The technology capital and O&M cost are extracted from the medium cost scenario in the same section above (ParsensBrinckerhoff, 2012). The capital cost is annualized using a 5 % discount rate and a 25-year lifetime.

Table 4-5 Indicator Performance of Solar PV on Hanimaadhoo

PV Panel	Capacity (kW_e)	Energy Generation (kWh_e)	Capital Cost ($)	O&M Cost ($/year)	Total Annual Cost ($/year)	Cost of Electricity ($/$kWh_e$)	Energy per Unit Capacity (kWh_e/kW_e)
Suntech	0.19	447	380	6.8	34.4	0.08	2352

The cost of diesel generation on the outer island of the Maldives is reported at 0.4 $ / kWh_e output (Mason, 2012). A PV unit generating 477 kWh_e will require a total annual cost of $ 34.5 to displace a $ 191 diesel cost and this technology is therefore performing better than grid parity.

4.3.2 Wind Turbine Assessment

This sub-section examines the energy generation and indicator performance of one wind turbine unit on the island of Hanimaadhoo. In order to identify the capacity and turbine hub height, a range of options are examined against the indicators and the combination with the most favourable performance is selected and used further in the design process.

Indicator Performance of Wind Turbines

To select the appropriate wind turbine and hub height, five manufacturers with installed capacities of 10 kW (30m), 55kW (30m), 100 kW (40m), 250 kW (50m) and 500 kW (50m) are modelled for the Hanimaadhoo site. The indicators for one unit of each turbine are shown in Table 4-6 below.

Table 4-6 Wind Turbine Indicator Performances - Hanimaadhoo Site

Manufacturer	Hub Height (m)	Capacity (kW_e)	Energy Generation (MWh/year)	Capital Cost ($'000s)	O&M Cost ($'000s/year)	Total Annual Cost ($'000s /year)
Excel Bergey	30	10	1.7	57	0.6	4.6
Coemi	30	55	10.0	128	4.0	12.3
Northern Wind Power	40	100	18.0	231	7.38	23.1
Wind Energy Solutions	50	250	28.0	577	18.5	60.0
NED Wind	50	500	73.0	1154	37.0	118.5

To select the required turbine, the energy generation cost per turbine is compared and the lowest cost is identified. The generated cost is shown graphically, per turbine, in Figure 4-12 below.

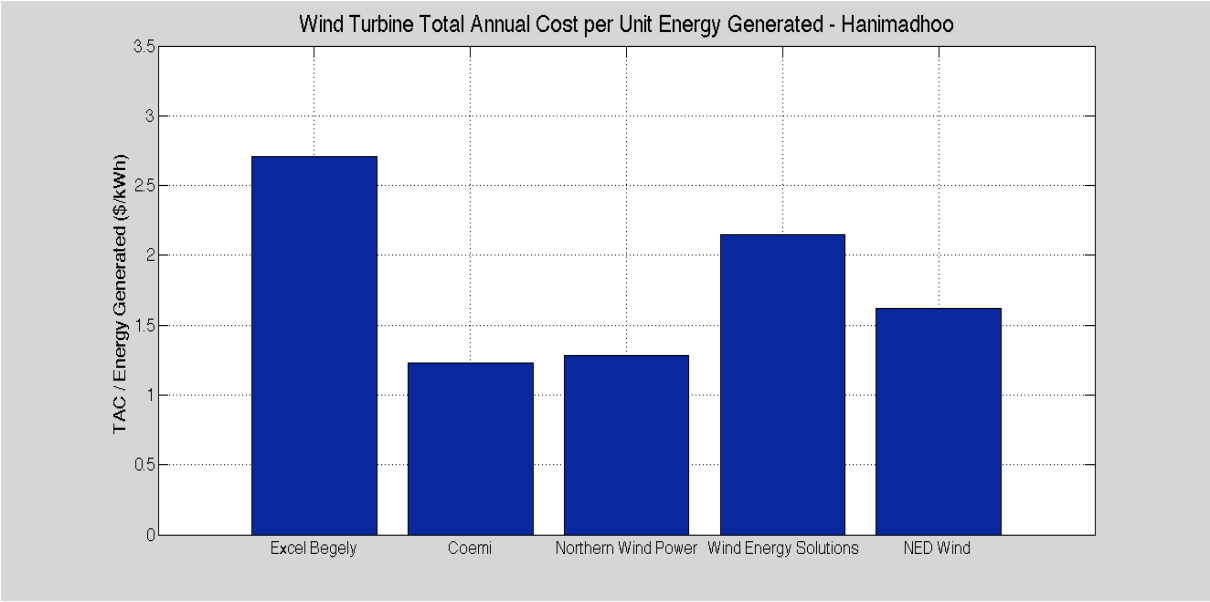


Figure 4-12 Total Annual Cost of Energy Generated Performance per Wind Turbine

From the graph in Figure 4-12 above, the Coemi 55 kW_e turbine is the most cost effective wind turbine solution for the annual electrical energy it can generate. It is, therefore, considered as the most appropriate turbine according to the decision-making indicators used in this study. It must be noted that, although it is the most cost-effective solution, the generation cost of $ 1.2 / kWh_e must still be considered

an expensive technology in comparison to the diesel generation cost ($ 0.4 / kWh_e) and the photovoltaic generation cost ($ 0.08 / kWh_e).

4.4 Renewable Energy Supply Mix Design – Hanimaadhoo Case Study

This section presents the implementation of the constrained exhaustive search renewable energy supply mix methodology in the Hanimaadhoo case study. The technologies considered are identified from the resource assessment as the wind turbine, PV and lead-acid battery storage systems. A diesel generator is also used as a back-up supply. The constrained exhaustive search space minimization technique is examined for the upper bound limits of these technologies on the island. The results present the optimum installed capacity based on the total annual cost and emissions reduction indicator performance.

4.4.1.1 Constrained Exhaustive Search Space Minimization

The following two sub-sections present the implementation of the constrained exhaustive search space minimization technique in the PV, wind turbine and lead-acid battery storage systems respectively in order to determine the upper bound limits of each technology for the final search space.

Photovoltaic and Wind Turbine Upper Bound Limits

The diesel generation to meet demand for a range of PV units is shown in Figure 4-13 below.

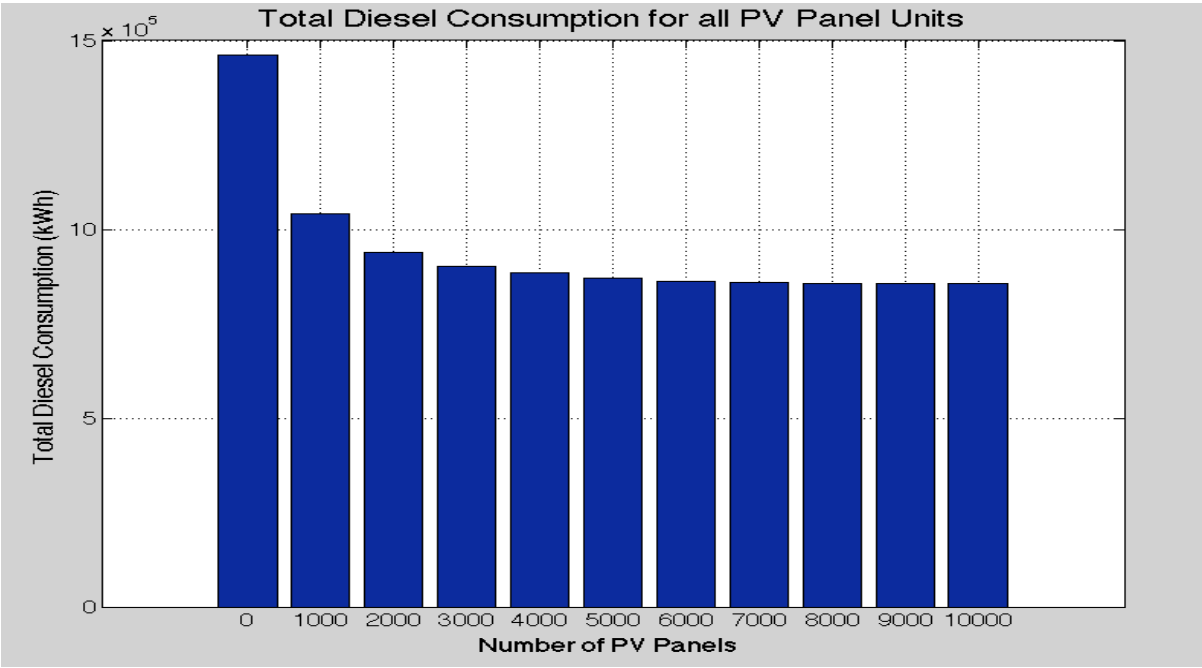


Figure 4-13 Total diesel generation against the number of PV panels (Suntech 190W)

The results above show that the "saturation point" is 9000 units. At this installed capacity, an increase in the number of panels does not have an effect on the diesel consumption required to meet demand on Hanimaadhoo. Therefore, the upper bound limit of the PV capacity is set at 1710 kW_e.

The diesel generation to meet demand for a range of wind turbine units is shown in Figure 4-14.

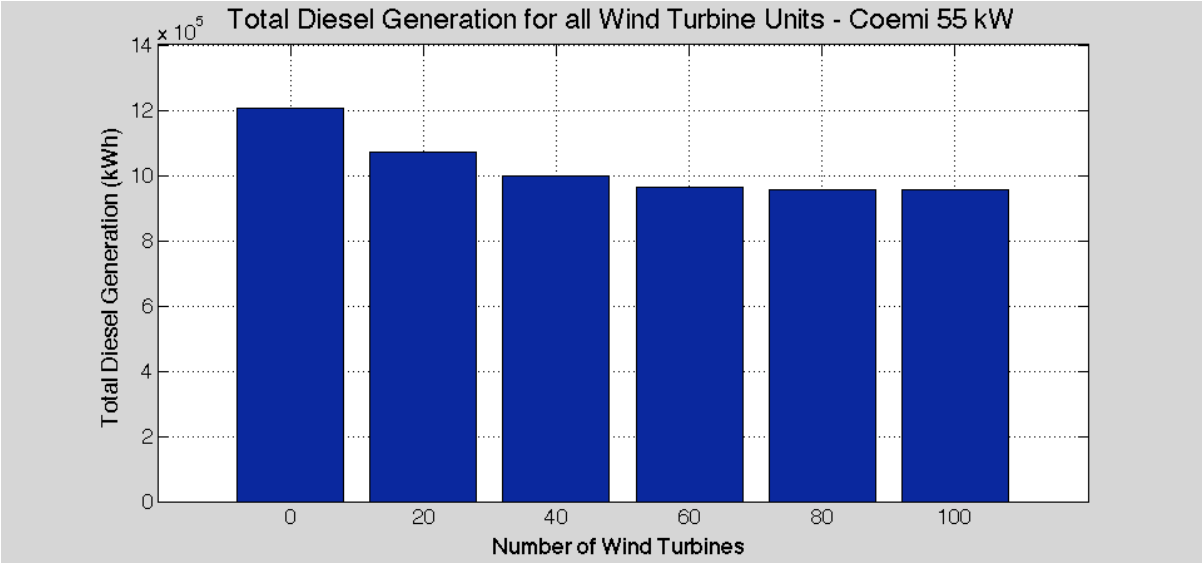


Figure 4-14 Total diesel consumption against number of Wind Turbine Units (Coemi 55 kW_e)

The results, in Figure 4-14 above, show that the "saturation point" of Wind Turbines is 80 units. At this installed capacity, an increase in the number of turbines does not have an effect on the diesel consumption required to meet demand. Therefore, the upper bound limit of the wind turbine in the constrained exhaustive search algorithm is set at 4000 kW_e.

Battery Storage Upper Bound Limits

Since the storage requirement for a PV only and a PV and wind turbine supply will have a different daily demand deficit and surplus, the upper bound battery limit is shown for both in Table 4-7 below assuming a 2 kWh_e battery with a minimum state of charge of 33 %.

Table 4-7 Daily Demand Indicators

Supply Mix	Maximum Daily Demand Deficit (MWh_e)	Maximum Daily Demand Surplus (MWh_e)	Utilizable Stored Electrical Energy (MWh_e)	Lead-acid Battery Capacity (kWh_e)	Upper Bound Number of Battery Units
• 9000 PV Panels • 80 Wind Turbines	3.2	48.8	3.2	4.8	2424
• 9000 PV Panels	4.27	44.9	4.27	6.5	3250

4.4.1.2 Final Renewable Energy Supply Mix Design

The final step in the renewable energy supply mix design is the implementation of the constrained exhaustive search algorithm using the minimized search space parameters per technology. Finally, a PV-battery storage supply mix, not including the wind turbine technology due to its relatively high generation cost is considered.

Photovoltaic, Wind Turbine and Lead-Acid Battery Storage Supply Mix

The total annual cost and emissions reduction indicator output for the PV, wind turbine and battery storage supply mix is shown in Figure 4-15 below.

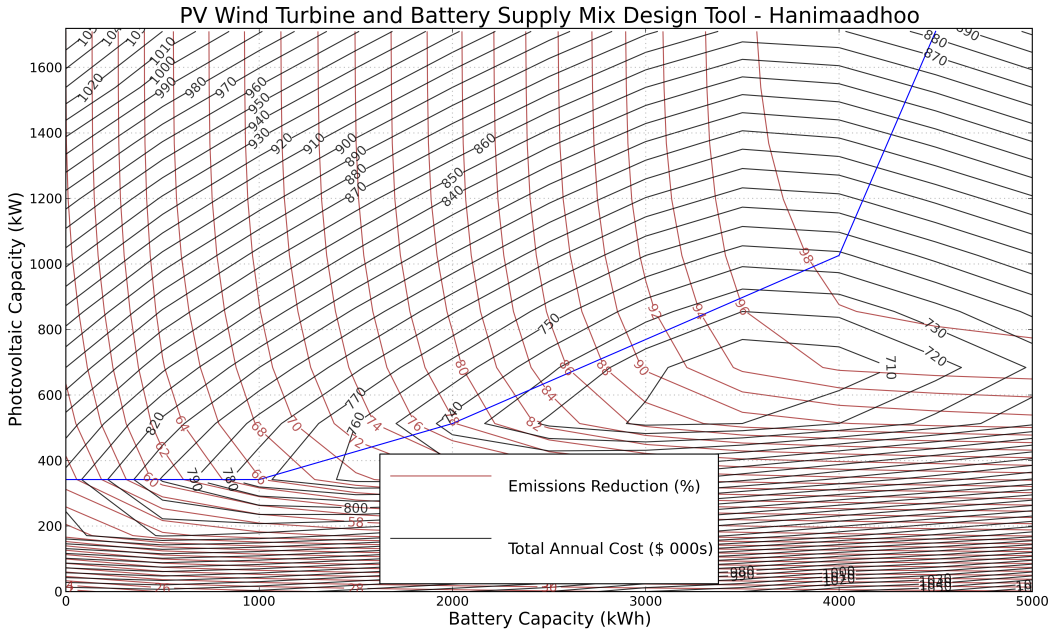


Figure 4-15 PV Wind Turbine and Battery Storage Supply Mix Design - Hanimaadhoo

It can be seen above that the supply mix that will achieve carbon neutrality and satisfy the total annual cost and emissions reduction indicators assuming the wind turbine saturation point of 4000 kW_e is 1000 kW_e PV, 3900 kW_e battery storage. The total annual cost of this system is $ 740,000/year, which is more expensive than the current total diesel generation cost including maintenance of $ 720,000 / year.

Photovoltaic and Lead-acid Battery Storage Supply Mix

The total annual cost and emissions reduction indicator output for the PV and battery storage supply mix is shown in Figure 4-16 below.

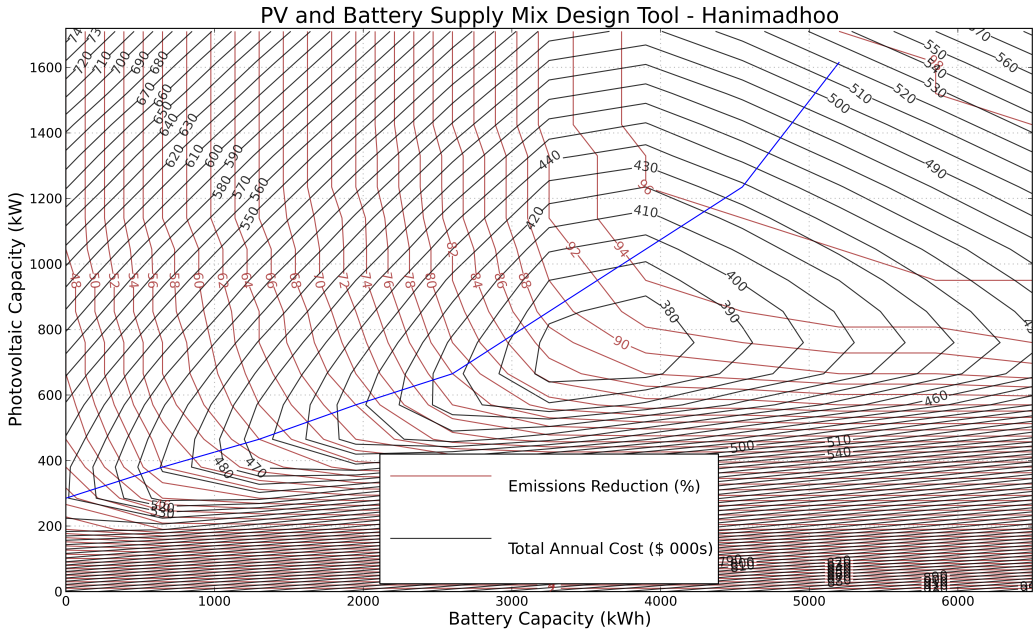


Figure 4-16 PV and Battery Supply Mix Design Tool - Hanimaadhoo

The supply mix that will achieve carbon neutrality and satisfy the total annual cost and emissions reduction indicators is 1710 kW_e PV and 6500 kWh_e of battery storage. The total annual cost of this system is $ 582,000 per year. It is important to note that carbon neutrality cannot be achieved within the scope of this study without the inclusion of energy storage.

Although the possibility of the wind resource complementing the solar resource at a seasonal time scale has been previously identified, its inclusion to approach carbon neutrality creates a supply mix that is less competitive than the current case that has no renewable energy element.

4.5 Chapter Summary

This chapter has conducted an energy demand analysis, renewable energy resource and conversion technology assessment, based on the methodology developed in Chapter 3, on the island of Hanimaadhoo in the Maldives. As expected, the island demonstrates a strong annual solar resource with a minimum level during the monsoon period between the months of May and July. A poor wind resource has been identified that has a maximum availability during the monsoon period and has, therefore, been further examined as a complement to the solar resource. The biomass resource has been determined as having minimal potential and has not been further investigated.

The PV generation has been determined to be at grid parity level as it generates electricity at a cost of $ 0.08/kWh$_e$ in comparison to the diesel cost of $ 0.4/kWh$_e$. This technology's saturation point with respect to demand is an installed capacity of 855 kW$_e$. The wind turbine saturation point with respect to demand is an installed capacity of 4000 kW$_e$.

The renewable energy supply mix methodology has been implemented for the solar PV, wind turbine and lead-acid battery storage conversion technologies. The inclusion of the wind turbine technology has proven to incur a higher cost than the current situation. The optimum supply mix only comprises of the PV and lead-acid battery technologies at a composition of 1710 kW$_e$ PV and 6500 kWh$_e$.

Chapter 5 – Oxfordshire Case Study

The previous chapter examined the implementation of the renewable energy supply mix design methodology, developed in Chapter 3, on the island of Hanimaadhoo in the Maldives, representing a tropical climate. This chapter considers the implementation of the methodology in a temperate climate represented by the county of Oxfordshire in the UK and the Christ Church site, located within the county boundaries and used as small-scale model establishment.

The Didcot A power station, located in south Oxfordshire, is a 2 GW_e capacity dual-fired coal and natural gas fired power station that began commercial operation in 1970. This station is able to provide power to approximately 2 million households, equivalent to over twice Oxfordshire's population. Didcot A operates as an "opted out station" with respect to the Large Combustion Plant Directive (LCPD), which enforces rigorous environmental compliance by limiting the emission of nitrogen oxide, sulphur dioxide and dust particulates. This power station is only authorized to operate for 20,000 hours, between 1st of January, 2008 and 31st December, 2015, and must be decommissioned by the end of 2015 (Npower, 2011). Some Non Governmental Organizations (NGOs), such as the Low Carbon Hub, have proposed that, since Didcot A is being decommissioned, there is an opportunity to install renewable technologies locally and, thus, reduce the replacement requirement of conventional fuels (LCH, 2012). Local installations are also beneficial since they can displace the requirement of transmitting renewable energy from long distances, such as wind energy from Scotland. Even though it is expected that the renewable generation potential in the county is insufficient to meet demand, this study prioritizes the maximization of the credible renewable energy potential and the usage of conventional power to meet the supply deficit. Oxfordshire's large surface area requires a mapping of the relevant resource to understand and assess the spatial distribution of each resource across the county using a GIS approach.

The Christ Church site, located in the county of Oxfordshire, has set a target of 60 % reduction in carbon dioxide emissions by 2020 (Harris, 2008). Christ Church has a demand mix, characterized by domestic and commercial users within one site, which is used in this study as an example of a case study geographically located within Oxfordshire.

The renewable energy supply mix design methodology, developed in Chapter 3 of this thesis, is implemented in the entire county of Oxfordshire in the first section of this chapter and in the individual Christ Church site in the second section of this chapter.

5.1 County of Oxfordshire

This section examines the design of a renewable energy supply mix to meet the demand of the county of Oxfordshire in the UK using the methodology developed in Chapter 3. In 2012, the Low Carbon Hub (LCH), a NGO in Oxford, commissioned this study as part of a broader investigation funded by the Department of Energy and Climate Change entitled "The Oxfordshire Energy Future". A brief review of the case study is initially conducted in terms of the county's population and current sources of carbon dioxide emissions. An energy demand analysis and potential resource and conversion technology assessment are presented and the results are used in the supply mix design.

Review of the Oxfordshire Case Study

The county of Oxfordshire is located at the northwest corner of the southeast region of England. The population is 650,000 occupying 260 thousand households, equivalent to an average of 2.48 people per household. Oxfordshire is comprised of 5 district authorities namely, Cherwell, Oxford, South Oxfordshire, Vale of White Horse and West Oxfordshire (OCC, 2012). Carbon dioxide emissions rose from 7.2 tonnes per capita in 2009 to 7.4 tonnes per capita in 2010[16]. This was the first time emissions had increased since 2005 and was due to the increased gas demand for space heating in 2010, the coldest winter since 1987 (DECC, 2010).

Figure 5-1 below shows that industrial and commercial sources account for over 40 % of CO_2 emissions, domestic sources for approximately 33 % and transportation for 27 % (OCC, 2012).

[16] The Oxfordshire emissions per head are above the national average of 6.6 t CO_2 per head

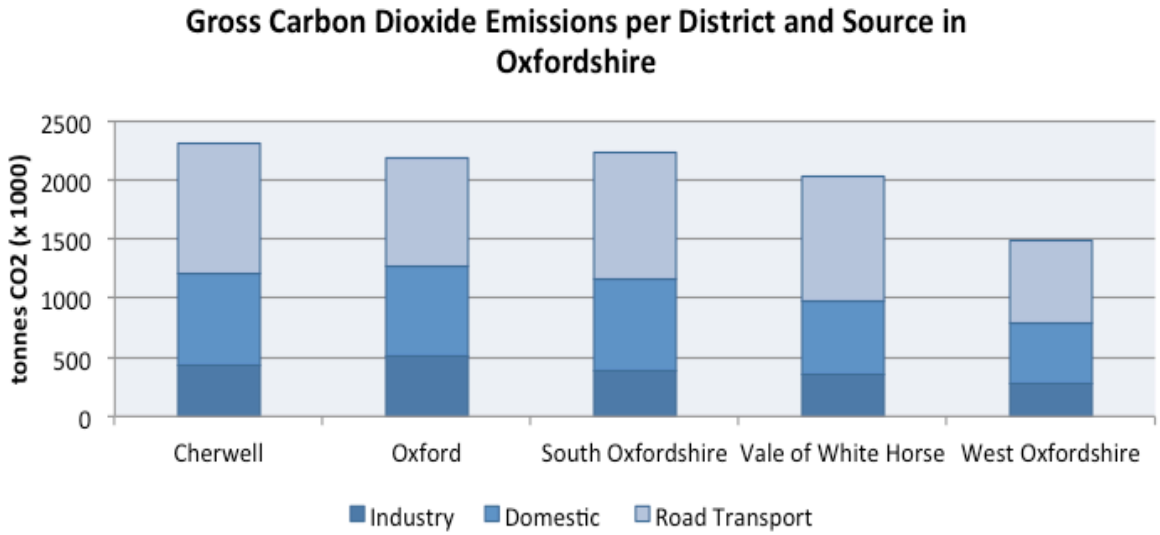


Figure 5-1 Gross CO_2 Emissions per District and Source in Oxfordshire. (Source: Oxfordshire County Council (OCC, 2012))

5.1.1 Energy Demand Analysis – Oxfordshire

This section examines the application of the energy demand analysis, developed in section 3.1, on the Oxfordshire demand. The results allow the assessment of the temporal analysis, climatic and growth factors on the demand.

Oxfordshire Electricity Demand

The Oxfordshire energy demand at an hourly time resolution is not available. The available data is the annual electricity consumption per district, published by the Department of Energy and Climate Change in a Sub-National Authority Electricity Statistics review (DECC, 2010a). To overcome the unavailable hourly demand data issue, it is assumed that Oxfordshire is a representation of the UK and so the half hourly demand recorded by the National Grid is adjusted using the Oxfordshire to England, Scotland and Wales population ratio for 2011-2012 (NationalGrid, 2012)[17]. The population of Oxfordshire is 0.65 million and of the UK is 59.6 million, giving a population ratio of 0.011 (ONS, 2007). The main assumption in this adjustment is that the Oxfordshire profile is consistent with the national profile and, thus, only the demand magnitude is estimated. The constructed data set is then converted to an annual energy demand and compared against the 2005 – 2011 recorded usage published by DECC. The average annual percentage difference is then used to shift the magnitude of the constructed hourly profile to

[17] The demand profile is referred to as the "constructed profile"

generate a final data set that is used in this chapter. To do this, the temporal analysis section initially presents the seasonal and annual change analysis.

5.1.1.1 Temporal Analysis

This section examines the temporal analysis of the Oxfordshire demand data.

Seasonal and Annual Change

A comparison of the recorded and constructed annual demand data for the period 2005 – 2011 is shown in Figure 5-2 below.

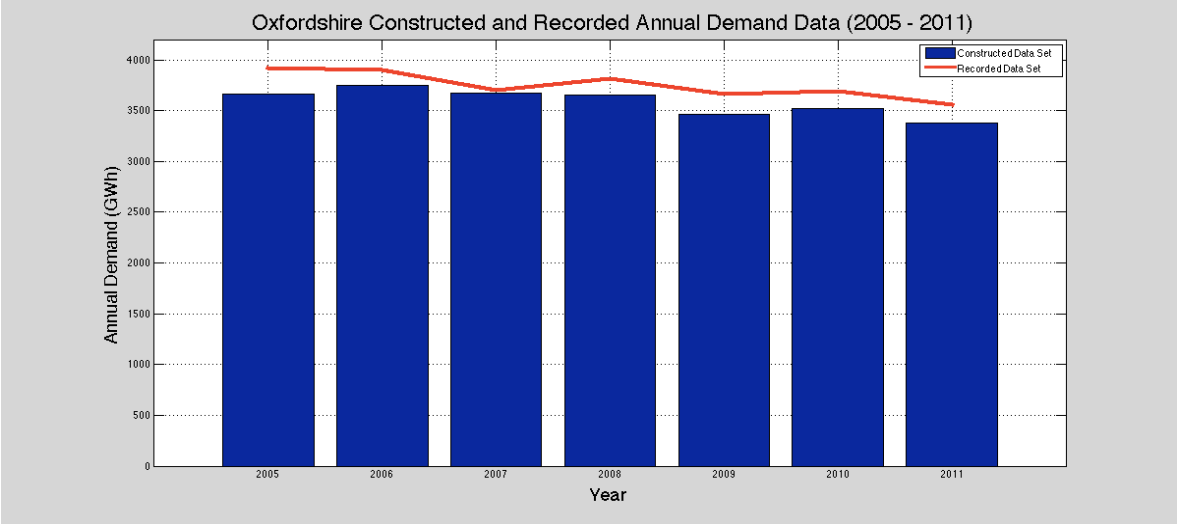


Figure 5-2 Comparison of the Oxfordshire Constructed and Recorded Annual Demand (2005 - 2011). (Source: Constructed Data Obtained from Adjusted National Grid Data (NationalGrid, 2012) and Recorded Data from DECC (DECC, 2010a))

The recorded data shows a consistently higher annual demand than the constructed data for all the periods examined. The average annual percentage difference between the two data sets used to adjust the constructed profile to its final form is 4.5 %.

The seasonal demand for 2011, using the final constructed data set, is shown in Figure 5-3 below.

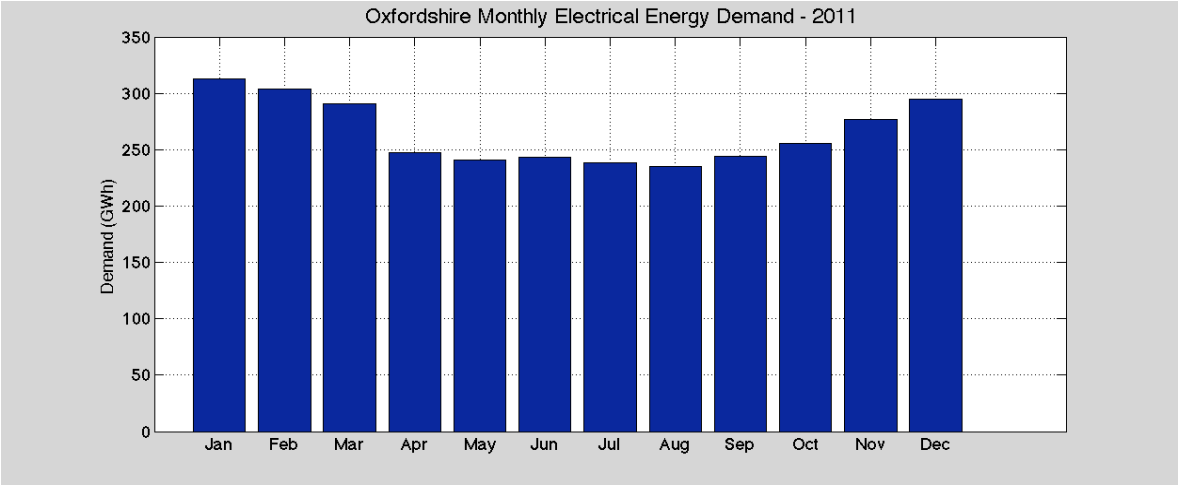


Figure 5-3 Oxfordshire Monthly Electricity Demand 2011 (Source: Adjusted National Grid Data (NationalGrid, 2012). Recorded Data from DECC (DECC, 2010a))

A summer/winter seasonal magnitude shift is present throughout the year, expected to be due to weather effects on demand, examined further in the climatic factor sub-section.

A further breakdown of the proportion each district has in the county's energy demand is shown in Table 5-1 below. The electricity demand ratio represents the ratio between each district's average annual demand between 2005 and 2011 and the county's average total annual demand. The electricity demand per person is also reported below.

Table 5-1 Electricity Demand Ratio and Population Ratio per District in Oxfordshire

District	Electricity Demand Ratio	Demand per Person (MWh/person)
Cherwell	0.21	5.3
Oxford	0.23	5.5
South Oxfordshire	0.23	6.1
Vale of White Horse	0.19	5.6
West Oxfordshire	0.14	4.8

The Oxfordshire average electricity demand per person is 5.5 MWh_e, which is 4.5 % less than the UK national average demand per person of 5.7 MWh_e (WorldBank, 2012). South Oxfordshire is the only district that has a higher demand per person than the national average, with a 7 % difference.

Average Power Analysis

The Average Power Analysis is presented graphically in Figure 5-4below for the minimum, maximum and Average Power in Oxfordshire.

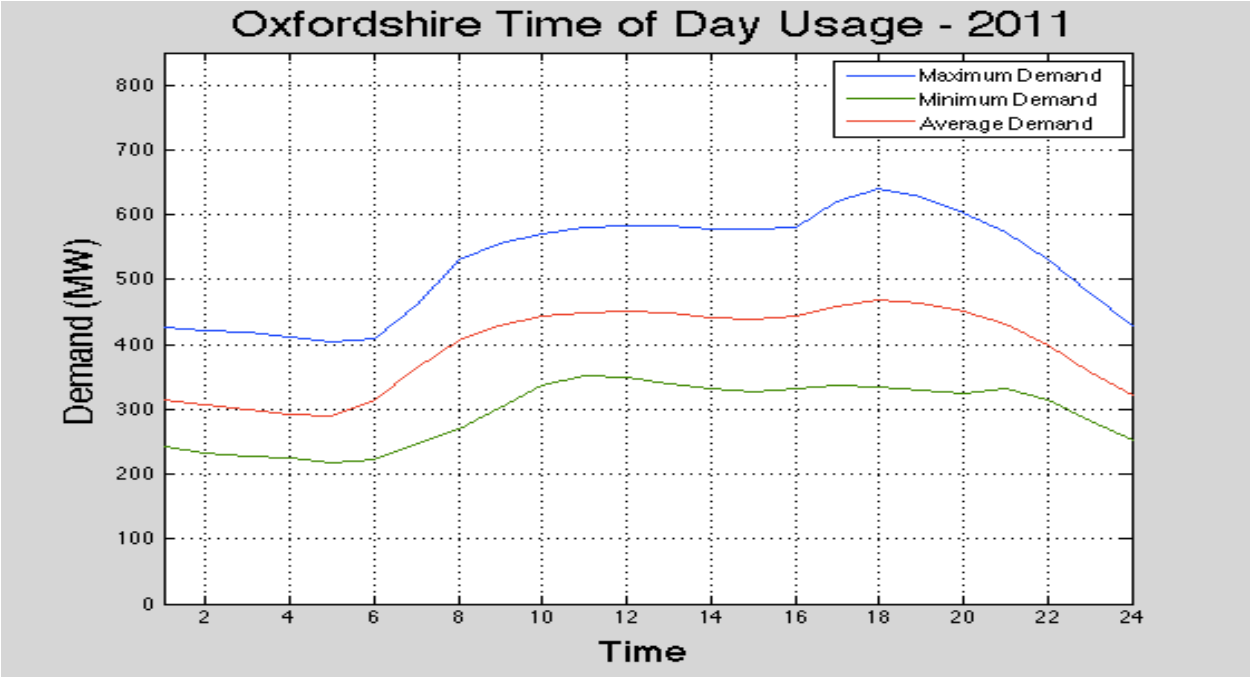


Figure 5-4 Oxfordshire Average Power Analysis (Source: Adjusted National Grid Data (NationalGrid, 2012))

The profile shape follows the typical daily UK consumption pattern, with the peak load especially evident in the maximum demand case between 1700 and 1900. The maximum case has a higher rate of demand increase between the morning hours of 0600 – 0800 and the afternoon peak hours between 1700 – 1900, than the flatter average and minimum cases.

5.1.1.2 Climatic Effects

The climatic effects on demand are examined in this sub-section. The monthly HDD data set constructed assumes an internal building temperature of 18ºC from the maximum available period of 2008 – 2012 (ECI, 2013). The temperature data set used to conduct this analysis represents the Benson Meteorological office. A linear regression analysis of the demand and monthly HDD is shown in Figure 5-5 below.

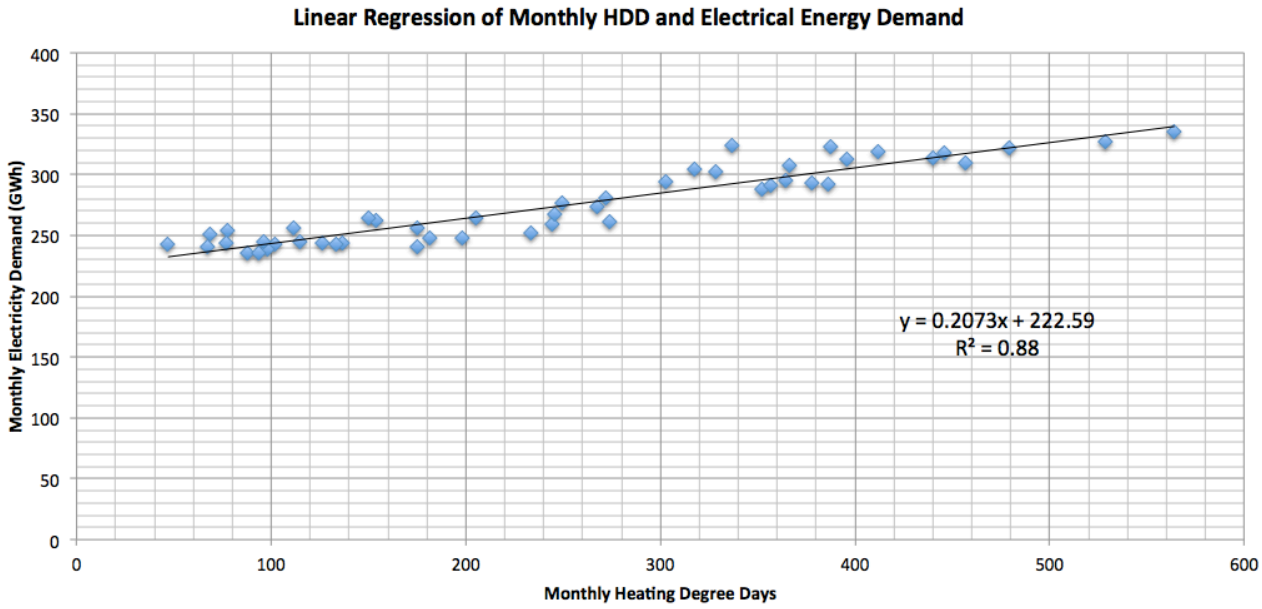


Figure 5-5 Linear Regression Analysis of Monthly HDD and Electricity Demand. (Source: HDD Data Extracted from Oxford University Environmental Change Institute. (ECI, 2013) Electricity Demand Data Extracted from DECC (DECC, 2010a))

A close fit between Oxfordshire's electrical energy demand and HDD is shown with a correlation coefficient of 0.88. The non-weather related factors of demand are the y-intercept of demand as 222.59 GWh_e. The strong coefficients of determination (>0.75) shown above allow the conclusion that the electricity demand shows a strong, positive linear relationship with the HDD and the external temperature in Oxfordshire. This is despite the fact that the monthly demand is derived using national demand data and the HDD are derived using ambient temperature recorded at a local meteorological station. This correlation allows further analysis on the relationship between energy demand and climatic effects. More specifically, the change in electricity demand per GWh is dependent on a 0.21 shift in the heating degree-day value. The deconstruction of the demand data to weather and non-weather related components allows the forecasting of demand reduction due to energy efficiency measures implemented for any type of electrical conversion technologies and appliances in the county.

Oxfordshire Gas Demand

The gas consumption recorded directly for the county of Oxfordshire is not available. The most relevant data set is the National Quarterly and Annual Gas Demand published by DECC in 2012 (DECC, 2012b). The main disadvantage of this data set is the limited information available on an hourly or even monthly time scale that does not allow a further analysis of time scale on demand. The population factor of 0.011, presented in the previous section, is used to convert the quarterly national demand to the quarterly

countywide demand.

5.1.1.3 Temporal Analysis

The average quarterly gas demand, derived from the 2005 – 2011 constructed data set, is shown in Figure 5-6 below (DECC, 2012b).

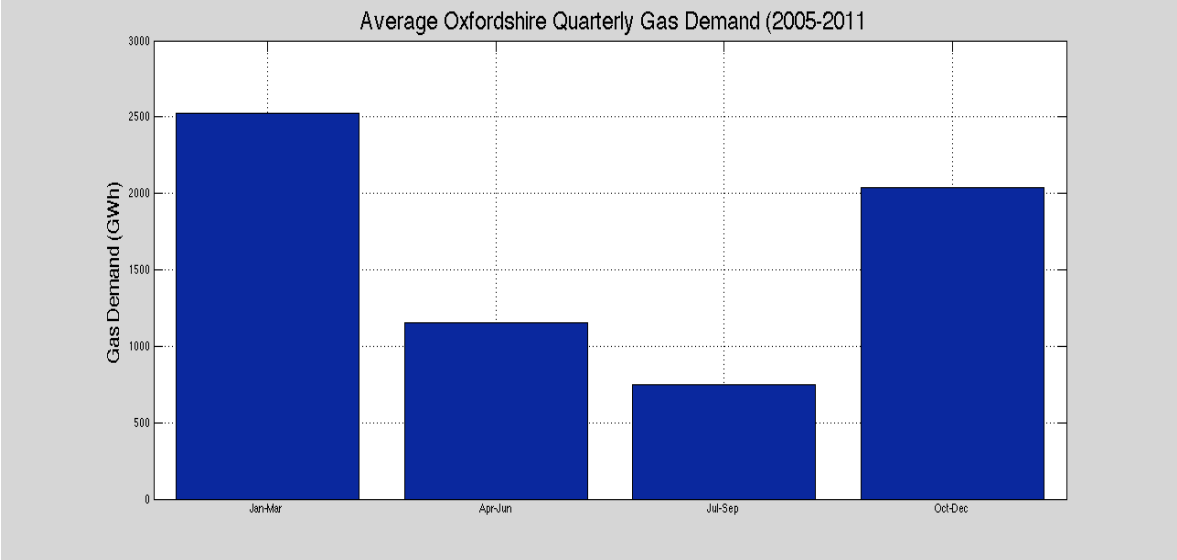


Figure 5-6 Average Quarterly Gas Demand Oxfordshire (2005 - 2011). (Data Source: Adjusted DECC (DECC, 2012b))

The quarterly gas demand is at a maximum during the winter months (October – March) and at a minimum during the summer season (April to June). The reduction in space heating requirements in the summer period is expected to be the main driver behind the difference in demand at quarterly levels. This is discussed further in the section examining Climatic Factors of demand.

The Oxfordshire annual gas demand for 2005 to 2011 is shown in Figure 5-7 below (DECC, 2012a).

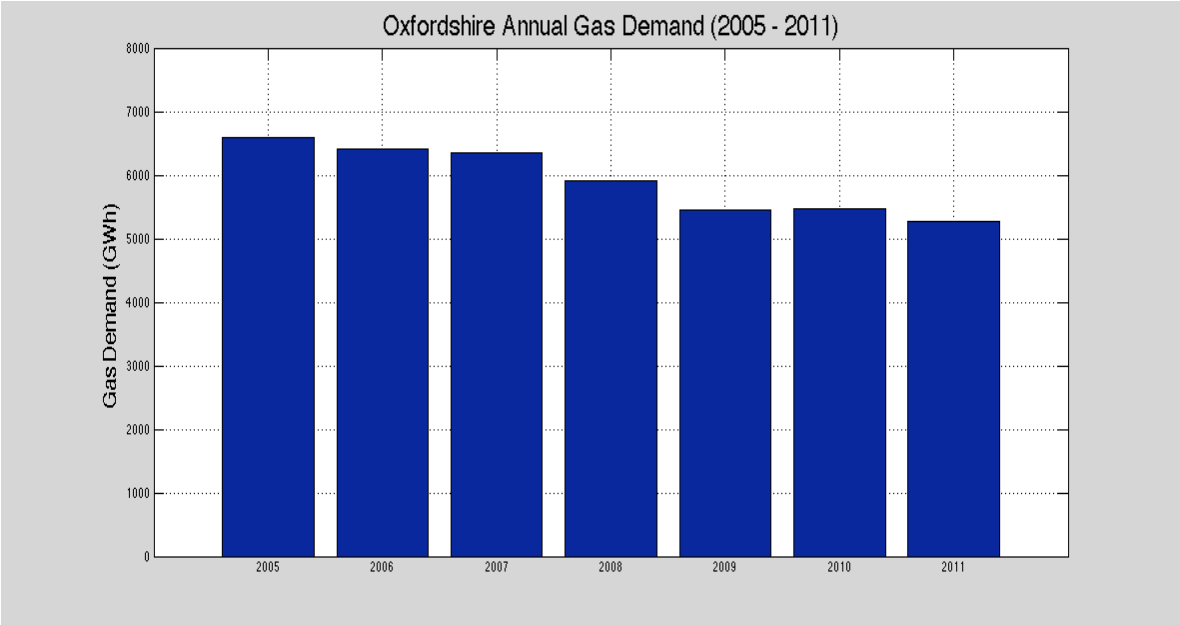


Figure 5-7 Oxfordshire Annual Gas Demand Data 2005 - 2011. (Source: Recorded Data from DECC (DECC, 2012a))

The annual change in demand shows a consistent reduction between 2005 and 2009. The relative change in annual demand is -2.6 % between 2005/2006, -1.1 % between 2006/2007, -7 % between 2007/2008 and -7.7 % between 2008/2009. There is a negligible difference between 2009/2010 and a -3.5 % change is evident between 2010/2011.

A further breakdown of the proportion each district has in the county's gas demand is shown in Table 5-2 below. The gas demand ratio is calculated as the ratio of the average annual demand per district to the total average annual demand for the county.

Table 5-2 Gas Demand and District Population Ratios - Oxfordshire

District	Gas Demand Ratio	Gas Demand per Person (MWh/person)
Cherwell	0.25	8.74
Oxford	0.28	9.07
South Oxfordshire	0.17	10.09
Vale of White Horse	0.18	9.23
West Oxfordshire	0.12	7.87

In 2011 the total UK gas consumption was 513 TWh (DECC, 2012a). As previously reported, the UK population is estimated as 59.6 million and, therefore, the national gas consumption per person is 7.9 MWh per year. This means that only West Oxfordshire is performing at a more efficient rate compared to the national average, with South Oxfordshire having the highest difference of 28 %.

5.1.1.4 Climatic Effects

The climatic effects on gas demand are examined in this sub-section. The data sets used are the constructed quarterly gas demand between 2008 and 2011 and the relevant quarterly HDD for the same period assuming an 18ºC internal building temperature. The temperature data set used to conduct this analysis has been extracted from the Benson Meteorological office. The linear regression analysis is shown in Figure 5-8 below.

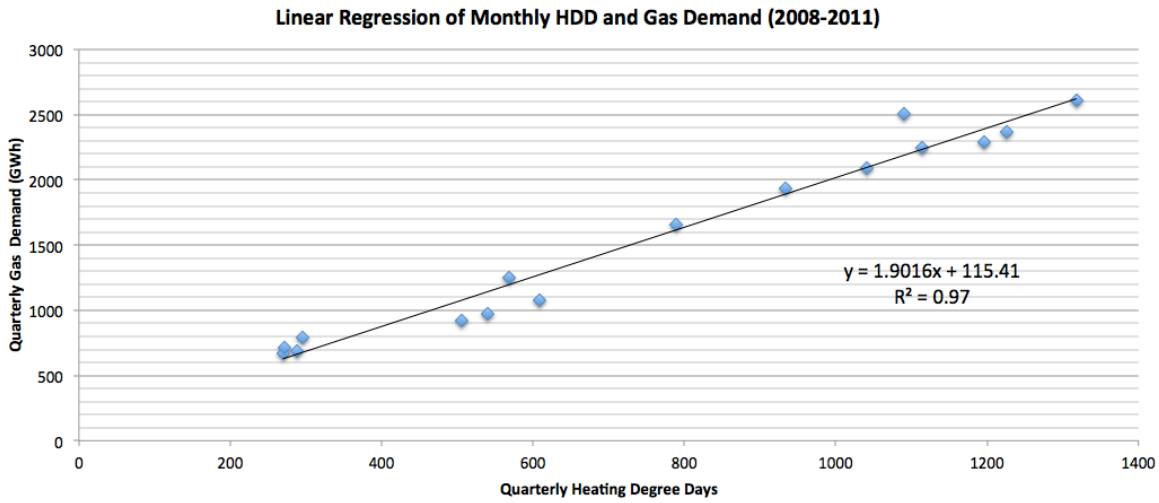


Figure 5-8 Linear Regression Analysis of Quarterly Gas and HDD between 2008 – 2011 (Source: HDD Data Set Extracted from Oxford University ECI (ECI, 2013). Gas Demand Data Extracted from DECC (DECC, 2012a))

A close fit between Oxfordshire's gas demand and HDD, with a correlation coefficient of 0.97, is shown. The non-weather related factors of demand are 115.41 GWh per quarter. The strong correlation is despite the fact that the monthly demand is derived using national data and the HDD are derived using local temperature data. This correlation allows further analysis on the relationship between gas demand and climatic effects. More specifically, the change in gas demand per GWh is dependent on a 1.9 shift in the heating degree-day value.

Growth

The Office of National Statistics (ONS) projects local and national populations based on recent birth, death and net migration trends. These projections do not account for factors such as local or national policies, area capacity and planned housing growth. If recent trends continue, the population in Oxfordshire could grow from 635,000 in 2008 to 675,000 in 2018 and 736,500 in 2033. Each district would experience an increase in population with Cherwell and West Oxfordshire seeing the largest

change (OCC, 2010). Table 5-3 below presents the change in the total energy demand in 2018, assuming the demand per person remains constant. Although the projected population in 2033 is known, the demand for this year is not accounted for due to the substantial changes expected in behaviour and conversion efficiency that greatly reduce the accuracy of this type of analysis.

Table 5-3 Projected Change in Energy Demand - Oxfordshire 2018

Energy Type	Change in Energy Demand 2018 (GWh)
Electricity	220
Gas	316

By assuming a capacity factor of 90 %, an increase of 220 GWh_e of electricity is equivalent to an additional conventional power capacity requirement of 27.5 MW_e.

Conversion of Gas Consumption to Energy Services

The gas demand analysis, presented above, is considered in potential energy terms which is then converted for space and water heating as well as for cooking requirements. According to the Energy Saving Trust, on average, 85 % of gas is converted to space and water heating in the UK (EnergySavingTrust, 2008). This fuel allocation is of particular interest as the introduction of renewable CHP systems, which can replace gas for space and water heating, is examined later in this chapter. The space and water heating demand is calculated using Equation (5-1) below.

$$Heating\ Demand\ (Space, Water) = \frac{Gas\ Demand}{\eta_{wab}} * Space\ and\ Water\ Proportion\ (85\%) \quad \textbf{(5-1)}$$

An investigation by BRE Housing, on behalf of the Department of Energy and Climate Change concluded that the proportion of domestic dwellings with condensing boilers in the UK in 2006 was 14.8 %. The same investigation reported a Weighted Average Boiler (WAB) efficiency in the UK of 74 % (Utley & Shorrock, 2008).

Oxfordshire Energy Demand Summary

This section has examined an analysis of the electricity and gas demand in the county of Oxfordshire. An overall drop of 4.5% in the annual electrical energy demand between 2005 and 2011 has been identified, with the minimum monthly demand occurring in August 2011. All the districts have a lower than national average demand per person, with the exception of South Oxfordshire that has a 7 % higher demand. A

very close fit is shown between the HDD and monthly electrical energy demand with a correlation coefficient of 0.88 and a non-weather related demand of 223 GWh_e.

Gas demand in the county shows a minimum average quarterly demand between 2005 and 2011 occurring between July and September. The annual gas demand shows a consistently reducing trend between 2005 and 2011 with an average decrease of 3.65 % per year. All the districts have a lower than national average demand per person, with the exception of South Oxfordshire that has a 28 % higher demand. As expected, a very close fit is shown between the HDD and quarterly gas demand with a correlation coefficient of 0.97 and a non-weather related demand of 115.41 GWh.

5.1.2 Renewable Energy Resource Assessment - Oxfordshire

This section examines the potential energy content and indicator assessment of the statistical resource types present in the county of Oxfordshire, using the relevant methodologies developed in Chapter 3. The outcome of this assessment allows an estimation of the total potential energy content of these resources in the county. Due to the large geographic coverage, the potential energy content of the county is mapped per resource in a GIS using the MapInfo software (MapInfo, 2007). The economic analysis estimates the cost incurred in utilizing these resources, as well as a cost comparison between renewable resources and the conventional fuel situation.

5.1.2.1 Determinative Resource Assessment – Oxfordshire

This section examines the implementation of the solar energy determinative resource assessment methodology, developed in section 3.2.1 of Chapter 3, in Oxfordshire. This section focuses of the rooftop solar energy potential only.

5.1.2.1.1 Solar Energy

To assess the solar energy potential, the optimum tilt angle of a solar energy collector is first identified. The urban solar rooftop potential estimation is then conducted for the locations of Abingdon, Banbury, Bicester and Oxford. This assessment provides a statistical overview of the utilization of credible solar energy in an urban context.

Optimum Solar Collector Tilt Angle

To determine the optimum collector position for maximum annual solar energy, the total radiation is calculated for a range of tilts with 5º intervals. This study assumes the same latitude throughout the county and uses the city of Oxford as the reference point. The total radiation is calculated as the sum of the direct, diffuse and reflected radiation using Equations (3-9) to (3-11). The ground reflectivity is assumed as 0.15 to represent an urban environment where the installation of rooftop systems is expected. The results are shown in Figure 5-9 below.

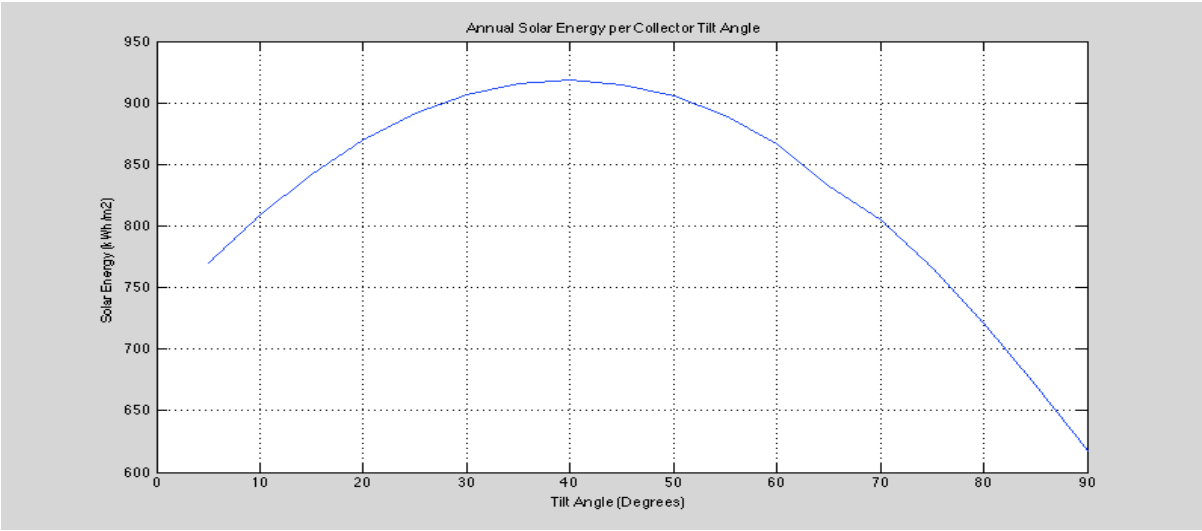


Figure 5-9 Solar Energy for a Range of Collector Tilt Angles

The maximum solar energy of 920 kWh/m^2, in Figure 5-9 above, corresponds to an optimum tilt angle for solar installations of 40º.

Urban Rooftop Solar Potential

This section examines the urban rooftop solar resource potential in the county using the GIS and Google Earth™ method, developed in this study. The results are extrapolated to represent the total number of buildings in the county.

GIS Component - Identification of Buildings with Orientation Constraints

The GIS algorithm, to identify the number of buildings within the 20º orientation constraints, is implemented in the MasterMap digital map version. The results are presented, in Table 5-4 below, and a map of each area is shown in Figure 5-10 to Figure 5-13 below. Section 3.2.1 of Chapter 3 has presented a detailed explanation of this methodology with accompanying Google Earth™ image extracts of a

specimen residential area in Abingdon.



Figure 5-10 Abingdon Rooftop Potential Solar Map

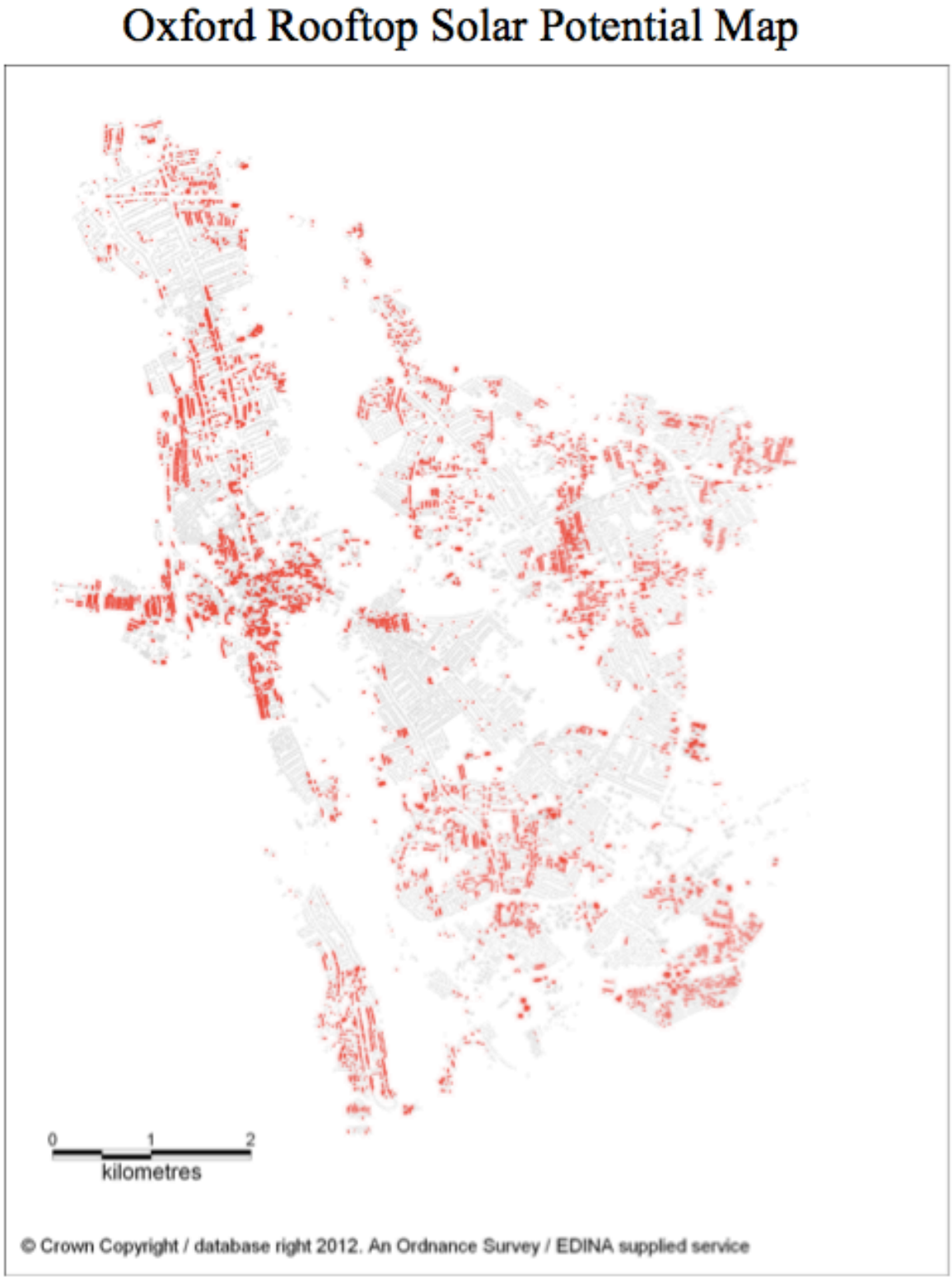


Figure 5-11 Oxford Rooftop Solar Potential Map



Figure 5-12 Banbury Rooftop Solar Potential Map

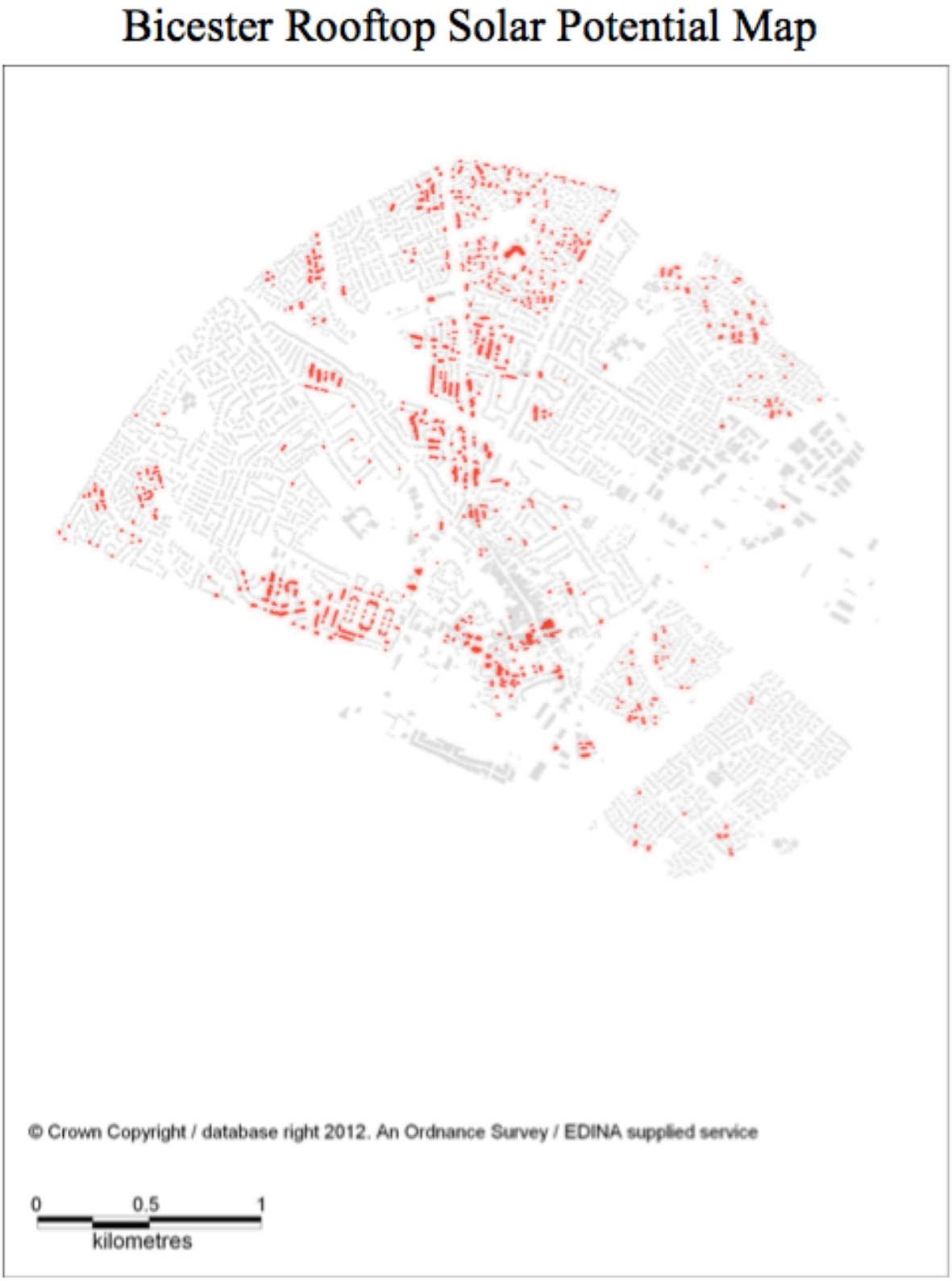


Figure 5-13 Bicester Rooftop Solar Potential Map

The towns above represent 40 % of the total buildings in the county. To extrapolate over the entire county, this percentage is used to calculate that there are approximately 56,100 suitable buildings for solar installations, equivalent to 4.4 million m^2 of total rooftop solar area, shown in further detail in Table 5-4 below.

Table 5-4 Numbers of Buildings within Solar Constraints in Oxfordshire

Town	Buildings within Orientation Constraint (x 1000)	Gross Rooftop Area (x 1000 m^2)
Abingdon	4.6	352
Banbury	4.5	338
Bicester	1.3	90
Oxford	12	1000
Remaining Towns	33.7	2685
Total	56.1	4465

Google Earth™ Component - Rooftop Type Mix

Section 3.2.1 of Chapter 3 identified 5 rooftop types, typical of UK architecture[18] that absorb different proportions of solar energy. A survey, via Google Earth™, to record the proportion of each rooftop type of a 1000 building sample set in Oxfordshire, has been conducted. To capture any difference in commercial and residential areas, this survey is geographically distributed across each town. The weighted average per rooftop type is used to represent the proportion of rooftop type in relation to the number of buildings per town. The results are shown in Table 5-5 below.

Table 5-5 Google Earth™ Survey Results for Rooftop Type Proportion

Town	Gable	Double Gable	Flat	Occupied Flat	Hipped
Abingdon	420	340	50	40	150
Banbury	500	100	120	80	200
Bicester	600	240	50	30	80
Oxford	200	300	100	150	250
Weighted Average	335	260	91	107	206

Total Rooftop Solar Potential

The total surface area in the county is calculated for the 56,100 suitable buildings using the statistical distribution per rooftop type, in Table 5-5 above, for the towns surveyed and the weighted average for the remainder of the county. The credible area and solar energy magnitude for urban rooftop utilization is shown in Table 5-6 below.

[18] The Rooftop Types are: Gable, Double Gable, Hipped, Flat and Occupied Flat

Table 5-6 Total Surface Area and Annual Solar Energy Striking Urban Rooftop Areas in Oxfordshire

Town	Total Buildings (x 1000)	Credible Rooftop Area (x 1000 m^2)	Solar Energy Potential (GWh/year)
Abingdon	4.6	260	235
Banbury	4.5	415	380
Bicester	1.3	70	65
Oxford	12	860	790
Other	33.6	2400	2200
Oxfordshire Total	56.1	4005	3670

The application of the solar potential results, in Table 5-6 above, is analyzed and discussed further in the photovoltaic conversion technology section later in this chapter.

5.1.2.2 Dispatchable Resource Assessment – Oxfordshire

This section examines the potential energy and decision making indicator assessment of the dispatchable resource type, using biomass energy in Oxfordshire as an example. To conduct this assessment, the relevant methodologies in Chapter 3 are implemented for the animal waste, energy crops, forestry waste and refuse biomass.

5.1.2.2.1 Biomass Energy

The biomass energy resource is categorized and examined, in section 3.2.2, in terms of the biogas and solid biomass fuel form generation. This section is divided into each of these two forms and their relevant types of biomass. The potential energy and geographic distribution of each type in the county is mapped in a GIS form and the decision-making indicator assessment is presented.

Energy crops for AD require arable land area for establishment. If land area is allocated to the energy chain, a competition between land for food and energy is created which, due to global food shortage supplies, is a major disadvantage of this resource. This is in contrast to solid biomass, such as Miscanthus and Short Rotation Coppice Willow that can be established on permanent and rough pasture, thus, avoiding the food and energy competition (Harvey & Pilgrim, 2011).

The initial part of this section is the presentation and re-allocation of Oxfordshire's agricultural land area under what are defined in this study as the "Energy Focus" and "Food Focus" usage scenarios that play an

integral role in the biomass assessment. The relevant strategy is then enforced with respect to the examination of the solid and biogas fuel forms.

Agricultural Land Area Allocation in Oxfordshire

Human diet in the UK has largely deviated from the optimum balance that has also created inefficiencies in land usage. The Landshare study has been conducted as part of the broader "Oxfordshire Energy Future" project to estimate the food supply and subsequent agricultural land area required if Oxford's population followed the Livewell diet (Landshare, 2012). Based on the proposed agricultural land area under this scenario, this study considers two land usage strategies that can be employed to prioritize either energy or food production, explained in Table 5-7 below.

Table 5-7 Land Usage Strategies

Land Usage Strategy	Description	Fuel Form
Energy Focus	The "Energy focus" strategy attempts to prioritize arable land area based on the required crop tonnage to co-digest the available animal waste. The remaining land is allocated for feeding	Biogas: • Maize / Animal Waste Co-Digestion
Food Focus	The "Food Focus" strategy attempts to allocate land usage based on the feeding demand and, if any surplus land area is used, may be considered for energy. The Livewell diet is used to construct the optimum feeding demand and the subsequent land area is reallocated to meet this.	Solid Biomass: • Miscanthus • SRC Willow

Energy Focus Land Usage Strategy

The animal waste sub-section below has identified that the annual cattle manure tonnage generated is 585,000 tonnes of manure per year based on a total cattle population of 66,000 (DEFRA, 2011b). Considering a fresh weight co-digestion ratio at 5:1 (manure: maize), 116,940 tonnes of maize are required under this strategy. Assuming a growth yield of 40 t/ha, approximately 2930 ha of arable land are required. The proposed land area allocation per usage type in the county, under the "Energy Focus" scenario, is shown in Table 5-8 below.

Table 5-8 Proposed Land usage in Oxfordshire: Energy Focus Strategy

Land type	Proposed land use (ha)	Current usage (ha)	Land status area (ha)
Arable (Human Feed)	58220	61150	- 2930
Arable (Animal Feed)	41500	41500	-
Temporary grass	11934	11900	-
Permanent and rough pasture	55272	55200	-
Horticulture and field vegetables	683	683	-
Energy crops (arable land)	2930	0	2930

Table 5-8 shows that the maize land area requirement is approximately 3 % of total arable land. Although this can be seen as a minimal proportion, its inclusion in the agricultural mix under the current status can only take place if there is a displacement of crops allocated to food production.

Food Focus Land Usage Strategy

Landshare's study proposes the implementation of the Livewell diet by Oxford's residents and projects the agricultural land mix under this scenario. This study considers that the county of Oxfordshire can be seen as a larger scale representation of the city of Oxford. The projected land mix is extrapolated in terms of population to represent the county of Oxfordshire. In 2009, the population of Oxfordshire was 648,000 and the population of Oxford was 150,000 (ONS, 2010). Therefore, the extrapolation factor used is 4.27 and the results are shown in Table 5-9 below (Landshare, 2012).

Table 5-9 Land use for farming in Oxford based on Livewell diet

Land type	Current land use (ha)	Proposed demand (ha)	Difference (ha)
Arable (Human Feed)	61150	47641	13510
Arable (Animal Feed)	41500	42196	- 696
Temporary grass	11900	19031	- 7131
Permanent and rough pasture	55200	12071	43129
Horticulture and field vegetables	680	15145	- 14465

Based on the difference between current and proposed land area, there is a surplus of land for the arable and permanent and rough pasture categories in Oxford. The feed crops, temporary grass and horticulture categories create a land deficit. To rearrange the Oxfordshire land usage, based on the Livewell diet implementation, the following steps are required.

1. The feed crop deficit is filled by the required area with surplus arable land
2. The temporary grass deficit is filled with surplus permanent and rough pasture. A land use conversion factor of 2:1 must be accounted for due to the superiority in land quality of the temporary grass category over rough pasture (Nix, 2012)
3. The horticulture and field vegetable deficit is filled, though not completely, with the remaining arable land area.

Table 5-10 below shows the agricultural land mix under the "Food Focus" scenario.

Table 5-10 Reallocation of Oxfordshire Land Use: Food Focus Scenario

Land Type	Proposed Land Use (ha)	Land Status	Land Status Area (ha)
Arable	47641	Neutral	-
Feed Crops	42196	Neutral	-
Temporary Grass	19031	Neutral	-
Permanent and Rough Pasture	12071	Surplus	28867
Horticulture and Field Vegetables	15145	Deficit	- 1651

In terms of its food supply, the results in Table 5-10 above, indicate that Oxfordshire has the potential to achieve a 99% level of self-reliance with a relatively small land deficit of 405 ha for horticulture and field vegetables. This reallocation shows that, even under an optimized dietary programme, no surplus arable land can be used for energy crops grown for anaerobic digestion systems without avoiding the food and energy competition. However, this strategy provides access to Permanent and Rough Pasture land with a 28867 ha surplus that can be used for solid biomass energy crops such as miscanthus and SRC willow.

5.1.2.2.1.1 Biogas Fuel Form Assessment

This section examines the assessment of animal waste, energy crops and refuse biomass in Oxfordshire. The energy focus strategy is enforced as it provides arable land area for growing energy crops, such as maize, for the co-digestion with animal waste for the production of biogas.

Animal Waste

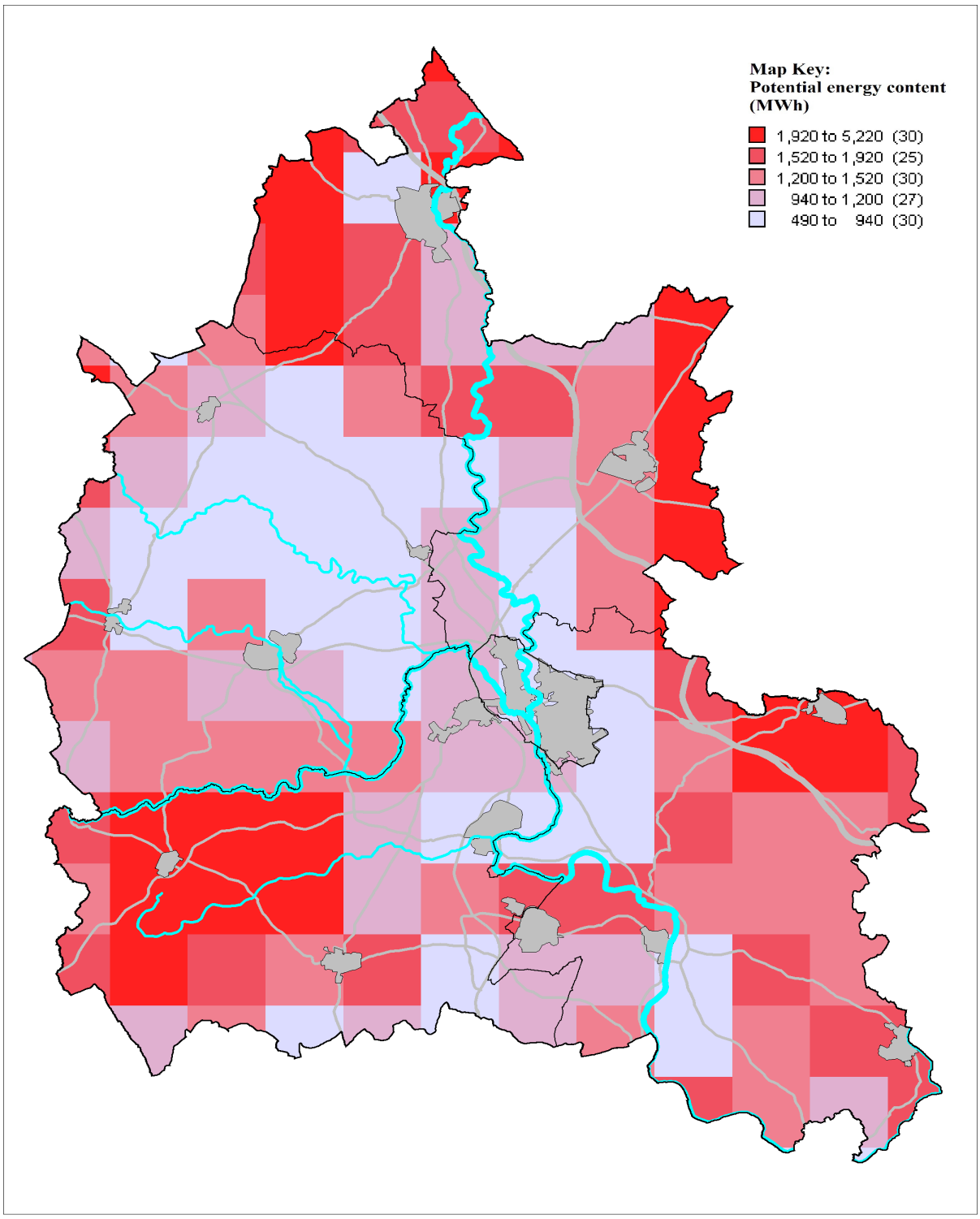
The population of Oxfordshire's livestock is extracted from the DEFRA June 2009 Livestock Numbers Survey. The survey records the livestock type, age and size and, hence, the annual generation of waste

tonnage can be calculated. The annual biogas LHV from single feedstock digestion of livestock waste in Oxfordshire is shown in Table 5-11 below (DEFRA, 2011b).

Table 5-11 LHV for Individual and Total Livestock in Oxfordshire

Livestock	Livestock population (x 1000s)	Waste Generation per Livestock (x 1000t/livestock)	LHV (GWh)
Dairy Cattle	15	166.5	20.9
Cattle	51	418.2	57.4
Pigs	74	118.4	22.2
Total	141	710.6	100.5

The spatial distribution of livestock population is converted to potential energy content by waste generation. Figure 5-14 presents the GIS map created to illustrate the potential energy and distribution of livestock manure across the county.



© Crown Copyright / database right 2012. An Ordnance Survey / EDINA supplied service

Figure 5-14 Geographical Distribution of Animal Waste in Oxfordshire

This distribution identifies the south-west as having the highest potential with 1.9 GWh – 5.2 GWh of biogas and the central and west area as having the lowest potential with 0.5 GWh to 0.9 GWh.

Co-Digestion of Energy Crops and Animal Waste

The energy focus strategy is implemented to assess the biogas generation from energy crops in the county. This strategy assumes that all the cattle and dairy cattle waste is allocated to energy crop co-digestion and the pig waste remains for single-feedstock digestion. As previously mentioned, the majority of European co-digestion plants use cattle manure and maize as feedstock. This combination is, therefore, investigated in further detail in this case study (IEA, 2010).

In order to co-digest the available cattle manure completely, the "Energy Focus" scenario, examined previously, has identified 117,200 t of maize for energy. Using the conversion factor of 277 m^3 of biogas per tonne of co-digestion mixture, calculated in section 3.2.2, this scenario generates 32.5 million m^3 of biogas with a potential energy content of 195 GWh.

Economic Analysis of Co-Digestion

A detailed breakdown of the £497/ha cost required to grow and harvest maize has been presented in section 3.2.2.1.2 generating a total cost of £ 1.45 million. The economics of animal waste, in section 3.2.2.1.1, have been assumed to be the transport cost to and from the digester as the digestate can be exchanged between the plant and the farmer and used as a fertilizer. The cost of biogas potential energy from co-digestion is shown, in Figure 5-15 below, with respect to the radius required to transport the animal waste to a centralized anaerobic digester.

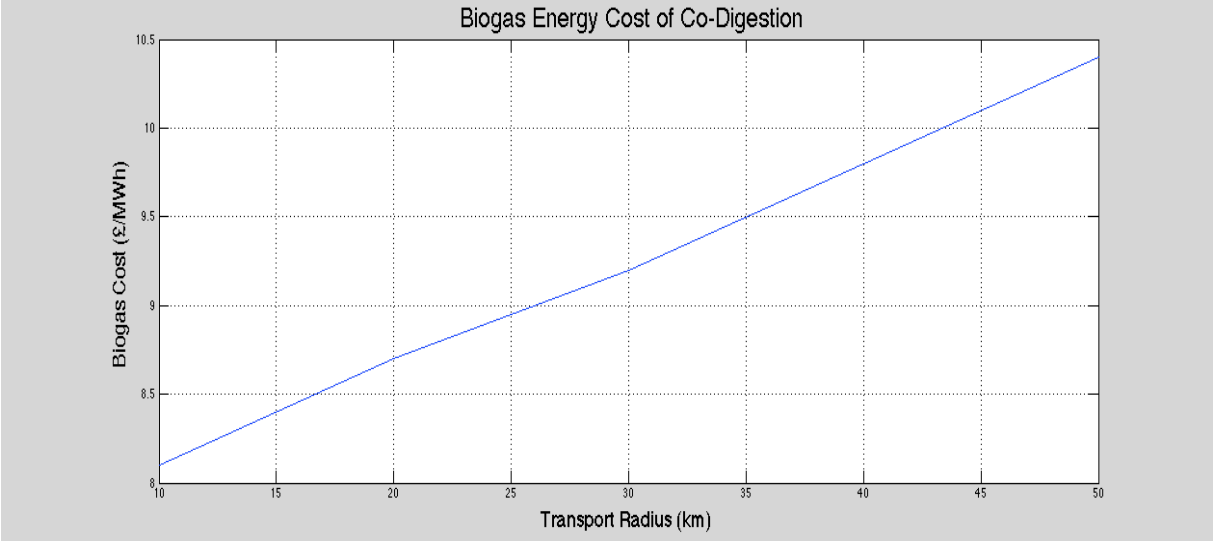


Figure 5-15 Biogas Energy Cost of Co-Digestion

Refuse

This sub-section examines the indicator assessment of refuse biomass in Oxfordshire. The forecasted gross tonnage per category, until 2030, is presented in Table 5-12 below (OCC, 2011). This data is recorded and forecasted by the council in terms of the total annual mass rather than per type of waste item. The total tonnage is converted to the suitable types of each refuse category, which are composed of a high organic content and preferable for the anaerobic digestion process, using the average waste composition values for England discussed in section 3.2.2.1.3.

Table 5-12 Potential energy content of waste in Oxfordshire (Raw Refuse Waste Data Source: Oxfordshire County Council (OCC, 2011))

Category	Year				
	2010	**2015**	**2020**	**2025**	**2030**
Total MSW (t)	308,700	325,100	337,900	351,700	366,000
Garden waste (t)	61,740	65,020	67,580	70,340	73,200
Kitchen waste (t)	52,480	55,270	57,445	59,790	62,220
Potential energy (GWh)	92.2	97.1	100.9	105	109.3
Total C&I Waste (t)	566,800	584,900	603,500	622,800	642,600
Green waste (t)	51,012	52,641	54,315	56,052	57,834
Food waste (t)	56,680	58,490	60,350	62,280	64,260
Potential energy (GWh)	64.7	66.9	68.9	71.2	73.5
Total Potential Energy (GWh)	157	164	170	176.2	182.8

From the results, in Table 5-12 above, it can be seen that there is an increasing trend in all categories of annual waste and consequent potential energy content in Oxfordshire. This increase is in the range of 1% per annual total of MSW and C&I waste. In 2010, the total accessible refuse in Oxfordshire that could be used as a feedstock for AD was 222,000 tonnes, equating to a potential energy content of 157 GWh. The average kitchen waste generation per person in Oxfordshire is 81 kg per year, corresponding to 22 kWh of potential energy per person.

Economic Analysis of Refuse Digestion

Section 3.2.2.1.3 of Chapter 3 reported the gate fee of food waste for Anaerobic Digestion to be £ 43 per tonne. Therefore, food waste in Oxfordshire can be assumed to have a market value of £ 4.5 million. If this food waste were considered in an incineration system with a median gate fee of £ 50, it would have a

market value of £ 5.5 million (WRAP, 2011). However, the 15 % higher value should not be a deciding factor in the choice of this type of technology. Further consideration, out of the scope of this study, should be given to the future values of gate fees for both technologies.

5.1.2.2.1.2 Solid Biomass Fuel Form Assessment

The solid biomass fuel form assessment is examined for Oxfordshire, assuming the implementation of the food focus strategy considering energy crops and forestry waste identified in Table 5-7 above. Regarding the energy crop species, a selection between the miscanthus and SRC willow is made using the solid biomass MCA analysis developed in section 3.2.2.2.1 An economic analysis of the optimum species is conducted to assess the establishment and operating cost of utilizing this crop in the county.

Solid Biomass Energy Crop Species Assessment Tool

The selection process of the crop species, envisaged as a biomass fuel form using the decision-making tool developed in this study, is conducted for Oxfordshire. Steps 1 – 4 of the process are followed assuming a land area utilization of 29 000 ha identified in Table 5-10 above.

Since the land area is fixed, and therefore constrained, the energy yield element is given a weighting of 2 to promote the maximum achievable biomass tonnage. Furthermore, as these crops will be newly introduced into the agricultural market, the establishment cost must be minimized and, thus, given a weighting of 2. The MCA analysis is populated with the relevant scoring and weighting in Table 5-13.

Table 5-13 Multi-Criteria Assessment Analysis for Miscanthus and SRC Willow in Oxfordshire

Criteria	Energy Yield	Economic		Environmental	Total Score (/60)
Elements	Energy Yield (MJ/ha) [LHV; Moisture; Growth]	Capital (£/ha)	O&M (£/ha)	Fertilizer Demand (MJ/MJ)	
Weighting	*2*	*2/2*	*1/2*	*1*	
Miscanthus	*8.3*	*8*	*10*	*10*	*40*
SRC Willow	*10*	*10*	*3*	*10*	*42*

The MCA analysis, in Table 5-13 above, identifies the SRC willow as the optimum solid biomass energy crop species with a marginal difference over miscanthus. An overview of the scoring shows that the outcome is mainly due to the higher willow yields and lower capital costs that are also the weighted elements in this analysis.

Economic Analysis of Energy Crops

The economic analysis is conducted by examining the production cost of the SRC willow supply chain, including pelletizing the crop, based on the data presented in section 3.2.2.2.1. The pellet format is preferred over the chip format due to its easier handling, storage and flow into the boilers (Jenkins, 2012). The transport cost assumed is a round-trip transport distance of 30 km and the final cost per land usage strategy is shown, in Table 5-14 below, assuming a 10 % moisture content considered to be an acceptable level for utilization.

Table 5-14 Production cost of SRC Willow in Oxfordshire

Land Usage	Annual Tonnage (x 1000 t)	Potential Energy (GWh)	Annual Cost (x £1000)
Energy Focus	302	1360	40800
Food Focus	1382	6220	186570

Forestry Waste

The potential energy from the forestry waste biomass category in Oxfordshire is examined. The Forestry Commission records the quantity and distribution of wood in terms of the broadleaf and coniferous species, which are further examined in this section (FC, 2012).

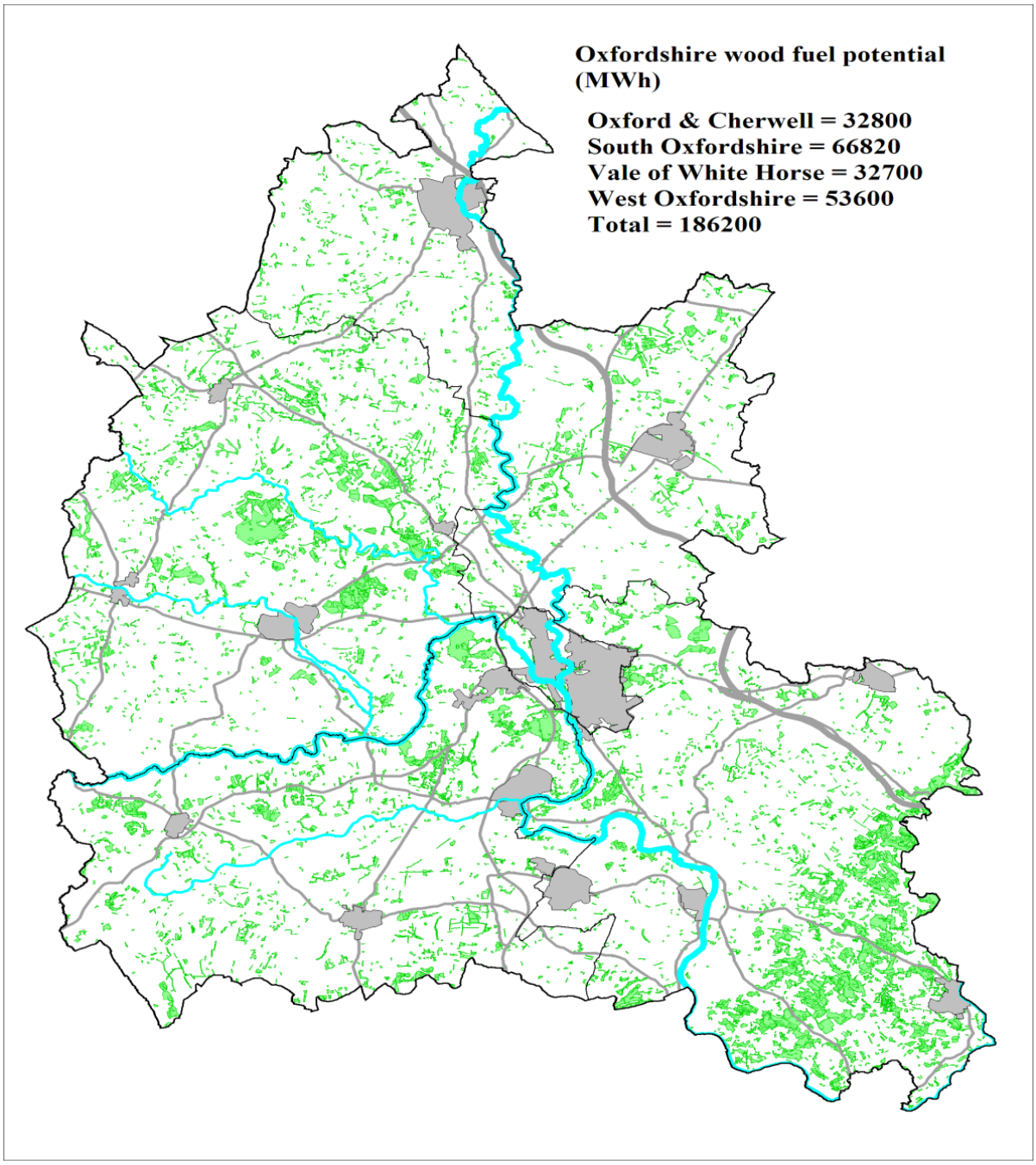
Forestry waste Potential Energy Content

The forestry area occupied by the broadleaf and coniferous wood species and the subsequent potential energy content in Oxfordshire is shown, by district, in Table 5-15 below (FC, 2012).

Table 5-15 Forestry Coverage in Oxfordshire

District	Total Area (ha)		Area for Forestry Waste as Fuel		Potential Energy Content (MWh)	
	Broadleaf	Conifer	Broadleaf	Conifer	Broadleaf	Conifer
Oxford and Cherwell	3015	784	1508	390	30000	2800
South Oxfordshire	6634	227	3317	114	66000	821
Vale of White Horse	3170	282	1585	140	31700	1000
West Oxfordshire	5100	733	2550	367	51000	2600
Total	17920	2026	8960	1013	179000	7221

The geographical distribution of this resource is mapped in Figure 5-16 below.



© Crown Copyright / database right 2012. An Ordnance Survey / EDINA supplied service

Figure 5-16 Geographical Distribution of Wood Fuel in Oxfordshire

The map, in Figure 5-16 above, illustrates that the majority of wood fuel is located in the south-eastern part of the county that falls within the South Oxfordshire district.

Economic Analysis of Forestry Waste

The sustainable utilization of the woodland resource for forestry waste production in Oxfordshire presents an economic benefit when considering its labour requirement. Section 3.2.2.2.2 calculated an average cost of £53 per tonne to produce a usable biomass format from forestry waste. The total broadleaf and conifer area is calculated at 9973 ha, in Table 5-15 above, and the total production cost is, therefore, £7.9 million.

5.1.2.3 Stochastic Resource Assessment

As part of the wider "Oxfordshire Capacity Study", the Oxfordshire Low Carbon Hub commissioned BVG associates, a technical consultancy that specializes in wind energy, to conduct the wind energy generation in the county. This thesis reports the main results concluded from the wind study and uses these further in the final renewable energy supply mix design algorithm.

BVG associates reported the top ten wind sites in Oxfordshire and their respective electricity generation, shown in Table 5-16 below. The capital cost is annualized using a 5 % discount rate over a 25-year operational lifetime.

Table 5-16 Oxfordshire Wind Energy Potential Generation

Site	Capacity (MW_e)	Energy Generation (GWh_e / year)	Capital Cost (£million)	O&M Cost (£million/year)	Total Annual Cost (£million/year)
Barn Hill	4.6	8.3	6.9	0.26	0.75
Drayton Copse	9.2	16.7	13.8	0.52	1.5
Edgecote	9.2	16.7	13.8	0.52	1.5
Gallows	18.4	33.4	27.6	1.1	3.0
Giddy Horne	9.2	16.7	13.8	0.52	1.5
White House	9.2	16.7	13.8	0.52	1.5
Didcot PS	6.9	12.5	10.4	0.40	1.1
Hutchin's Copse	9.2	16.7	13.8	0.52	1.5
Over Norton Common	6.9	12.5	10.4	0.39	1.1
Rosey Copse	11.5	20.9	17.3	0.66	1.9
Total	94.3	171.1	141.5	5.4	15.4

The identified sites have then been mapped in a GIS format using MapInfo™ by the authors of this thesis and are presented in Figure 5-17 below.

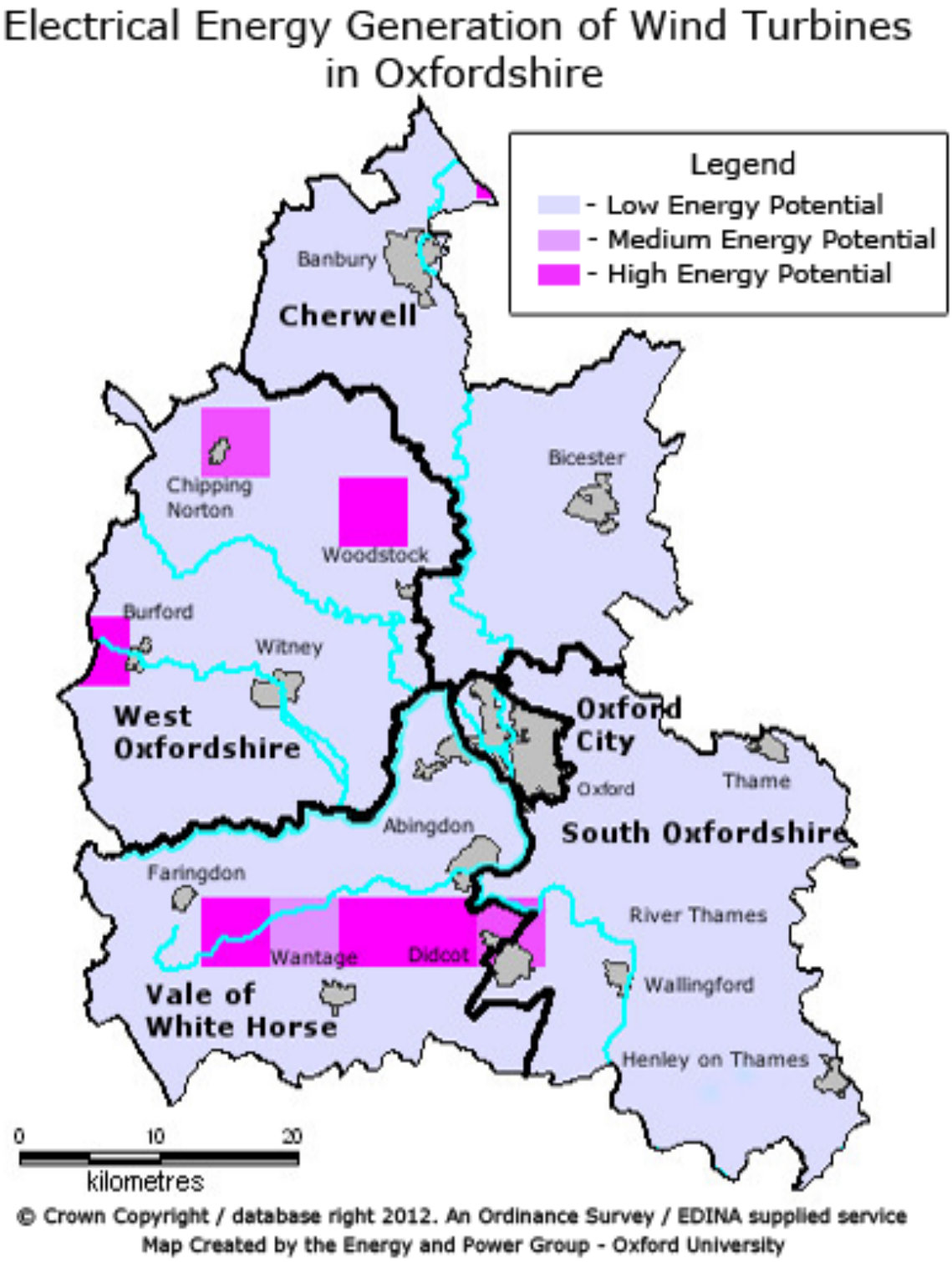


Figure 5-17 Electrical Energy Generation Map of Wind Turbines in Oxfordshire

The wind generation map, in Figure 5-17, shows that the south-west region has the highest wind energy potential in the county. The north and south-east regions have no wind potential and can be eliminated from further analysis of detailed siting and wind farm development in Oxfordshire.

5.1.3 Available Conversion Technology Assessment – Oxfordshire

This section examines the implementation of the available conversion technology assessment methodologies, examined in Chapter 3, for the solar PV, wind turbine and AD technologies in Oxfordshire. The indicator performance of each individual technology in the county is examined and discussed in further detail.

5.1.3.1 Solar Photovoltaic Assessment

This sub-section examines the energy generation and indicator performance of rooftop PV in Oxfordshire. Assuming that all the available suitable rooftop space, previously identified in Table 5-6, is allocated to PV installations, the indicator performance of PV in Oxfordshire is shown in Table 5-17. The total annual cost is calculated using a discount rate of 5 % over 25 years. The low cost scenario, reported in section 3.2.1 is used in anticipation of the continuing reduction in PV prices.

Table 5-17 Indicator Performances of Rooftop Solar Photovoltaics in Oxfordshire

Location	Capacity (MW_e)	Electrical Energy (GWh_e)	Capital Cost (£ Million)	Total Annual Cost (£ Million/year)	Cost per unit Energy (£/kWh_e)
Abingdon	24	19.8	47.5	4.6	0.23
Banbury	39	32.3	77.1	7.5	0.23
Bicester	7	5.8	13.8	1.3	0.22
Oxford	82	67.8	163	15.7	0.23
Other	227	187	449	43.5	0.23
Total	379	313	750	72.6	0.23

Table 5-17 shows that Oxfordshire can accommodate up to 379 MW_e of rooftop solar PV capacity at a total annual cost of £ 72.6 million per year. This component of the supply mix can achieve an emissions reduction performance of up to 8.9 % with respect to Oxfordshire's electrical emissions.

5.1.3.2 Wind Turbine Technology Assessment

The results, in Table 5-16 above, show that Oxfordshire has the potential to accommodate 41 wind turbines with a total installed capacity of 94.3 MW_e generating 171 GWh_e of electricity per annum. This

generation is equivalent to 4.7 % of the county's electricity demand recorded in 2009. Assuming that the entire resource potential is utilized, the total annual cost and emissions reduction indicator of the wind turbine technology in Oxfordshire is shown in Table 5-18 below. This study assumes that, as the minimum annual energy demand is greater than the installed turbine capacity, the entire magnitude of energy generated is absorbed by the demand. The cost of the wind turbine technology is extracted from section 3.3.5 using the medium capital and O&M cost options for installed capacities greater than 5 MW_e (ARUP, 2011).

Table 5-18 Indicator Performance of the Wind Turbine Technology in Oxfordshire

Technology	Capacity (MW_e)	Electrical Energy (GWh_e/year)	Capital Cost (£ Million)	O&M Cost (£ Million/year)	Total Annual Cost (£ Million/year)	Cost per unit Energy (£/kWh)
Wind Turbine	94.3	171.1	141.5	5.4	14.6	0.09

The results, in Table 5-18 above, show that Oxfordshire's wind capacity factor is 21 %. The wind performance in the county is at a substantially lower level than the reported long-term average UK wind capacity factor of 27 % (DUKES, 2005). Furthermore, by utilizing the entire wind potential in the county, an electrical emissions reduction of 2 % can be achieved.

5.1.3.3 Anaerobic Digestion Combined Heat and Power Assessment

This sub-section examines the energy generation and indicator performance of AD CHP in Oxfordshire. Each of the feedstock assessed is considered in a final total AD CHP for the "Energy Focus" land usage, shown in Table 5-19 below, and the "Food Focus" land usage, shown in Table 5-20 below. The "Energy Focus" strategy is also considered and compared against the base-case scenario for AD energy crops. The electrical conversion efficiency is assumed as 41 % and the thermal conversion efficiency is assumed as 35 % (Alfagy, 2011a). Furthermore, the median costs are assumed from the economic analysis of AD in section 3.3.1. The capital cost is annualized using a discount rate of 5 % over a 30-year lifetime.

Table 5-19 Energy Focus Anaerobic Digestion Combined Heat and Power - 2011 Demand

Energy Focus	Electrical Capacity (MW_e)	Thermal Capacity (MW_{th})	Electrical Energy (MWh_e)	Thermal Energy (MWh_{th})	Capital Cost (£ Million)	O&M Cost (£ Million)/year)	Total Annual Cost (£ Million/year)
Co-digestion (Maize + Manure)	10	8.5	80000	68000	39	8.4	10.9
Animal Waste (Pig)	1.1	1	8800	8000	4	0.92	1.2
Refuse	8	6.9	64000	55200	41.9	3.8	6.5
Total	19.1	16.4	152800	131200	81.3	13.1	18.6

The combined emissions reduction from the electricity and heat generated is calculated using the emissions reduction factors calculated in Table 3-25 of section 3.3.1. The proportion of total emissions reduction (from both electricity and heat), due to the anaerobic digestion of biomass, is 4.5 %.

The "Food Focus" usage, shown in Table 5-20 uses the same cost scenario and discount rate as above.

Table 5-20 Food Focus Anaerobic Digestion Combined Heat and Power - 2011 Demand

Biomass	Electrical Capacity (MW_e)	Thermal Capacity (MW_{th})	Electrical Energy (MWh_e)	Thermal Energy (MWh_{th})	Capital Cost (£ Million)	O&M Cost (£ Million)	Total Annual Cost (£ Million)
Animal Waste	7.3	6.2	58400	49600	28.5	6.1	8
Refuse	8	6.9	64000	55200	41.9	3.8	6.5
Total	15.3	13.1	122400	104800	70.4	9.9	14.5

The proportion of total emissions reduction (from both electricity and heat), due to the anaerobic digestion of biomass, is 3.1 %.

A comparison of both strategies shows that the "Energy Focus" requires an additional total annual cost of £ 4.1 million per year compared to the "Food Focus" land usage. This increase is required to achieve an increase of 30.4 GWh of electrical energy and 26.4 GWh of thermal energy per year.

5.1.3.4 Gasification Combined Heat and Power Assessment

The examination of the gasification technology, in section 3.3.2, identified the preference for utilizing solid biomass fuels such as miscanthus or SRC willow energy crops and wood. This section examines the

indicator performance of a centralized large scale Gasification CHP system under both land strategies. The "Energy Focus" strategy has allocated 55270 ha of permanent and rough pasture, a land type suitable for the establishment of SRC willow. The "Food Focus" strategy has allocated 12070 ha of the same land type for the establishment of SRC willow. The gasification of wood from forestry waste is considered to be constant under any land usage strategy and is, thus, an independent fuel supply component. The median cost scenario is assumed from the economic analysis of gasification conducted. The capital cost is annualized using a discount rate of 5 % over a 30-year lifetime.

Table 5-21 Gasification Combined Heat and Power Assessment – 2011 Demand Case

Solid Biomass	Electrical Capacity (MW_e)	Thermal Capacity (MW_{th})	Electrical Energy (MWh_e)	Thermal Energy (MWh_{th})	Capital Cost (£ million)	O&M Cost (£ million)	Total Annual Cost (£ Million)
Energy Focus	54	48	432000	384000	296	19.8	40.8
Food Focus	249	218	1992000	1744000	1193	80	165
Forestry Waste	7.4	6.5	59200	52000	35.5	2.4	4.9
Total Energy Focus	61.4	54.5	491200	436000	331.5	22.2	45.7
Total Food Focus	256.4	224.5	2051200	1796000	1228.5	82.4	170

A comparison of both strategies shows that the "Food Focus" land usage requires an additional total annual cost of £ 124.3 million per year compared to the "Food Focus" land usage. This increase is required to achieve an increase of 1560 GWh_e of electrical energy and 1360 GWh_{th} of thermal energy per year. The proportion of total emissions reduction (from both electricity and heat), due to the gasification of energy crops and forestry waste under the "Energy Focus" scenario, is 4 %. The proportion of total emissions reduction (from both electricity and heat), due to the gasification of energy crops and forestry waste under the "Food Focus" scenario, is 14.8 %.

5.2 Renewable Energy Supply Mix Design – Oxfordshire

The final renewable energy supply mix is assessed in this section under the resource type and availability of the "Energy Focus" and "Food Focus" land usage scenarios. The 2013 wholesale electricity price has been projected by DECC at a cost of £ 57 / MWh_e (DECC, 2012). A summary of the maximum renewable energy capacity per scenario is shown in Table 5-22 below.

Table 5-22 Maximum Renewable Energy Capacity per Land Usage Scenario

Land Usage	Anaerobic Digestion (MW_e)	Gasification (MW_e)	Solar Photovoltaic (MW_e)	Wind (MW_e)
Energy Focus	19.1	61.4	379	94.3
Food Focus	15.3	256.4	379	94.3

Biomass has been identified in this study as a dispatchable resource. To maximize the baseload generation by renewable energy, this study examines a scenario where that the AD and gasification technologies are sized to consume all the available resource. The solar and wind resources are considered in the Exhaustive Search algorithm for both land usage scenarios.

Exhaustive Search Space Minimization

The total grid generation required to meet demand for a PV capacity up to the maximum rooftop availability is shown in Figure 5-18 below. The total grid generation required to meet demand for a wind turbine capacity up to the maximum availability is shown in Figure 5-19 below.

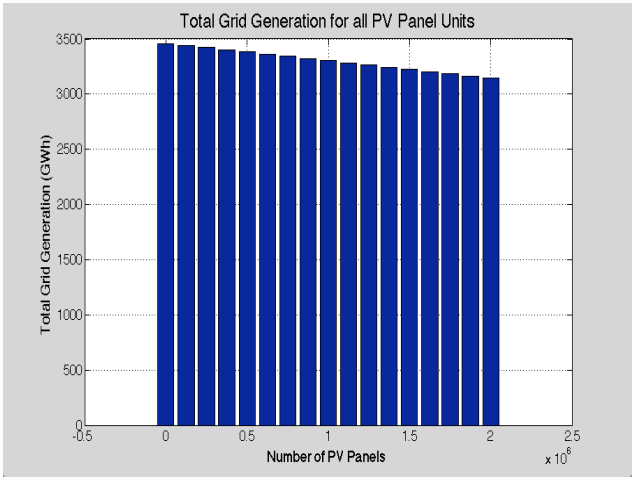


Figure 5-18 Grid Generation Vs Photovoltaics

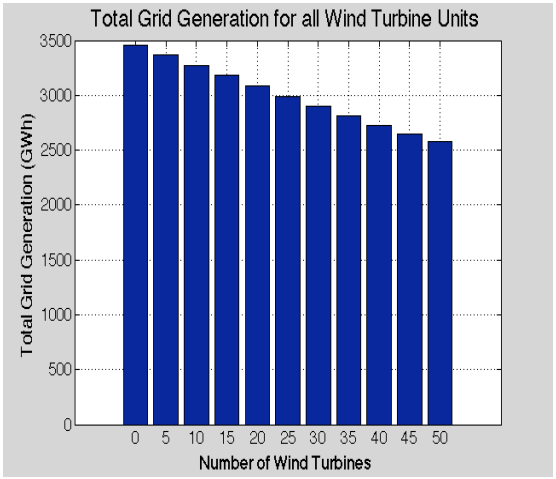


Figure 5-19 Grid Demand Vs Wind Turbine

Due to the fact that the grid generation does not saturate, the upper bound limit of each technology is equivalent to the maximum credible resource available.

5.2.1 Renewable Energy Supply Mix Design – Energy Focus Land Usage

The contour plot of total annual cost and emissions reduction for the "Energy Focus" land usage scenario is shown in Figure 5-20 below.

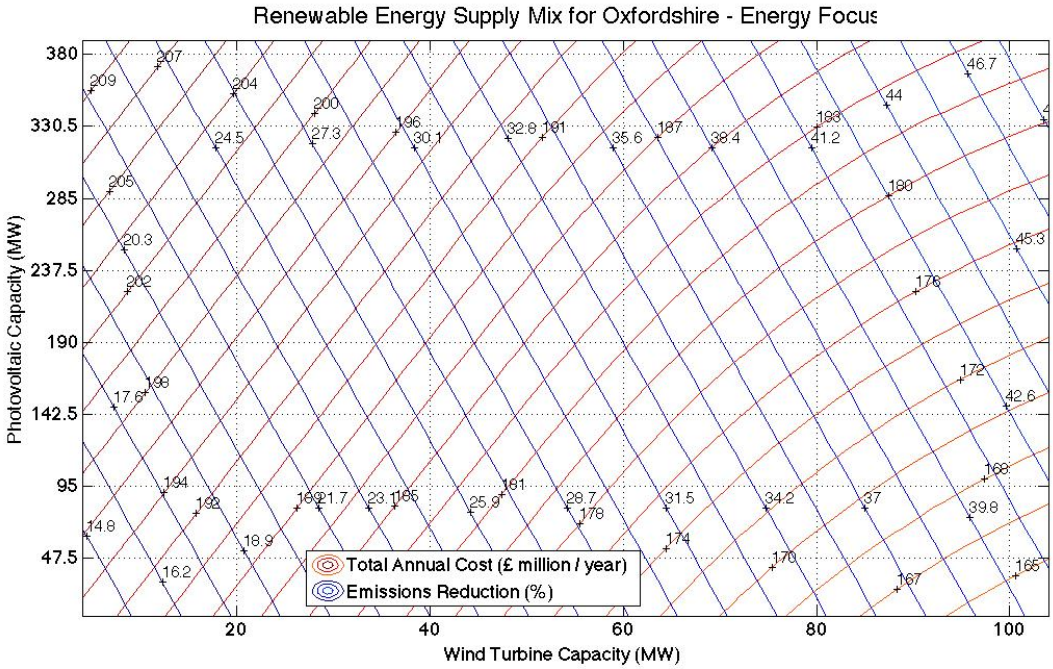


Figure 5-20 Renewable Energy Supply Mix Design - Energy Focus

The results in in Figure 5-20 above show that even under the utilization of all the renewable energy resource examined, the county cannot reach carbon neutrality. The main conclusion that can be drawn is that the total annual cost of increasing wind capacity is lower than the total annual cost of increasing PV capacity. Furthermore, the graph indicates that a further increase in wind turbine capacity would further reduce cost while increasing the reduction in emissions. However, as the maximum capacity, identified by BVG associates is 95 MW, investigating a larger system is not considered a realistic option.

5.2.2 Renewable Energy Supply Mix Design – Food Focus Land Usage

The contour plot of total annual cost and emissions reduction for the "Energy Focus" land usage scenario is shown in Figure 5-21 below.

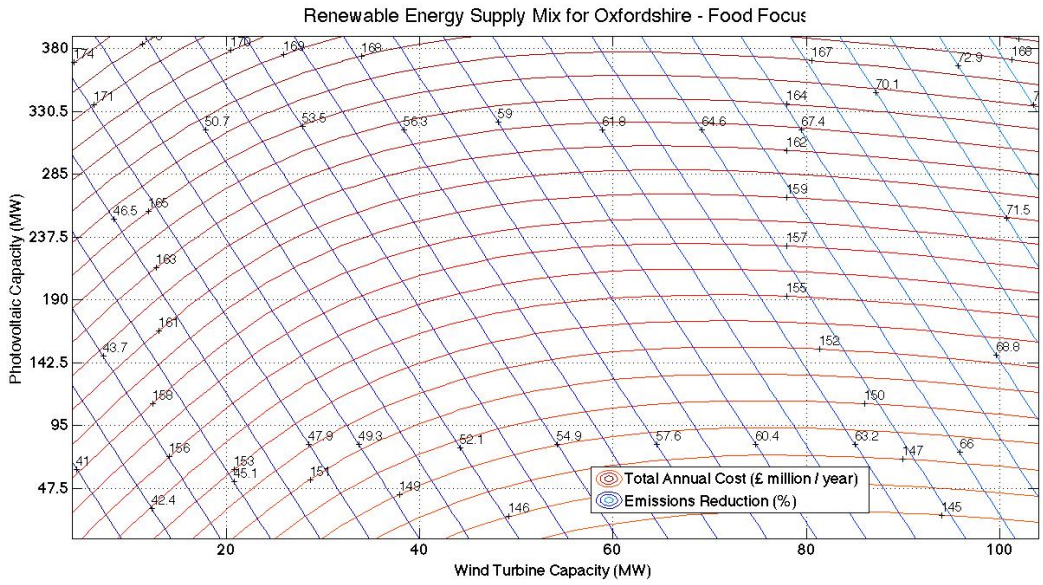


Figure 5-21 Renewable Energy Supply Mix Design - Food Focus Land Usage

The results in Figure 5-21 above show that even under the utilization of all the renewable energy resource examined, the county cannot reach carbon neutrality. The trend shown in the graph is similar to the "Energy Focus" scenario with the exception that that total annual cost reduces at a faster rate with respect to increasing wind turbine capacity. This is due to the greater biomass utilization via the gasification of SRC willow that increases the total renewable energy supply to demand.

5.3 Case Study Summary

This chapter has conducted an energy demand analysis and potential resource and conversion technology assessment for the county of Oxfordshire in the UK.

The electrical energy demand analysis has shown a generally decreasing trend in the annual consumption of 3 % between the years 2005 and 2011. Electrical energy demand and climatic effects have shown a strong correlation (R^2=0.88). Furthermore, as expected, the Average Power Analysis demonstrates a typical intraday profile with an average peak demand of 820 MW_e. The gas demand analysis has also shown a generally decreasing trend in the annual consumption of 23 % between the years 2005 and 2011. Gas demand and climatic effects have shown a close correlation (R^2=0.93).

The determinative resource assessment has examined solar energy. The optimum collector tilt has been determined at 40º and the annual resource striking this plane is 920 kWh/m^2. Rooftop solar installations have been examined as technique to utilize this solar energy. Due to the large number of buildings in the county, a computational methodology has been required in this assessment. A GIS algorithm has been developed to analyze the number of buildings within the south-facing orientation constraints suitable for solar installations. A methodology, using Google Earth™, has been used to calculate the number of rooftop type mix in the county based on typical UK building architecture. This methodology has identified 56,100 buildings suitable for solar utilization, equivalent to 4.5 million m^2 of rooftop area absorbing 1690 GWh of potential solar energy per year.

The biomass resource has been examined as an example of the dispatchable resource assessment. Two land usage strategies have been identified through collaboration with the LandShare organization. The "Energy Focus" strategy prioritizes arable land to maximize the growth of energy crops for co-digestion with the available animal waste. The co-digestion potential under this strategy has been identified as an installed capacity of 10 MW_e generating 80 GWh_e of electrical energy and 60 GWh_{th} of thermal energy per year. The "Food Focus" strategy prioritizes an optimum diet for Oxfordshire's population and attempts to create a neutral net food import/export position. The animal waste, energy crop, organic refuse and co-digestion (animal waste/energy crops) biomass categories have been examined under each land usage scenario.

The reallocation of land usage indicates that the county can reach a self-reliance level of 99 % with a relatively small land deficit of 405 ha for Horticulture and Field Vegetables. No surplus arable land for biogas energy crops can be provided without creating a food and energy land usage competition. This strategy has the potential to utilize Permanent and Rough Pasture with 28867 ha used for the establishment of solid biomass species. The energy crop MCA methodology has been implemented for solid biomass energy crops and the optimum species has been identified as SRC willow. The optimum species for biogas energy crops has been identified as maize.

A wind resource assessment of the county has been conducted by BVG associates, an engineering consultancy firm, who also participated in the "Oxfordshire Capacity Study". The results of this analysis

have been presented as an example of the stochastic resource and have identified a total wind capacity installation of 94.3 MW_e with a generation availability of 171.1 GWh_e / year.

The Exhaustive Search algorithm shows that carbon neutrality cannot be achieved in Oxfordshire under the land usage scenarios examined. The main conclusion drawn is that the increasing installation of PV capacity incurs a higher total annual cost compared to an increasing installation of wind turbine capacity. Also, the "Food Focus" land usage scenario performs at a lower total annual cost and higher emissions reduction performance than the "Energy Focus" scenario due to the larger biomass utilization.

5.4 Christ Church Site

This section examines the design of a renewable energy supply mix to meet the demand of the Christ Church site, located within the County of Oxfordshire. To start with, a review of the site and the existing energy supply is presented. The demand analysis and resource and conversion technology assessment is then presented and the results are used in the final supply mix design.

Review of the Christ Church Site

Christ Church is located in the city of Oxford in the UK and is a constituent college of the University of Oxford. The site has committed to reducing its carbon emissions by 60 % by 2050. Relative actions include a Power Purchase Agreement (PPA) to supply Scottish hydropower from the electricity utility, expiring in 2012 (Harris, 2008). However, no renewable technologies are currently in operation on-site. A plan of the electrical infrastructure is shown over the site layout, shown in Figure 5-22 (Pareto, 2009).

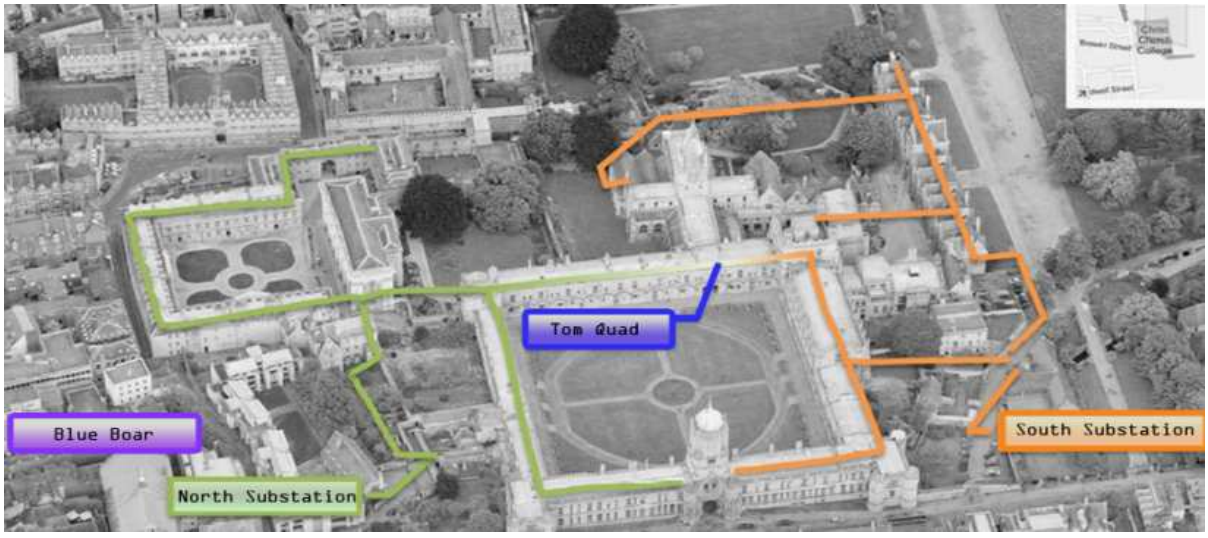


Figure 5-22 Christ Church Electricity Infrastructure

Review of the Christ Church Energy Demand Profile

The energy requirement at Christ Church is currently met by the site's connection to the national electricity and gas grids. Figure 5-22 shows that the site's electricity infrastructure is geographically divided into the north and south substations. The energy demand category has been divided into two forms, commercial and residential, based on the usage purposes of each building. The commercial energy demand category is used to describe the buildings for the administrative and academic requirements of the site where the expected majority of energy demand is between 0900 and 1700 on a weekday basis. The residential energy demand category is used to describe student residences, which have a longer energy demand requirement on an intraday basis as well as throughout the weekend. Table 5-23 lists the building and respective demand categories powered by each substation.

Table 5-23 Major Buildings Located on the Christ Church Site

Building	Energy demand category	Substation Connection
Tom Quad (1,2,3,4,5)	Residential and Commercial	South SS
Meadows Building	Residential	South SS
Peckwater Quad	Residential	North SS
Canterbury Quad	Residential	North SS
Blue Boar	Residential (with substantial night-storage)	North SS

Based on information obtained by the Manciple, the connection to the national electricity grid is priced according to the Economy 7 tariff scheme, which is on between 0000 and 0700 every day. The day units are priced at 6.5 p/kWh$_e$ and the Economy 7 units are charged at 5.5 p/kWh$_e$ (SouthernElectric, 2010). The gas connection to the national grid is distributed to all the main buildings on site except for the Blue Boar residences and is priced at an average rate of 3 p/kWh. It is important to note the presence of night storage heaters within the energy demand mix, the majority of which are powered by the north substation and a small number by the south substation.

5.4.1 Energy Demand Analysis - Christ Church Site

This section examines the implementation of the energy demand analysis, developed in section of Chapter 3, in the Christ Church demand profiles. This study uses the electrical Half-Hourly Demand (HHD) data obtained by the college Manciple. This data has been recorded using half-hourly meters

installed at both substations between January 2011 and December 2012. The results allow the assessment of the temporal, climatic and growth factors in relation to demand.

5.4.1.1 Temporal Analysis

The Average Power Analysis and seasonal factors are analyzed in this section to assess the electricity and gas demand at Christ Church.

Average Power Analysis – Electricity

The Average Power Analysis in terms of the minimum, average and maximum power is shown for the north substation in Figure 5-23 and the south substation in Figure 5-24 below.

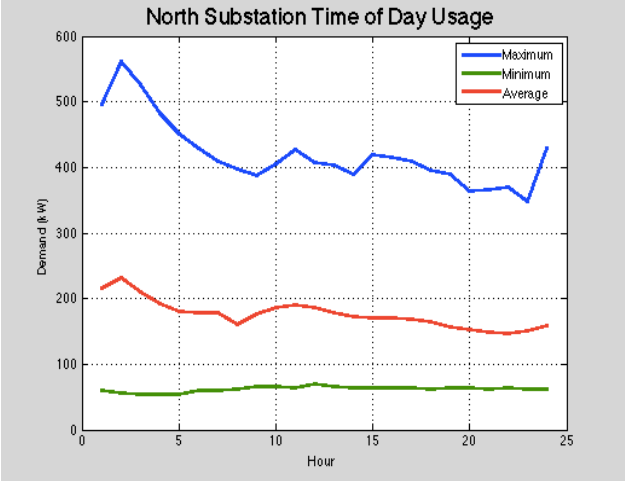


Figure 5-23 North Substation ToU

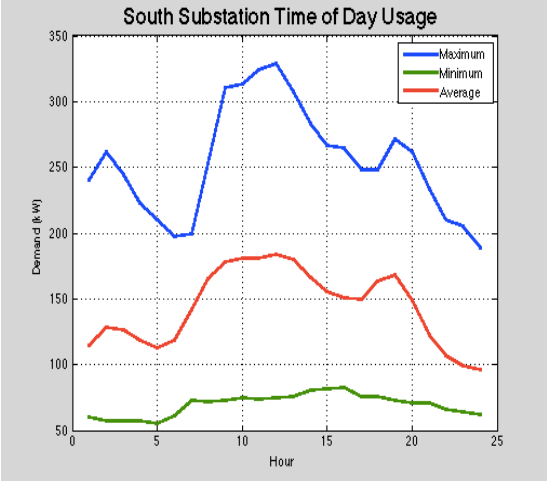


Figure 5-24 South Substation ToU

The night storage heating operation at the north substation is particularly obvious in Figure 5-23 during the Economy 7 hours, due to a profile with an average peak demand at 0200 that minimizes when the Economy 7 tariff changes to the peak hour tariff after 0700.

The daily energy demand, during the Economy 7 hours, is the integral of the hourly power demand between the hours of 0000 and 0700. To calculate the night storage requirement, the minimum demand, which occurs during the last hour of Economy 7, is subtracted from the total power demand throughout these hours and is equal to 398 kW_e. The electrical energy allocated by the north substation to the night storage heaters is, therefore, 569 kWh_e per day, equivalent to 6 % of the daily demand. This heating service costs £32.8 and emits 0.26 tCO_2/day[19] (DEFRA, 2012).

[19] The equivalent carbon dioxide emissions factor for electricity generated by the UK national grid supply mix is 0.457 $kgCO_2$ / kWh_e (DECC, 2010)

To generate the same heating service, a natural gas fired boiler, with a combustion efficiency of 90% costing 3 p/kWh, could replace the night storage system by consuming 632 kWh of natural gas per day (Means, 2010). The daily operation of the gas boiler would cost £19 and emit 0.12 tCO_2/day [20] (DEFRA, 2012). These results show that, in both project metrics, a gas-fired system achieves a higher performance than the night storage system. However, the building design and infrastructure prohibit the installation of such a system so this option cannot be considered further.

Average Power Analysis – Gas

The analogue gas meters at the site do not allow for monitoring and recording of hourly or daily gas demand. The highest available data resolution is on a monthly scale. This study assumes a linear base load gas demand at the magnitude required to meet the monthly data using Equation (5-2) below.

$$Hourly\ Gas\ Demand = \frac{Monthly\ Gas\ Demand}{Hours\ per\ Month} \quad \textbf{(5-2)}$$

Seasonal and Annual Change

The monthly electricity and gas demand between 2008 and 2009 is shown, in Figure 5-25 below, and the three-year annual energy consumption data is shown in Figure 5-26 below.

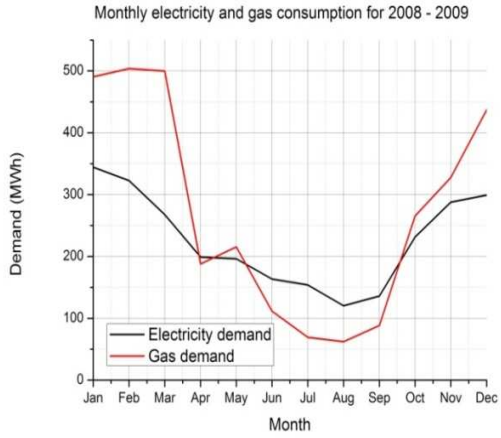


Figure 5-25 Monthly Electricity and Gas Demand 2008 - 2009

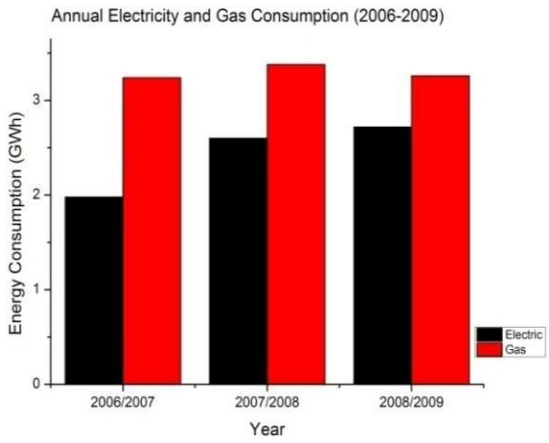


Figure 5-26 Annual Electricity and Gas Demand 2006 - 2009

The monthly electricity demand pattern shows that there is a greater demand over the winter periods compared to the summer periods. This is due to the population reduction over the academic holidays and also the potential relationship between the external temperature and the electricity consumption discussed

[20] The equivalent carbon dioxide emissions factor for natural gas combustion by the UK national gas grid is 0.184 $kgCO_2/kWh_{th}$ section (DECC, 2010)

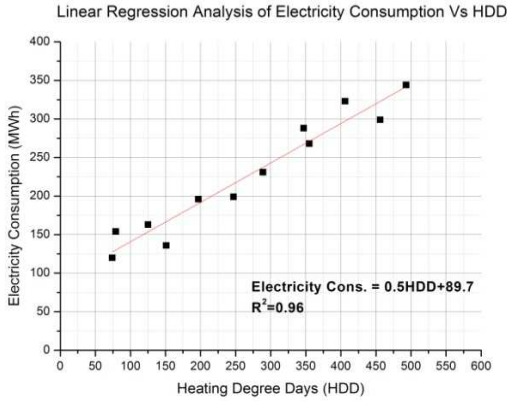
in the next sub-section. With respect to the monthly gas demand, there is a difference between the winter and summer months, due to the heating requirements of these periods.

Annual electricity demand has increased by 37 % from 1.98 GWh_e in the period 2006/2007 to 2.72 GWh_e in the period 2008/2009. Gas demand has increased by 0.6 % from an annual total of 3.23 GWh in the period 2006/2007 to 3.26 GWh in the period 2008/2009.

To convert the gas consumption to a thermal energy demand, which is later examined against the thermal energy generation of a CHP unit, a LHV efficiency of 85 % is assumed for the gas boiler operating at the Christ Church site.

5.4.1.2 Climatic Effects

The external temperature effects on the Christ Church electricity and gas demand are examined in this sub-section. This assessment uses the total electricity and gas demand of the site, shown in Figure 5-25 above. The temperature data set used to conduct this analysis has been extracted from the Benson Meteorological office because it is the closest geographical site to the case study that records the data required for this analysis (ECI REFERENCE). The typical internal building temperature is set at 18°C (McCulloch, 2010). The majority of degree-days recorded at the Benson Meteorological station, using the aforementioned internal temperature, are the HDD that have, therefore, been used in this analysis. The linear regression analysis between electrical energy demand and HDD is shown in Figure 5-27 and between gas demand and HDD in Figure 5-28 below.



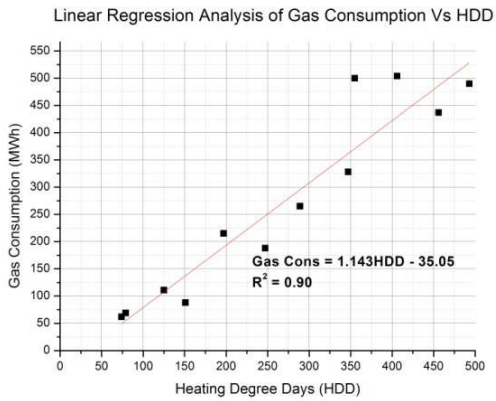


Figure 5-27 Electricity Consumption and HDD Regression **Figure 5-28 Gas Consumption and HDD Analysis**

The strong coefficients of determination (>0.75), shown in both graphs above, allow the conclusion that

both the electricity and gas demand show a strong, positive linear relationship with the HDD and climate. This correlation allows further analysis on the relationship between both types of energy demand and the heating degree-day unit. More specifically, the change in electricity demand per MWh is dependent on a 0.5 shift in the heating degree-day value. It has been concluded from the graph, in Figure 5-27 above, that the electrical consumption at Christ Church, unrelated to the space heating service on a monthly basis, is 89.7 MWh_e. The change in the gas demand per MWh is dependent on a 1.1 shift in the HDD.

5.4.1.3 Growth

The main change in infrastructure at Christ Church occurred in the 2007-2009 period when the Blue Boar residences were closed for renovation (ChristChurch, 2010). The energy intensive construction process may have caused the 37 % demand increase between the 2006/2007 and 2007/2008 periods. Furthermore, a projection for future increase in population and infrastructure must be accounted for, as this will change the demand profile and magnitudes, which the supply is designed to meet.

Christ Church Energy Demand Analysis Summary

This section has conducted an energy demand analysis of the Christ Church site. The Average Power Analysis is mainly driven by the night storage heating at the north substation. Both electricity and gas show a strong correlation with climate, allowing for the extraction of non-weather related demand magnitude.

5.4.2 Renewable Energy Resource Assessment - Christ Church Site

This section examines the implementation of the renewable energy resource assessment methodologies, by statistical characteristic type, presented in section 3.2. The usefulness of these assessments is two-fold: firstly, they propose the resources that should be further considered; and, secondly, they present the magnitude and occurrence of each resource that will permit the power and energy estimation.

5.4.2.1 Determinative Resource Assessment

This section examines the solar energy resource assessment for the Christ Church Site.

5.4.2.1.1 Solar Energy

The solar energy assessment conducted for the county of Oxfordshire above, calculated an optimum tilt

angle of 40º and potential energy production of 920 kWh/m^2. As Christ Church is located in Oxfordshire, this study assumes the same optimum tilt angle and potential energy content. The assessment is investigated further by a survey, via Google Earth, to determine the surface area and tilt angle of the suitable rooftop solar installations.

Rooftop Solar Energy - Christ Church

The suitable rooftops for solar installation are highlighted on the Google Earth image of the Christ Church site, presented in Figure 5-29 below. If the rooftop tilt angle is less than the optimum tilt, previously calculated at 40°, the photovoltaic panels can be mounted to the optimum angle and, thus, generate at the highest potential. If a rooftop angle is greater than the optimum tilt, the photovoltaic panels can only be physically installed at this angle and further investigation must be conducted to assess if the generation potential is at a cost-effective level. The identified rooftops are all under the 40º slope and so this study assumes that the panels are mounted to the optimum tilt.

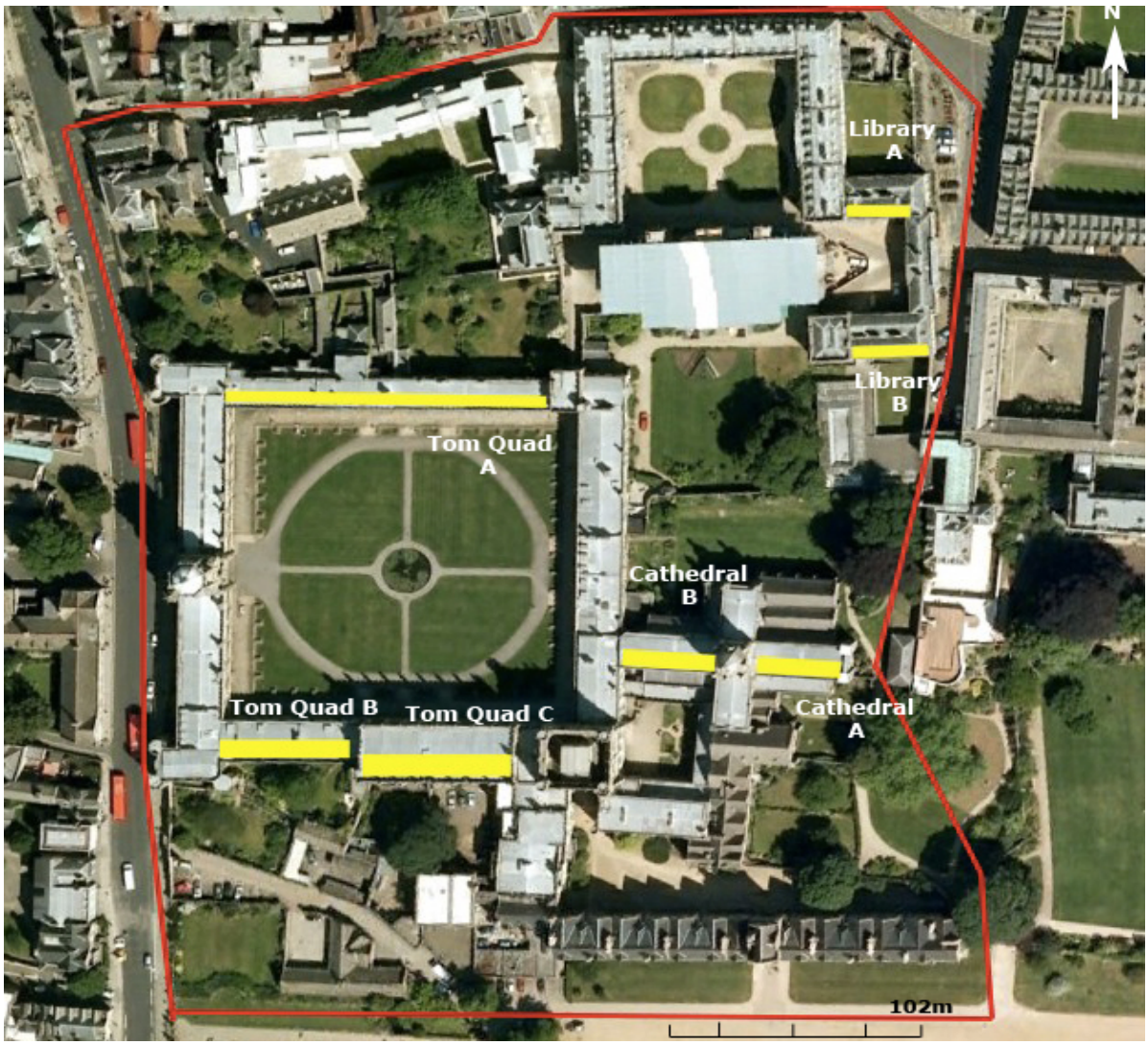


Figure 5-29 Christ Church Solar Rooftop Potential

The suitable rooftops, labelled in the map above, are individually presented in terms of their surface area and annual solar energy potential in Table 5-24 below. The tilt angles have been obtained from the site's maintenance manager who conducted a site visit to assess each rooftop (Coles, 2012).

Table 5-24 Rooftop Solar Energy at Christ Church

Rooftop	Dimensions (m)	Tilt Angle (°)	Rooftop Area (m^2)	Annual Solar Energy (MWh)
Tom Quad A	77 x 3.5	30	270	248
Tom Quad B	28 x 4.5	30	125	115
Tom Quad C	36 x 6	30	215	197
Cathedral A	20 x 4	40	80	74
Cathedral B	20 x 4	40	80	74
Library A	15 x 3	35	45	41
Library B	15 x 3	35	45	41
Total Rooftop	-	-	860	790

5.4.2.2 Dispatchable Resource Assessment

This section examines the implementation of the biomass energy dispatchable resource assessment for the suitable category, developed in section 3.2.2, on the Christ Church site.

5.4.2.2.1 Biomass Energy

Christ Church owns large areas of agricultural land throughout Oxfordshire and the UK. Therefore, the possibility of growing and harvesting energy crops is presented. The crop availability provides the site with the ability to monitor the entire supply chain, from the growth stages to electricity generation. This characteristic of the supply chain is expected to reduce the annual cost of this project as the site does not need to purchase any product or service from a third party. The animal waste and refuse categories are not considered relevant to the site and are not examined further in this section.

In order to establish the preferred energy crop species between crops for solid biomass and biogas utilization, both MCA analyses, developed in Chapter 3, are implemented on the Christ Church site. The optimum species of each form is then compared on an energy yield per unit area of land (kWh/ha) basis. The highest energy yielding crop is further considered with its respective conversion technology component in the overall supply mix design.

Biogas Fuel Form Energy Crop Species Assessment Tool

This sub-section examines the selection process of the crop species, envisaged as a biogas fuel form, using the decision-making tool developed in section 3.2.2.1.2.

Steps 1 – 4 of the process are followed using the information on the most popular energy crop species in the UK, shown in Table 3-7 of section 3.2.2.1.2. Due to the main constraint being the land requirement and its limited availability in an urban area such as Oxford, the main emphasis is given on identifying the species with the highest energy yield. Therefore, the energy yield is given a weighting of 2 and the remaining elements a weighting of 1, as shown in Table 5-25 below.

Table 5-25 Implementation of Energy Crop Species Assessment Tool for the Christ Church Site

Criteria	Energy Yield	Economic	Environmental	Total Score (/40)
Elements	Energy Yield (MJ/ha) [VS; BMP; Growth]	O&M (£/ha)	Fertilizer Demand (MJ/MJ)	
Weighting	***2***	***1***	***1***	
Barley	6.3	10	6	***29***
Maize	7.7	9	10	***34***
Oilseed Rape	4.3	9	6	***24***
Sugar Beet	7.0	5	8	***27***

From the MCA results, shown in Table 5-25 above, the most favourable species, using the average range values of each element, is maize and least favourable is oil seed rape which shows a particularly low performance under the energy yield element examined due to its poor crop growth yield.

Solid Biomass Fuel Form Energy Crop Species Assessment Tool

This sub-section examines the selection process of the crop species, envisaged as a solid biomass fuel form, using the decision-making tool developed in this study.

Steps 1 – 4 of the process are followed using the information of the most popular energy crop species in the UK, shown in Table 3-13 of section 3.2.2.2.1. To maintain a consistent comparison between the energy crops envisaged for the biogas fuel form, the MCA analysis weightings are similar to Table 5-25 above. The implementation of this analysis for the solid biomass fuel form at the Christ Church site is shown in Table 5-26 below.

Table 5-26 Multi-Criteria Assessment Analysis for Solid Biomass Energy Crops at Christ Church

Criteria	Energy Yield	Economic		Environmental	Total Score (/60)
Elements	Energy Yield (MWh/ha) [LHV; Moisture; Growth]	Capital (£/ha)	O&M (£/ha)	Fertilizer Demand (MJ/MJ)	
Weighting	*2*	*1*	*1*	*1*	
Miscanthus	*8.7*	*8*	*10*	*10*	*45*
SRC Willow	*9.3*	*10*	*3*	*10*	*42*

The MCA results indicate that Miscanthus is the optimum solid biomass species under the decision-making criteria and weighting factors allocated in this analysis.

The following sub-section compares the optimum species for solid and biogas applications to decide which of the two pathways should be used in designing the site's supply mix.

Optimum Energy Crop Species – Christ Church

The Miscanthus and Maize species have been identified as the optimum energy crop feedstock at the Christ Church site. As only one option can be utilized and examined further, a selection must be made between the two. The anaerobic digestion of energy crops is considered a mature and commercially available technology as opposed to their gasification which is still at a research and development stage (IRENA, 2012a). Furthermore, the operational philosophy of an energy crop anaerobic digestion system requires the digestate to be used as the crop fertilizer, thereby, creating an autonomous power generation system. This is a feature that gasification does not offer. The two aforementioned points are the main reasons why the anaerobic digestion of energy crops is the sole method considered further to meet demand at the Christ Church site.

5.4.2.3 Available Conversion Technology Assessment - Christ Church Site

The previous section identified the solar and biomass resources as the renewable energy resource elements of the proposed supply mix. This section examines the implementation of the available conversion technology methodologies, examined in Chapter 3, in the solar PV and AD CHP technologies. Since Christ Church is a grid-connected site, the grid effectively acts as a battery bank and, therefore, storage is not considered in this analysis.

5.4.2.3.1 Solar Photovoltaic Assessment

This sub-section examines the energy generation and indicator performance of the PV technology at Christ Church. The 5-parameter single diode model is used to represent the Suntech STP 190 W device assuming a tilt of 40º and a south-facing orientation.

The indicator performance of one PV unit and the entire array is shown in Table 5-27 below. This study assumes that, due to the small size of the array, there is a negligible O&M cost and that the annualized

capital cost is calculated using a discount factor of 5 % over a 25-year period. The energy yield generated per kW of installed capacity at Christ Church is 845 kWh/kW_p.

Table 5-27 Christ Church Solar PV Performance

Technology Module	Capacity (kW_e)	Capital Cost (£'000s)	Total Annual Cost (£'000s/year)	Annual Energy Generation (MWh_e)
Suntech 190 W	0.19	0.25	17.3	0.16
Suntech 190 W	93	121	8.7	76.6

The composition of the total PV array is shown in Table 5-28 below.

Table 5-28 Composition of Photovoltaic Array at Christ Church

Rooftop	Installed Capacity (kW_e)	Capital Cost (£'000s)	Total Annual Cost (£'000s/year)	Annual Energy Generation (MWh_e/year)
Tom Quad A	36.5	47.5	3.4	30.1
Tom Quad B	13.3	17.3	1.3	10.9
Tom Quad C	17.1	22.2	1.6	14.1
Cathedral A	9.5	12.4	0.9	7.9
Cathedral B	9.5	12.4	0.9	7.9
Library A	3.4	4.4	0.3	2.8
Library B	3.4	4.4	0.3	2.8
Total	92.7	120.6	8.7	76.5

The seasonal variation of the 93 kW_e PV array against demand is shown in Figure 5-30 below.

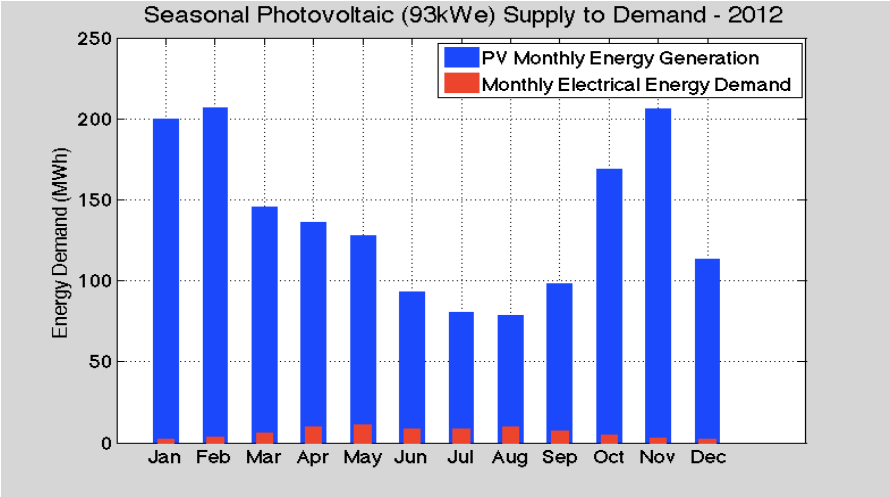


Figure 5-30 Seasonal 93 kWe PV Supply to Demand

The summer period shows the highest proportion of PV energy to demand due to the favourable climatic conditions and reduced demand because of vacation time.

5.4.2.3.2 Anaerobic Digestion Combined Heat and Power Assessment

This sub-section examines the performance of a maize AD system at Christ Church, identified as the optimum species by the energy crop selection tool. A range of available units, extracted from the Alfagy manufacturer, is shown in Table 5-29 below with the respective indicator performance and land area required for feedstock growth (Alfagy, 2010). The energy demand column represents the percentage of CHP energy generated that meets demand and discounts any oversupplied energy.

The peak electrical demand at Christ Church is 789 kW_e. Installing an AD system greater than this leads to an oversizing of supply, which is unnecessary due to the dispatchable nature of the biomass. Table 5-29 below considers system sizes less than the peak load currently available on the market.

Table 5-29 Alfagy AD Performance at Christ Church

Electrical Capacity (kW_e)	Thermal Capacity (kW_{th})	Land Usage (ha/year)	Annual Energy Generation		Capital Cost (£'000s)	O&M Cost (£/year)	Total Annual Cost (£/year)
			Electrical (MWh_e)	Thermal (MWh_{th})[21]			
250	260	95	2232	2321	975	420	485
500	427	190	4464	3812	1950	840	970

The seasonal variation of the 250 kW_e AD CHP system is shown against the electrical energy demand in Figure 5-31 and the thermal energy demand in Figure 5-32 below.

[21] Thermal energy demand assumes a gas boiler η = 90 % from the Christ Church gas consumption

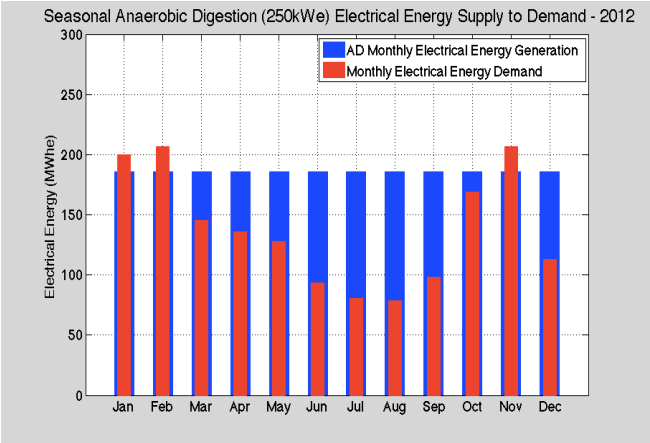


Figure 5-31 AD Electrical Energy to Demand

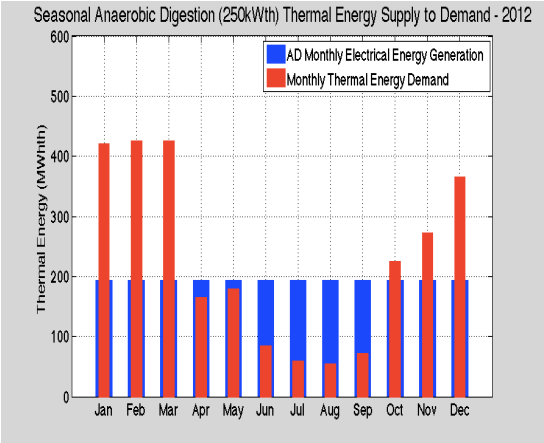


Figure 5-32 AD Thermal Energy to Demand

The monthly AD electrical generation oversupplies demand for the majority of the year except for January, February and November when the demand is seen to be at a minimally higher level. As expected, the AD thermal supply is able to meet the entire summer demand and a thermal demand deficit is present over the winter. Although the monthly time scale may show a supply surplus, further analysis is required, at higher time resolutions, to investigate the average power supply and demand patterns in order to determine if all of the supply is in fact required by the demand. This is examined further in the renewable energy supply mix methodology.

The seasonal variation of the 500 kW_e AD CHP system is shown against the electrical energy demand in Figure 5-33 and the thermal energy demand in Figure 5-34 below.

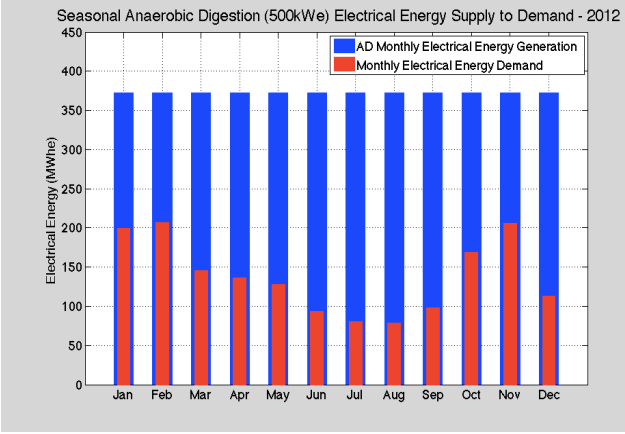


Figure 5-33 AD Electrical Energy to Demand

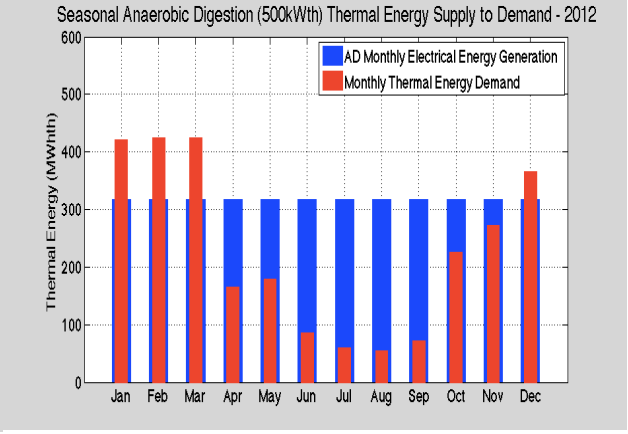


Figure 5-34 AD Thermal Energy to Demand

The larger 500 kW_e unit generates at a sufficiently high monthly level to oversupply the electrical demand throughout the entire year. The thermal energy supply is able to surpass demand for the spring season as well as just the summer as is the case for the 250 kW_e unit.

The next sub-section will investigate both AD systems and their combination with other technologies as well as compare the hourly supply and demand to identify the hourly operation of the supply mix.

5.4.2.4 Renewable Energy Supply Mix Design – Christ Church Site

This section presents the implementation of the constrained exhaustive search renewable energy supply mix methodology on the Christ Church site. The technologies considered are identified from the resource assessment as the PV and AD CHP systems. The electricity and gas grids are considered as a back-up supply to meet demand when the renewable element is insufficient.

The constrained exhaustive search space minimization technique for the upper bound limits of the PV and AD CHP technologies is examined. Although there is a maximum rooftop space available, this technique examines the need for utilizing all the available space. The search is conducted individually for each AD unit, in Table 5-29 above, with the subsequent PV supply.

5.4.2.4.1 Exhaustive Search Space Minimization

This sub-section presents the implementation of the exhaustive search space minimization technique, on the PV and AD CHP systems, to determine the upper bound limits of the final search space.

Photovoltaic Upper Bound Limits

The maximum suitable rooftop capacity is presented in Table 5-27 as 93 kW_e. This sub-section examines the PV generation of the array against the national grid demand to identify if there is a saturation point prior to the 93 kW_e. This sweep is shown in Figure 5-35 below. The saturation point, assuming unlimited rooftop area, is shown in Figure 5-36 below.

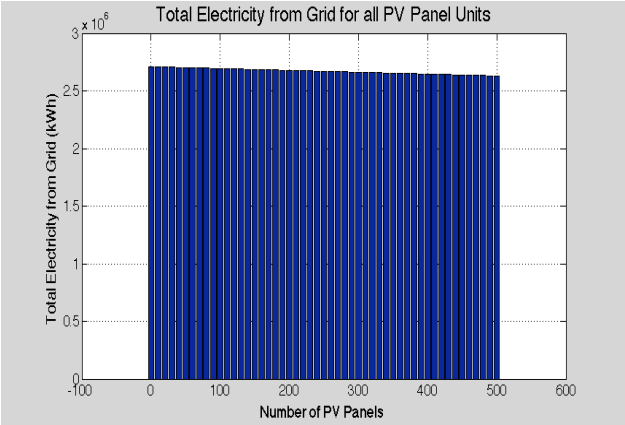


Figure 5-35 Total Grid Electricity for PV Units up to 93 kW_e

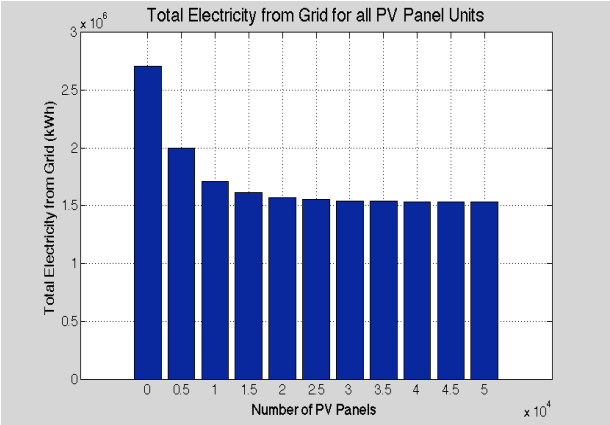


Figure 5-36 Total Grid Electricity for all PV Units

Figure 5-35 shows that the maximum PV installation of 93 kW_e does not saturate the supply and, thus, the entire 93 kW can be considered without oversizing the search space. Figure 5-36 illustrates that, if the installation space were unlimited, the supply would saturate at 40000 units equivalent to 7.6 MW_e. This saturation point is greater than the available installation space of 93 kW_e, so it can be concluded that the entire rooftop can be utilized for PV arrays without an oversupply to demand.

5.4.2.5 Final Renewable Energy Supply Mix Design

This sub-section presents the implementation of the constrained exhaustive search on the Christ Church site, using the minimum search space presented per technology in the previous sub-section. The total annual cost and emissions reduction performance of the 250 kW_e and the 500 kW_e AD systems with a PV supply range up to the rooftop saturation point is shown in Figure 5-37 below.

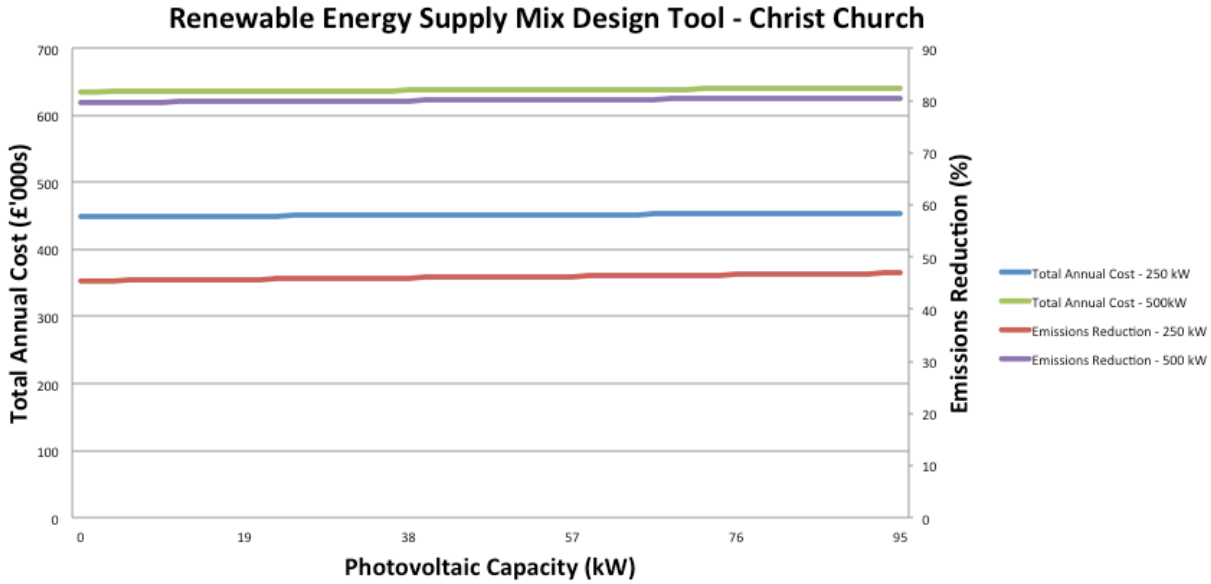


Figure 5-37 Renewable Energy Supply Mix Design Tool - Christ Church

The main influence of total annual cost and emissions reduction is the size of the AD generator. A small change in cost and emissions is made as the PV capacity increases due to the relatively small PV search space examined. More specifically, the 93 kW_e PV array generates 1.4 % of the total annual demand.

As mentioned previously, the targeted emissions reduction at Christ Church is 60 %. This can be met by installing a 250 kW_e AD and 93 kW_e PV supply mix. However, under the scope of technologies and capacities examined in this study, it has been concluded that carbon neutrality cannot be achieved at the Christ Church site. It is expected that oversizing the AD generator will improve the emissions reduction performance but a trade-off must be decided for the oversupply of renewable energy to demand and a higher emissions reduction performance.

5.5 Case Study Summary

This case study has conducted an energy demand analysis and resource assessment and has implemented the renewable energy supply mix methodology, developed in Chapter 3, on the Christ Church site located within the county of Oxfordshire.

The electricity and gas demand shows a high correlation with HDD (R^2 = 0.96) and the gas demand (R^2=0.90). It has been concluded that both the electrical and thermal requirements of the site are directly related to external climatic effects. The high correlation of electrical energy to HDD is due to the large element of night storage heating installed on-site.

The dispatchable resource assessment has been conducted by the implementation of the energy crop MCA methodology developed in Chapter 3. The MCA has been implemented, for both the solid energy crops and biogas energy crops, as a potential renewable fuel used for on-site generation. Miscanthus has been identified as the optimum solid biomass species and maize as the optimum species for biogas production. The anaerobic digestion of energy crops is considered a mature and commercially available technology, as opposed to gasification that is still in the development phase. The anaerobic digestion of maize has been selected for further analysis as a component of the renewable energy supply mix.

The conversion technology assessment has identified an available rooftop space of 93 kW_e PV capacity on the south facing rooftops at a tilt angle less than or equal to the 40º optimum tilt. The AD analysis identified the 250 kW_e and 500 kW_e systems as potential components of the supply mix as larger capacities are greater than the annual peak demand and, thus, oversize system supply. The PV upper bound of 7.6 MW_e has been calculated as saturating the site's grid requirement. However, as the available rooftop space is only 93 kW_e, this capacity has been considered as the upper bound limit for the analysis. The supply mix that can achieve the 60 % emissions reduction target at the lowest total annual cost is comprised of a 250 kW_e AD and 93 kW_e PV. Carbon neutrality cannot be met using the technologies and capacities within the scope of this study.

Chapter 6 - Conclusion

This thesis addresses the topic of designing a renewable energy supply mix to meet demand. The criteria used in this exercise are based on the economic and environmental metrics of sustainability, as defined by the United Nations World Commission on Environment and Development.

Renewable Energy Supply Mix Assessment Metrics Applied

The economic metric is assessed by the total annual cost of the proposed supply mix. This cost is calculated as the summation of the annualized capital cost, annual operation and maintenance cost and the conventional fuel cost required to meet demand. The environmental metric is assessed by the equivalent carbon dioxide emissions reduction of the proposed supply mix. The social metrics of sustainability have not been examined as they are considered out of the research scope of this thesis.

Since the main aim of this study is to meet energy demand, a series of techniques have been developed to analyze demand profiles. Three factors have been identified as suitable to provide a complete view of a site's demand profile. These are the temporal, climatic and growth factors of demand. The temporal factors examine the diurnal, seasonal and annual energy demand. The climatic factors examine the effect weather has on demand to find if there is a relation between the two and, if so, what the requirements are for space heating and cooling. The growth factors examine the expected long-term shift in infrastructure and population in order to conclude if there is a requirement to add supply capacity or other infrastructural changes to meet demand.

Renewable Energy Resources and Conversion Technologies Examined

The renewable energy supply mix is separated in terms of the renewable energy resource and available conversion technology. Renewable energy resources have been generally divided in terms of their statistical availability, which are the determinative, dispatchable and stochastic statistical types. To account for each statistical type, a specific resource has been used as an example of each. Each resource is considered in terms of the economic and environmental indicators. Determinative resources have a predictable magnitude and diurnal and seasonal profile over the annual time scale. Solar energy is used as an example of the determinative resource. Dispatchable resources can provide spatial and temporal energy storage. Biomass energy is used as an example of the dispatchable resource. Biomass energy is

comprised of animal waste, energy crops, forestry waste and refuse. All of these types of biomass are examined in this study. Since energy crops are grown specifically for the purpose of use as a fuel, a multi-criteria assessment analysis has been developed to determine optimum crop species under the economic and environmental indicators. This assessment has been developed for high organic content energy crops envisaged in an AD system and woody crops envisaged in a gasification system. Stochastic resources have an intermittent nature with high levels of randomness involved in their availability and can be assessed using probability distributions. Wind energy is used as an example of a stochastic resource.

The conversion technologies that operate using each of the above resources are then examined in terms of the economic and environmental indicators. The photovoltaic technology is used as the available technology that operates with solar energy. Anaerobic digestion is used as the available technology that operates with animal waste, energy crops with high organic content, such as maize, and organic household waste in the refuse category. Gasification is used as the available technology that operates with woody energy crops, such as miscanthus and short rotation coppice willow and forestry waste. Since there is a higher total system efficiency and thermal energy is also generated in a useful energy form, both anaerobic digestion and gasification are assumed to power a CHP generator.

Renewable Energy Supply Mix Design Methodology Developed

Following the resource and conversion technology assessment of the supply mix, the system sizing methodology is then applied using the constrained exhaustive search algorithm. Due to the large search space involved with this algorithm, a minimization technique has been developed in this study to confine the search space and maximize computational efficiency. This technique functions by comparing an increasing number of units of each individual technology against the demand profile on the diurnal (or highest resolution time scale possible) and finding the conventional fuel requirement to meet demand. The number of units per technology that do not require a further increase in conventional fuel is defined as the “saturation point” and is subsequently the upper bound limit of the search space. This methodology allows the application of the constrained exhaustive search algorithm within a useful system capacity as it ensures that there is no oversizing of the system and unnecessary examination of system capacities.

Case Studies Used for Renewable Energy Supply Mix Design

Two case studies have been used to assess the functionality of the supply mix design methodology developed in this study. These are the island of Hanimaadhoo, located in the Republic of the Maldives, and the county of Oxfordshire in the UK. This case study has been further examined using the Christ Church site, a college member of the University of Oxford, located in the city of Oxford.

Case Study 1: Island of Hanimaadhoo, Republic of the Maldives

Chapter 4 of this thesis investigates the island of Hanimaadhoo in the Maldives. Solar and wind energy in Hanimaadhoo has been assessed using data obtained from the on-site United Nations Development Program meteorological office that records direct and diffuse solar radiation and wind speed, direction and air density on an hourly scale. The solar energy potential is calculated as 2700 kWh / m^2 and an initial assessment of refuse biomass from organic household waste has the potential to power a 5 kW_e anaerobic digester for 8000 hours per year. As this type of system is not commercially available at this scale, the biomass resource has not been further examined. The wind energy potential is categorized as a class 1 (poor) wind site at vertical heights ranging between 15 and 80 m. The average wind speed at 15 m is 2.8 m/s and the average wind speed at 80 m is 3.3 m/s due to the relatively low surface roughness constant of 0.003 used, based on the topographical mixture between open sea and agriculture observed on the island. Between May and July, the seasonal availability of wind is at a maximum when solar energy is at a minimum. Therefore, this resource has been further considered in the supply mix design as a potential complement to the available solar resource on a seasonal scale. The PV technology has shown a cost of energy generation of $ 0.08 / kWh_e, which is highly competitive when compared to the current diesel cost of $ 0.4/kWh_e.

The implementation of the renewable energy supply mix design methodology has then been applied considering a supply mix comprised of the PV, wind turbine and Lead-Acid battery technologies. This supply mix can achieve carbon neutrality at a total annual cost of $ 740,000 by installing a wind capacity of 4000 kW_e, 1000 kW_e PV capacity and 3900 kWh_e of battery storage. The total annual cost of this system is $ 740,000/year, which is more expensive than the current cost of $ 720,000 / year. Due to the poor wind regime in the area, the design methodology has been implemented again by not including the wind turbine technology. This supply mix can achieve carbon neutrality at a total annual cost of $

582,000 by installing 1710 kW_e of PV and 6500 kWh_e battery storage. It is shown that not including the wind turbine technology achieves carbon neutrality at a lower cost and so, for the purposes of this study, is the proposed supply mix design for the island.

Case Study 2: County of Oxfordshire, UK

Chapter 5 investigates the county of Oxfordshire and is divided into two sections. The first part of the chapter investigates the county of Oxfordshire and the second part of the chapter investigates the Christ Church site, used as a smaller scale model example case study within the county.

The hourly electricity demand for Oxfordshire follows a typical profile with an average peak load of 950 MW_e at 1800 and a minimum average demand of 440 MW_e at 0500. The climatic factor of electricity demand shows a strong correlation with HDD ($R^2 = 0.88$) and the gas demand shows a strong correlation with HDD ($R^2 = 0.97$).

The solar potential in Oxford has been calculated as 920 kWh/m^2. The available rooftop space for solar PV has been extrapolated from Abingdon, Banbury, Bicester and Oxford to identify 56,100 suitable buildings absorbing 1690 GWh of potential solar energy per year in the county. The available space is equivalent to a total PV capacity of 379 MW_e.

The "Energy Focus" scenario can accommodate a total of 19.1 MW_e AD capacity. This is comprised of 10 MW_e using maize and cattle waste co-digestion feedstock, a 1.1 MW_e AD using pig waste feedstock and 8 MW_e of organic refuse. A further 61.4 MW_e can also be included from 54 MW_e willow and 7.4 MW_e of forestry waste. The "Food Focus" scenario can accommodate a total of 15.3 MW_e AD capacity. This is comprised of 7.3 MW_e AD, using animal waste (cattle, pig) feedstock and 8 MW_e of organic refuse. A further gasification capacity of 256.4 MW_e can also be included from 249 MW_e willow and 7.4 MW_e of forestry waste. This scenario shows that Oxfordshire can achieve a self-reliance level of 99 % if the residents adapt to the examined Livewell diet.

The BVG wind resource assessment has identified a total wind capacity installation of 94.3 MW_e providing an electrical energy generation of 171.1 GWh_e / year.

Both land usage scenarios have then been investigated using the Exhaustive Search Space algorithm. The "Energy Focus" scenario cannot achieve carbon neutrality by the utilization of the resources within the

scope of this study. An increase in PV capacity up to the utilization of all suitable rooftops county shows a decrease in total annual cost, while an increasing wind turbine capacity increases the total annual cost.

The "Food Focus" scenario cannot achieve carbon neutrality by the utilization of the resources within the scope of this study. An increasing PV capacity has a higher rate of reduction of total annual cost compared to the "Energy Focus" due to the larger gasification capacity that enhances the total performance of the supply mix.

Case Study 2: Christ Church Site, Oxfordshire

The total peak electrical demand at the Christ Church site is 789 kW_e. The climatic factor shows a strong correlation between both electricity and gas consumption and HDD. Similarly to the county, the correlation coefficient for the electricity and HDD relationship is 0.96 and the annual non-weather related demand is 89.7 MWh_e per year. The correlation coefficient for the gas and HDD relationship is 0.90.

The constrained infrastructure at Christ Church only allows the installation of a 93 kW_e PV array installed on the Tom Quad, Cathedral and Library buildings. The ownership of large areas of arable land has created the opportunity to investigate the establishment of energy crops as a fuel for an AD or gasification system. The multi-criteria assessment identified maize as the optimum species to fuel an AD system and miscanthus as the optimum species to fuel a gasification system. However, as the AD of energy crops is a more mature and commercially available technology than the gasification of energy crops, the former technology has only been considered in the supply mix design process.

The implementation of the renewable energy supply mix design methodology has been implemented for an energy crop AD, PV and Lead-Acid battery supply. The 250 kW_e and 500 kW_e AD systems have been considered in this study, as the commercially available equipment that are less than the peak load. The PV technology search minimization has identified a saturation point of 7.6 MW_e, but 93 kW_e is assumed in this analysis as it reflects the available space for PV installation on-site.

Critical Reflection on the Strengths and Weaknesses of the Proposed Methodology

This study has attempted to develop a general methodology that could be applied to a case study aiming to achieve carbon neutrality. The main strengths and weaknesses are outlined in this section.

The key assumption made in the methodology is that the average performance of each technology was considered. The supply modelling assumed that the conventional energy technologies would meet any deficit from the renewable technologies. There is a technical constraint with this assumption as the ramping capabilities of these technologies are not accounted for and so a time mismatch in power supply levels against demand may be evident. More detailed operational optimization could output different results than those shown in this study particularly for sites with rapidly changing operational conditions. This is much more of a concern in the Oxfordshire case study where effects such as short term cloud cover on PV generation is a continuous effect as opposed to the Maldives that mainly experiences expected cloud coverage specifically throughout the monsoon season. Furthermore, the assessment assumes that the load and generation profiles remained constant over time. However, the lifetime of the technologies examined span over at least 20 years and due account needs to be made for future growth and changing climatic conditions. Finally, this methodology functions with detailed resource and demand profiles and so the outputs generated are dependent on the quality of these inputs and may also be difficult to obtain.

The main strengths of this methodology are that it allows the visual understanding of the compromise between total annual cost and emissions reduction indicators and allows an optimum trajectory between the 2 constraints. Once this optimum solution has been found, the basis is set for a more detailed operational analysis. The methodology has minimized the time requirements to complete the modelling process (<1 hour), which is also computer resource efficient. This has been achieved via a heuristic approach in identifying the upper bound limits of each renewable technology, thereby, omitting unnecessary combinations of units in the Exhaustive Search. Finally, this methodology functions on real half hourly data and attempts to balance a system over a complete 24-hour period by applying technologies with varying operational characteristics.

Contribution to Knowledge of Designing a Renewable Energy Supply Mix to Meet Demand

This sub-section highlights several methodologies developed and used in this study.

The literature review conducted in this thesis has shown a gap in knowledge of available methodologies that focus on designing a renewable energy supply mix to meet demand under sustainability metrics such as those used in the United Nations sustainability definition. This thesis presents an approach that focuses on the economic and environmental metrics and uses the total annual cost as an indicator of the economic metric and the reduction in carbon dioxide emissions as an indicator of the environmental metric.

In terms of the renewable energy resources, this study has developed a cost effective and resource efficient methodology to identify the specific suitable rooftops and total surface area for solar PV installations in an urban area. This methodology is particularly useful as there is limited software in the market that can perform this type of function. The available software is highly complex to work with and extremely resource expensive to use for high rooftop number (>1000) case studies.

This study has developed a selection technique using a Multi-Criteria Assessment approach to identify the optimum energy crop species using the decision-making indicators as the main criteria. An assessment methodology has been developed to represent the solid biomass energy crop types suitable as fuel for technologies such as gasification and domestic boilers. A second assessment methodology has been developed for energy crops used as feedstock in the AD technology. These methodologies are useful in the overall decision-making process of the supply mix design, as they help assess and compare the large number of available energy crop species that are potential feedstock candidates.

To design the optimum supply mix, the Lagrangian multipliers, calculated by finding the point where a total annual cost and emissions reduction contour are tangential has been used to determine the size the supply mix with respect to the installed capacity of the individual technologies. This methodology is beneficial in situations where two indicators are considered simultaneously in a design process. Furthermore, it is a tool that drives the design process by proposing the supply mix either from a predetermined total annual cost cap or a minimum emissions reduction performance required by the user.

Appendix A

The information in Appendix A is designated to represent Chapter 3 (Methodology) of this thesis.

Visual Basic Code for Solar Rooftop Assessment Methodology

The code in Table 0-1 below has been developed in the Visual Basic language to identify the buildings in the MapInfo software that are suitable for rooftop solar utilization.

Table 0-1 Visual Basic Code Developed to Identify Rooftops Suitable for Solar Utilization in the MapInfo GIS Software

```
            End If
        'iv.
        End If
        If Cell.Offset(12, 0) = "" Then
            IsEnd = "Yes"
        End If
         'ii.  Calculate the length of this segment (Current Length)
        If IsEnd = "No" Then
            CurrentLength = ((Cell.Offset(11, 0) - Cell.Offset(12, 0)) ^ 2 + (Cell.Offset(11, 1) -
Cell.Offset(12, 1)) ^ 2) ^ 0.5
        End If
        'iii.  If CurrentLenth if greater than MaximumLength, Then
        If CurrentLength > MaximumLength Then
            '1.  Set MaximumLength to CurrentLength
            MaximumLength = CurrentLength
            '2. Calculate the orientation of this segment and set this as ObjectOrientation
            If Cell.Offset(12, 0) > Cell.Offset(11, 0) And Cell.Offset(12, 1) > Cell.Offset(11, 1) Then
                ObjectOrientation = 180 / 3.141592654 * (Atn((Cell.Offset(12, 0) - Cell.Offset(11, 0)) /
(Cell.Offset(12, 1) - Cell.Offset(11, 1))))
            End If
            If Cell.Offset(12, 0) > Cell.Offset(11, 0) And Cell.Offset(12, 1) < Cell.Offset(11, 1) Then
```

```
                ObjectOrientation = 90 + Abs(180 / 3.141592654 * (Atn((Cell.Offset(12, 1) - Cell.Offset(11,
1)) / (Cell.Offset(12, 0) - Cell.Offset(11, 0)))))
            End If
            If Cell.Offset(12, 0) < Cell.Offset(11, 0) And Cell.Offset(12, 1) < Cell.Offset(11, 1) Then
               ObjectOrientation = 180 + 180 / 3.141592654 * (Atn((Cell.Offset(12, 0) - Cell.Offset(11, 0))
/ (Cell.Offset(12, 1) - Cell.Offset(11, 1))))
            End If
            If Cell.Offset(12, 0) < Cell.Offset(11, 0) And Cell.Offset(12, 1) > Cell.Offset(11, 1) Then
               ObjectOrientation = 270 + Abs(180 / 3.141592654 * (Atn((Cell.Offset(12, 1) -
Cell.Offset(11, 1)) / (Cell.Offset(12, 0) - Cell.Offset(11, 0)))))
            End If
         'iv.
         End If
   'b.  End clause for processing this object
  End If
   'c.  Output the results for this object
   If Cell.Offset(0, 1) = "Center" Then
      outputText = Cell.Offset(0, 2) & ", " & Cell.Offset(0, 3) & ", " & MaximumLength & ", " &
ObjectOrientation
      Print #1, outputText
   End If
   'd.  If this is the end of the list (a blank cell followed by another blank three rows below) then exit the
for loop
   If Cell.Offset(0, 0) = "" And Cell.Offset(1, 0) = "" And Cell.Offset(2, 0) = "" And Cell.Offset(3, 0) = ""
And Cell.Offset(4, 0) = "" Then
               outputText = "Found EOF"
               Print #1, outputText
                  Close #1
```

```
        Exit For
    End If
'4.  Proceed to next row
Next
End Sub
```

Typical Rooftop Architecture in the UK

The images below represent the typical UK rooftop architecture used in the solar rooftop assessment methodology (GeographBritainandIreland, 2009).



Figure 7.1 Gable Rooftop



Figure 7.2 Double Gable



Figure 7.3 Hipped Rooftop



Figure 7.4 Flat Rooftop

Municipal and Commercial & Industrial Solid Waste Composition

The chart in **Error! Reference source not found.** below shows the average percentage composition by mass of MSW in England (Hogg et al., 2008).

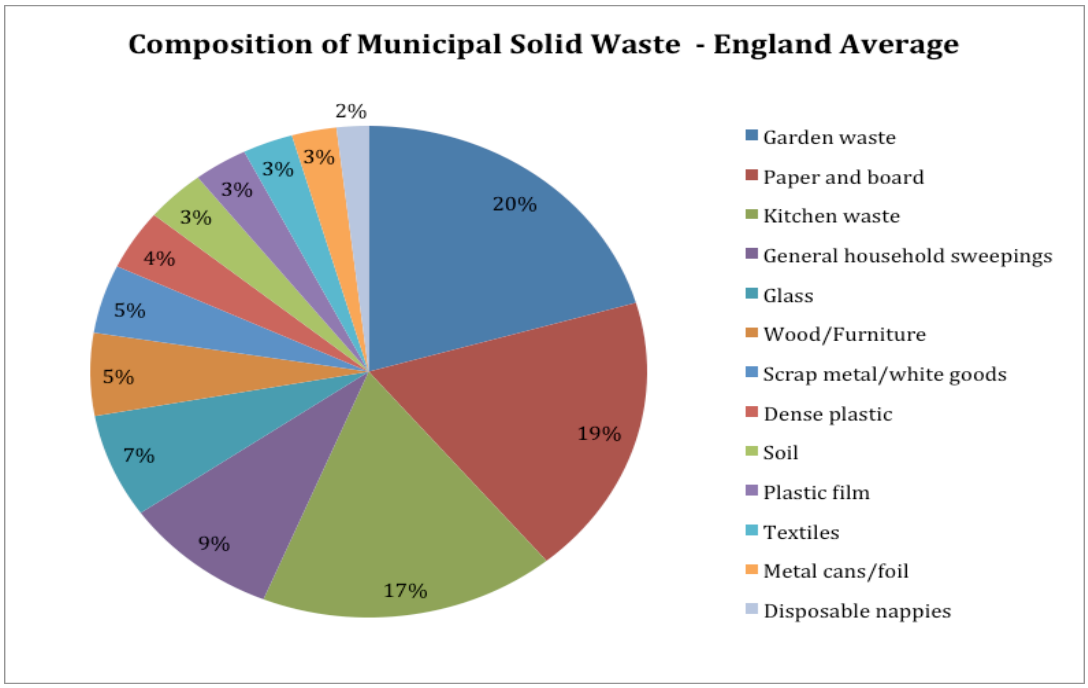


Figure 7.5 Composition of Residential Waste - England Average

The chart in **Error! Reference source not found.** below shows the average percentage composition by mass of C&I waste in England (Hogg et al., 2008).

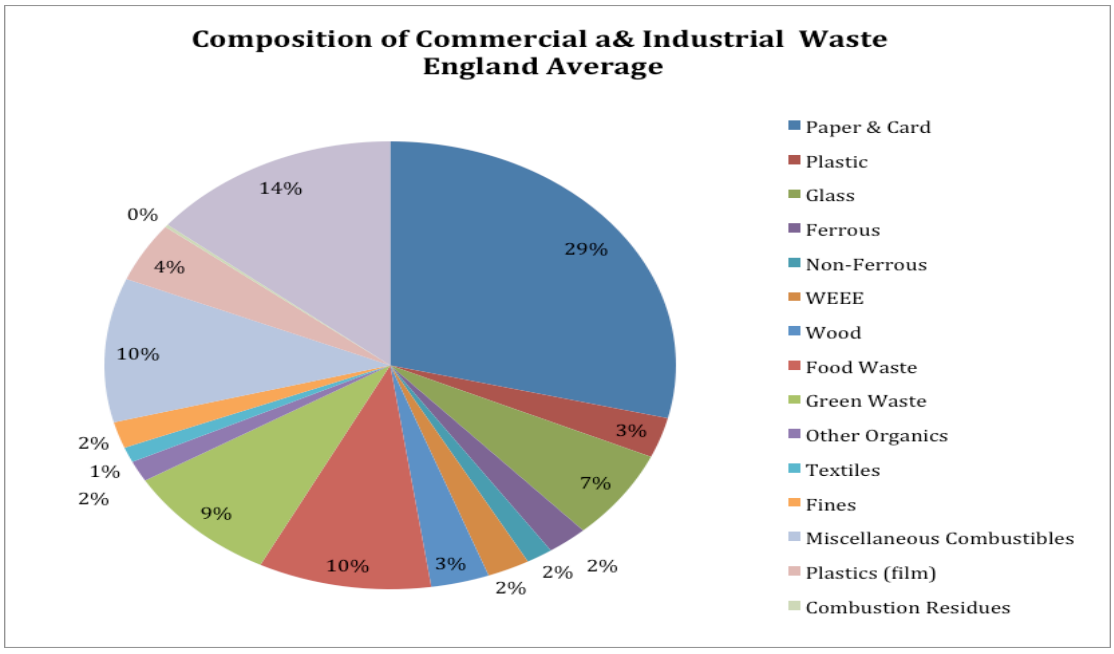


Figure 7.6 Composition of Commercial and Industrial Waste - England Average

Suntech STP190S Photovoltaic Module Data Sheet

The Suntech STP190S Photovoltaic module data sheet that shows the electrical and technical characteristics as well as the current – voltage relationship is shown in Figure 7 (Solar2000, 2013).

SOLAR2000 Spec Sheet

STP190S - 24/Ad+

SUNTECH
Solar powering a green future™

190 Watt
MONOCRYSTALLINE SOLAR MODULE



Features

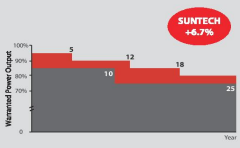
- **High module conversion efficiency** (14.9%)
  Up to 14.9%, through superior cell technology and leading manufacturing capability
- **Positive tolerance** (0/+5%)
  Guaranteed positive tolerance 0/+5% ensures power output reliability
- **Extended wind and snow load tests** (3800Pa 5400Pa)
  Entire module certified to withstand extreme wind (3800 Pascal) and snow loads (5400 Pascal) *
- **Self clean effect** (Self-clean)
  Anti-reflective, hydrophobic layer improves light absorption and reduces surface dust
- **Excellent weak light performance** (Weak light)
  Excellent performance under low light environments (mornings, evenings, and cloudy days)
- **Suntech current sorting process** (2%)
  All Suntech modules sorted and packaged by amperage, maximizing system output by reducing mismatch losses by up to 2%

Certifications and standards:
IEC 61215, IEC 61730, conformity to CE

Trust Suntech to Deliver Reliable Performance Over Time

- World's No.1 manufacturer of crystalline silicon photovoltaic modules
- Unrivaled manufacturing capacity and world-class technology
- Rigorous quality control meeting the highest international standards : ISO 9001: 2008, ISO 14001: 2004 and ISO17025: 2005

Industry-leading Warranty based on Pnom



- Based on nominal power (Pnom)
- 25-year transferrable power output warranty: 5 years/95%, 12 years/90%, 18 years/85%, 25 years/80% **
- Warrants 6.7% more power than the market standard over 25 years
- 10-year material and workmanship warranty



Superior Frame Design
Specially designed drainage holes and rigid construction prevent frames from deforming. Screwless frame design for a long term durability.



Most Modern IP67 Rated Junction Box
Supports any orientation installation. High performance low resistance connectors ensure maximum module power output for highest energy production.

* Please refer to Suntech Standard Module Installation Manual for details.
** Please refer to Suntech Product Warranty for details.

©Copyright 2011 Suntech Power

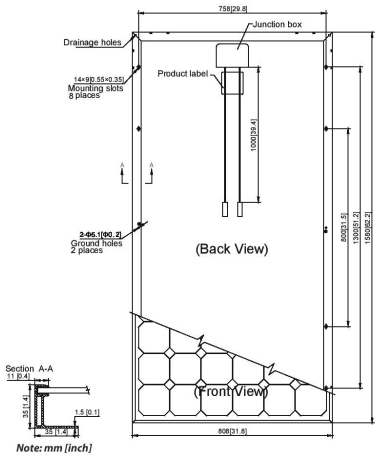
www.suntech-power.com EN-STD-Ad+-NO2.01-Rev 2011

Address: Solar 2000 (Storage 2000 Complex)
34 Barndioota Rd Salisbury Plain SA 5109
Tel: 08 8282 5929
Fax: 08 8282 5989
Email us: enquiries@solar2000.com.au

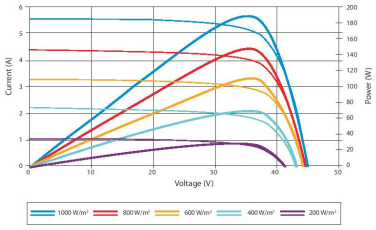
SOLAR2000

Spec Sheet

STP190S - 24/Ad+



Current-Voltage & Power-Voltage Curve (190S-24)



Excellent performance under weak light conditions: at an irradiation intensity of 200 W/m² (AM 1.5, 25 °C), 95.5% or higher of the STC efficiency (1000 W/m²) is achieved

Electrical Characteristics

STC	STP190S-24/Ad+
Optimum Operating Voltage (Vmp)	36.6 V
Optimum Operating Current (Imp)	5.20 A
Open Circuit Voltage (Voc)	45.2 V
Short Circuit Current (Isc)	5.62 A
Maximum Power at STC (Pmax)	190 W
Module Efficiency	14.9%
Operating Module Temperature	-40 °C to +85 °C
Maximum System Voltage	1000 V DC (IEC) / 600 V DC (UL)
Maximum Series Fuse Rating	15 A
Power Tolerance	0/+5 %

STC: Irradiance 1000 W/m², module temperature 25 °C, AM=1.5;
Best in Class AAA solar simulator (IEC 60904-9) used, power measurement uncertainty is within +/- 3%

NOCT	STP190S-24/Ad+
Maximum Power at NOCT (Pmax)	139 W
Optimum Operating Voltage (Vmp)	33.1 V
Optimum Operating Current (Imp)	4.19 A
Open Circuit Voltage (Voc)	41.3 V
Short Circuit Current (Isc)	4.56 A

NOCT: Irradiance 800 W/m², ambient temperature 20 °C, AM=1.5, wind speed 1 m/s;
Best in Class AAA solar simulator (IEC 60904-9) used, power measurement uncertainty is within +/- 3%

Mechanical Characteristics

Solar Cell	Monocrystalline 125 × 125 mm (5 inches)
No. of Cells	72 (6 × 12)
Dimensions	1580 × 808 × 35mm (62.2 × 31.8 × 1.4 inches)
Weight	15.5 kgs (34.1 lbs.)
Front Glass	3.2 mm (0.13 inches) tempered glass
Frame	Anodized aluminium alloy
Junction Box	IP67 rated
Output Cables	TUV (2Pfg1169:2007), UL 4703, UL 44 4.0 mm² (0.006 inches²), symmetrical lengths (-) 1000 mm (39.4 inches) and (+) 1000 mm (39.4 inches)
Connectors	H4 connectors (MC4 compatible)

Temperature Characteristics

Nominal Operating Cell Temperature (**NOCT**)	45±2°C
Temperature Coefficient of Pmax	-0.45 %/°C
Temperature Coefficient of Voc	-0.34 %/°C
Temperature Coefficient of Isc	0.050 %/°C

Packing Configuration

Container	20' GP	40' GP
Pieces per pallet	26	26
Pallets per container	12	28
Pieces per container	312	728

Dealer information

Specifications are subject to change without further notification

www.suntech-power.com | E-mail: sales@suntech-power.com EN-STD-Ad+-NO2.01-Rev 2011

Address: Solar 2000 (Storage 2000 Complex)
34 Barndioota Rd Salisbury Plain SA 5109
Tel: 08 8282 5929
Fax: 08 8282 5989
Email us: enquiries@solar2000.com.au

Figure 7.7 Suntech STP 190S - Product Data Sheet

Works Cited

Afgan, N. & Carvalho, M., 2002. Multi-criteriaassessment of new and renewableenergy power plants. *Energy*, 27(8), pp.739-55.

Akai, T., 1994. *Applied Numerical Methods for Engineers*. 1st ed. New York: John Wiley & Sons.

Alfagy, 2010. *Biogas CHP to power Anaerobic Digestion (AD) plants*. [Online] Available at: http://www.alfagy.com/products-chp,-boilers-other/91-combined-heat-power-products/biogas-chp.html [Accessed 5 January 2011].

Alfagy, 2011a. *Alfagy*. Product Specifications. Moreton-in-Marsh: Alfagy Alfagy AD and CHP Systems.

ARUP, 2011. *Review of the generation costs and deployment potential of renewable electricity technologies in the UK*. Study Report. London : Department of Energy and Climate Change ARUP.

Ashok, S., 2007. Optimised model for community-based hybrid energy system. *Renewable Energy*, 32(7), pp.1155-64.

Baldwin, A. & Katers, J., 2009. *Performance Analysis of Anaerobic Digestion Systems At Two Dairy Farms in Northeastern Wisconsin*. Focus on Energy Final Report. Wisconsin: Focus on Energy University of Wisconsin-Green Bay.

Balfour, J.R., Shaw, M. & Nash, N., 2011. *Review Guide for the NABCEP Entry-Level Exam*. Burlington: Jones & Bartlett Publishers.

Banks, C., 2007. *Renewable energy from crops and agrowastes - CROPGEN*. Database. Southampton: University of Southampton University of Southampton.

Bates, J., Edberg, O. & Nuttall, C., 2009. *Minimizing greenhouse gas emissions from biomass energy generation*. Science Report. Bristol: Environment Agency Environment Agency. Research Contractor : AEA.

BEC, 2011. *Moisture Content*. [Online] UK Forestry Commission Available at: http://www.biomassenergycentre.org.uk/portal/page?_pageid=75,177178&_dad=portal&_schema=PORTAL [Accessed 1 December 2010].

Begic, F. & Afgan, N., 2007. Sustainability assessmenttool for the decisionmaking in selection of energysystem—Bosniancase. *Energy*, 32(10), p.1979–1985.

Bernstein, R. & Bernstein, S., 1999. *Schaum's Outline of Elements of Statistics II: Inferential Statistics*. McGraw-Hill Professional.

Betz, A., 1920. Das maximum der theoretisch möglichen ausnützung des windes durch windmotoren. *Z. Gesamte Turbinenw*, 26, p.307–309.

Boiteux, M. & Bessiere, F., 1961. Sur l'emploi des méthodes globale et marginale dans le choix des investissements. *Revue Francaise de Recherche Opérationelle*, 20, pp.65-78.

Borowy, B.S., 1996. Methodology for optimally sizing the combination of a battery bank and PV array in a wind/PV hybrid system. *IEEE Transactions on Energy Conversion*, 11(2), pp.367 - 375.

Boucher, O., Friedlingstein, P., Collins, B. & Shine, K.P., 2009. The indirect global warming potential and global temperature change potential due to methane oxidation. *Environmental Research Letters*, IV(4).

Boxwell, M., 2010. *Solar Electricity Handbook*. 3rd ed. Ryton on Dunsmore: Greenstream Publishing.

BP, 2012a. *BP Statistical Review of World Energy June 2012*. Statistical Review. London: BP p.l.c. BP p.l.c. 61st Annual Edition.

BP, 2012. *BP Energy Outlook 2030*. Presentation. London: BP BP.

Braun, R., Weiland, P. & Wellinger, A., 2011. *Biogas From Energy Crops Digestion*. Technical Brochure. Westerduinweg: International Energy Agency - Task 37 IEA Bioenergy.

Breeze, P., 2005. *Power Generation Technologies*. 1st ed. Oxford: Newnes.

Brundtland, G., 1987. *Our common future: The World Commission on Environment and Development*. Mandate. New York: Oxford University Press United Nations World Commission on Environment and Development.

Caslin, B., Finnan, J. & McCracken, A., 2010. *Short Rotation Coppice Willow Best Practice Guidelines*. Best Practice Guidelines. Belfast: Teagasc Agri-Food and Biosciences Institute.

Cesaraccio, C., Spano, D., Duce, P. & Snyder, R., 2001. An improved model for determining degree-day values from daily temperature data. *International Journal of Biometeorology*, 45(4), pp.161-69.

Chedid, R., Karaki, S. & Rifai, A., 2005. A multi-objective design methodology for hybrid renewable energy systems. Moscow, 2005. Power Techn.

Chedid, R. & Saliba, Y., 1996. Optimization and control of autonomous renewable energy systems. *Internatioanl Journal of Energy Resources* , 20(7), p.609–24.

Cherni, J.A. et al., 2007. Energy supply for sustainable rural livelihoods. A multi-criteria decision-support system. *Energy Policy*, 35(3), p.1493–1504.

Cho, J.K. & Park, S.C., 1995. Biochemical methane potential and solid state anaerobic digestion of Korean food wastes. *Bioresource Technology*, 52(3), p.245–253.

ChristChurch, 2010. *Blue Boar Opening*. [Online] Available at: http://www.chch.ox.ac.uk/news/2009/blue-boar-opening [Accessed 9 January 2011].

ChristChurch, 2013a. *Christ Church Oxford*. [Online] Available at: http://www.chch.ox.ac.uk/visiting/history [Accessed 24 May 2013].

ChristChurch, 2013. *Christ Church, Oxford*. [Online] Available at: http://www.chch.ox.ac.uk/college/academic-research-staff [Accessed 24 May 2013].

Chynoweth, D.P. et al., 1993. Biochemical methane potential of biomass and waste feedstocks. *Biomass and Bioenergy*, 5(1), p.95–111.

Climaco, J., 1997. *Multicriteria analysis*. New York: Springer-Verlag.

Coles, S., 2012. *Discussion on the rooftop tilt angles at Christ Church*. Personal Communication. Oxford: Oxford University.

Connolly, D., 2010. *Review of Energy Storage Technologies For the integration of fluctuating renewable energy*. Technology Review. Limerick: University of Limerick University of Limerick.

Connollya, D., Lundb, H., Mathiesenb, B. & Leahya, M., 2010. A review of computer tools for analyzing the integration of renewable energy into various systems. *Applied Energy*, 87(4), p.1059 – 1082.

DAF, 2007. *The contribution of road transport to a cleaner environment*. Product Specifications. Thame: DAF Trucks NV i DAF Trucks NV.

Dalgaard, T., Halberg, N. & Porter, J., 2001. A model for fossil energy use in Danish agriculture used to compare organic and conventional farming. *Agriculture, Ecosystems and Environment*, 87(1), pp.51-65.

DCLG, 2009. *Multi criteria analysis : a manual*. Manual. London: Crown Department for Communities and Local Government.

de Vries, J.W., Corré, W.J. & van Dooren, H.J.C., 2010. *Environmental assessment of untreated manure use, manure digestion and co-digestion with silage maize*. Project Deliverable. Lelystad: Wageningen UR Livestock Research Wageningen UR Livestock Research. Deliverable for the 'EU-AGRO-BIOGAS' project.

DECC, 2010. *2010 UK carbon dioxide emissions for Local Authority and Government Office region level (local authority influenced emissions only so excludes motorway transport emissions).*. Emissions

Statistics. London: Departmenr of Energy and Climate Change Department of Energy and Climate Change.

DECC, 2010a. *Sub-National Authority Electricity Statistics*. Review. London: DECC Department of Energy and Climate Change.

DECC, 2012a. *Sub-National Gas Sales and Numbers of Customers 2005 - 2011*. Energy statistics digest. London: DECC Department of Energy and Climate Change.

DECC, 2012b. *Table 4.1. Natural gas supply and consumption*. Energy Statistics. London: Department of Energy and Climate Change Department of Energy and Climate Change.

DECC, 2012. *DECC Updated Energy & Emissions Projections - Annex F*. Forecast Report. London: Department of Energy and Climate Change Department of Energy and Climate Change.

DEFRA, 2007. *Waste Strategy for 2007*. London: The Stationary Office Department for Energy, Food and Rural Affairs.

DEFRA, 2009. *BNXS01: Carbon Dioxide Emission Factors for UK Energy:Market Transformation Programme*. Market Transformation Report. London: DEFRA Department of Energy, Food and Rural Affairs.

DEFRA, 2011a. *Applying the Waste Hierarchy: evidence summary*. Current research summary. London: Crown Department for Energy, Food and Rural Affairs.

DEFRA, 2011. *Anaerobic Digestion Strategy and Action Plan*. Strategy Action Plan. London: Crown Department for Environment, Food and Rural Affairs and Department of Energy and Climate Change.

DEFRA, 2011b. *Maps of livestock populations in 2000 and 2010 across England*. Survey. London: DEFRA Department for Energy, Food and Rural Affairs.

DEFRA, 2012. *2012 Guidelines to Defra/DECC's GHG Conversion Factors for Company Reporting*. Guidelines. London: Defra & DECC Produced by AEA for the Department of Energy and Climate Change (DECC) and the Department for Environment, Food and Rural Affairs (Defra). Study Commissioned to AEA.

DegreeDays.net, 2011. *Degree Days.net - Custom Degree Day Data*. [Online] BizEE Software Available at: http://www.degreedays.net/ [Accessed 3 July 2011].

Diaf, S. et al., 2007. A methodology for optimal sizing of autonomous hybrid PV/wind system. *Energy Policy*, 35(11), pp.5708-18.

Diakaki, C. et al., 2004. A multi-objective decision model for the improvement of energy efficiency in buildings. *Energy*, 35(12), p.5483–5496.

DUKES, 2005. *Digest of UK Energy Statistics*. Report. London: Department of Trade and Industry.

E4tech, 2010. *Biomass prices in the heat and electricity sectors in the UK*. Department of Energy and Climate Change.

EC, 2008. *Directive 2008/98/EC of the european parliament and of the council on waste and repealing certain Directives*. Directive. Official Journal of the European Union.

ECI, 2013. *Weekly Updated: Monthly Degree Days for energy management*. [Online] School of Geography and the Environment, Oxford University Available at: http://www.eci.ox.ac.uk/research/energy/degreedays-weekly-monthly.php [Accessed 18 January 2013].

El-Hefnawi, S.H., 1998. Photovoltaic Diesel-generator hybrid power system sizing. *Renewable Energy* , 13(1), pp.33-40.

Elliott, D.L. et al., 1986. *Wind Energy Resource Atlas of the United States*. Resource Atlas. Richland, Washington: Solar Technical Information Program Solar Energy Research Institute Pacific North West National Laboratory.

EnergySavingTrust, 2008. *Domestic heating by gas: boiler systems – guidance for installers and specifiers*. Guidance for Installer and Suppliers. London: Energy Saving Trust Energy Saving Trust.

EnvironmentalImpact, 2008. *Fertilizer Impact*. [Online] Available at: http://envimpact.org/node/ [Accessed 1 April 2012].

Evans, A., Strezov, V. & Evans, T., 2009. Assessment of sustainability indicators for renewable energy technologies. *Renewable and Sustainable Energy Reviews*, 13(5), pp.1082-88.

FAO, 2007. *Fertilizer Use Statistics*. [Online] Available at: http://www.fao.org/ag/agp/fertistat/fst_fubc1_en.asp?country=GBR&commodity=%25&year=%25&search=Search+%21 [Accessed 14 March 2012].

FC, 2009a. *Woodfuel scoping study*. Research Summary. Midlothian: Forestry Commission Forestry Commission and Biomass Energy Centre (BEC).

FC, 2009. *Wood as Fuel : A Guide to Choosing and Drying Logs*. Practice Guidelines. Surrey: Crown Copyright Forestry Comission.

FC, 2012. *Oxfordshire - Woodland Cover*. Presentation. Surrey: Forestry Commission Forestry Commission.

FEC, 2003. *Anaerobic digestion, storage, oligolysis,lime, heat and aerobic treatment of livestock manures*. Final Report. Kenilworth: FEC Services.

Fereidouni, A., 2012. *Least Cost Analysis of Energy Efficiency Upgrades for Ontario Using Trnsys*. MSc Thesis. Ontario: Digital Commons @ Ryerson. Ryerson University.

Frost, J.P. & Gilkinson, S.R., 2010. *First Year Performance Summary for Anaerobic Digestion of Dairy Cow Slurry at AFBI Hillsborough*. [Online] Available at: www.afbini.gov.uk [Accessed 25 March 2012].

Garag, H.P. & Prakash, J., 2000. *Solar Energy : Fundamentals and Applications*. 1st ed. New Delhi: Tata McGraw Hill.

GCMAP, 2009. *HAQ - Airport*. [Online] Available at: http://www.gcmap.com/airport/HAQ [Accessed 2 April 2011].

GeographBritainandIreland, 2009. *Roof Types*. [Online] Available at: http://www.geograph.org.uk/article/Roof-Types#gabled [Accessed 25 April 2012].

Gipe, P., 2004. *Wind Power : Renewable Energy for Home, Farm, and Business*. Vermont: Chelsea Green Publishing Company.

Goetzberger, A. & Hoffmann, V.U., 2005. *Photovoltaic Solar Energy Generation*. Berlin: Springer.

Golding, E.W., 1958. The combination of local sources of energy for isolated communities. *Solar Energy*, 2(1), p.7–12.

Goodge, M., 2006. *Listed Buildings in Oxford, Oxfordshire, England*. [Online] Available at: http://www.britishlistedbuildings.co.uk/england/oxfordshire/oxford [Accessed 12 January 2013].

GoogleEarth, 2010. *Google Maps*. [Online] Available at: https://maps.google.co.uk/maps?client=safari&oe=UTF-8&q=headington&ie=UTF-8&hq=&hnear=0x4876c157f53ee125:0x831c30a1f0c7ecd5,Headington,+Oxfordshire&gl=uk&ei=W6Y8UKbOLsnH0QXEtIGwBA&ved=0CIsBELYD [Accessed 14 July 2012].

GunaTravel, 2013. *Maldives Hotels and Resorts*. [Online] Available at: http://www.guna-travel.com/maldives/#prettyPhoto [Accessed 4 March 2013].

Harris, J., 2008. *Christ Church to become 'The 40 % House' and on track to cut carbon emissions by 60 % by 2050*. Media Release. Oxford: Christ Church.

Hart, C.E., 1991. *Practical Forestry for the Agent and Surveyor*. 1st ed. Gloucestershire: Alla Sutton Publishing.

Harvey, M. & Pilgrim, S., 2011. The new competition for land: Food, energy, and climate change. *Food Policy*, 36(1), p.40–51.

Herren, R., 2011. *The Science of Agriculture: A Biological Approach*. 4th ed. New York: Cengage Learning.

Herzog, T., 2005. *World Greenhouse Gas Emissions in 2005*. Working Paper. Washington: World Resources Institute.

Hester, R.E. & Harrison, R.M., 1999. *Environmental Impact of Power Generation*. Cambridge: Royal Society of Chemistry.

Hester, R.E. & Harrison, R.M., 2003. *Sustainability and Environmental Impact of Renewable Energy Sources*. Cambridge: Royal Society of Chemistry.

Hoffman, K.C., 1973. *A linear programming model of the nation's energy system*. New York: Brookhaven National Laboratory.

Hogg, D., Baddeley, A., Ballinger, A. & Elliott, T., 2008. *Development of Marginal Abatement Cost Curves for the Waste Sector*. Consultation Report. Bristol: Committee on Climate Change, DEFRA and Environment Agency Eunomia research and consulting.

IEA, 2010. *Potential for co-digestion*. Technical Brochure. Tulln: International Energy Agency International Energy Agency.

IPCC, 2012. *Renewable Energy Sources and Climate Change Mitigation*. 1st ed. New York: Cambridge University Press.

IRENA, 2012. *30 Years of Policies for Wind Energy Lessons from 12 Wind Energy Markets*. Policy Review. Abu Dhabi: International Renewable Energy Agency and the Global Wind Energy Council International Renewable Energy Agency.

IRENA, 2012a. *Biomass for Power Generation*. Working Paper. Bonn: International Renewable Energy Agency International Renewable Energy Agency.

IRENA, 2012b. *Electricity Storage and Renewables for Island Power A Guide for Decision Makers*. Decicion Makers Guide. Bonn: International Renewable Energy Agency International Renewable Energy Agency.

Jacobson, M.Z., 1999. *Atmospheric Modeling*. Cambridge: Cambridge University Press.

Jenkins, D., 2012. *Wood Pellet Heating Systems: The Earthscan Expert Handbook on Planning, Design and Installation*. 2nd ed. London: Routledge.

Jepma, C.J. & Munasinghe, M., 1998. *Climate Change Policy: Facts, Issues and Analyses*. Cambridge: Cambridge University Press.

Jordan, R.C. & Liu, B.Y.U., 1962. Daily insolation on surfaces tilted towards the equator. *Trans SHRAE*, (67), pp.526 - 541.

Josephson, P., 2002. *Industrialized Nature: Brute Force Technology and the Transformation of the Natural World*. Washington : Island Press.

Karp, A. & Shield, I., 2008. Bioenergy from plants and the sustainable yield challenge. *New Phytologist*, 179(1), pp.15-32.

Kaya, T. & Kahramanb, C., 2010. Multi criteria renewable energy planning using an integrated fuzzy VIKOR & AHP methodology: The case of Istanbul. *Energy*, 35(6), p.2517–2527.

Khoiyangbam, R.S. et al., 2011. *Biogas Technology: Towards Sustainable Development*. New Dheli: The Energy and Resources Institute (TERI).

King, M.R. & Mody, N.A., 2010. *Numerical and Statistical Methods for Bioengineering: Applications in MATLAB*. 1st ed. Cambridge: Cambridge University Press.

Koroneos, C., Michailidis, M. & Moussiopoulos, N., 2004. Multi-objective optimization in energy systems: the case study of Lesvos Island, Greece. *Renewable and Sustainable Energy Reviews*, 8(1), pp.91-100.

Koutroulis, E., Kolokotsab, D., Potirakisa, A. & Kalaitzakisa, K., 2006. Methodology for optimalsizing of stand-alonephotovoltaic/wind-generatorsystems using geneticalgorithms. *Solar Energy*, 80(9), pp.1072-88.

Kubik, M., Coker, P. & Hunt, C., 2011. Using meteorological wind data to estimate turbine generation output: a sensitivity analysis. In *World Renewable Energy Congress 2011*. Linkoping, 2011. Elsevier.

La Roche, P., 2011. *Carbon-Neutral Architectural Design*. 1st ed. Boca Raton, Florida: CRC Press, Taylor & Francis Group.

Landshare, 2012. *FoodPrinting Oxford*. Oxford: Local Energy Assessment Fund, Department of Energy and Climate Change Landshare.

Layberry, R., 2008. Degree days for building energy management - presentation of a new data set. *Building Services Engineering and Technology*, 29(3), pp.273-82.

LCH, 2012. *Investor*. [Online] Available at: http://www.lowcarbonhub.org/about/the-big-idea/investors [Accessed 15 July 2012].

LCH, 2013. *About Us*. [Online] Available at: http://www.lowcarbonhub.org/about/low-carbon-hub [Accessed 2013 April March].

Liu, B.Y.H. & Jordan, R.C., 1960. The interrelationship and characteristics and distribution of direct, diffuse, and total solar radiation. *Solar Energy*, 4, pp.1-10.

Lukehurst, C., Frost, P. & Al Sead, T., 2010. *Utilisation of digestate from biogas plants as biofertilizer*. Technical Brochure. Kent: IEA Bioenergy IEA Bioenergy.

Manwel, J., McGowan, J. & Rogers, A., 2002. *Wind Energy Explained: Theory, Design and Application*. 1st ed. Chichester: Wiley-Blackwell.

MapInfo, 2007. *MapInfo Professional User Guide Abridged*. User Guide. New York: Pitney Bowes Pitney Bowes.

Markvart, T., 2000. *Solar Electricity*. 2nd ed. Chichester : John Wiley & Sons.

Mason, M., 2012. *Maldives SREP Investment Plan*. Investment Plan. Male: Renewable Energy Investment Office Renewable Energy Investment Office, Republic of the Maldives.

Masters, T., 2009. *Maldives*. 7th ed. London: Lonely Planet.

McCulloch, M., 2010. *Discussion on Degree Day's at Christ Church*. Personal Communication. Oxford: Oxford University.

McKendry, P., 2001. Energy Production from biomass (part 1): overview of biomass. *Bioresource technology* , 1(83), pp.37-46.

McLoughlin, F., Duffy, A. & Conlon, M., 2011. A Parametric Analysis of Domestic Electricity Consumption Patterns in Ireland. In *enth International Conference on Environment and Electrical Engineering (EEIC)*. Rome, 2011. Dublin Energy Lab.

Means, R.S., 2010. *Green Building: Project Planning and Cost Estimating*. 3rd ed. Hoboken, New Jersey: John Wiley & Sons.

Meck, R., 2012. *Calculating Tilted Array Spacing*. [Online] Available at: http://www.affordable-solar.com/Learning-Center/Building-a-System/Calculating-Tilted-Array-Spacing [Accessed 5 October 2012].

Mellita, A., Kalogiroub, S.A., Hontoriac, L. & Shaarid, S., 2009. Artificialintelligencetechniques for sizingphotovoltaic systems: Areview. *Renewable and Sustainable Energy Reviews*, 13(2), pp.406-19.

Metz, B., 2001. *Climate Change 2001: Mitigation: Contribution of Working Group III to the Third Assessment Report of the Intergovernmental Panel on Climate Change*. Cambridge: Cambridge University Press.

Metz, B. et al., 2007. *Contribution of Working Group III to the Fourth Assessment Report of the Intergovernmental Panel on Climate Change*. Assessment Report. Cambridge: Cambridge University Press.

Mohamed, I., 2011. *Country Analysis Paper, Maldives*. Forum Country Analysis. Singapore: United Nations Environmental Protection Agency. Third Meeting of the Regional 3R Forum in Asia "Technology Transfer for promoting the 3Rs –Adapting, implementing, and scaling up appropriate technologies".

Mokyr, J., 1985. *The Economics of the Industrial Revolution*. 1st ed. Rowman & Littlefiels Publishers Inc.

MPND, 2006. *Island Level Tables - Population and Housing Census 2006*. [Online] Available at: http://www.planning.gov.mv/publications/census2006_island_level_tables/islandTables.htm [Accessed 5 May 2011].

MPND, 2007. *Population, percentage share of population and population density by islands, 2000 & 2006*. Census. Male: Ministry of Planning and National Development Maldives, Population and Housing Census.

MTCA, 2005. *Ministry of Tourism and Civil Aviation - Maldives Third Tourism Masterplan*. Masterplan. Male: Ministry of Tourism and Civil Aviation Ministry of Tourism and Civil Aviation.

NAPEE, 2008. *Understanding Cost-Effectiveness of Energy Efficiency Programs: Best Practices, Technical Methods, and Emerging Issues for Policy- Makers*. National Action Plan. Seattle: U.S. Department of Energy and U.S. Environmental Protection Agency National Action Plan for Energy Efficiency.

NationalGrid, 2012. *Metered half-hourly electricity demands*. [Online] National Grid (1) Available at: http://www.nationalgrid.com/uk/Electricity/Data/Demand+Data/ [Accessed 25 January 2013].

Nix, J., 2012. *John Nix Farm Management Pocketbook*. 42nd ed. Leicester: Agro Business Consultants.

Npower, 2011. *Didcot Power Stations*. Brochure. Didcot: RWE RWE Npower.

NREL, 2011a. *U.S Wind Resource Map*. [Online] Available at: http://www.nrel.gov/gis/wind.html [Accessed 15 November 2011].

NREL, 2011. *Getting Started Guide for HOMER Legacy (Version 2.68)*. User Manual. Golden, Colorado: NREL National Renewable Energy Laboratory.

NREL, 2012. *Cost and Performance Data for Power Generation Technologies*. Cost Report. Washington DC: National Renewable Energy Laboratory Black & Veatch.

OCC, 2010. *Oxfordshire Data Observatory Briefing Note, July 2010 Oxfordshire's population estimates and projections, June 2010 Oxfordshire's population*. Briefing Note. Oxford: Oxford City Council Oxford City Council.

OCC, 2011. *Oxfordshire Minerals and Waste Development Framework*. Policy Framework. Oxford: Oxfordshire County Council Oxfordshire County Council.

OCC, 2012. *Oxfordshire Economic Assessment: Part Two - Update of evidence*. Draft Asessment Plan. Oxford: Oxfordshire County Council.

ONS, 2007. *Key Population and Vital Statistics 2007*. Correction Notice. London: Crown Copyright Office for National Statistics.

ONS, 2010. *Oxfordshire Data Observatory Briefing Note, July 2010*. Population report. Oxford: Oxfordshire Data Observatory Office of National Statistics.

OS, 2012. *OS Master Map - Making all the difference*. [Online] Available at: http://www.ordnancesurvey.co.uk/oswebsite/products/os-mastermap/index.html [Accessed 15 March 2012].

Ozerdem, B., Ozer, S. & Tosun, M., 2006. Feasibilty study of wind farms : A case study for Izmir, Turkey. *Journal of Wind Engineering and Industrial Aerodynamics*, 94(10), pp.725-43.

Pareto, 2009. *Microgrid Preliminary Feasibility Analysis Christ Church, Oxford, UK*. Feasibility Analysis. Oxford: Pareto Energy Consultants.

ParsensBrinckerhoff, 2012. *Solar PV cost update*. Cost Update. London: Department of Energy and Climate Change Parsens Brinckerhoff.

Peacocke, C., 2008. *Biomass Gasification and Biomass CHP Lecture I*. Presentation. Belfast,: Care Demon Care Demon.

Petchers, N., 2003. *Combined heating, cooling, and power handbook*. Lilburn: The Fairmont Press.

Pohekar, S. & Ramachandran, M., 2004. Application of multi-criteria decision making to sustainable energy planning—A review. *Renewable and Sustainable Energy Reviews*, 8(4), p.365–381.

Prasad, R., 2005. *Fundamentals of Electrical Engineering*. 1st ed. New Dheli: Prentice-Hall of India.

PresidentOffice, 2009. *President announces the government's intention to make the Maldives world's first carbon neutral country*. [Online] Available at: http://www.presidencymaldives.gov.mv/Index.aspx?lid=11&dcid=180 [Accessed 23 October 2010].

Protogeropoulos, C., Brinkworth, B.J. & Marshall, R.H., 1997. Sizing and techno-economical optimization for hybrid solar photovoltaic/wind power systems with battery storage. *International Journal of Energy Resources*, 21(6), pp.465-79.

Provey, J.R. & Barber, E.M., 2010. *Convert Your Home to Solar Energy*. Newton: Taunton Press.

Quareshi, S., 1984. Renewable Energy - The Key to a Better Future. *Solar and Wind Technology*, 1(1), pp.25-35.

Rivkin, D., Anderson, L. & Silk, V., 2012. *Wind Turbine Control Systems*. 1st ed. Burlington : Jones & Bartlett Publishers.

Schweizer, P., 1974. Determining Optimal Fuel Mix for Environmental Dispatch. *IEEE Transactions on Automation and Control*, pp.534-37. Short Papers.

Sepulveda, J., Souder, W. & Gottfried, B., 1984. *Schaum's Outline of Engineering Economics*. New York: McGraw-Hill Professional.

Sera, D., Teodorescu, R. & Rodriguez, P., 2007. *PV panel model based on datasheet values*. Conference Publications. Aalborg: IEEE IEEE International Symposium on Industrial Electronics.

Soetaert, W. & Vandamme, E., 2005. *Biofuels*. 1st ed. Ghent: Wiley.

Solar2000, 2013. *Solar2000 Spec Sheet*. [Online] Solar2000 Available at: http://solar2000.com.au/wp-content/uploads/2011/08/Suntech-STP190S-24-Ad-spec-sheet.pdf [Accessed 12 January 2012].

SouthernElectric, 2010. *Christ Church Utility Costs 09.10*. Invoice. Gay, J. (2010). Christ Church Utility Costs 09.10. Christ Church. Oxford: Christ Church.: Christ Church Christ Church. Oxford.

STELCO, 2009. *Electricity Production Report 2007-2009*. Electricity Production Report. Hanimaadhoo: State Electricity Company Limited State Electricity Company Limited.

Stevens, M. & Smulders, P., 1979. The estimation of the parameters of the Weibull wind speed distribution for wind energy utilization purposes. *Wind Engineering*, 3(2), pp.132 - 145.

Suntech, 2010. *190 Watt Monocrystalline Solar Module*. Product Datasheet. San Francisco: SunTech Power Ltd SunTech Power Ltd.

Surles, W., Watrous, A., Horanyi, E. & Schaefer, M., 2011. *Solar Angles and Tracking System*. [Online] Available at: http://www.teachengineering.org/view_lesson.php?url=collection/cub_/lessons/cub_pveff/cub_pveff_lesson01.xml [Accessed 22 April 2012].

Thomas, R., 2003. *Sustainable Urban Design: An Environmental Approach*. 1st ed. Oxford: Spon Press.

Tong, W., 2010. *Wind Power Generation and Wind turbine Design*. Southampton: WIT Press.

Towler, G. & Sinnott, R.K., 2012. *Chemical Engineering Design: Principles, Practice and Economics of Plant and Process Design*. 2nd ed. Oxford: Elsevier.

Tzeng, G.-H., Shiau, T.-a. & Chien-Yuan, L., 1992. Application of multicriteria decision making to the evaluation of new energy system development in Taiwan. *Energy*, 17(10), pp.983-92.

Uellendahl, H. et al., 2008. *Energy balance and cost-benefit analysis of biogas production from perennial energy crops pretreated by wet oxidation*. Working Paper. Roskilde: Riso DTU Riso DTU, Technical University of Denmark and Aarhus University.

UNFCCC, 1992. *United Nations framework convention on climate change*. Framework convention. New York: United Nations United Nations.

UNFCCC, 2007. *Impacts, vulnerabilities and adaption in developing countries*. Framework Convention. Bonn,: Information Services of the UNFCCC secretariat United Nations.

UNWCED, 1987. *United Nations World Commission on Environment and Development. Our Common Future (Brundtland Report)*. Oxford: Oxford University Press United Nations.

USAID, 2012. *Climate Vulnerability Assessment - Islands of Dhidhdhoo and Hinnavaru, The Maldives*. Climate Assessment. United States Agency for International Development.

Utley, J. & Shorrock, L., 2008. *Domestic Energy Fact File 2008*. Fact File. London: Crown Copyright BRE Housing.

van Alphen, K., van Sark, W.G.J.H.M. & Hekkert, M.P., 2007. Renewable energy technologies in the Maldives—determining the potential. *Renewable and Sustainable Energy Reviews*, 11(8), pp.1650-74.

Vesma, 2011. *What are degree days?* [Online] Available at: http://www.vesma.com/ddd/whatthey.htm [Accessed 2 December 2011].

von Karman, T., 1931. *Mechanical Similitude and Turbulance*. Technical Memorandum. Springfield: NACA US Department of Commerce.

Wang, M., 2010. The comparison between MAUT and PROMETHEE. *2010 IEEE International Conference on Industrial Engineering and Engineering Management (IEEM)*, pp.753 - 757.

Wilkie, A., 2005. Anaerobic Digestion of Manure : Design Process and Considerations. In *dairy manure management : Treatment, Handling and Community Relations*. New York, 2005. Natural Resource, Agriculture, and Engineering Service.

Winter, M. & Lobley, M., 2009. *What Is Land For?: The Food, Fuel and Climate Change Debate*. 1st ed. Sterling, Virginia: Earthscan.

Wizelius, T., 2007. *Developing wind power projects: theory and practice*. London: Earthscan.

Woodcock, M., 2012. *Woodfuel potential and progress in South East England February 2012*. Progress Report. Surry: Forestry Commission Forestry Commission.

WorldBank, 2010. *World Development Indicators 2010*. 14th ed. Washington: Development Data Group, World Bank.

WorldBank, 2012. *World Development Indicators 2012*. Washington: World Bank Publications.

WRAP, 2011. *Comparing the cost of alternative waste treatment options*. Gate fees cost. Banbury: Waste Resources and Actions Programme.

WRAP, 2012. *Gate Fees Report, 2012 Comparing the cost of alternative waste treatment options*. Cost Survey. Banbury: Waste and Resources action Programme Waste and Resources action Programme.

Yang, H., Lu, L. & Zhou, W., 2007. A novel optimization sizing model for hybrid solar-wind power generation system. *Solar Energy*, 81(1), pp.76-84.

Yang, H., Zhoua, W., Lua, L. & Fangb, Z., 2008. Optimal sizing method for stand-alone hybrid solar–wind system with LPSP technology by using genetic algorithm. *Solar Energy*, 82(4), pp.354-67.

Yergin, D., 1991. *The Prize: The Epic Quest for Oil, Money & Power*. New York: Simon & Schuster.

Zoumakis, N.M., 1993. The dependace of the power law exponent on surface roughness and stabiltiy in a neutraly and stably stratified surface boundary layer. *Atmosphera*, 6, pp.69-73.

Zwart, K.B. & Kuikman, P.J., 2011. *Co-digestion of animal manure and maize: is it sustainable? - an update*. Alterra report 2169. Wageningen: SenterNovem Alterra.